Characterization of Environmental Health Risk Assessment Models based on the Releases from a PCB Incineration Facility

by

Glenn M. Ferguson

A thesis
presented to the University of Waterloo
in fulfillment of the
thesis requirement for the degree of
Doctor of Philosophy
in
Health Studies

Waterloo, Ontario, Canada, 2001

© Glenn M. Ferguson 2001

National Library of Canada
Acquisitions and Bibliographic Services
395 Wellington Street
Ottawa ON K1A 0N4
Canada

Bibliothèque nationale du Canada
Acquisitions et services bibliographiques
395, rue Wellington
Ottawa ON K1A 0N4
Canada

Your file Votre référence

Our file Notre référence

The author has granted a non-exclusive licence allowing the National Library of Canada to reproduce, loan, distribute or sell copies of this thesis in microform, paper or electronic formats.

L'auteur a accordé une licence non exclusive permettant à la Bibliothèque nationale du Canada de reproduire, prêter, distribuer ou vendre des copies de cette thèse sous la forme de microfiche/film, de reproduction sur papier ou sur format électronique.

The author retains ownership of the copyright in this thesis. Neither the thesis nor substantial extracts from it may be printed or otherwise reproduced without the author's permission.

L'auteur conserve la propriété du droit d'auteur qui protège cette thèse. Ni la thèse ni des extraits substantiels de celle-ci ne doivent être imprimés ou autrement reproduits sans son autorisation.

0-612-65237-8

Canada

The University of Waterloo requires the signatures of all persons using or photocopying this thesis. Please sign below, and give address and date.

ACKNOWLEDGMENTS

I would like to gratefully acknowledge the contribution of a number people on this research project. First and foremost is my supervisor, Dr. R. Stephen McColl, who provided invaluable time, effort, and guidance throughout my research, to help shape and improve the study theory and design. His efforts and assistance with breaking down and debugging the various problems in the Evans and Andersen (2000) equilibrium model was particular life-saving, and allowed me to "share the pain" a bit. Above all, he was always there as a sounding board for my various ideas and theories, as well as when my frustration over ill-mannered PBPK models and software got the best of me. For that I will be eternally grateful.

I would also like to thank my initial committee members, Drs. George Dixon and John Hicks for their advice and input at the planning stages, and my statistics advisor, Dr. Hugh Chipman, for his tireless patience in my attempts to come up with reasonable statistical tests to evaluate the relative validity of the various models, when faced with relatively small data sets of environmental and experimental information.

Douglas Skinner and other researchers at Westworth Associates Environmental Limited provided invaluable advice on BOVAR's environmental monitoring program and the terrestrial receptor biology and behaviour. Dr. Frank F. Mallory, of the Department of Biology at Laurentian University, provided essential tissue-specific information on the Gapper's red-backed vole. Dr. Victor Clulow, Dr. Mallory's collegue at Laurentian University, also provided suggestions with respect to obtaining field-derived data on red-backed voles. I would also like to thank Dr. Xiaofeng Wang at InnaPhase Corporation for his help with the low-level working of the original Wang *et al.* (1997) PBPK model, Dr. Marina Evans at U.S. EPA's National Health and Environmental Effects Research Laboratory for providing the source code to the Evans and Andersen (2000) equilibrium model, and Dr. Stephen Safe at Texas A&M University for his insights into PCDD/F congener-specific Ah binding kinetics.

The current research project was wholly funded through industrial grants provided by BOVAR Waste Management Limited and Cantox Environmental Inc. BOVAR also provided the full monitoring data set and associated information, with technical support being provided by both BOVAR and Cantox Environmental Inc. It is very encouraging to see the continued high level of support from industrial partners into methodological research in the field of environmental risk assessment.

Finally, I would especially like to thank my family and friends who have always been there to provide the love and encouragement that helped me make my way through the long process that is a doctoral degree. It has been a long road ... but one well worth traveling.

ABSTRACT

The current study characterizes the principal uncertainties surrounding the application of environmental models in the assessment of potential health risks related to dioxin emissions from a PCB incineration facility. The objectives of the current research involved: (1) the empirical characterization and preliminary validation of computer-based models used for exposure assessment and toxicological assessment; (2) characterization of the potential environmental consequences from ambient exposure to bioaccumulative chemicals; and (3) improved scientific support for risk management decisions concerning such industrial activities.

Based upon model specifications from the scientific literature, a physiologically-based pharmacokinetic (PBPK) model was adapted and revised to characterize the dispositional kinetics of the key polychlorinated dibenzo-*p*-dioxin and dibenzofuran congeners (*i.e.*, 2,3,7,8-tetrachlorodibenzo-*p*-dioxin [TCDD], 2,3,7,8-tetrachlorodibenzofuran, 1,2,3,7,8-pentachlorodibenzofuran, and 2,3,4,7,8-pentachlorodibenzofuran) in the Sprague-Dawley rat (*Rattus norvegicus*) laboratory species and the Gapper's red-backed vole (*Clethrionomys gapperi*) sentinel species.

Results of the current application of the PBPK model developed for the vole sentinel species indicated that the revised model appears to provide a reasonably accurate estimation of chemical-specific disposition and elimination patterns. Furthermore, model results suggest that the internationally established methodology for Toxic Equivalency Factors (TEFs) may overestimate the apparent toxicity of the 2,3,4,7,8-PeCDF congener in relation to TCDD in the red-backed vole. Given that the 2,3,4,7,8-PeCDF congener represents the preponderance of the mass- and TEF-based concentration of dioxin/furan congeners measured in biota near incineration facilities, a systematic over-estimation of the TEF for this congener would have significant impacts on the outcome of an environmental risk assessment, based upon the red-backed vole as a sentinel species.

TABLE OF CONTENTS

Page

ACKNOWLEDGMENTS iv

ABSTRACT vi

TABLE OF CONTENTS vii

LIST OF FIGURES ix

LIST OF TABLES xiv

1.0 INTRODUCTION 1
1.1 Research Objectives 7

2.0 BACKGROUND 10
2.1 Environmental Monitoring Program at Swan Hills Treatment Centre 12
2.2 Biological Receptors 16
2.2.1 The Gapper's Red-backed vole (Clethrionomys gapperi) 17
2.2.2 Labrador Tea (Ledum groenlandicum) 20
2.2.3 Live Moss 22
2.3 Criteria Chemicals 22
2.3.1 Polychlorinated Dibenzo-p-dioxins and Dibenzofurans (Dioxins and Furans) 23
2.4 Environmental Properties and Fate of Criteria Chemicals 40

3.0 PHYSIOLOGICALLY-BASED PHARMACOKINETIC (PBPK) MODELLING OF POLYCHLORINATED DIOXINS AND FURANS 43
3.1 Introduction 43
3.2 Overview of PBPK Modelling 44
3.3 Physiologically-Based Pharmacokinetic Modelling of Dioxin Exposures 49
3.2 Evaluation of Uncertainty Inherent in PBPK Model Methodologies 58
3.2.1 Overview of Model Uncertainty and Variability 58
3.2.2 Application of Sensitivity Analyses 59
3.2.3 Techniques for the Evaluation of Uncertainty and Sensitivity 60
3.2.4 Application of Validation to Environmental Models 61

4.0 METHODOLOGY 64
4.1 Gathering of Field Monitoring Data 64
4.1.1 Objective Overview 64
4.1.2 Environmental Sampling of PCDD/F Concentrations 65
4.1.3 Collation and Selection of SHTC Monitoring Data 65
4.1.4 Data Cleanup and Quality Assurance/Quality Control 68

Page

4.2 Development of TCDD PBPK Prototype Models 68
4.2.1 Steady- State PBPK Model 69
4.2.2 Equilibrium-Based Model 94
4.3 Congener-Specific PBPK Modelling of Test Organisms 100
4.3.1 Time-Series Modelling of Congener-Specific Deposition Patterns 100

5.0 RESULTS 102
5.1 Summary of Field-Monitoring Results 102
5.1.1 Temporal Congener-Specific Biota Concentrations 102
5.1.2 Estimated Congener-Specific Consumption Rates for Red-backed voles 115
5.2 Validation of Prototype Steady-State PBPK Model 116
5.2.1 Comparison of Modelled Results versus Wang et al. (1997) Graphs 116
5.2.2 Comparison of Experimental versus Modelled Disposition Results ... 122
5.2.3 Sensitivity Analysis of Prototype Steady-State PBPK Model 130
5.3 Validation of Prototype Equilibrium-based Model 136
5.2.1 Comparison of Modelled Results versus Evans and Andersen (2000) Graph 137
5.2.2 Comparison of Steady-State versus Equilibrium-based Model 139
5.3 Dose-Dependent Application of PBPK Model 143

6.0 DISCUSSION 174
6.1 Modelling Issues 174
6.2 Empirical Issues 182
6.3 Application Issues 189

7.0 CONCLUSIONS 200

8.0 REFERENCES 203

APPENDIX A Detailed Overview of Mathematical Equations used in Prototype PBPK Models

APPENDIX B Detailed Results of Sensitivity Analyses of PBPK Model System

LIST OF FIGURES

Page

Figure 1.1 Progression of Potential Chemical Impacts on Biological Systems from Exposure to Disease (NRC, 1989) 3

Figure 1.2 The roles of physiologically based pharmacokinetic and pharmacodynamic modelling in a refined health risk assessment paradigm (Leung and Paustenbach, 1995) 4

Figure 2.1 Photograph of the primary Kiln Incinerator at the SHTC Facility 11

Figure 2.2 Map of Alberta Depicting the Relative Position of the Town of Swan Hills and the Swan Hills Treatment Centre (SHTC) 14

Figure 2.3 Localized Map Depicting Relative Locations of each Monitoring Program Sampling Sites (AGRA, 1997) 15

Figure 2.4 The Red-backed Vole, *Clethrionomys gapperi* (Erwin, 2000) 18

Figure 2.5 North American Dispersion Pattern for *Clethrionomys gapperi* (Hall, 1981) ... 19

Figure 2.6 Photograph of Labrador Tea and Other Commonly Prevalent Plant Species found in the Sampling Plot Understoreys 21

Figure 2.7 Generic structural diagram of the PCDD and PCDF chemical families, as well as the specific TCDD and TCDF congeners 24

Figure 2.8 Proposed Ah-Receptor Mediated Mechanism of Action for Dioxin-like Exposures (adapted from Hu and Bunce, 1999 and Santostefano *et al.*, 1998) .. 30

Figure 3.1 Overview of sequence of events following chemical exposure (Hoang, 1995) .. 46

Figure 3.2 A schematic representation of a steady-state based PBPK model for TCDD (Wang *et al.*, 1997) 51

Figure 3.3 A schematic representation of an equilibrium-based model for TCDD (Evans and Andersen, 2000) 56

Figure 4.1 Screenshot of TCDD PBPK Model developed in the ACSL Modelling System 70

Figure 4.2 Example of TCDD Tissue Concentration Fluctuations in Model Predictions at Low Administered Doses 71

Page

Figure 4.3 Scenario-specific Data Entry for Excel-Based Interface to the Prototype PBPK Model 74

Figure 4.4 Chemical-specific Data Entry for Excel-Based Interface to the Prototype PBPK Model 74

Figure 4.5 Species-specific Data Entry for Excel-Based Interface to the Prototype PBPK Model 75

Figure 4.6 Interactive Model Run Results Displayed in Excel-Based Interface to Prototype PBPK Model 75

Figure 4.7 Overview of PBPK Model Results Displayed in Excel-Based Interface to Prototype PBPK Model 76

Figure 4.8 Receptor Binding Run Results Displayed in Excel-Based Interface to Prototype PBPK Model 76

Figure 4.9 Screenshot of equilibrium-based model developed based upon Evans and Andersen (2000) 95

Figure 5.1 SHTC Congener-Specific PCDD/F Disposition Pattern in Biological Samples from Fall 1996 at Site 11 106

Figure 5.2 SHTC Congener-Specific PCDD/F Disposition Pattern in Biological Samples from Winter 1996 at Site 11 106

Figure 5.3 SHTC Congener-Specific PCDD/F Disposition Pattern in Biological Samples from Summer 1996 at Site 107 107

Figure 5.4 SHTC Congener-Specific PCDD/F Disposition Pattern in Biological Samples from Winter 1996 at Site 107 107

Figure 5.5 SHTC Congener-Specific PCDD/F Disposition Pattern in Biological Samples from Fall 1996 at Site 114 108

Figure 5.6 SHTC Congener-Specific PCDD/F Disposition Pattern in Biological Samples from Winter 1996 at Site 114 108

Figure 5.7 Congener-Specific PCDD/F Mass and TEF-Adjusted Percentages for Red-backed Voles and Labrador Tea sampled at Site 107 during Summer 1996 (Pre-Incident) 112

Page

Figure 5.8 Congener-Specific PCDD/F Mass and TEF-Adjusted Percentages for Red-backed Voles and Labrador Tea sampled at Site 107 during Winter 1996 (Post-Incident) 112

Figure 5.9 Experimentally-derived TCDD concentrations in rats compared to curves describing model simulation results in accumulative tissue compartments (Wang *et al.*, 1997) 118

Figure 5.10 Comparison of experimental (Wang *et al.*, 1997) *versus* predicted (with reproduced model) TCDD timeseries tissue concentrations in various accumulative tissue compartments 118

Figure 5.11 Experimentally-derived TCDD concentrations in rats compared to curves describing model simulation results in non-accumulative tissue compartments (Wang *et al.*, 1997) 119

Figure 5.12 Comparison of experimental (Wang *et al.*, 1997) *versus* predicted (with reproduced model) TCDD timeseries tissue concentrations in various non-accumulative tissue compartments 119

Figure 5.13 Experimentally-derived TCDD concentrations in rats compared to curves describing model simulation results in accumulative tissue compartments, at early time points (Wang *et al.*, 1997) 120

Figure 5.14 Comparison of experimental (Wang *et al.*, 1997) *versus* predicted (with reproduced model) TCDD timeseries tissue concentrations in various accumulative tissue compartments, at early time points 120

Figure 5.15 Experimentally-derived TCDD concentrations in rats compared to curves describing model simulation results in non-accumulative tissue compartments, at early time points (Wang *et al.*, 1997) 121

Figure 5.16 Comparison of experimental (Wang *et al.*, 1997) *versus* modelled TCDD timeseries tissue concentrations in various non-accumulative tissue compartments, at early time points 121

Figure 5.17 Comparison of experimental (with 95% confidence intervals) *versus* modelled liver and adipose tissue compartmental TCDD distribution 126

Figure 5.18 Comparison of experimental and modelled compartment-specific TCDD concentrations (% administered dose/gram) after oral administration of 25 µg/kg to C57BL/6J mice, 4-days post-treatment 128

Page

Figure 5.19 Comparison of experimental and modelled compartment-specific 4-PeCDF concentrations (% administered dose/gram) after oral administration of 300 μg/kg to C57BL/6J mice, 4-days post-treatment 129

Figure 5.20 Comparison of experimental and modelled compartment-specific 4-PeCDF concentrations (% administered dose/gram) after oral administration of 300 μg/kg to C57BL/6J mice, 4-days post-treatment (only lungs, kidneys, spleen and skin) 130

Figure 5.21 Comparison of contribution of variance (%) for key parameter groups at each administered dose level, 8-hours after exposure 132

Figure 5.22 Comparison of contribution of variance (%) for key parameter groups at each administered dose level, 24-hours after exposure 132

Figure 5.23 Comparison of contribution of variance (%) for key parameter groups at each administered dose level, 72-hours after exposure 133

Figure 5.24 Simulation results for the liver fraction (FH) presented in Evans and Andersen (2000) 138

Figure 5.25 Reproduction of dose-dependency curve based on original Evans and Andersen (2000) methodology 138

Figure 5.26 Reproduction of dose-dependency curve using both the original and corrected Evans and Andersen (2000) methodology 139

Figure 5.27 Graphical plot of time-series chemical concentrations in the liver and fat compartments following a 10 μg/kg bodyweight dose, using the steady-state PBPK model with excretion eliminated 140

Figure 5.28 Graphical plot of time-series chemical concentrations in the liver and fat compartments following a 0.01 μg/kg bodyweight dose, using the steady-state PBPK model with excretion eliminated 140

Figure 5.29 Modelled red-backed vole time-series whole body concentration results for each assessed PCDD/F congener for an administered dose of 0.001 μg/kg ... 163

Figure 5.30 Modelled red-backed vole time-series liver-to-fat ratios for each assessed PCDD/F congener for an administered dose of 0.001 μg/kg 163

Figure 5.31 Modelled red-backed vole time-series whole body concentration results for each assessed PCDD/F congener for an administered dose of 0.01 μg/kg 164

Page

Figure 5.32 Modelled red-backed vole time-series liver-to-fat ratios for each assessed PCDD/F congener for an administered dose of 0.01 μg/kg 164

Figure 5.33 Modelled red-backed vole time-series whole body concentration results for each assessed PCDD/F congener for an administered dose of 0.1 μg/kg 165

Figure 5.34 Modelled red-backed vole time-series liver-to-fat ratios for each assessed PCDD/F congener for an administered dose of 0.1 μg/kg 165

Figure 5.35 Modelled red-backed vole time-series whole body concentration results for each assessed PCDD/F congener for an administered dose of 1 μg/kg 166

Figure 5.36 Modelled red-backed vole time-series liver-to-fat ratios for each assessed PCDD/F congener for an administered dose of 1 μg/kg 166

Figure 5.37 Modelled red-backed vole time-series whole body concentration results for each assessed PCDD/F congener for an administered dose of 10 μg/kg 167

Figure 5.38 Modelled red-backed vole time-series liver-to-fat ratios for each assessed PCDD/F congener for an administered dose of 10 μg/kg 167

Figure 5.39 Modelled red-backed vole time-series whole body concentration results for each assessed PCDD/F congener for an administered dose of 100 μg/kg 168

Figure 5.40 Modelled red-backed vole time-series liver-to-fat ratios for each assessed PCDD/F congener for an administered dose of 100 μg/kg 168

Figure 5.41 Congener-specific liver-to-fat ratios for various administered doses (μg/kg bodyweight) for the Sprague-Dawley rat after 24 hours 169

Figure 5.42 Congener-specific liver-to-fat ratios for various administered doses (μg/kg bodyweight) for the red-backed vole after 24 hours 169

Figure 5.43 Congener-specific CYP1A2 fold induction for various administered doses (μg/kg bodyweight) for the Sprague-Dawley rat after 24 hours 170

Figure 5.44 Congener-specific CYP1A2 fold induction for various administered doses (μg/kg bodyweight) for the red-backed vole after 24 hours 170

LIST OF TABLES

Page

Table 2.1 Various Toxic Equivalency Factors (TEFs) Schemes Recommended for Mammalian Risk Assessments (Van den Berg *et al.*, 1998) 39

Table 3.1 Sprague-Dawley Rat Physiological Parameters used in TCDD Equilibrium-Based PBPK Model (Wang *et al.*, 1997) 53

Table 3.2 Sprague-Dawley Rat Physiological Parameters used in TCDD Steady-State PBPK Model (Evans and Andersen, 2000) 57

Table 4.1 Overview of Red-Backed Voles Bodyweights Sampled as part of the SHTC Monitoring Program between June 1995 and June1998 66

Table 4.2 Available PCDD/F Congener-Specific Data in Vole Receptors for Specific Exposure Impact Periods 67

Table 4.3 Available PCDD/F Congener-Specific Data in Labrador Tea for Specific Exposure Periods 67

Table 4.4 Available PCDD/F Congener-Specific Data in Moss Samples for Specific Exposure Periods 67

Table 4.5 Summary of Parameter Revisions made to Better Fit the Prototype PBPK Model to C57BL/6J Mice Experimental Results (Diliberto *et al.*, 1999) 78

Table 4.6 Red-backed Vole Summary Organ Weights (Mallory, 2001) 79

Table 4.7 PBPK Physiological Parameters Selected for each Test Species 80

Table 4.8 Specific parameters used in the calculation of congener-specific lipophilicity adjustments 84

Table 4.9 Chemical-specific dissociation constants and calculated adjustment factors for Ah receptor affinity 87

Table 4.10 Chemical-specific dissociation constants and calculated adjustment factors for CYP1A2 receptor affinity 89

Table 4.11 Congener-Specific Fecal Excretion Half-Lives and Calculated Adjustment Factor 91

Table 4.12 Default physiological parameters specified for the equilibrium-based model by Evans and Andersen (2000) 98

		Page
Table 5.1	PCDD/F Congener Concentrations (ppt) in Various Environmental Media at Monitoring Site 11	103
Table 5.2	PCDD/F Congener Concentrations (ppt) in Various Environmental Media at Monitoring Site 107	104
Table 5.3	PCDD/F Congener Concentrations (ppt) in Various Environmental Media at Monitoring Site 114	105
Table 5.4	Congener-Specific PCDD/F Mass and TEF-Adjusted[a] Concentrations (ppt) and their Relative Overall Percentages for the Vole and Labrador Tea Samples taken at each Key Monitoring Site during Summer and Winter 1996	108
Table 5.5	Calculated Vole-to-Plant Bioaccumulation Factors (BAFs) for Site 11	113
Table 5.6	Calculated Vole-to-Plant Bioaccumulation Factors (BAFs) for Site 107	114
Table 5.7	Calculated Vole-to-Plant Bioaccumulation Factors (BAFs) for Site 114	115
Table 5.8	Summary of Highest Biota Concentrations Measured during Winter 1996 for the Key Congeners, and Related Estimated Daily Intakes	116
Table 5.9	Comparison of experimental and modelled compartment-specific time course distribution of TCDD (% administered dose/g) after oral administration to Sprague-Dawley rats	122
Table 5.10	Evaluation of Time Course Compartment-Specific Concentration (% Administered Dose/Gram) for Modelled *versus* Experimental Data.	124
Table 5.11	Comparison of experimental and modelled compartment-specific time course distribution of TCDD (% administered dose/g) after oral administration to C57BL/6J mice, 4-days Post-treatment	127
Table 5.12	Comparison of experimental and modelled compartment-specific time course distribution of 4-PeCDF (% administered dose/g) after oral administration to C57BL/6J mice, 4-days Post-treatment	128
Table 5.13	Sensitivity Analysis of Contribution to Variance between TCDD PBPK Model Variables and Sequestration Outcome for Specific Parameter Groups[a] the Sprague-Dawley Rat	131
Table 5.14	Top 15 Physiological Parameters by Contribution to Variance to TCDD Disposition, 24-Hours at each Administered Dose Level	135

		Page
Table 5.15	Comparison of steady-state results of the three assessed models of TCDD disposition in the Sprague-Dawley Rat	141
Table 5.16	Revised parameters used in the updated equilibrium-based model	142
Table 5.17	Comparison of steady-state results with an updated version of the equilibrium-based model of TCDD disposition in the Sprague-Dawley Rat	142
Table 5.18	Time-Series Dose-Dependent Modelled Disposition of TCDD for the Sprague-Dawley Rat	145
Table 5.19	Time-Series Dose-Dependent Modelled Disposition of TCDF for the Sprague-Dawley Rat	147
Table 5.20	Time-Series Dose-Dependent Modelled Disposition of 1-PeCDF for the Sprague-Dawley Rat	149
Table 5.21	Time-Series Dose-Dependent Modelled Disposition of 4-PeCDF for the Sprague-Dawley Rat	151
Table 5.22	Time-Series Dose-Dependent Modelled Disposition of TCDD for the Gapper's Red-Backed Vole	153
Table 5.23	Time-Series Dose-Dependent Modelled Disposition of TCDF for the Gapper's Red-Backed Vole	155
Table 5.24	Time-Series Dose-Dependent Modelled Disposition of 1-PeCDF for the Gapper's Red-Backed Vole	157
Table 5.25	Time-Series Dose-Dependent Modelled Disposition of 4-PeCDF for the Gapper's Red-Backed Vole	159
Table 5.26	Time-Series Modelled Disposition of each Assessed PCDD/F Congener for the Gapper's Red-Backed Vole, based upon Intake Rates at Site 107 following Emission Incident	161
Table 5.27	Comparison of Liver-To-Fat Ratios between TCDF, 1-PeCDF, and 4-PeCDF to that of TCDD for the Sprague-Dawley Rat and Gapper's Red-Backed Vole	171
Table 5.28	Dose-Specific Comparison of Modelled *versus* Measured Vole-to-Plant BAF values for each Assessed PCDD/F Congener	172
Table 5.29	Comparison of Congener-Specific to TCDD BAF values in based on Modelled and Environmental Data	173

Page

Table 6.1 Comparison of Prototype Models based upon Several Validity Criteria 180

Table 6.2 Overview of Log Octanol-Water Partition Coefficient Values for the key Dioxin and Furan Congeners 182

Table 6.3 Examples of Antagonistic Interactions of Halogenated Aromatic Hydrocarbons through Inhibition of TCDD or 3,3',4,4',5-PentaCB-induced Responses (Safe, 1998c) 191

1.0 INTRODUCTION

Inadvertent exposure to xenobiotic chemicals is an unavoidable consequence of living in an industrialized society. While the environment, and those organisms which dwell within it, has an incredible ability to absorb and neutralize the potential adverse impacts of released chemicals, often realization of the true impact these compounds have on biological systems comes too late to prevent adverse environmental effects. To this end, environmental modelling solutions are often used to provide an early warning of the potential impact of chemicals on human health and ecosystem integrity -- either to evaluate the acceptability of various human activities, or to develop acceptable mitigation approaches for existing problems arising from human activities (e.g., rezoning, pathway-specific cleanup, *etc.*).

Typically, the goal of environmental risk analysis is to develop methods of assessing the risk of adverse health effects from exposure to toxic chemicals, as an initial step in prioritizing and managing the risk. To be effective as a tool in the decision-making process for assessing environmental health risks, exposure and toxicological assessment models must be "predictive" in nature, allowing a future projection of the potential for exposure, and consequent risk to human and ecosystem health, arising from a given exposure scenario. These assessment models typically use "sentinel" monitoring species as indicators of potential early warnings of risk to the surrounding ecosystems (*i.e.*, canaries in a mineshaft). While these models are constructed using the best available knowledge in the areas of environmental fate, toxicology, pharmacology, and environmental health risk assessment as a whole, they are simplistic representations of natural processes that are incompletely understood.

Consequently, to improve the usefulness and confidence of decision makers in the predictions of environmental health risk models, it is imperative that they be validated to "test" their predictive abilities in real-world scenarios. As the scientific underpinnings of environmental processes increase, the intricate components of environmental models will be tested by researchers and subsequently modified to improve their reliability in predicting human health risks. However, in the short term, more empirical testing approaches are needed to provide decision makers with greater confidence in using environmental exposure assessment models in arriving at

management solutions for immediate health problems. This philosophy provides the basis for conducting the investigations proposed in this research study.

The process of assessing the health risks associated with human exposure to toxic environmental chemicals inevitably relies on a number of assumptions, estimates, and rationalizations. Adverse impacts due to environmental contamination typically occur as a result of a sequence of events, beginning with the initial release of a contaminant from a specific source into the environment, movement *via* environmental fate and transport, accumulation in microenvironments, uptake by human and ecological receptors, biological transport to sensitive tissues/sites within the organisms, and ultimately resulting in a dose-response within the organisms expressing an adverse effect (Lioy, 1995).

Some of the greatest challenges for toxicological assessments result from the necessity to extrapolate outside the range of conditions found in experimental studies (Clewell III, 1995; Bailer and Dankovic, 1997). As such, due to the use of animal data as the basis of many human health risk assessments, the need for tools and techniques that address these dose and species extrapolation questions becomes a vital concern.

In the past, simple extrapolation approaches, such as allometric scaling, have been used to project from a test species to another species of concern. These approaches are rooted in the assumption that all biological and physiological processes are inherently similar in nature, and differ only relationally to the relative size of the species being evaluated. As such, it is possible to extrapolate from an experimental outcome from one species to another by simply adjusting the endpoint in question by a ratio of the body weights of the two species to a specific power. Thus, this can be expressed through the following:

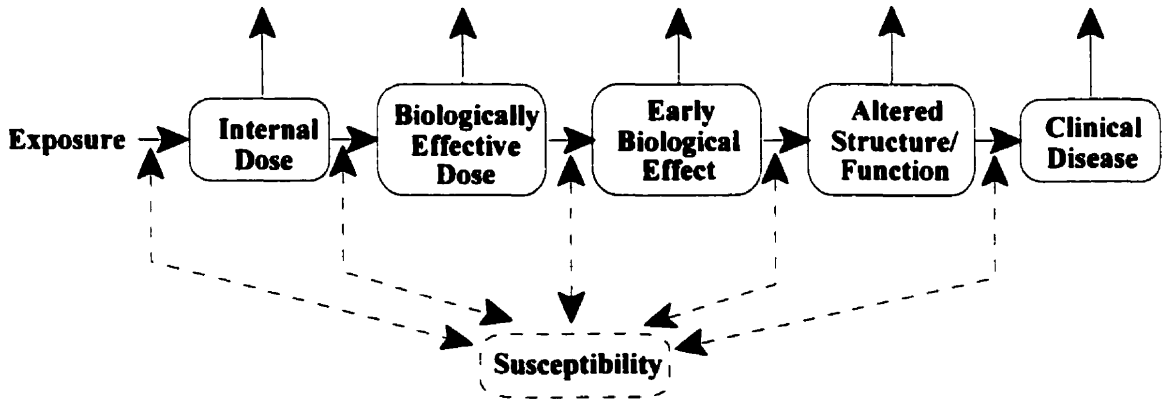
$$y = a\, w^b$$

where y is the variable in question, a is the allometric coefficient, and b is the allometric exponent. For example, the allometric relationship between blood circulation time (seconds) and total body weight (kilograms) has been expressed as $21\ w^{0.21}$, resulting in a blood circulation time of 15 seconds in a 250 gram rat and 50 seconds in a 70 kilogram human (Lin, 1998). While the simplicity of this approach makes it a useful technique, it does result in a considerable amount of

uncertainty due to its generic, empirical nature and lack of specification for the internal physiology of a given species of concern.

When evaluating the potential impact of chemical exposures to a species of concern, it is also very important to properly assess the transition from external exposure, or dose, to what is termed the *biologically effective dose* (see Figure 1.1). The biologically effective (equivalent) dose represents the actual concentration of chemical which reaches the target site within the organism, resulting in a specified biological effect or outcome (beneficial or detrimental). In the past, many simple models calculated potential health risks based upon the administered, or *external* dose. While more readily quantifiable (*i.e.*, ongoing ambient air monitoring programs), depending on the internal pharmacokinetics of the compound, very little of the external dose may actually result in a biological impact at a target tissue site. As such, actual quantification of the internal dose (*i.e.*, chemical concentration found in the tissues or blood), or preferably the biologically effective dose, would provide a better representation of the actual health risk posed by exposure to the chemical of concern. However, as internal dose typically depends on more than just the administered (or external) dose, using internal doses in risk assessment models generally requires a considerable increase in model complexity and specificity.

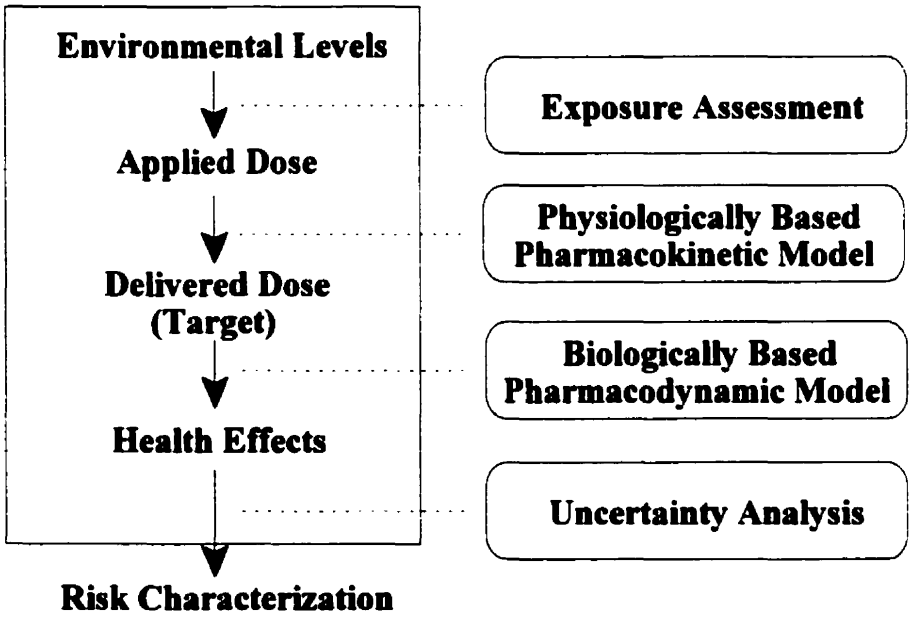
Figure 1.1 Progression of Potential Chemical Impacts on Biological Systems from Exposure to Disease (NRC, 1989).



Pharmacokinetic models are used to provide a functional relationship between external measures of chemical exposure and internal, target tissue measures of exposure to the actual toxic moiety. Pharmacokinetic models can provide a more appropriate basis for translating risk in animals to human risk and in some instances provide the ability to extrapolate between experimental doses/routes and potential human exposure patterns. The use of physiologically based pharmacokinetic (PBPK) modelling provides a scientifically attractive method of conducting this aspect of risk assessments.

The uptake and disposition of chemicals by living organisms, notably humans, has long been one of the primary concerns of toxicological research. The study of the disposition of chemicals in animal bodies falls under the field of pharmacokinetics. In broad terms, pharmacokinetics (PK) involves the study of absorption, distribution, metabolism, and excretion (ADME) of chemicals and their metabolites. Pharmacokinetics essentially provides the link between exposure analysis and toxicology, to provide a biologically-realistic evaluation of potential health risks (Figure 1.2).

Figure 1.2 The roles of physiologically based pharmacokinetic and pharmacodynamic modelling in a refined health risk assessment paradigm (Leung and Paustenbach, 1995)



The closely related subject of pharmacokinetic modelling is the process of developing mathematical descriptions for these critical biological processes. Due to their quantitative nature, PK models underwent considerable development for use in research by the drug and pharmaceutical industry. However, more recently applied pharmacokinetic research has also proved highly useful in describing the distributions of potentially toxic environmental chemicals, such as benzene, pentachlorophenol, pesticides, and their metabolites, within the body after inadvertent exposure.

From the late 1950's through the late 1970's, the majority of pharmacokinetic models described in the literature were variations of two, three or more compartments with a central pool representing the blood, with a number of secondary, peripheral compartments representing tissues, typically grouped into "slow" and "fast" equilibrating compartments (Roth *et al.*, 1995). These "classical" PK models represent the body as a system of homogenous compartments, which usually have no definite physiological or anatomical reality (Krishnan and Andersen, 1994; Klaassen and Rozman, 1991).

Within this "classical" model approach, the rate constants and concentrations describing the chemical, as well as the actual "topology" of the model itself (*i.e.*, the number and size of compartments and the interconnections between them) are dependent on the experimental data. As such, these models are also dependent on the chemical under study, the setup of the experiment, the route of exposure, and the dosing regime. Furthermore, while these data-based models can be used for interpolation under specific conditions, due to their inherent calibration to a specific experimental situation, they should not be used for extrapolation outside the range of doses, dose routes, and species used in the study on which they were based. As such, due to the lack of an authentic depiction of actual anatomical, physiological, and biochemical processes, these data-based compartmental models cannot easily be used in interspecies extrapolation, particularly to predict pharmacokinetic behaviour in humans (Krishnan and Andersen, 1994).

Given these limitations, the use of more biologically-based models incorporating pharmacokinetic and pharmacodynamic processes has become wide-spread over the past decade. The recent development of biologically-based models to describe the pharmacokinetics of

chemicals of concern such as 2,3,7,8-tetrachlorodibenzo-*p*-dioxin (TCDD) has provided insight into the various biological factors which influence the disposition, metabolism, and excretion of this compound and related, lipophilic xenobiotics (Buckley, 1995).

Physiologically based pharmacokinetic (PBPK) modelling is a powerful toxicological tool designed to convert an exposure, regardless of the applied route, into an ultimate target tissue dose. PBPK models are typically designed based upon known physiological processes (*e.g.*, blood flow rates, tissue volumes, breathing rates, *etc.*), on chemical-specific processes (*e.g.*, partition coefficients, chemical volatility, metabolic constants, molecular weight, *etc.*), and on species- and dose-dependent processes (due to non-linear kinetics), especially enzyme biotransformation. These models are also particularly well suited for evaluating the potential impacts of non-linearity (*e.g.*, threshold) in complex dose-response systems. Through the use of mechanisms, such as Hill or Michaelis-Menton kinetics, biological models representing the dose-dependent kinetics of a particular compound can be more accurately evaluated.

Thus, a detailed PBPK model can be developed and validated against the more readily available experimental animal data, and then extrapolated by computerized numerical simulation to predict concentrations of toxic compounds in the tissues of specific target organisms (*i.e.*, typically humans) following exposure. Through this physiologically-based process, risk assessors can avoid many of the uncertainties associated with interspecies differences between test (laboratory) animals and humans, and improve the predictive accuracy of human health and environmental risk assessments.

While providing a viable tool for the toxicological evaluation of chemicals, PBPK models do have a number of limitations. The major disadvantage of the use of PBPK modelling in quantitative risk assessment is that the measured parameters are often difficult to obtain and require knowledge of human metabolic processes that may be highly variable and difficult to assess (Klaasen and Eaton, 1991). For example, despite considerable study in recent years, many of the underlying metabolic processes within the liver (*i.e.*, specific P450 isomer binding efficiencies, potentially saturable pathways, *etc.*) remain unclear and subject to considerable uncertainty.

Other potential limitations to the use of PBPK modelling within a risk assessment include:

i) accuracy is lacking for individual dosing (*i.e.*, unlike laboratory studies, it is not always possible to accurately estimate chemical exposure doses for a specific individual outside such a controlled setting);

ii) despite the development of a number of commercial PBPK simulation packages, the mathematically complex equations are difficult for most toxicologists and clinicians to handle, and;

iii) physiological parameters are often poorly defined across species and strains, disease states, and the like, diminishing the accuracy of the predictions of this type of modelling (Klaassen and Rozman, 1991).

Nevertheless, despite these limitations, physiologically based toxicokinetic models have proven to be very useful investigative tools, and offer considerable opportunity for insights into the kinetics of xenobiotics beyond what can be provided by classical toxicokinetic methodologies.

1.1 Research Objectives

Using the extensive environmental monitoring database collated in conjunction with the operation of the Swan Hills Treatment Centre (a hazardous waste incineration facility) in Swan Hills, Alberta, the collected data will be used to attempt to characterize and validate environmental modelling methodologies for polychlorinated dioxins and furans. While polychlorinated biphenyls (PCBs) are also present in such an environment, their concentrations are not significantly elevated above the typical background levels encountered in regions such as western Canada, and therefore PCBs will not be addressed directly in this study.

The principal objectives of the research include: (1) the empirical characterization and preliminary validation of computer-based models used for exposure and toxicological (*i.e.*, PBPK modeling) assessment; (2) characterization of the potential health consequences related to

environmental exposure to bioaccumulative chemicals; and (3) improved scientific support for risk management decisions concerning such industrial activities.

Based upon the above methodological overview, the following are the key research aims and questions to be addressed through this doctoral research project. They are divided into three specific categories and follow a chronological order of implementation: a) modelling issues; b) empirical issues, and; c) application issues.

Modelling Issues

1. Evaluation of relative merits of simpler (*i.e.*, two-compartment or equilibrium-based) pharmacokinetic models *versus* complex (*i.e.*, multi-compartmental) PBPK models for the assessment of health risks related to environmental exposures to dioxins and furans;
2. Evaluation of the feasibility of using a PBPK model developed using laboratory rodents for use with the vole sentinel species (*i.e.*, availability of detailed physiological data for the vole receptors or adequate allometric methodologies to produce equivalent data for the appropriate biological receptor), and;
3. Discussion of the relative strengths and weaknesses of the selected PBPK model for dioxins and furans. Objective measures of model strength and weakness such as i) robustness, ii) sensitivity, iii) parsimony, and iv) explanatory value will be evaluated to provide a better indication of the potential uncertainty related to the application of this particular model design.

Empirical Issues

1. Evaluate the apparent empirical relationship between the octanol-water partitioning coefficient (log K_{ow}) and Bioaccumulation Factor (BAF) or Bioconcentration Factor (BCF) of dioxins and furans in the vole sentinel receptor;

2. Evaluate whether the Toxic Equivalency Factors (TEFs) for dioxins and furans provide a suitable surrogate for toxicity in the vole species, considering such parameters as chemical bioavailability, pharmacokinetic factors, and toxicodynamic equivalency, and;
3. Evaluate the "fractionation" characteristics of the dioxin/furan congener emission mixtures in both the environment and within the vole receptor, on a (i) mass ratio and (ii) TEQ ratio. More specifically, the relative congener and isomeric "fingerprint" breakdown of dioxin and furan concentrations present in both environmental (*e.g.*, water, soil, and sediment) and biological (*e.g.*, Labrador tea plants and voles) sinks are highly dependent upon a variety factors. For example, each specific congener group has differing physico-chemical properties, leading to differing physiological disposition, metabolism and ultimately toxicological impacts on biological receptors, such as the red-backed vole. These "fractionation" characteristics provide much of the basis for the TEQ methodology for evaluating the toxicity of individual dioxin-like congeners as an overall functional group.

Application Issues

1. Discuss the implications of research results on mammalian (both vole and human) risk assessments, and the applicability of laboratory developed TEF values under environmental conditions;
2. Using uncertainty analyses, evaluate the potential impacts of leverage variables on the PBPK model, and accordingly the results of a health assessment involving these variables, and;
3. Discuss the value of the results of the research as well as future empirical research needs.

The key empirical question for the current research study is whether it is feasible to use physiologically-based pharmacokinetic models with existing biological monitoring data to predict potential toxicological risk to human populations. Ultimately, this can only be answered by determining whether the Gapper's red-backed vole is a valid sentinel species to evaluate the pharmacokinetic and pharmacodynamic implications of environmental exposure to POPs, such as polychlorinated dibenzo-*p*-dioxins and furans.

2.0 BACKGROUND

Incineration, as a method for the permanent destruction of persistent hazardous wastes, has received significant concern from many environmental groups, members of the public, and, consequently, some governments. This opposition arose from public apprehensions related to quantities of chemicals in incinerator stack emissions, in some cases without consideration of the rates of exposure to the chemical emissions, how rates of exposure may compare to those from ambient background sources and the likelihood of adverse effects to human and/or ecological health from such exposures (Delzell *et al.*, 1994). Trace concentrations of a variety of chemicals remain following combustion even in properly designed and operated incinerators. These chemicals typically arise from two general sources: a) unburned organic constituents, metals and metallic chemicals, and residual ash (*i.e.*, bottom ash and fly ash), and; b) products of incomplete combustion (PICs) that are formed within the incinerator by the combination of atoms from dissociated molecules. Typically these emissions are thought to be well below levels at which human or environmental health risks would be evident. However, if the incinerator is not properly designed and/or operated, the concentrations of chemicals from these sources increase in the incinerator emissions and in the residual ash (Travis and Cook, 1989; Lee and Huffman, 1990; Acharya *et al.*, 1991; Delzell *et al.*, 1994), and could result in an elevated health risk.

Of particular concern with respect to the typical emission releases from incineration facilities are a group of bioaccumulative chemicals called *persistent organic pollutants* (POPs). This group of compounds is so-named due to its extreme stability in the environment, and long residency half-life within the fatty tissues of biological organisms. Perhaps the most important member of this group is the highly toxic compound, 2,3,7,8-tetrachlorodibenzo-*p*-dioxin (also widely referred to as TCDD or dioxin). TCDD belongs to the halogenated aromatic hydrocarbon family, which includes polychlorinated dibenzo-*p*-dioxins (PCDDs), dibenzofurans (PCDFs), biphenyls (PCBs), and naphthalenes (PCNs) (Safe, 1986). They are well known as environmental contaminants due to the extreme toxic potency of some members of the family, the wide variety of their toxic responses, and their ubiquitous presence within both biological organisms and the environment, as a whole (Safe, 1986). Given the high level of concern related to potential emissions of these persistent compounds, significant importance is typically placed on the

monitoring of both emissions and biota (both plant and animal) concentrations of these compounds in the area surrounding incineration facilities.

The Swan Hills Treatment Centre (SHTC), operated by BOVAR Waste Management Limited, is Canada's only permanent, large-scale incinerator facility capable of destroying hazardous wastes such as environmentally persistent polychlorinated biphenyls (PCBs). It is located approximately 12 kilometres northeast of the Town of Swan Hills (approximately 200 kilometres northwest of Edmonton), Alberta, and has been in operation since 1987. To the end of 1996, 143,000 tonnes of hazardous waste material, including 20,225 tonnes of PCBs, have been processed and destroyed at this facility. The normal destruction of these hazardous waste materials results in the controlled air emissions of waste gases from the facility's incinerators, transformer furnace, and other sources on the plant site.

Figure 2.1 Photograph of the primary Kiln Incinerator at the SHTC Facility



A comprehensive monitoring program to provide environmental indicators of the performance of the SHTC has been in place since 1985, before the facility was operational. The current program includes ambient air, surface water, ground water, soils, vegetation, aquatic resources and wildlife indicator studies. This monitoring data has demonstrated that concentrations of PCBs, dioxins and furans in the environment were relatively stable at most monitoring locations through 1995, but showed increases at some locations from 1995 to 1996, largely attributed to fugitive emissions.

However, environmental concentrations of PCBs, dioxins and furans increased significantly around the SHTC following an accidental release from the transformer furnace of the C.E. Raymond incinerator in mid-October 1996. The release was the result of the mechanical failure of an isolation flange and expansion joint that separated process gases from the flue gas duct. A stack emission survey being conducted at the time in the transformer furnace later showed that approximately 4.2 kilograms of total PCBs and 3.4 grams TEQ (toxic equivalent) of dioxins and furans were released over the estimated 8-hour duration of the incident (CanTox, 1998). A detailed investigation of this event and statistical evaluation of potential congener-specific "fingerprints" related to normal and incident-related emissions from the SHTC was conducted for the candidate's Masters thesis work (Ferguson, 1998).

The resulting elevated concentrations of both dioxins and furans in the environmental biota in the area surrounding the facility following the incident provide an excellent temporal "sign post" by which to attempt to evaluate the short-term disposition impact of PCDD/PCDF concentrations in vole sentinel species.

2.1 Environmental Monitoring Program at Swan Hills Treatment Centre

The Swan Hills site for the Treatment Centre was selected in 1985 following studies to determine the suitability of a number of potential sites in various regions and public consultations with local residents. The following features contributed to the overall environmental acceptability of the site: i) thick clay soils providing a relatively impervious site; ii) location remote from population centres; iii) good access route; iv) central provincial location; and v) lack of land use conflict

(*e.g.*, agriculture). The Treatment Centre is located on 130 ha of land owned by BOVAR Waste Management Limited. In addition, it is surrounded by 0.8 km development exclusion zone (Chem-Security, 1991). Construction of the Treatment Centre began in March of 1985, and it was officially opened September 11, 1987. In the winter of 1993-1994, a new rotary kiln was added to the facility, which increased its capacity by 35,000 tonnes/year.

A comprehensive environmental monitoring program was initiated in the vicinity of the SHTC in 1985, prior to the initiation of plant operations (a year after the siting of the facility was finalized). Baseline data were collected over a two-year period prior to the Treatment Centre's operation. The baseline monitoring provided an unique opportunity to establish existing environmental conditions in the vicinity of the plant site. In addition to environmental monitoring, the program also included incoming waste assessment, personnel sampling, health surveillance, industrial hygiene and plant boundary air quality monitoring (Chem-Security, 1991).

The current monitoring program includes ambient air, surface water, ground water, soils, vegetation, aquatic resources and wildlife indicator studies. The program has been modified on several occasions since 1987 in response to changes in monitoring priorities. These modifications have involved the consolidation of some monitoring sites and the addition of others (Penner, 1994; Westworth, 1997). The normal monitoring program was also expanded following a release incident in 1996 to address concerns raised by the Alberta Department of Health, Department of the Environment, residents of the Town of Swan Hills, and nearby Indian band councils.

Figure 2.3 provides a site map of the SHTC, indicating the relative positions of each key monitoring location, both near the facility (*i.e.*, sites 11, 107, and 144) and in what would be termed "background" locations (*i.e.*, sites 70 and 71).

Figure 2.2 **Map of Alberta Depicting the Relative Position of the Town of Swan Hills and the Swan Hills Treatment Centre (SHTC)**

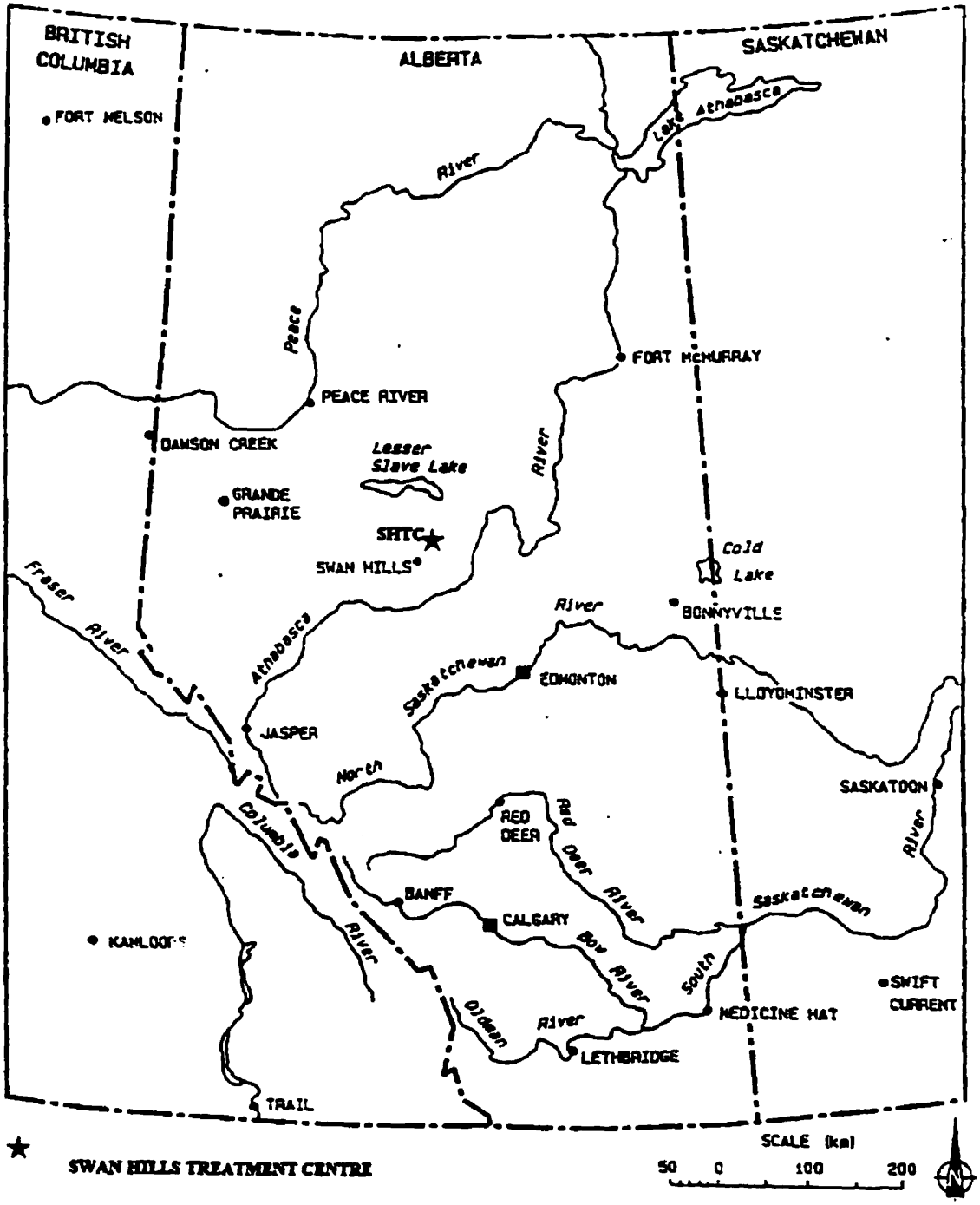
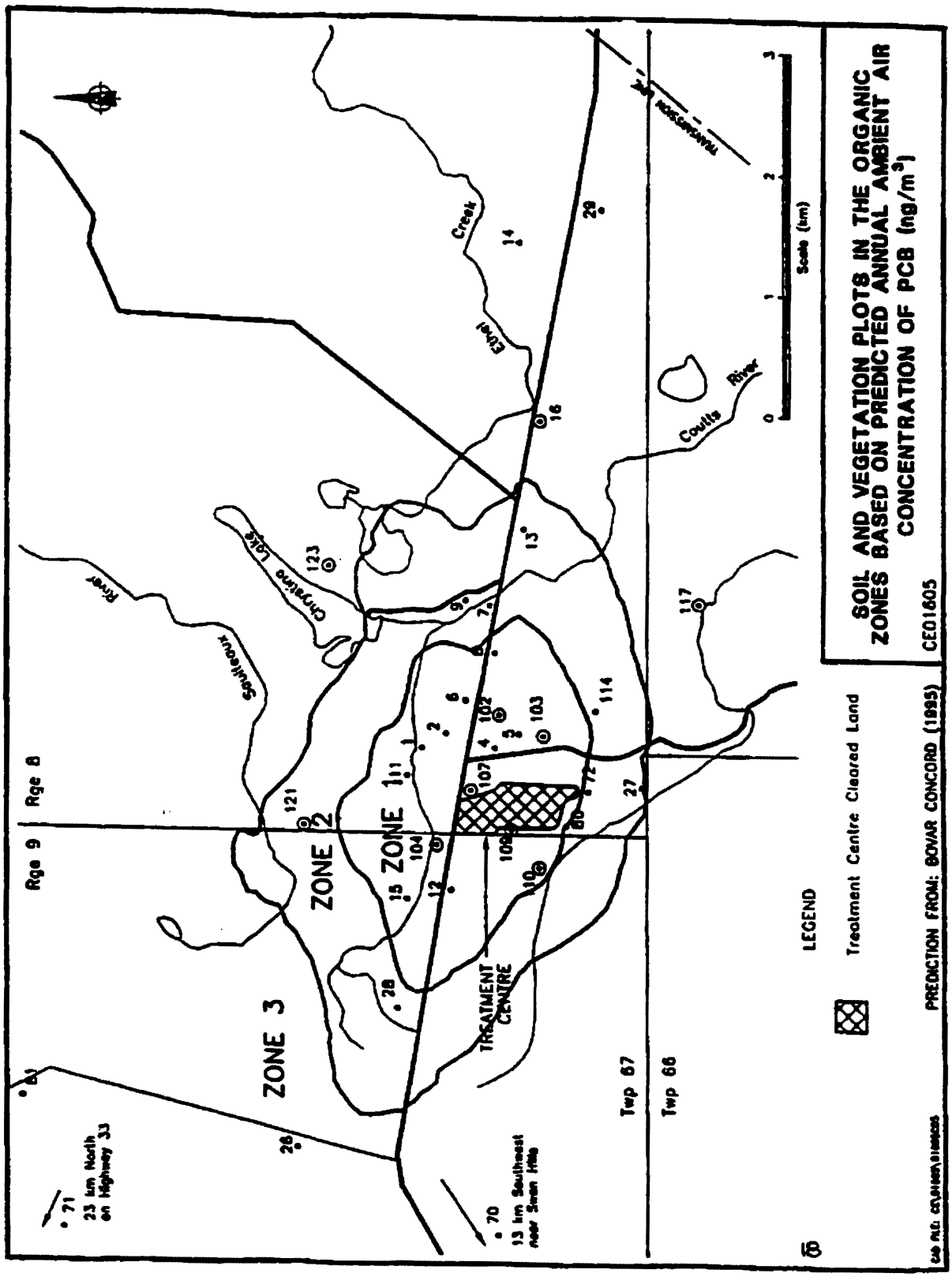


Figure 2.3 **Localized Map Depicting Relative Locations of each Monitoring Program Sampling Sites (AGRA, 1997)**



The small mammal population monitoring program involved two annual livetrapping sessions, a spring/summer session, which was conducted in June, and a fall session, which was conducted in September. During each session, population monitoring was conducted on 15 livetrapping plots, each approximately 1.1 hectares in area. Each plot consisted of 48 trapping stations spaced at 15 metre intervals in a 7 by 7 sampling grid (Westworth, 1998). Animals were also collected for the analysis of tissue chemistry in two snap-trapping sessions annually (in February and June) by SHTC consultants. It is the results of these sampling sessions which will be used to evaluate potential red-backed vole dioxin and furan body burden concentrations.

The vegetation monitoring program typically involved two annual sampling sessions, a winter session, which was conducted in February, and a fall session, which was conducted in September. Additional sampling was also conducted in November of 1996 to assess potential deposition and surficial concentrations arising from emissions during the October 1996 incident. As part of this sampling program, Labrador tea shrubs were sampled at 21 plots and analyzed for a suite of chemical parameters. Lesser amounts of wildlife browse, lichen and moss, and berries were also sampled as part of the program (AGRA, 1997).

2.2 Biological Receptors

As noted previously, the ongoing environmental monitoring program includes ambient air, surface water, ground water, soils, vegetation, aquatic resources and wildlife indicator studies. The selection of wildlife receptors for the ongoing assessment of SHTC facility emissions was based upon a combination of factors, which included: i) the availability of long-term monitoring data; ii) trophic level; iii) year-round residency in the study area, and; iv) the likelihood of being consumed or handled by humans (Chem-Security, 1999).

For the purpose of the current study, two biological indicator species were initially selected as the most appropriate receptors to evaluate: i) the Gapper's red-backed vole (*Clethrionomys gapperi*), and ii) Labrador tea (*Ledum groenlandicum*). Both selected receptor species have been historically sampled since the beginning of the environmental monitoring program at all of the key sites surrounding the facility and in background locations. While historically not sampled as

consistently or extensively as the Labrador tea, monitoring data has also demonstrated that sampling data on live moss provided more accurate reflections of environmental concentrations immediately following the accidental release event. As such, these three species provide excellent biological indicators, on a historical basis, for relative dioxin and furan emissions for the incinerator facility into the surrounding environment.

2.2.1 The Gapper's Red-Backed Vole (Clethrionomys gapperi)

The Gapper's red-backed vole, a small rodent typically weighing approximately 16-42 grams, was chosen as the primary wildlife indicator species for the overall environmental monitoring program because of its relative abundance in the area and its sedentary nature, allowing information obtained to be related to specific locations in the study area. The red-backed vole also has a short life span and is easily trapped, making it an ideal sentinel species for the long-term monitoring study. The red-backed vole, which typically comprises over 90% of the animals captured during the small mammal monitoring program, is the most abundant small mammal in the Swan Hills Study area (Westworth, 1998).

The Gapper's red-backed vole (*Clethrionomys gapperi*) is a dark gray microtine rodent (*i.e.*, a member of the rodent subfamily Microtinae, sometimes called Arvicolinae) with a prominent rust-coloured dorsal stripe extending from the eyes to the tail, and a dark slate gray to almost white underbelly (see Figure 2.4). It's head and body length is typically 70-112 mm, with a short tail approximately 25-60 mm long. The fur is dense, long, and soft in the winter, but changes to shorter, coarser fur during the summer months. Males and females tend to be similar in size and colour, with the younger, immature voles tending to be darker than the adults (Hoffmeister, 1986; Ballenger, 1996).

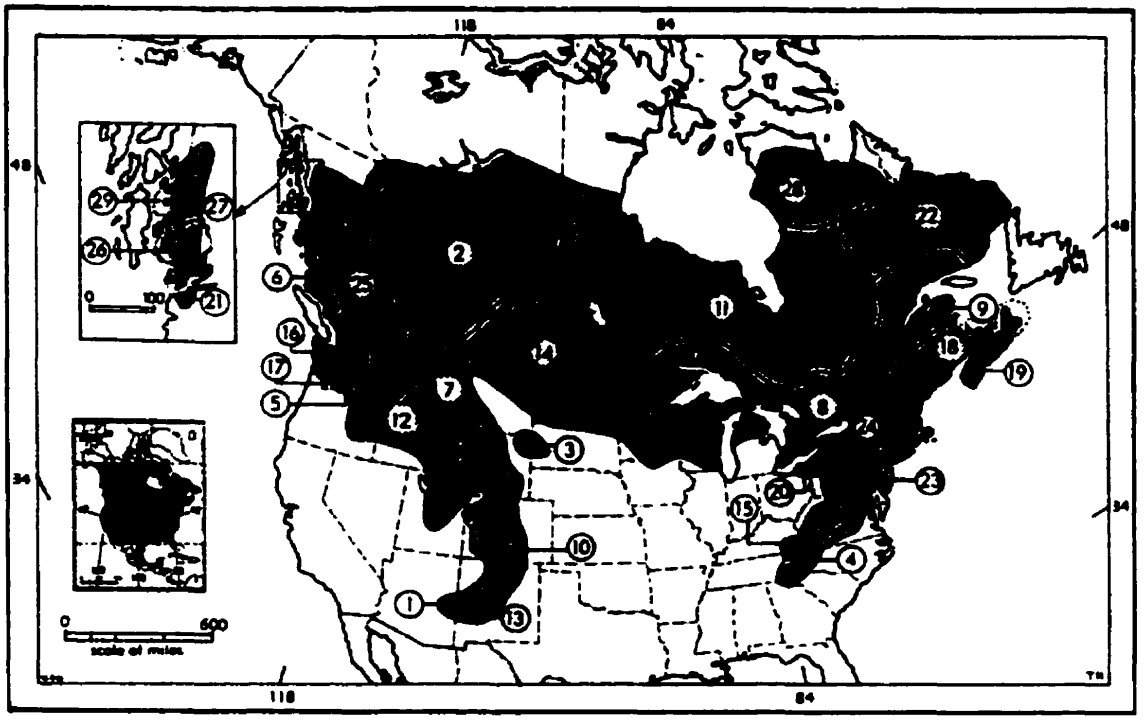
Figure 2.4 The Red-backed Vole, *Clethrionomys gapperi* (Erwin, 2000)



The habitat for red-backed voles range from British Columbia to Labrador and throughout the northern United States from the Rocky Mountains to the Appalachians (see Figure 2.5). They tend to inhabit cool, mossy and rocky boreal forests (typically coniferous, although deciduous or mixed forests are also accepted) in both dry and moist areas (Burt and Grossenheider, 1976; Nowak and Paradiso, 1983; Ballenger, 1996). Their nests are typically constructed under the roots of stumps, logs, or brush piles. The home range of the red-backed vole is about 1/4 acre (0.1 hectares). While populations of *C. gapperi* often fluctuate widely from year to year with no apparent periodicity, their numbers are fairly low with approximately 2-3 voles per acre, in favourable habitat (Ballenger, 1986).

During the SHTC monitoring program, vole density has fluctuated widely (6 to 35 voles/ha) with peak numbers occurring at 2 to 4 year intervals. Year-to-year variations in other demographic characteristics, such as the percentage of adult voles in breeding condition, age structure, sex ratios and survival rates, are fairly consistent and appear to be largely related to events associated with population cycling (Westworth, 1998).

Figure 2.5 North American Dispersion Pattern for *Clethrionomys gapperi* (Hall, 1981)



Guide to *Clethrionomys gapperi* Subspecies

1. *C. g. arizonensis*
2. *C. g. athabascae*
3. *C. g. brevicaudus*
4. *C. g. carolinensis*
5. *C. g. cascadensis*
6. *C. g. caurinus*
7. *C. g. galei*
8. *C. g. gapperi*
9. *C. g. gaspeanus*
10. *C. g. gauti*
11. *C. g. hudsonius*
12. *C. g. idahoensis*
13. *C. g. limitis*
14. *C. g. loringi*
15. *C. g. maurus*
16. *C. g. nivarius*
17. *C. g. occidentalis*
18. *C. g. ochaceus*
19. *C. g. pallescens*
20. *C. g. paludicola*
21. *C. g. phaeus*
22. *C. g. proteus*
23. *C. g. rhoadsii*
24. *C. g. rupicola*
25. *C. g. saturatus*
26. *C. g. solus*
27. *C. g. stikinensis*
28. *C. g. ungava*
29. *C. g. wrangeli*

Red-backed voles exhibit seasonal changes in food habits consume a variety of plant materials during the year. Field research has indicated a daily consumption rate of approximately 0.31 g/g/day (McManus, 1974). They tend to be opportunistic feeders and change their diet as the seasons progress. They tend to eat leaf petioles and young shoots in the spring, add fruits and berries to their diet in the summer, and then switch to nuts and seeds in the autumn months. While underground fungi also comprise an important part of the diet, especially in the fall, they also consume some bark, roots, lichens, and insects. They sometimes store food (*i.e.*, bulbs, stems, tubers, and nuts) in their nests for use in the winter when it becomes difficult to forage (Ballenger, 1986).

Red-backed voles are active night and day (more so during the night) year round (*i.e.*, they do not hibernate), staying close to fallen logs or rocks, and frequently travel through underground passages to reach their foraging areas. They are highly susceptible to predation. Their maximum longevity is approximately 20 months, but most individuals do not survive more than 10 to 12 months, due to predation and mortality during the winter months (Burt and Grossenheider, 1976; eNature, 2000; Ballenger, 1996).

Their young are born typically between March and October, with a litter size of averaging between 3 to 7 pups, depending on environmental conditions. Females are typically able to rear 2 or 3 litters per year, with breeding beginning as early as late winter and continuing into the late fall. The offspring are weaned at 17 to 16 days, with sexual maturity occurring at approximately 3 months of age (Burt and Grossenheider, 1979; Ballenger, 1986).

As the voles can live to about 12 to 18 months of age, and have very small foraging and habitat territories, they make excellent indicator species for an environmental monitoring study. The red-backed vole also represents a key species in avian and mammalian food chains in Alberta's boreal forests (Westworth, 1997).

2.2.2 Labrador Tea (Ledum groenlandicum)

The use of vascular plants is primarily an indirect and long-term technique to monitor airborne pollution. Research has demonstrated that the uptake of metal or organic-complexed particulates is primarily a function of the availability of the pollutant in the soil and secondarily a result of direct absorption by the leaves and the needles of the plant species (Martin and Coughtrey, 1992). The sampling of plant leaves is useful as it is a relatively inexpensive and simple method of monitoring the relative pattern and levels of stack-related releases from the incinerator facility.

Labrador tea is a small (up to 1 metre in height) evergreen shrub with green leaves and dense rusty hairs on its twigs. They are typically found in moist to wet forest and bogs in lowland and montane zones. They typically grow in wet, usually very acid and poor organic soils (Douglas *et al.*, 1990; Angove and Bancroft, 1983).

Figure 2.6 Photograph of Labrador Tea and Other Commonly Prevalent Plant Species found in the Sampling Plot Understoreys



Labrador tea leaves were chosen as the primary foliar analysis because of their abundance, ease of sampling and low susceptibility to trampling. Furthermore, the leaves represent an annual deposition because their leaves are retained through the year, including the winter months. While these plants are classified as evergreens, they do gradually exchange their leaves, typically on a yearly basis (generally in the late spring). As such, new leaves can be collected during the fall sampling period after a 3 to 4 month period of exposure. As there appears to be minimal translocation of PCBs and dioxin/furan compounds within the plant's vascular system, only the current years' accumulation of the assessed compound would likely be present in the leaves (Mahanty, 1990). Labrador tea is also viewed as an excellent receptor of airborne pollutants due to the fine hairs on the underside of the leaves which capture airborne contaminated particulate complexes (AGRA, 1997).

Based upon these characteristics, ambient chemical concentrations detected on the surface of the Labrador tea was deemed an acceptable conservative surrogate for ambient chemical concentrations found upon food sources utilized by the red-backed vole.

2.2.3 Live Moss

Vegetation data collected from near the SHTC indicates that, after an incident such as that in October 1996, PCBs, dioxins and furans tend to persist much longer in moss than in other vegetation, such as Labrador tea or browse. These compounds tend to accumulate in moss *via* both vapour uptake and particulate deposition. Prior to the accidental release in 1996, vegetative data indicated that there was no consistent difference between concentrations in moss and Labrador tea. However, for a number of years following the incident, concentrations in moss remained relatively high, particularly for dioxins and furans, while concentrations in Labrador tea and browse decreased significantly and rapidly (within one year) after a short-term peak following the incident (likely due to the annual turnover of exposed leaves) (Chem-Security, 1999).

As moss, particularly those that contain fungi, is a primary food of choice for the red-backed vole, use of the Labrador tea concentrations as a surrogate for the overall concentration in all food source may underestimate dietary exposures. As such, moss were also selected as an appropriate environmental indicator species for the current assessment.

2.3 Criteria Chemicals

The environmental monitoring program at the SHTC has historically monitored a large number of chemical compounds, both organic and inorganic. However, as the SHTC is primarily a PCB incineration facility, environmental concentrations of PCBs, dioxins and furans have always been of chief concern to all parties involved.

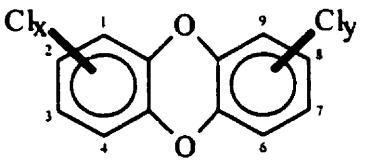
Both polychlorinated biphenyls (PCBs) and polychlorinated dibenzo-*p*-dioxins and dibenzofurans (PCDD/Fs) belong to a family of chemicals called halogenated aromatics, a group of environmental pollutants which have been identified worldwide in diverse environmental media (Safe, 1994; Environment Canada, 1997a;b). Due to their persistent (*i.e.*, bioaccumulative) nature and widespread distribution in the environment, they have been the subject of considerable study with respect to the hazards they pose to both humans and the environment, as a whole. As noted previously, this group of bioaccumulative chemicals, and others like them, have become known as *Persistent Organic Pollutants* (POPs).

2.3.1 Polychlorinated Dibenzo-p-dioxins and Dibenzofurans (Dioxins and Furans)

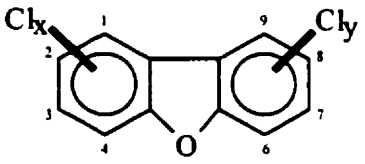
What are dioxins and furans?

2,3,7,8-Tetrachlorodibenzo-*p*-dioxin (TCDD) is the prototype for a family of chemicals which have the same mechanism of action, are structurally related, and induce a common spectrum of biochemical responses and adverse effects. The polychlorinated dibenzo-*p*-dioxins (PCDDs) and polychlorinated dibenzofurans (PCDFs) are structural homologues (see Figure 2.7), which produce a similar spectrum of biological and toxicological responses in living organisms, at varying degrees of potency. Chlorine substitution at the 2,3,7, and 8 position is generally considered necessary for dioxin-like behaviour, with TCDD representing the most potent and extensively studied of the PCDDs and PCDFs (Safe, 1986).

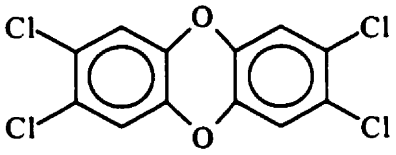
Figure 2.7 Generic structural diagrams of the PCDD and PCDF chemical families, as well as the specific TCDD and TCDF congeners.



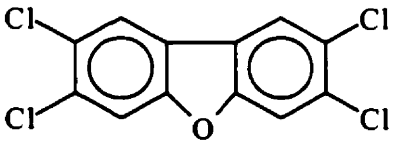
Polychlorinated dibenzo-p-dioxin



Polychlorinated dibenzofuran



2,3,7,8-tetrachlorodibenzo-p-dioxin



2,3,7,8-tetrachlorodibenzofuran

There are 75 chlorinated dibenzo-*p*-dioxins, ranging in degree of chlorination from the two monochlorinated congeners to the fully chlorinated octachlorodibenzo-*p*-dioxin congener. Similarly, there are 135 chlorinated dibenzofurans ranging in degree of chlorination from the four monochlorinated congeners to the fully chlorinated octachlorodibenzofuran congener. There is a wide range in the physical/chemical properties of chlorinated dioxins and furans both within isomeric groups and between congener families (Delzell *et al.*, 1994). Each of the dioxin and furan isomers are never found alone in either the environment or living tissue, but are typically found in mixture with other isomers at varying percentages depending on the source and environmental and biological degradation processes.

It is important to note that both dioxins and furans are not produced commercially. Rather, mixtures of specific congeners of these substances are released into the environment as contaminants or by-products associated with various anthropogenic activities and natural processes (*e.g.*, forest fires). Specifically, chlorinated dioxins and furans are formed during a variety of combustion processes, including the incineration of hazardous chemicals (*e.g.*, PCBs) and municipal waste incineration, although their concentrations are typically small in emissions of incinerators employing best-available technologies (BAT), such as the SHTC. They are also produced through the chlorine bleaching of paper and pulp products, production of certain

herbicides, metal smelting, and other industrial processes. As a result of this production, dioxins and furans are ubiquitously present at low concentrations in the environment in industrialized countries. Long-range airborne transport of these compounds has also resulted in their distribution to more pristine environments around the world (*i.e.*, the arctic).

As a result of their high lipid solubility and resistance to metabolic breakdown in biological systems, PCDD/Fs tend to bioaccumulate in the food chain, and ultimately end up in the human body where they can be detected in fatty tissues (*i.e.*, serum, adipose) and in mother's milk. Their presence has also been shown to change normal fat metabolism at higher doses, and result in decreased food consumption, wasting, hyperlipidemia, and fatty liver (Delzell *et al.*, 1994). As a result, TCDD has become a model compound for the pharmacokinetic study of transport of such chemicals between pools of lipid within biological systems (Roth *et al.*, 1994).

In broad terms, interactions between chemicals and living organisms in the environment typically initiate a chain of biological events within the organism which can lead to either beneficial (*i.e.*, pharmaceutical drugs) or harmful (*i.e.*, toxic compounds) impacts upon health. These interactions can be associated with direct "reactivity" with target molecules, or through the binding of the compound to specific biological receptors within the organism. In recent years, considerable effort has been made by the toxicological community to understand the potential interactions of chemicals with membrane-localized or cytoplasmic receptors (Andersen, 1995). Perhaps one of the best examples of this scientific research is the investigation of how PCDD/Fs, and some PCBs, interact at the pharmacokinetic (and pharmacodynamic) level with a cellular protein known as the aryl hydrocarbon *(Ah)* receptor.

The PBPK models proposed for PCBs, dioxins and furans, in recent years, are all rather similar. They typically involve five or six notional physiologic compartments (distinguished by their perfusion and tissue binding kinetics), consisting of the blood, slowly perfused tissues, and richly perfused tissues, with separate compartments for the principal target tissues: the fat and liver. However, it is how these compounds interact with the hepatocellular *Ah* protein receptor which determines their ultimate toxicological (pharmacodynamic) impacts on a given biological system.

The Toxicity of Dioxins and Furans

The toxicity of polychlorinated dioxins and furans differ markedly among species, as do their pharmacokinetics and disposition. The chlorinated dibenzodioxins and dibenzofurans tend to accumulate in the liver and adipose tissue, although considerable species and strain differences in their relative tissue distribution has been noted in the scientific literature (discussed in detail in the following section). This is likely due in part to differing binding tendencies (affinity) and efficacies to the *Ah* and other cellular receptor proteins, as well as basal levels of hepatic microsomal monooxygenases such as CYP1A2, in responsive and nonresponsive biological species (Krewski *et al.*, 1994).

The overt signs of toxicity in animals from exposures to chlorinated dioxins and furans are characterized by a general wasting syndrome, with an overall loss in body weight, even though food consumption is normal. These effects are typically accompanied by abnormalities in functions of the reproductive, adrenocortical, and thyroid endocrine systems (Delzell *et al.*, 1994). Dioxins and furans, particularly the most toxic TCDD congener, have been identified as carcinogenic and tumour promoters in rodents, in addition to demonstrating immunotoxic, reproductive, and teratogenic effects (Krewski *et al.*, 1994).

Several possible mechanisms have been postulated in the scientific literature to explain the toxic actions of chlorinated dioxins and furans. Two relate to their effects on enzyme systems within cells of the body, and one is based on their potential interference with the functions of DNA. The potential impacts upon enzyme systems relate to the induction of the CYP1A family of aryl hydrocarbon hydroxylase (AHH) enzymes associated with the Ah receptor system and the inhibition of glucocorticoid-regulated enzymes (Delzell, 1994). Research has also indicated that the Ah receptor-TCDD complex can impact negatively on levels of growth factor receptors (*e.g.*, *c-fos* proto-oncogenes, epidermal growth factor receptors [EGFR], transforming growth factor [TGF], *etc.*), resulting in the induction of various important growth factors. For example, TCDD's interaction with the Ah receptor has been shown to up-regulate an EGF-like peptide (treated nominally as transforming growth factor-alpha, TGF-α) by synergistically reacting with the estrogen receptor-estrogen complex (Kohn *et al.*, 1993; Portier *et al.*, 1993) and decreasing

concentrations of the plasma membrane EGF receptor (Lee *et al.*, 1996). TCDD binding to the Ah receptor complex has also been noted to result in endocrine disruption activities which mimic or antagonize endogenous hormone action (*i.e.*, estrogens) *in vivo*. While the mechanisms underlying these antiestrogenic impacts are unknown, they are thought to be mediated by "cross-talk" (*i.e.*, a sharing of common intermediates in signaling pathways) between the TCDD/Ah complex and estrogen response elements (EREs) (Klinge *et al.*, 2000). This impacts are discussed in greater depth in the section on Ah receptor mediated toxicity.

To properly characterize a physiologically-based pharmacokinetic model describing the toxic impacts of dioxins and furans on a biological system, one must first evaluate these potential mechanisms to determine their relative impacts. Based on information on PCBs of similar structure, some researchers believe that the metabolic activation of various PCDD/F isomers to reactive intermediates may interfere with DNA function, resulting in toxic action. However, the available information on this theory is fragmentary, and the relevance of these mechanisms to environmental concentrations of dioxins and furans remains unclear. The important information from the mechanistic studies of chlorinated dioxins and furans indicate that they do not produce self-replicating lesions (*i.e.*, mutations or other self-replicating effects on DNA), and as such are not considered toxicants with nonthreshold dose-response relationships. Furthermore, the available literature indicates an exposure threshold in their dose-response relationship, and that below this exposure threshold, no adverse effects would be expected (Delzell *et al.*, 1994).

Based on this information, the current scientific consensus indicates that the toxic effects of PCDD/Fs are likely dependent on the interaction of dioxin, and dioxin-like compounds, with a specific cellular protein, the *Ah* (aryl hydrocarbon) receptor. While none of the correlations between the various adverse effects associated with PCDD/F and interactions with the Ah receptor conclusively proves that the Ah receptor system is the primary mechanism of toxicity of chlorinated dioxins and furans, weight-of-evidence evaluations (Safe, 1990; Borlakoglu and Haegele, 1991) concluded that the Ah receptor-mediated response was a critical component in their action (Delzell *et al.*, 1994).

What is the Ah Receptor?

Over the past twenty years, much research has been directed at clarifying the occurrence, structure, and function of a cytosolic protein called the aryl hydrocarbon (Ah) receptor (AhR). The Ah receptor protein evolved about 450 million years ago, early in vertebrate evolution (Hengstler *et al.*, 1999), and exists in teleost fish, birds, and mammals (Hahn *et al.*, 1994). A variety of anthropogenic and natural chemicals have been shown to bind to the AhR and act as receptor agonists to elicit the prototypical AhR-mediated biochemical responses. Interestingly enough, no endogenous ligand for the Ah receptor has been identified. However, indolo[3,2-*b*]carbazole, which is formed from the acid-catalyzed conversion of the natural plant dietary metabolite indole-3-carbinol, binds with moderately high affinity to the Ah receptor (Santostefano *et al.*, 1992). One of the major differences between many anthropogenic and natural chemicals is their pharmacokinetics and its ultimate toxic impact on the organism. Many anthropogenic chemicals capable of binding to the Ah receptor are persistent and bioaccumulate in wildlife and humans. In contrast, most if not all of the natural Ah receptor ligands are rapidly metabolized and eliminated from biological systems (U.S. EPA, 2000).

Briefly, the Ah receptor is a ligand-activated transcription factor that is a member of the basic-helix-loop-helix-Per-Arnt-Sim (bHLH-PAS) superfamily. The basic-helix-loop-helix (referred to individually as bHLH) DNA binding and dimerization motif also identifies the Ah receptor as a member of the broad class of bHLH gene regulatory factors. Members of this large family of transcription factors are often involved in regulation of cell type differentiation and proliferation, and are typically characterized by the requirement of formation of homo- or heterodimeric complexes with other bHLH-demonstrating partner factors to achieve DNA binding activity (Poellinger, 2000; U.S. EPA, 2000). These proteins are known to regulate such diverse areas as circadian rhythms and steroid receptor signaling, and are involved in sensing oxygen tension (Hahn, 1998). Interestingly, the AhR is the only member of the bHLH class known to require ligand-dependent activation for heterodimerization and transcriptional activity (Gasiewicz *et al.*, 1996; Hushka *et al.*, 1998). The classification of the AhR as part of the bHLH-PAS superfamily and its evolutionary conservatism (*i.e.*, present in all vertebrate classes examined) appears to

imply that this protein may play an important, but yet unknown, role in normal physiological function (U.S. EPA, 2000).

The unbound (*i.e.*, non-ligated) Ah receptor is an oligomeric complex located in the cytoplasm, where it is associated with two molecules of the 90-kDa heat-shock protein and the another protein which may be a 60-kDa c-Src protein (Andersen, 1995; Alexander *et al.*, 1999; Hengstler *et al.*, 1999; Hu and Bunce, 1999). This complex is termed the *unligated aryl hydrocarbon receptor complex.*

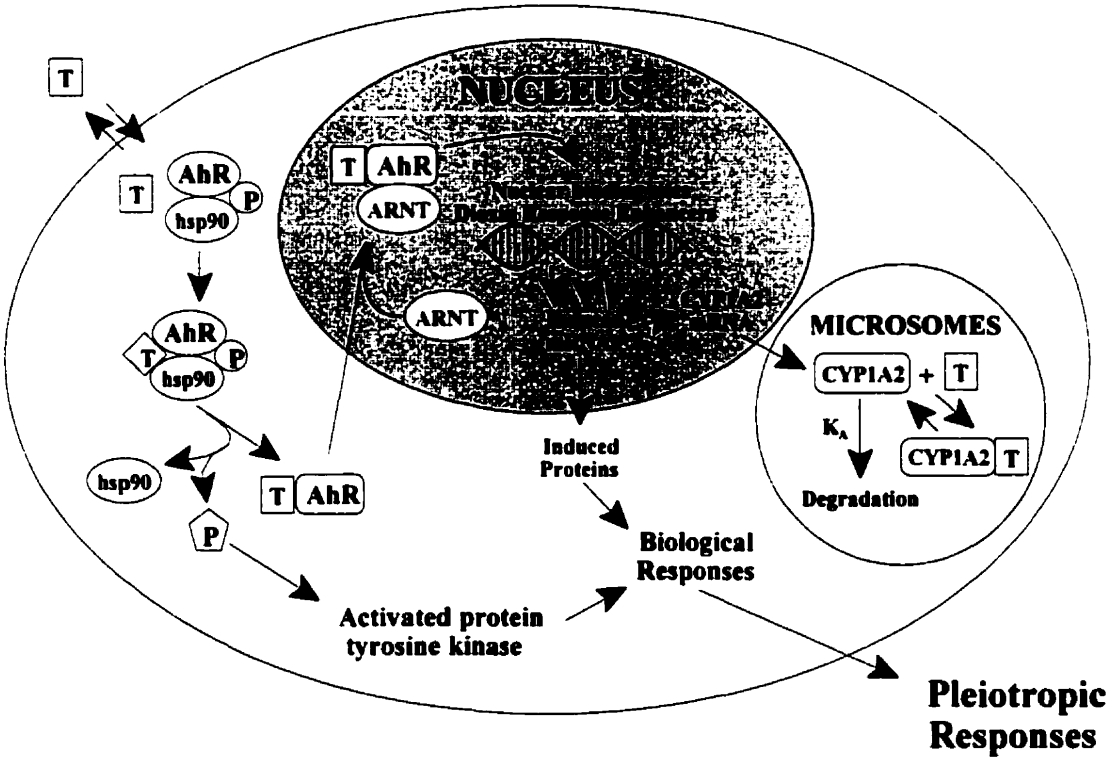
The 90 kDa molecular chaperone hsp90 proteins appear to be required for maintaining the receptor in a non-activated, ligand binding conformation. For example, research has demonstrated that ligand binding to the Ah receptor is severely impaired upon expression in a yeast strain in which hsp90 expression levels are down-regulated to about 5% of wild-type levels (Poellinger, 2000).

There is considerable uncertainty in the scientific literature as to the true size and nature of the smaller associated protein. A number of researchers (described in Hu and Bunce, 1999) feel it is possibly the 60-kD protein c-Src, and ultimately results in biological responses due to impacts on tyrosine kinase activity. Other researchers feel it is a 23-kDa (Kazlauskas *et al.*, 1999) or 50-kDa (Santostefano *et al.*, 1998) co-chaperone protein thought to play a role in stabilizing the complex containing the receptor and hsp90. Ongoing research should provide a more accurate depiction of this protein and its true role in the Ah receptor binding process.

The cascade of biological effects is initiated by TCDD entering the cell *via* passive diffusion through the cell membrane, and the process of binding to the Ah receptor (see Figure 2.8). After binding of a dioxin molecule or similar ligand, the Ah receptor is released from the 90-kDa heat-shock proteins and the other smaller chaperone protein (as discussed previously, possibly a 60-kDa c-Src protein), and becomes associated with the Ah receptor nuclear translocator protein (*Arnt*) after entering the nucleus of the cell. This translocator complex also contains the bHLH domain, which allows for binding to specific asymmetrical recognition motifs of DNA in

promoter regions of specific genes, resulting in enhanced transcriptional activity (*i.e.*, production of mRNA). For example, these DNA recognition sequences, termed a *dioxin-responsive element* (DREs) or *xenobiotic-responsive element* (XREs), have a consensus sequence [T(T/A]GCGTG] located in the 5'-flanking region upstream of the cytochrome P450 CYP1A1 gene (Andersen *et al.*, 1995; Hengstler *et al.*, 1999; Poellinger, 2000). While it is essential for the binding of the Ah receptor to the DNA sequence, contrary to what its name suggests, the *Arnt* protein is not involved in translocating the Ah receptor to the nucleus (when first identified, it was thought to be a transporter protein). Studies have demonstrated TCDD-induced nuclear translocation of the liganded Ah receptor also in *Arnt*-deficient mouse Hepa-1 cells (Hankinson *et al.*, 1996).

Figure 2.8 Proposed Ah-Receptor Mediated Mechanism of Action for Dioxin-like Exposures (adapted from Hu and Bunce, 1999 and Santostefano *et al.*, 1998)



The mRNA produced from the transcribed genes serve as templates for protein synthesis. Among the genes transcriptionally regulated by the Ah receptor-dioxin complex (although not necessarily in conjunction with *Arnt*) are several that regulate cell growth and differentiation.

Ah Receptor Binding Affinity

Studies involving the Ah receptor have demonstrated it to have a saturable, high-affinity binding site (typically with a K_d of around 1 nM) for TCDD and similar ligands, and has been identified in a variety of animal tissues (Poellinger, 2000; Delzell *et al.*, 1994). The Ah receptor is highly polymorphic, particularly when compared with other nuclear receptors. This polymorphism has been shown to extend beyond the classical responsive and nonresponsive phenotypes (*i.e.*, C57 strains of mice have been shown to be highly responsive, while DBA and AKR strains have been described as nonresponsive) to include significant differences in receptor primary structure. For example, three different murine Ahr alleles (typically denoted with a "b" subscript from the prototype C57BL strain) have been identified that encode high-affinity receptors in responsive strains (Schmidt and Bradfield, 1996), and differ by only a few point mutations in the common open reading frame (also known as ORF) and by additional sequences at their carboxyl ends (Poland *et al.*, 1994). Specifically, the allele found in C57 strains (Ahr^{b-1}) encodes a 95-kDa (805 amino acids) receptor with high affinity for agonists, whereas the 104-kDa (848 amino acids) high-affinity allele (Ahr^{b-2}) is found in most other commonly used laboratory strains, such as C3H/He and BALB/c (Poland *et al.*, 1987). Finally, several wild-mouse strains (*Mus sp.*) demonstrate a third high-affinity allele (Ahr^{b-3}) encoding a 105-kDa (883 amino acids) receptor protein (Poland and Glover, 1990; Poland *et al.*, 1994).

However, only a single allele (Ahr^{d}) has been identified which encodes for the low-affinity receptor (~104 kDa) found in nonresponsive strains. This allele is denoted with a "d" superscript based upon the prototype nonresponsive DBA strain, and is most appropriately compared with the Ahr^{b-2} allele because the two alleles express proteins of the same size that differ in only two amino acids (Swanson and Bradfield, 1993; Poland and Glover, 1990; Smith *et al.*, 1998; Poland *et al.*, 1994). As a result of these differences in receptor binding affinity, studies into the induction of hepatic AHH activity by TCDD have noted a 9-fold difference between activity levels of C57BL/6J and DBA/2 mice, and an approximate 10-fold difference between strains demonstrating the high-affinity Ahr^{b-1} or Ahr^{b-2} alleles and the low-affinity Ahr^{d} allele (Poland *et al.* ,1994).

It is also important to note that the structural and functional variability of the Ah receptor is also significant across species. Research conducted into photoaffinity labelling of hepatic cytosol has indicated that the Ah receptor can vary in molecular weight by nearly 30 kDa (*e.g.*, 95 kDa in C57 mouse, 101 kDa in chickens, 103 kDa in guinea pigs, 104 kDa in rabbits, 106 kDa in rats and humans, 113 kDa in monkeys, and 124 kDa in hamsters) (Poland *et al.*, 1987). As such, the considerable species and strain variability in size and specificity of the Ah receptor can have large impacts on the binding affinity of the TCDD ligand to the receptor. Research has demonstrated that while the binding affinity to the Ah receptor varies significantly between mouse strains (Poland *et al.*, 1994), it does not appear to vary dramatically between strains of rats (Pohjanvirta and Tuomisto, 1994). However, there is some evidence indicating that the binding affinity of TCDD to the Ah receptor can vary by a factor of approximately10 to 20 in humans, and this range encompasses binding affinities similar to those observed in sensitive (*i.e.*, responsive) and resistant, nonresponsive mice (Micka *et al.*, 1997; Okey *et al.*, 1997).

Interestingly enough, there are also gender- and age-specific differences in the toxicity of dioxins and furans. A number of studies have identified a clear, although small, gender difference in the acute, subchronic, and chronic toxicities of TCDD in rats. In general, females have been demonstrated to be more sensitive to TCDD than males, and while the profile of TCDD distribution in female rats is similar to that in male rats, the concentration of TCDD in most tissues were higher in females than in males (Li *et al.*, 1995). Recent investigations in mice have indicated that this can likely be linked to an increased biliary excretion level in males, as compared to females, and even older senescent males (Jackson *et al.*, 1998). Other studies have suggested that advanced age may have differential effects on Ah receptor-mediated enzyme induction, resulting in potential toxicological implications for older animals (Pegram *et al.*, 1995).

Ah Receptor Mediated Toxicity

Exogenous ligands for the Ah receptor, particularly TCDD, can cause several toxic effects, including cancer, progressive weight loss, toxicity to the immune system, fetal toxicity, birth defects, dysregulation of endocrine (thyroid, androgen, estrogen, and growth factor) homeostasis,

and decreases in male and female reproductive performance. TCDD has also proven to be the most potent tumour promoter analyzed and some researchers believe it can act as a complete carcinogen (*i.e.*, has initiator and a promoter capabilities) because rodents demonstrate an increased incidence of specific tumours in chronic toxicity studies, without prior exposure to an experimental initiator (Schmidt and Bradfield, 1996). However, unlike many potent carcinogens such as polycyclic aromatic hydrocarbons (PAHs) or heterocyclic amines, dioxins are not genotoxic and do not covalently bind DNA, RNA, or protein, and are not mutagenic in the Ames assay (Hengstler *et al.*, 1999; Schmidt and Bradfield, 1996), calling into question their ability as an carcinogenic initiator. Proposed mechanisms for the carcinogenic effects of TCDD on biological systems include: i) increased cytochrome P450-mediated metabolic activation of other carcinogens or endogenous compounds such as estrogen; ii) DNA single-strand breaks resulting from lipid peroxidation, and; iii) alterations in cell proliferation through transcriptional regulation of cytokines and growth factors (Huff *et al.*, 1994).

The impact of dioxin on these critical processes can result in broad spectrum toxicity on multiple organ systems, including action as a hepatic tumour promoter (Andersen *et al.*, 1995). Genes which have been shown to exhibit increased transcriptional rates by this mechanism include microsomal monooxygenases (*i.e.*, P450 CYP1A1, 1A2, and 1B1), the glutathione *S*-transferases, UDP-glucuronosyltransferase, aldehyde dehydrogenase, and NAD(P)H:quinone reductase (Santostefano *et al.*, 1998; Hengstler *et al.*, 1999).

Dioxins also mediate increases in the liver concentration of transforming growth factor-α (TGF-α) by a mechanism which requires the Ah receptor. TGF-α subsequently binds to the epidermal growth factor (EGF) receptor, a process which is known to cause internalization of this receptor in hepatocytes. This action is thought to be an early event in the generation of a mitogenic signal (Kohn *et al.*, 1993). EGF is a potent mitogen with tumour-promoting activity *in vivo*, and alterations in EGF receptor (EGFR) regulatory systems may play a role in carcinogenesis. Research has indicated that the EGFR (encoded by the c-*erb* proto-oncogene) is a transmembrane glycoprotein with a ligand-dependent intrinsic tyrosine kinase activity (Sewell and Lucier, 1995). As TCDD decreases binding of EGF in the livers of intact female rats but not in ovariectomized rats, this effect was further assumed to be dependent on estrogen action. Given these AhR-

mediated impacts, dioxins and furans have also been widely labelled as *endocrine disruptor chemicals* (EDCs).

TCDD and related compounds have been shown to modulate several intracellular endocrine response pathways. For example, in the rodent uterus, in addition to the impacts outlined above (*i.e.*, epidermal growth factor receptor binding, *c-fos* and EGF receptor mRNA levels, *etc.*), TCDD inhibits such 17β-estradiol (E2)-induced responses as uterine wet weight increase, peroxidase activity, and progesterone receptor binding. Despite these effects, TCDD does not bind either the uterine estrogen receptor (ER) or progesterone receptor (PR) (Safe *et al.*, 1998).

The mechanisms underlying these observations are unknown, but are thought to be mediated by "cross-talk" (*i.e.*, a sharing of common intermediates in intracellular signaling pathways) between TCDD and hormones including estrogens (Klinge *et al.*, 2000), typically in extrahepatic tissue. TCDD has been shown to cause a rapid downregulation of nuclear ERα levels and this is typically accompanied by induction of CYP1A1 resulting in the rapid oxidative metabolism of any available E2 (Safe *et al.*, 1998a). One proposed mechanism of this inhibitory AhR-ER crosstalk involves direct interaction of the AhR complex with inhibitory DREs identified in the 5'-promoter regions of E2-responsive cathepsin D, pS2 and c-*fos* genes. However, other studies have identified AhR agonists which can inhibit E2-induced expression of several genes that do not have functional DREs (Wormke *et al.*, 2000). While the molecular mechanisms underlying the apparent "cross-talk" between ER- and Ah receptor-mediated activities are unknown, recent research has suggested that this rapid inhibition of available ERα may be facilitated through the unidirectional activation of proteasomes, and that the E2-activated degradation of ERα by proteasomes may be an important pathway for limiting the duration of estrogenic responses in target tissues. Thus, TCDD not only activates proteasome-dependent downregulation of the Ah receptor, but also induces degradation of ERα protein *via* other proteasome-dependent pathways (Wormke *et al.*, 2000). Additional mechanisms by which TCDD may interfere with the ER action include inhibition of ER-DNA binding and interference with critical ER-protein interactions that mitigate transcriptional activation. As transcription factors of many different families appear to use common coactivator proteins, competition for these proteins may provide another mechanism for the antiestrogenic behaviour of TCDD (Klinge *et al.*, 2000).

As noted previously, dioxin and dioxin-like compounds that bind these regulatory genes demonstrate dose-dependent kinetics. In other words, as the administered dose increases, a larger proportion of the total dose is found in the liver. For example, it appears likely that dose-dependent hepatic sequestration is related to induction of CYP1A2, but other proteins may also be involved (Diliberto *et al.*, 1997, 1999; Wang *et al.*, 2000). Thus, any comprehensive model of dioxin pharmacokinetics must include the induction of these dioxin-binding proteins, mediated by the interaction of a dioxin-*Ah*-receptor complex with specific DRE binding sites on DNA (Leung *et al.*, 1988, 1990a,b; Andersen *et al.*, 1993).

What are cytochrome P450?

The cytochrome P450s are a group of hemoproteins associated with the smooth endoplasmic reticulum, which mediate the primary (phase I) oxidative metabolism of a broad spectrum of lipophilic substrates, both endogenous and exogenous (xenobiotic) in nature (Nims and Lubet, 1995). For example, the cytochrome P4501A1 (CYP1A1) enzyme catalyzes oxygenation of polycyclic aromatic substances as the initial step in their metabolic processing to water-soluble derivatives, and ultimate excretion from the body. While most CYP induction response occurs in the liver (as the main site of detoxification and metabolism in the body), these CYP genes are present in an uninduced state throughout the body, and play a significant role in many tissue organs (*i.e.*, small intestine, lung, kidney, and placenta).

The CYP1A subfamily includes two genes, CYP1A1 and CYP1A2, which show a relatively high degree of nucleotide homology (~75% in rats). Typically, the same compounds will induce both of these proteins, usually with similar kinetic patterns (Nerurkar *et al.*, 1993). The CYP1A subfamily is associated with the metabolic activation of planar, hydrophobic compounds such as polycyclic aromatic hydrocarbons (PAHs), PCDD/Fs, and other related compounds (Nims and Lubet, 1995; Ziegler, 1991). CYP1A1 preferentially catalyzes the oxidation of PAHs, while CYP1A2 preferentially metabolizes a variety of heteroaromatic amines through *N*-hydroxylation (Nerurkar *et al.*, 1993). Exposure to such a xenobiotic can also markedly enhance the ability of an organism to metabolize the same xenobiotic (and other similar compounds) through a process termed *enzyme induction*. This process is discussed in further depth in Section 3.0.

When exposed to such a ligand, CYP1A2 induction is largely limited to hepatic (liver) cells, while CYP1A1 is expressed both in liver and many extrahepatic tissues, such as the lungs, skin, and kidneys (DeVito *et al.*, 1996; Gonzalez, 1988). Particularly relevant to the disposition, metabolism, and excretion of dioxin and dioxin-like compounds is the ability of CYP1A2 to temporarily sequester these compounds in the liver, on a dose-dependent basis. As such, sequestration of TCDD by binding to CYP1A2 can result in a considerable shift of localized TCDD tissue concentrations from the more lipophilic adipose tissue to the liver, and have significant impacts on the organism's ability to sequester and excrete the compound. Thus, it is vital to address this pharmacokinetic and pharmacodynamic issues when designing an accurate PBPK model of TCDD exposure.

There have historically been four distinct methodological approaches for determining CYP induction following potential exposure to a contaminant. These included: i) quantification of total CYP *via* UV spectrophotometry; ii) substrate conversion assays; iii) immunochemical detection of protein, and; iv) quantification of gene-specific RNA (Nims and Lubet, 1995). Research has demonstrated that the spectral technique for assessing CYP induction is relatively insensitive, and does not provide sufficient detail with respect to the specific subfamilies or isozymes being induced (*i.e.*, it may indicate that a CYP1A family member has been induced, but not which one). Each of the remaining techniques, while demonstrating much greater sensitivity, have certain specific advantages and disadvantages, depending on the circumstance (Nims and Lubet, 1995). Perhaps the most commonly used methodology is that of the *substrate conversion assay*. This assay relies on the ability of the individual CYP isozymes to catalyze a reaction in a specific substrate, which can then be quantified through laboratory analysis. For example, induction of the CYP1A1 isoform has been linked to the *O*-deethylation of the substrate *ethoxyresorufin* (otherwise known as EROD), while other researchers have linked CYP1A2 induction to the *O*-demethylation of the substrate *methoxyresorufin* (otherwise known as MROD). Acetanilide 4-hydroxylase (ACOH) has also been proposed as a potential enzymatic marker for CYP1A2 induction (DeVito *et al.*, 1996). Many researchers believe that conversion levels of these substrates can be used as enzymatic biomarkers to estimate the relative induction of the related CYP isozyme following an exposure event (DeVito *et al.*, 1996). However, considerable uncertainty has been expressed in the scientific literature as to the selectivity and

specificity of these substrates for one particular isozyme. This issue will be discussed in greater depth later in this paper.

Use of Toxic Equivalency Factors (TEFs)

Biological species, including humans, are constantly exposed to complex mixtures of polyhalogenated aromatic hydrocarbons (PHAHs), such as PCDDs, PCDFs, and PCBs through a variety of routes of exposure. The composition of these complex mixtures of PHAHs can vary dramatically in both the environment and living biota, with environmental and biological degradation (*i.e.*, differing environmental fates of congeners with different solubilities, volatilities, and rates of degradation/metabolism) playing a key role. According to their inherent physical-chemical nature, each of these compounds is variably persistent, undergoes environmental transport, and can preferentially bioconcentrate in higher tropic levels of the food chain (Safe, 1998a). As a result, the congener profile of PHAH mixtures can change both spatially and temporally within the environment, and are usually very different from the source mixtures originally released into the environment (Van den Berg *et al.*, 1998). The complex nature of these PHAH mixtures complicates the risk assessment for humans, fish and wildlife. To allow risk assessors to better evaluate their potential mixture-based toxicities, these compounds are typically classified as either "dioxin-like" or "nondioxin-like" (Birnbaum and DeVito, 1995). The dioxin-like compounds are grouped according to their common structure (*i.e.*, coplanar and non-ortho substituted aromatic rings) and mechanism of action (i.e., they induce their biochemical and toxicological effects by specific, high-affinity binding to the Ah receptor) (DeVito *et al.*, 2000; Van den Berg *et al.*, 1998).

In order to estimate the toxic potential of a mixture of such dioxin-like compounds and better facilitate their evaluation in hazard and risk assessments, the scientific community has developed a system of *toxic equivalency factors* (TEFs). The idea behind this is to produce a "standardized" estimate of potency of a specific chemical within a complex mixture of dioxin-like compounds, for which relatively little direct toxicological information is available, based upon information on another structurally-similar congener for which there is substantial toxicity data and an understanding of the inherent mechanism of action (DeVito and Birnbaum, 1995;

Birnbaum, 1999) or the same chemical under a different exposure scenario (*e.g.*, individual *versus* mixtures, different species, different exposure biological exposure systems, *etc.*). TEFs for these PHAHs are typically calculated by determining the relative biological potency (REP) of a compound compared to that of the keystone chemical 2,3,7,8-tetrachlorodibenzo-*p*-dioxin (TCDD), which is the most potent and best characterized of this "family" of dioxin-like compounds. The TEF approach assumes that the effects of the individual compounds are strictly additive and proportional to their individual potencies and concentrations (Safe, 1998a).

The concentration of each specific congener is multiplied by its corresponding TEF value, and the resulting potency-weighted concentration values are summed to form an expression of the mixture's overall toxic equivalency (TEQ) to TCDD. This value can then be employed as a concentration of TCDD toxic equivalents (*i.e.*, TCDD TEQ-equiv.) representing the overall toxicity of the assessed mixture.

$$TEQ = \sum [PCDD_i] \times TEF_i + \sum [PCDF_j] \times TEF_j + \sum [PCB_k] \times TEF_k$$

Chemicals included in this TEQ methodology must meet certain criteria. They must be: a) persistent; b) bioacumulative, and; c) induce toxicities by binding to the Ah receptor (Van den Berg *et al.*, 1998). Ultimately, the REP of a dioxin-like chemical is dependent upon both binding affinity to the Ah receptor and pharmacokinetic properties of the chemical, when compared to TCDD (DeVito *et al.*, 1997). In developing TEFs, the relative potency for each assessed chemical is evaluated using both *in vitro* and *in vivo* experimental methodologies, comparing enzyme induction, thymic atrophy, immunotoxicity, teratogenicity, and several other related criteria endpoints (*e.g.*, reproduction, development, endocrine function, *etc.*) (DeVito and Birnbaum, 1995).

The TEF approach first began to be introduced as a viable approach in the late 1980s to early 1990s, with proposed sets of guidelines and TEF values provided by various researchers and regulatory agencies. The first international set of TEFs (I-TEFs) was presented and adopted after a 3-year study conducted by the North Atlantic Treaty Organization Committee on the Challenges of Modern Society (NATO/CCMS). The most recent re-evaluation of the TEF

scheme was conducted at an expert meeting organized by the World Health Organization and held in Stockholm, Sweden, on June 15-18, 1997. The objective of this meeting was to derive consensus TEFs for PCDDs, PCDFs, and dioxinlike PCBs for both humans, fish, and wildlife risk assessment (Van den Berg *et al.*, 1998).

Table 2.1, below, provides a list of previous TEF schemes, in addition to the current scientifically accepted set of TEF values for the dioxin and furan congeners, proposed by WHO.

Table 2.1 Various Toxic Equivalency Factors (TEFs) Schemes Recommended for Mammalian Risk Assessments (Van den Berg *et al.*, 1998).

Congener	I-TEF [a]	CEPA [b]	Safe [c]	WHO [d]
Dioxins				
2,3,7,8-TetraCDD	1	1	1	1
1,2,3,7,8-PentaCDD	0.5	0.5	0.5	1
1,2,3,4,7,8-HexaCDD	0.1	0.1	0.1	0.1
1,2,3,6,7,8-HexaCDD	0.1	0.1	0.1	0.1
1,2,3,7,8,9-HexaCDD	0.1	0.1	0.1	0.1
1,2,3,4,6,7,8-HeptaCDD	0.01	0.01	0.01	0.01
OctaCDD	0.001	0.001	0.001	0.0001
Furans				
2,3,7,8-TetraCDF	0.1	0.1	0.1	0.1
1,2,3,7,8-PentaCDF	0.01	0.05	0.1	0.05
2,3,4,7,8-PentaCDF	0.5	0.5	0.5	0.5
1,2,3,4,7,8-HexaCDF	0.1	0.1	0.1	0.1
1,2,3,6,7,8-HexaCDF	0.1	0.1	0.1	0.1
1,2,3,7,8,9-HexaCDF	0.1	0.1	0.1	0.1
2,3,4,6,7,8-HexaCDF	0.1	0.1	0.1	0.1
1,2,3,4,6,7,8-HeptaCDF	0.01	0.01	0.1	0.01
1,2,3,4,7,8,9-HeptaCDF	0.01	0.01	0.1	0.01
OctaCDF	0.001	0.001	0.001	0.0001

[a] Initial international scheme for TEF proposed by Health and Welfare Canada (HWC) and the Ontario Ministry of the Environment (OMOE) and adopted by NATO/CCMS (Boddington, 1988).
[b] Initial Canada-wide standard outlined in the first CEPA Priority Substance List Assessment Report (CEPA, 1990).
[c] Safe proposed a set of TEFs based on structure-activity relationships, laboratory enzyme induction studies, and acute and chronic *in vivo* studies (Safe, 1990).
[d] Set of mammalian TEF values recommended by the WHO expert panel (Van den Berg *et al.*, 1998).

The TEF approach is not without a degree of uncertainty, and is still the subject of much debate in the scientific literature. In addition to the large variance in assay studies used to quantify the relative toxic potentials, uncertainties such as the potential impacts of differences in shape of the

dose-response curve (*e.g.*, questionable low-dose linearity of REP responses), species responsiveness, and the antagonistic non-additive role of certain non-dioxinlike PCBs all call into question the applicability of the TEF approach in the environmental risk assessment process. Furthermore, the high monetary and labour costs of determining these TEQ values in environmental samples has limited the practicality of mounting extensive environmental monitoring programs for these compounds (Bunce, 1997). Despite all these uncertainties, the consensus from the WHO expert panel was that the additive TEF model remains the most feasible risk assessment methodology for assessing complex mixtures of dioxin-like PHAHs (US EPA, 2000).

2.4 Environmental Properties and Fate of Criteria Chemicals

Polychlorinated dioxins and furans, as well as dioxin-like PCBs, have been found throughout the world in practically all media including air, soil, water, sediment, and biota. Their widespread occurrence is not unexpected given the numerous sources that have emitted these compounds into the atmosphere and the overall resistance of these chemicals to both abiotic and biotic transformation/degradation (U.S. EPA, 2000). While TCDD is commonly the primary focus of environmental risk assessments due to its inherent toxicity, it is important to note that chemical analysis of environmental media and biotic receptors have indicated that TCDD is a minor component (by mass) representing less than 1%, whereas the higher isomers typically account for over 99% of the total PCDD/F mass (Czuczwa and Hites, 1995; Rappe *et al.*, 1987).

The primary mechanism by which both PCBs and dioxins/furans are believed to enter the food chain is via atmospheric deposition. Consequently, they can be transported long distances in the atmosphere before they are deposited onto vegetation, soil, and water *via* dry and wet deposition. Deposition onto vegetation and subsequent ingestion of that plant material by animals is thought to be the primary mechanism by which these compounds enter and bioaccumulate within the terrestrial food chain (U.S. EPA, 2000). After direct deposition onto water bodies or indirectly *via* soil erosion and runoff, PCBs and dioxins/furans (since they are relatively insoluble in water) tend to become incorporated into suspended particulates and bottom sediments where they can enter the aquatic food chain (Delzell *et al.*, 1994).

These chemicals tend to be quite stable and persistent in the environment, particularly the higher chlorinated congeners. Available information indicates that while variability in the sampling data can be significant, the more highly chlorinated (tetra-CDD/F and above) congeners of dioxins and furans and certain PCB congeners do accumulate in biota, as demonstrated by ambient levels detected in human breast milk and in animals at the top of the food chain (U.S. EPA, 2000; Delzell *et al.*, 1994). The only environmentally significant transformation processes for these congeners are believed to be atmospheric photo-oxidation and photolysis of nonsorbed species in the gaseous phase or at the soil or water-air interface (U.S. EPA, 2000). As such, burial in-place or erosive movement of soil to nearby water bodies appears to be the predominant environmental fate (*i.e.*, sink) of dioxins and furans sorbed to soils (U.S. EPA, 2000).

Since PCB production was banned in the late 1970s, the major source of PCB exposure in the general environment appears to be the redistribution of PCB previously introduced into the environment as well as releases associated with the disposal of commercial PCB products. Such redistribution typically involves volatilisation from soil and water into the atmosphere with subsequent deposition and then re-volatilization (WHO, 1993). As a result of this redistribution, PCBs can be ultimately transported over great distances.

Chlorinated dioxins and furans also appear to be widespread in the environment due to numerous chemical reactions occurring during the combustion of naturally occurring and man-made organic materials in the presence of chlorine. Thus, dioxins and furans can arise from a diverse variety of combustion sources, including incinerators, chemical tar burners, fossil-fueled power plants, vehicle mufflers, chimneys of wood burning stoves/fireplaces, cigarette smoke, backyard trash burning, and even charcoal-broiled foods. Research has also demonstrated that natural combustion during forest fires and slash burning are also contributors to the concentrations of these chemicals in the environment (Delzell *et al.*, 1994). Given the ubiquitous nature of these chemicals in the environment, it is important to realize that all Canadians are exposed to background concentrations of PCBs, dioxins and furans to varying degrees.

This has particular importance when evaluating potential ambient concentrations of these POPs observed as part of a long-term monitoring program, such as that in place at the SHTC. By

evaluating concentrations prior to the operation of the facility and in localized regions outside the potential "area of influence" of the facility, a more accurate characterization of the actual facility impacts on the surrounding ecosystem can be achieved.

While environmental fate modelling can play an important role in evaluating risk as part of a environmental risk assessment, given the similar physical-chemical properties of PCDD/F congeners, it is likely that the greatest amount of uncertainty in a health assessment would be represented by toxicokinetic and toxicodynamic properties of the individual congeners. Exposure concentrations of chemicals in air, food, water, soil dust, or other media with which populations are in contact are the dose scales most commonly used when evaluating potential health effects of chemicals in the environment. However, external exposure is often only a rough estimate for internal exposure delivered at the critical target in the body. An estimate of the internal dose is a more appropriate measure for use in mechanism-based risk assessments (Bernillon and Bois, 2000). As such, biologically-based toxicological analyses, such as physiologically-based pharmacokinetic modelling, of key sentinel organisms (*i.e.*, a vole) can play a vital role in evaluating health risks as part of an overall environmental health risk assessment process.

3.0 PHYSIOLOGICALLY-BASED PHARMACOKINETIC (PBPK) MODELLING OF POLYCHLORINATED DIOXINS AND FURANS

3.1 Introduction

The uptake and disposition of chemicals by living organisms, notably humans, has long been one of primary concern to pharmacological and toxicological research. The study of the dispersion of chemicals in animal bodies entails the field of *pharmacokinetics*. Pharmacokinetics combines the words *pharmacology* and *kinetics*, and studies the rates of absorption, distribution, metabolism, and elimination of chemicals and metabolites in biological systems (Wen *et al.*, 1999). The closely related subject of pharmacokinetic modelling is the process of developing mathematical descriptions for these critical flow rates. As such, pharmacokinetic modelling can be best described as the process of developing mathematical descriptions for absorption, distribution, metabolism, and excretion of chemicals in biota (Krishnan and Andersen, 1994).

There are two commonly used types of pharmacokinetic models: a) the classical (empirical) model, and b) physiologically-based (PBPK) pharmacokinetic models. With the former, an unique set of experimentally-derived kinetic data are used to statistically fit an unique (non-generalizable) model and determine the value of each rate constants. In the case of the PBPK models, the description of the distribution relies on standardized physiological parameters which are appropriate values determined *a priori*, independently of the kinetic data. Even with PBPK models, however, a few "fitted" parameters, usually the ones describing metabolism, are adjusted using statistical goodness-of-fit criteria to optimize the model parameters, until an acceptable fit to the data is obtained. However, as PBPK models use standardized physiological parameters, they can presumably serve as appropriate vehicles for inter-route and interspecies extrapolation (Woodruff *et al.*, 1992).

To fully understand the potential implications and uses of pharmacokinetic modelling on the assessment of human health risks associated with exposures to persistent organic pollutants, one must first have an adequate understanding of the basis behind these forms of pharmacokinetic research methodologies. While the use of classical pharmacokinetic modelling is of some

interest in addressing this goal, the current discussion paper will focus on the PBPK methodology as the majority of recent toxicological research into POPs has been primarily concentrated on the development of more efficient and accurate physiologically-based pharmacokinetic models.

Physiologically based pharmacokinetic (PBPK) modelling refers to the development of mathematical descriptions of the uptake and disposition of chemicals based on quantitative interrelationships among the critical biological factors and systems within a specific test species. Perhaps Andersen (1994) provided one of the best overviews of the area when he described PBPK models as an "... attempt to provide both a realistic anatomic description of the animal to which a drug or toxic chemical has been administered and a biologically accurate representation of the physiological pathways for chemical storage, metabolism, and elimination in the animal." As such, the ultimate aim of using PBPK modelling in risk assessment is to accurately provide a measure of dose which better represents the internal tissue dose (a pharmacokinetic measure) or the "biologically effective dose" (a pharmacodynamic measure) which causally results in the potentially toxic outcome (Clewell III, 1995).

3.2 Overview of PBPK Modelling

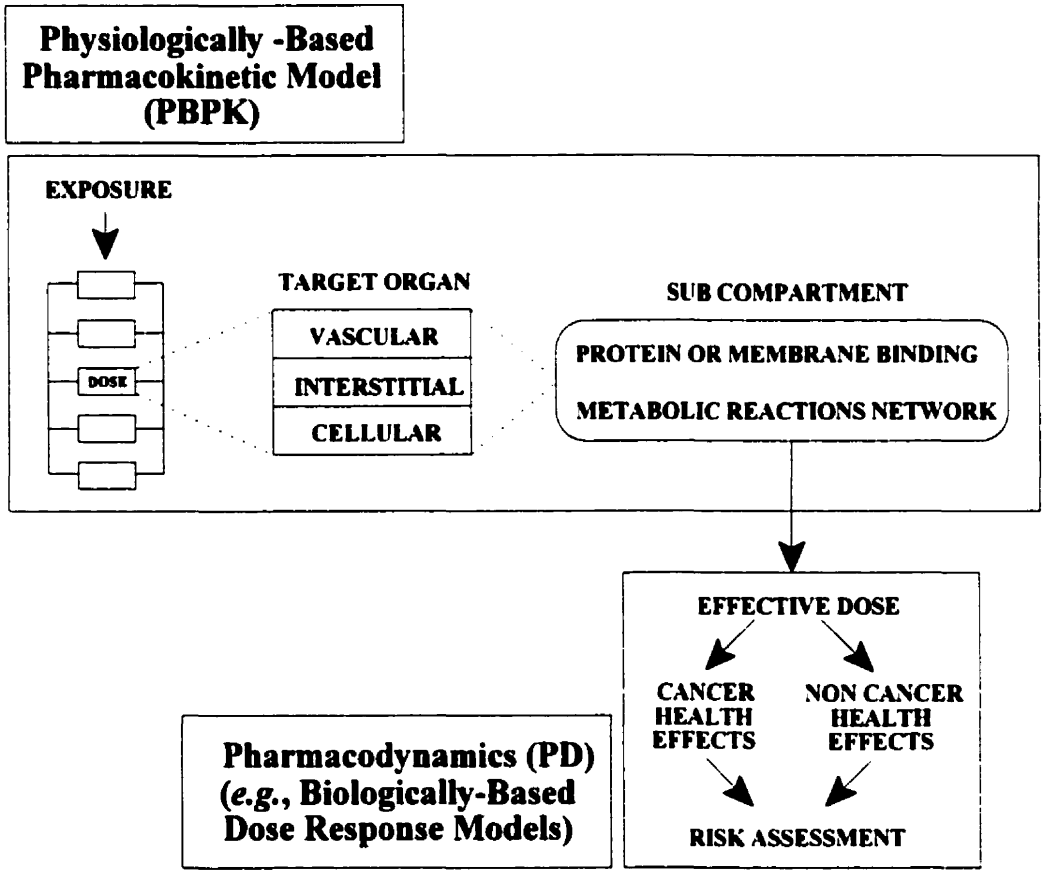
PBPK modelling has been used for more than 70 years to evaluate the disposition (*i.e.*, absorption, distribution, metabolism, and elimination) of pharmaceuticals and other foreign substances (*i.e.*, xenobiotics) within living organisms. Research in this area began in 1924 with studies of volatile anaesthetics, using fairly simple models that evaluated the impact of ventilation, blood flow and blood:air solubilities on chemical uptake within the body (Aarons *et al.*, 1999). PBPK models have since evolved over the past nearly 80 years to the current state-of-the-art tools, capable of evaluating chemical disposition within complex, multi-compartmental systems, and incorporating many aspects involving the pharmacodynamics of particular compounds.

As noted previously, the ultimate aim of using PBPK modelling in risk assessment is to provide a measurement of dose which better reflects the internal dose (delivered to target and non-target organs) or the "biologically effective dose" which is causally related to the ultimate toxic

outcome. As such, PBPK modelling attempts to describe the relationship between the external measures of applied dose (*e.g.*, amount administered or concentration in food, water, or air) and measures of internal dose or biologically effective dose (*e.g.*, amount metabolized or concentration in the tissue displaying the toxic response), using as realistic a description of mammalian physiology and biochemistry as is necessary and feasible (Figure 3.1). PBPK models differ from the more traditional empirical compartmental approaches in that the model compartments are based largely on the actual physiology and anatomy of the test species (Andersen, 1994). For example, in PBPK models the compartments represent actual tissues, or groupings of tissues, with realistic weights and blood flows derived from the literature, or determined through experimental study. Thus nonlinear biological processes (*i.e.*, saturable systems, complex receptor binding arrangements, *etc.*) can be incorporated into the model and evaluations of the potential interactions between the chemical and animal systems can be attempted over a wide range of conditions (Clewell III, 1995).

At their core, PBPK models envisage the organism as a network of compartments representing individual organs or tissue groups interconnected by the arterial and venous blood flow. Uptake, distribution, metabolism, and excretion in a PBPK model are described in terms of quantitative interrelationships among certain physiological, physicochemical, and biochemical parameters. Intercompartmental transfer rate constants are developed based upon blood flow rates, tissue to blood partition coefficients, and tissue volumes for that particular test species (Krewski *et al.*, 1995; Mason and Wilson, 1999).

Figure 3.1 Overview of sequence of events following chemical exposure (Hoang, 1995)



In general, even the most minimal PBPK model (*i.e.*, for aqueous or lipid soluble substances) will generally contain at least three compartments: 1) rapidly perfused tissues, 2) slowly perfused tissues, and 3) fat. These tissue groupings are chosen by virtue of characteristic differences in perfusion-to-volume ratio and chemical composition; properties which jointly determine the rate and magnitude of equilibration between chemicals transported in the blood and those isolated in tissues. (Bailer and Dankovic, 1997). Absorption of chemicals in the environmental medium may be *via* pulmonary, dermal, or oral routes. The amount absorbed per unit time can either be calculated within the model, or the change in chemical concentration in blood or the tissue representing the portal of entry may be simulated using appropriate equations. The chemical in the arterial supply binds to blood components and/or enters the various tissue compartments where it may be dissolved in lipid and water components and be bound to tissue macro-molecules. The rate of change in the amount of chemical in each tissue compartment is

described with mass balance differential equations (MBDEs), defined and solved by numerical methods.

In the case of metabolizing tissues, these MBDEs represent appropriate mathematical descriptions of the processes involved. This is typically achieved by modifying the basic differential equation by including terms describing either a first order clearance process (k_f) or saturable metabolism characterized by Michaelis-Menten type enzyme kinetics (involving K_m and V_{max}). As with other model parameters, these constants can be either obtained from the scientific literature, or estimated using either *in vitro* (*e.g.*, vial equilibration technique with homogenates) or *in vivo* (*e.g.*, measuring gas uptake or exhalation rates of animals in an exposure chamber) techniques (Leung, 1993).

Xenobiotic metabolism or biotransformation is the principle process that determines the fate of most persistent organic pollutants (POPs) in the body. A primary characteristic of phase 1 (*e.g.*, cytochrome P450 enzymes) and phase 2 (*e.g.*, glucuronidation, sulfatation, *etc.*) metabolism is often to render lipophilic compounds more water soluble, which in most cases permits their rapid excretion from the body through urine and bile. Lipophilic compounds, such as POPs, are readily absorbed into the body and have a greater potential for bioaccumulation. Thus, the ability of the organism to clear these lipophilic compounds *via* biotransformation reactions influences the apparent toxicity displayed by these POPs by determining the delivered dose at critical target organs and tissues (Larsen, 1995). It is also important to note that the bioaccumulative nature of these compounds typically results in non-linearity in the dose-response relationship. This is often referred to as the "dose-dependency" of the compound as a function of the concentration, duration, and pattern of long-term exposure. As such, multicompartmental mass-balance PBPK models allow for the integrated use of saturable enzyme kinetics (*i.e.*, Michaelis-Menton or Hill) to better describe disposition, metabolism and excretion kinetics of these compounds.

Finally, the concentration of chemical excreted in biological fluids (*e.g.*, exhaled air, urine, *etc.*) can be calculated using algebraic or differential equations (Haddad and Krishnan, 1998; Krewski *et al.*, 1995; Mason and Wilson, 1999). The key consideration when constructing such a model is to maintain the correct mass balance within each tissue compartment as well as the entire

model by carefully accounting for the input and output mass flows of the chemical in various compartments.

PBPK models are primarily limited by the availability of congener- and species-specific data that accurately represent the dose- and time-dependent disposition of TCDD and related PHAH compounds. Thus, congener- and species-specific rate constants for metabolism and excretion are considered essential in developing accurate PBPK models for these compounds in a given target species.

Typically, the modelling of TCDD disposition within an organism by a PBPK model system can be divided into two specific methodologies: i) steady-state (time-dependent), and; ii) equilibrium-based (time-independent). Both models assume an existing PBPK methodological framework, and allow for the movement of TCDD between the various model compartment groups. However, models incorporating equilibrium-based kinetics assume that a stable concentration relationship exists between all physiological compartments, regardless of time after exposure. As such, the chemical concentrations in each compartment will not change over time, once this equilibrium condition has been reached. Steady-state models, on the other hand, assume that the influx and outflow of chemical will be variable over time, and that chemical concentrations within the various compartmental groups will be governed by rate and mass transport kinetics of the individual compartments. Each type of model design has its advantages and disadvantages, depending on the desired modelling application, and will be discussed in further depth within this study.

A complete literature review of the historical up to most recent development of PBPK models for dioxins and furans was conducted for the current research project. This review will be used as the basis of the current model development and application to address the key objectives for this research project.

3.3 Physiologically-Based Pharmacokinetic Modelling of Dioxin Exposures

Over the past 20 years, a variety of methodological approaches have been used to describe the pharmacokinetic behaviour of PCDDs and dioxin-like compounds in mammalian biological systems. These approaches have mirrored the continuing refinements in dosimetry modelling associated with increasing sophistication both in mathematical modelling techniques, as well as the methodological understanding by the scientific community of the modes of action of PCDD/Fs within biological systems (Wang *et al.*, 1997a,b; Andersen *et al.*, 1997a).

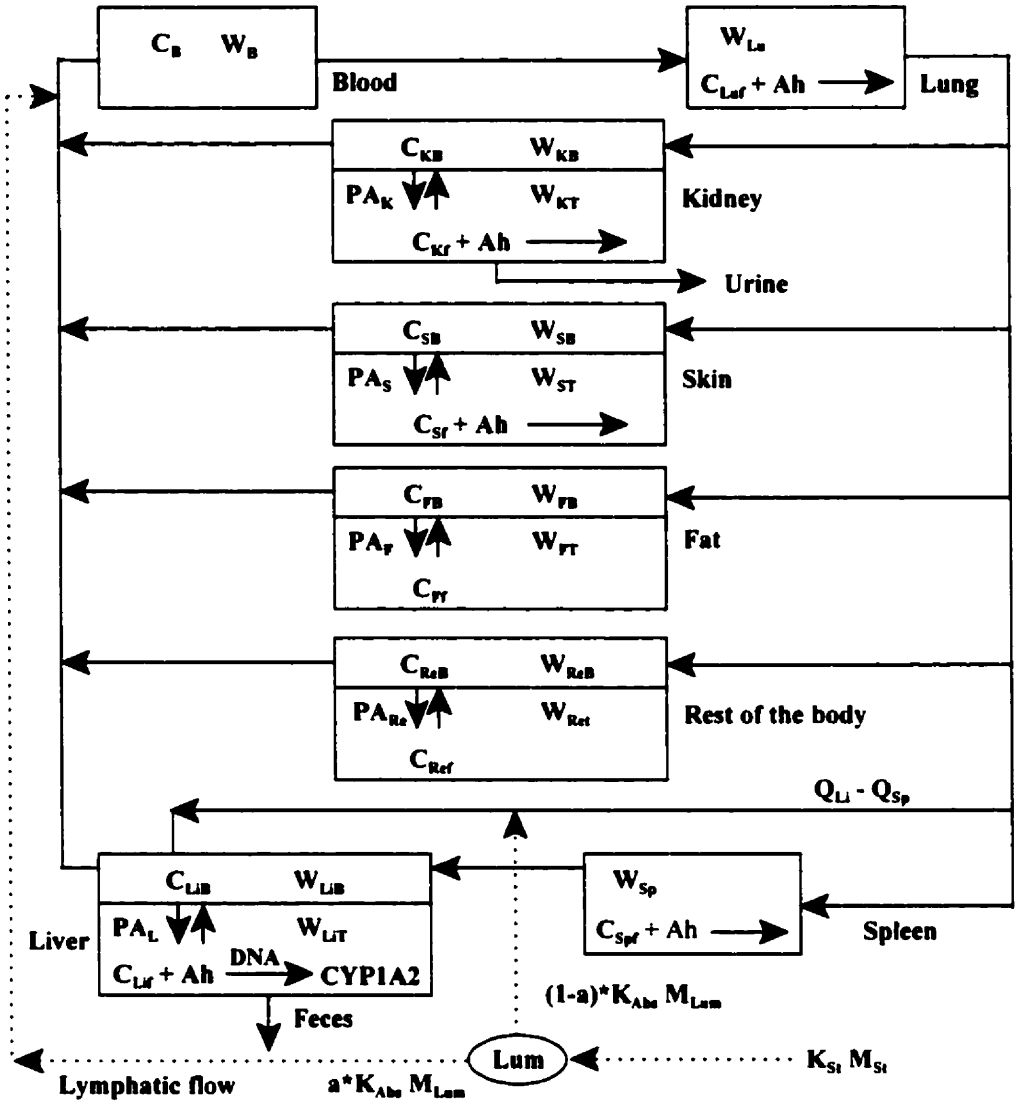
The early PBPK models evaluated the disposition of PCDD/Fs (and PCBs) by taking into account the role of lipid solubility in tissue uptake. Unfortunately, these earlier models were unable to explain the greater concentration of the PCDD/Fs in the liver than in the adipose tissue at high doses, as well as the increase of the compounds in the liver over time (Birnbaum *et al.*, 1980; Birnbaum, 1986; Wang *et al.*, 1997). TCDD model tissue concentration ratios, especially those present in the liver compartment, were demonstrated to be complexly related to both the intrinsic partitioning and to the presence of specific cytosolic and microsomal TCDD-binding proteins. This discrepancy led to the development of the next generation of PCDD/F PBPK models, based upon the hypothesis of an inducible hepatic protein responsible for hepatic sequestration of the PCDD/F compounds (Leung *et al.*, 1988, 1990a,b; Andersen *et al.*, 1993). These models were extended with the inclusion of hepatic binding proteins in response to interactions of TCDD, the Ah receptor, and the corresponding dioxin response elements (DRE) on the DNA (Andersen *et al.*, 1993). These model methodologies continued to evolve through the early and into the late 1990s, further delineating the role of hepatic binding on the absorption, distribution, and excretion of dioxin-like compounds within biological systems.

A review of the scientific literature has indicated that the current state-of-the-art equilibrium-based PBPK model for dioxins and furans (Wang *et al.*, 1997a) was established based on the anatomy and preliminary analysis of time course tissue distribution of TCDD in female Sprague-Dawley rats. Eight compartments (see Figure 3.1) were chosen based upon TCDD-induced response (Birnbaum, 1994) and experimental data, and the model is largely similar in structure to the predecessor Andersen *et al.* (1993) and Leung *et al.* (1990a,b) versions. The Wang *et al.*

(1997) PBPK model for dioxin incorporates four main determinants: i) a high fat/blood partition coefficient; ii) specific, inducible binding in the liver; iii) diffusion-limited tissue distribution, and; iv) first-order biliary excretion/elimination of TCDD. This model was developed with the time course tissue distribution data obtained following a single oral dose of 10 μg [^{3}H]TCDD/kg to female Sprague-Dawley rats, and later validated using other dosing regimes (*i.e.*, 0.001, 0.1, 0.3, 1.0, 10, and 30 μg [^{3}H]TCDD/kg). Tissue distribution information at early time points was gathered to allow for better approximation of some unique parameters related to mass transfer, such as capillary:tissue permeability. The interaction between TCDD and the Ah receptor and the binding of TCDD to hepatic induced protein (*i.e.*, CYP1A2) was also based on a time series analyses, and previous work done in this area. As with previous models, hepatic induction of CYP1A2 was assumed to be a direct result of the formation of a TCDD-Ah receptor-DNA complex (Andersen *et al.*, 1993). The Hill equation was used to describe the induction dose-response interaction between the TCDD-Ah receptor complex with DRE binding sites on DNA. The model described the change of CYP1A2 with time based upon a stimulation process proposed by Dayneka *et al.* (1993), and the process governing quantification of TCDD specifically bound to either the Ah receptor or CYP1A2 was simplified using a Michaelis-Menton saturable binding kinetics equation (Lauffenburg and Lindermann, 1993).

The Hill equation is commonly used for modelling ligand-receptor binding data and allows for both sigmoidal and proportional response below a given maximal induction level (Portier *et al.*, 1993). In general, standard Michaelis-Menten kinetics can be thought of as one specific type of Hill model, where the Hill exponent is estimated to be 1. In the case of CYP1A2, a Hill exponent of 0.5 indicates a strong degree of negative cooperativity in binding.

Figure 3.2 **A schematic representation of a steady-state based PBPK model for TCDD (Wang *et al.*, 1997)**



Typically, a PBPK model includes a large number of equations and parameters. To obtain the unique value of each parameter, model simplification is important. In addition, the appropriate approach for parameter estimation and the experimental design to obtain the complete time course data for parameter estimation are critical (Wang *et al.*, 1997). As noted previously, species differences in response are largely due to differences in pharmacokinetics and biotransformation. However, mammals, including primates, have similar anatomy, physiology, biochemistry and cellular structure. As numerous research studies have noted that organ size and

physiological function can be correlated with the body weight of the test species (Rhodes *et al.*, 1993), allometric scaling by weight is commonly employed to extrapolate from one biological system to another.

The primary means by which xenobiotic chemicals are transported throughout the body is *via* the blood. Chemicals in blood typically partition into free and protein bound fractions, with the free fraction typically driving the movement of the chemical into tissue *via* passive transport. In basic PBPK models, the transport of these chemicals between blood and tissues is assumed to be *perfusion-* or *flow-limited*. This means that barriers to transport of the chemical between the blood and tissue are negligible, and that equilibrium between the free and bound fractions in blood and tissue is rapid (Andersen, 1994; Bailer and Dankovic, 1997). As such, concentrations of chemicals in specific tissue groups and the venous blood exiting the tissue are assumed to be at equilibrium. The flow-limited assumption is usually employed to simplify the PBPK model due to the lack of information on membrane transfer, and is typically appropriate for lipophilic or low molecular weight compounds, which easily partition or diffuse through cell membranes. In the current model, the lungs and the spleen are considered flow-limited tissue compartments due to the similarity of their time course concentration profiles to that of blood (Wang *et al.*, 1997).

Other tissue compartments demonstrate what is termed *membrane-limited* behaviour in which membrane permeability is the dominant mass transfer factor in tissue uptake. Under these conditions, equilibrium between the free and bound fractions in blood and tissue is much slower and entirely dependent on the ability of the chemical to penetrate tissue membranes in the compartment. In the current model, compartments representing the kidneys, adipose tissue, and the rest of the body were considered to be membrane-limited.

A third form of compartmental mass transfer behaviour, termed *membrane-influenced*, is also attributed to certain tissue groups within this model. The membrane-influenced condition is a more general case than either flow-limited or membrane-limited condition, in which both blood flow (perfusion) rate and membrane permeability contribute to tissue uptake. In the current model, the skin and liver tissue groups were considered to be membrane-influenced compartments (Wang *et al.*, 1997).

Some of the physiological data, for a female Sprague-Dawley rat, originally used in this equilibrium-based model are described below in Table 3.1.

Table 3.1 Sprague-Dawley Rat Physiological Parameters used in TCDD Equilibrium-Based PBPK Model (Wang *et al.*, 1997).

Model Parameters	Abbrev.	Physiological Parameters	Parameter Estimation
Body weight (g)	W_t	250	Measured
Tissue weight (g)			
Adipose tissue	W_F	17.3	Measured tissue weight-tissue blood weight
Kidney	W_K	1.64	
Skin	W_S	45.8	
Rest of the body	W_{Re}	117.6	
Liver	W_{Li}	9.05	
Lung	W_{Lu}	0.81	
Spleen	W_{Sp}	0.44	
Blood	W_B	18.9	
Tissue blood weight (g)			
Adipose tissue	W_{FB}	0.78	ILSI, 1994
Kidney	W_{KB}	0.31	
Skin	W_{SB}	0.92	
Rest of the body	W_{ReB}	3.5	
Liver	W_{LiB}	2.41	
Lung	W_{LuB}	0.46	
Spleen	W_{SpB}	0.12	
Blood flow rate (ml/hr)			
Adipose tissue	Q_F	462	ILSI, 1994
Kidney	Q_K	930	
Skin	Q_S	383	
Rest of the body	Q_{Re}	3620	
Liver	Q_{Li}	1208	
Lung	Q_{Lu}	6624	
Spleen	Q_{Sp}	112	
Permeability (ml/hr)			
Adipose tissue	PA_F	$PA_F/Q_F = 0.08$	Fitted to experimental data
Kidney	PA_K	$PA_K/Q_K = 0.01$	
Skin	PA_S	$PA_S/Q_S = 0.09$	
Rest of the body	PA_{Re}	$PA_{re}/Q_{re} = 0.03$	
Liver	PA_{Li}	$PA_{Li}/Q_{Li} = 0.35$	

Table 3.1 Sprague-Dawley Rat Physiological Parameters used in TCDD Equilibrium-Based PBPK Model (Wang *et al.*, 1997).

Model Parameters	Abbrev.	Physiological Parameters	Parameter Estimation
Equilibrium distribution ratio			
Adipose tissue	P_F	100	Fitted to experimental data
Kidney	P_K	6	
Skin	P_S	10	
Rest of the body	P_{Re}	1.5	
Liver	P_{Li}	6	
Lung	P_{Lu}	6	
Spleen	P_{Sp}	5	
Ah receptor level (nM)			
Adipose tissue	Ah_F	—	Fitted to experimental data
Kidney	Ah_K	0.25	
Skin	Ah_S	0.05	
Rest of the body	Ah_{Re}	—	
Liver	Ah_{Li}	0.35	
Lung	Ah_{Lu}	0.35	
Spleen	Ah_{Sp}	0.1	
Dissociation constant (nM)			
TCDD-Ah	K_{Dah}	0.1	Gasiewicz and Rucci, 1984; Safe, 1988
TCDD-CYP1A2	K_{DA2}	30 nM	
CYP1A2			
Basal level	C_{A2base}	1.6 nmoles/g	Kedderis *et al.*, 1991
Basal induction rate	$K_0 = K_2C_{A2base}$	160 nM/hr	Webber *et al.*, 1993
Maximum induction fold	In_{A2}	600	Adjusted
Degradation rate	K_2	0.1 liter/hr	
TCDD-Ah-DNA interaction constant	IC_{A2}	130 nM	Adjusted based on Tritscher *et al.*, 1992
Hill coefficient	h	0.6	Fitted
Holding time	τ	0.25 hour	Fitted
Oral absorption (1/hr)			
Stomic empty rate	K_{sto}	0.36	Roth *et al.*, 1993
Absorption rate	K_{Abs}	0.2	Fitted to experimental data
Elimination (1/hr)			
Urinary	V_{uri}	1	Estimated from Allen *et al.*, 1975 and Diliberto *et al.*, 1996
Fecal	K_{per}	2.2	

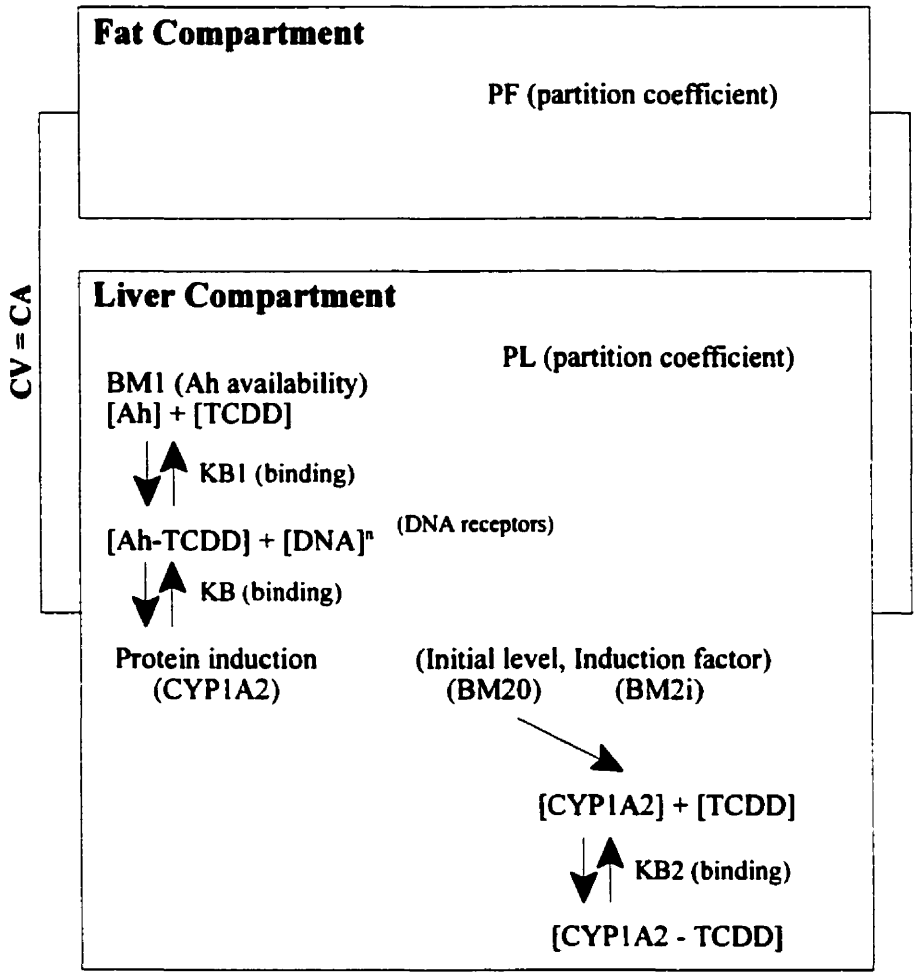
Note:'—' indicates the parameter is not sensitive to tissue distribution

Recently, an alternative equilibrium-based model has been described by Evans and Andersen (2000). The goal of this particular model was to restructure the available PBPK models in order to calculate TCDD dose-dependencies in terms of the total dose of TCDD in the animal. The authors attempted to achieve this objective by calculating a fraction of administered dose in liver

or liver-to-fat concentration ratios for multiple doses to produce a typical dose-response representation of these variables. The PBPK model used to generate these dose-response representations was based on an earlier TCDD model for the rat described by Andersen *et al.* (1993), adapted for what was termed "steady-state" conditions (based upon methodologies presented in Carrier *et al.*, 1995). It is questionable as to whether this methodology can be correctly specified as "steady-state" given the lack of time-dependencies within the model.

The equilibrium-based model was represented by two compartments (liver and fat) connected by a pooling blood supply (see Figure 3.2). As with the Wang *et al.* (1997) methodology, the induction of CYP1A2 was described through the formation of the Ah-TCDD complex and its binding to DNA using the Hill equation. Transport of TCDD into the cell by diffusion (*i.e.*, application of a permeability coefficient) was assumed to be very rapid and thus not included to maintain quasi "steady-state" conditions. The model methodology used assumed that all body stores of TCDD were in fat and liver, and as the model was at equilibrium, all blood concentrations leaving each compartment and re-entering as arterial blood had achieved the same level (*i.e.*, $C_V = C_A$).

Figure 3.3 A schematic representation of an equilibrium-based model for TCDD (Evans and Andersen, 2000)



Some of the physiological data, for a female Sprague-Dawley rat, used in this equilibrium-based model are described below in Table 3.2.

Table 3.2 Sprague-Dawley Rat Physiological Parameters used in TCDD Steady-State PBPK Model (Evans and Andersen, 2000).

Model Parameters	Abbrev.	Physiological Parameters	Parameter Estimation
Liver-to-blood partition coefficient	P_L	10	Estimated
Fat-to-blood partition coefficient	P_F	350	Estimated
Percent liver/body volume	V_{LC}	4%	Andersen *et al.*, 1993
Percent fat/body volume	V_{FC}	6%	Andersen *et al.*, 1993
Ah receptor availability	BM1	0.054 nmoles/liver	Gasiewicz and Rucci, 1984
Ah receptor binding constant	KB1	0.04 nM	Estimated
CYP1A2 basal levels	BM20	10 nmoles/liver	Estimated
CYP1A2 induction factor	BM2i	85 fold	Estimated
CYP1A2 binding constant to TCDD	KB2	6.5 nM	Estimated
Hill coefficient	N	1	Estimated
Ah receptor complex and DNA receptor binding constant	Kd	0.05 nM	Estimated

3.2 Evaluation of Uncertainty Inherent in PBPK Model Methodologies

3.2.1 Overview of Model Uncertainty and Variability

The evolution of physiologically based pharmacokinetic (PBPK) models for the assessment of risk related to persistent organic pollutants has not been restricted to advancements in the understanding of underlying physiological processes (*e.g.*, hepatic protein binding and sequestration within the liver). Considerable work has also been invested in establishing the inherent uncertainties present within a given model, and the sensitivity of each contributing physiological parameter. Since all empirical data have inherent errors, any model will have a certain degree of uncertainty associated with it. As Lao Tzu aptly stated in *The Tao*, "to know one's ignorance is the best part of knowledge", and the potential impacts of uncertainty can have significant implications on the true validity of any environmental risk assessment model.

Two factors play a key role when evaluating the validating and applicability of a model and its results to a specific risk assessment scenario: i) uncertainty, and ii) variability. Uncertainty refers to a lack of knowledge about specific factors, parameters, or models. Regulatory agencies, such as the U.S. EPA, typically classify uncertainty based upon a framework presented by Dr. Adam Finkle of OSHA. In addition to natural variability, this framework recognizes three different types of uncertainty: i) parameter uncertainty, ii) model uncertainty, and iii) decision rule uncertainty. Parameter uncertainty is the uncertainty associated with the model inputs used in a calculation (*i.e.*, measurement errors, sampling errors, or systematic errors). Model uncertainty results from the effect of simplifying nature for use in models and the associated uncertainty (*i.e.*, uncertainty due to necessary simplification of real-world process, mis-specification of the model structure, misuse of the model, or use of inappropriate surrogate/parameter variables). Finally, decision rule uncertainty addresses disagreements or poor specification of social objectives (*i.e.*, descriptive errors, aggregation errors, errors in professional judgement, or incomplete analysis) (U.S. EPA, 1997). The uncertainty inherent within a model or its parameters can be potentially reduced by more detailed study of the parameters or processes involved.

Variability, on the other hand, refers to observed differences attributable to true heterogeneity or diversity in a population or exposure parameter. Sources of variability are generally viewed the result of natural random processes, and can arise from environmental or genetic differences among the species being evaluated (*i.e.*, natural variation in the bodyweights of sampled voles) (U.S. EPA, 1997). It is important to note that while further study can better characterize the variability within a given population, this type of uncertainty is usually not reducible by further measurement or study.

Pharmacokinetic variability can have a large influence on the toxicity of a chemical by affecting the extent to which the chemical is absorbed, distributed, metabolized, and excreted. One of the main advantages of using PBPK models to describe pharmacokinetic variability is that parameters developed for these models are physiologically meaningful, and can in principle be estimated by independent methods. Generally, more information is available on chemical independent PBPK model parameters (such as blood flows and tissue volume) than on chemical specific parameters (such as partition coefficients and metabolic constants). Despite the best efforts, there will always be some uncertainty associated with the values of model parameters for an individual due to random error (or systematic bias) in the data used to estimate the parameter, intra-individual variability, and assumptions that are inherent in any model of physical processes (Krewski *et al.*, 1995; Frederick, 1995). Furthermore, inter-individual variability among individuals in a population will ultimately lead to a distribution of values for a given PBPK model parameter, making the selection of a "best" singular value a difficult task.

3.2.2 Application of Sensitivity Analyses

Given this variability and uncertainty within the model parameters, systematic testing of the effects of these parameters on the model predictions within the PBPK model should be also be conducted to validate the developed methodology. This systematic testing is typically termed *sensitivity* or *variability analysis*. Sensitivity generally refers to the variation in output of a mathematical model with respect to changes in the values of the model's input. A sensitivity analysis typically attempts to provide a mathematical characterization of the model's parameter values (*i.e.*, parameter uncertainty) and input assumptions (*i.e.*, model uncertainty) with respect

to the magnitude of their contribution to the overall model output variability or uncertainty. It also attempts to characterize the magnitude of prediction error associated with model parameter errors and the extent to which model structure affects the relationship between parameter and output errors (U.S. EPA, 1997; Clewell *et al.*, 1994). As such, a sensitivity analysis is able to focus on changes in model predictions due to changes in specific model parameters, and evaluate the contribution that the variability of each specific parameter has on the overall calculation of the chemical's internal dose within a specific tissue. Based upon this information, further research efforts can be focused on the evaluation of the parameters which most strongly impact upon the model output. This process would also assist in the prioritization of data-gathering efforts to verify experimentally derived model parameters during future sampling, and further reduce model uncertainty (Clewell *et al.*, 1994).

Certain caveats must be expressed when conducting uncertainty and sensitivity analyses on PBPK model methodologies. Many researchers have indicated that models which incorporate nonlinear responses (*i.e.*, receptor-binding kinetics) may be sensitive to certain parameters during low dose simulations, but sensitive to other parameters during high dose simulations (*i.e.*, parameter sensitivity may be dose-dependent) (Frederick, 1995). As such, it is important to conduct a careful and complete evaluation of the model response over a wide range of hypothetical conditions (*e.g.*, doses) to ensure the overall effectiveness of the sensitivity analysis.

3.2.3 Techniques for the Evaluation of Uncertainty and Sensitivity

The general purpose of sensitivity and uncertainty analysis, as applied to PBPK models, is to evaluate the degree of uncertainty in model predictions of tissue-delivered doses induced by uncertainty in the model parameters (Krewski *et al.*, 1995). The results of the sensitivity and uncertainty analyses can also be used to estimate the potential impact of proceeding with a risk assessment without filling specific data gaps (Clewell III, 1995). The methods most frequently used for determining the uncertainty and sensitivity of model parameters include Monte Carlo simulation, response surface analysis, and univariate sensitivity techniques (Krewski *et al.*, 1995). Other techniques, such as the application of numerical Bayesian methods for reducing uncertainty, can also be applied.

Briefly, Monte Carlo simulations involve establishing a probability distribution for each of the model input parameters, based upon available experimental/observation data or incorporating expert opinion (*i.e.*, Bayesian priors). The uncertainty distributions of parameter estimates are then derived based upon their individual probability distributions (*e.g.*, uniform, normal, log-normal, triangular, *etc.*), and used to calculate the outcome variables based upon the model methodology. This sampling process is repeated a large number of times, termed model *iterations*, until a statistically significant probability distribution for the desired model output has been created. Latin Hypercube sampling methodology is also one widely used variant of the standard Monte Carlo method. In this method, the typical range of probable values for each of the uncertain input variables is divided into ordered segments of equal probability. This allows for more "efficient" sampling of each parameter once from each of its possible segments, and ensures that the random samples are generated from all the ranges of possible values, thus giving insight into the extremes of the probability distributions of the outputs (Morgan and Henrion, 1990). The main disadvantage to this methodology is that it greatly increases the computational and computer memory requirements in conducting the model runs.

3.2.4 Application of Validation to Environmental Models

The ultimate goal of pharmacokinetic modelling is prediction, and model validation is a necessary step to ensure the overall predictive quality with respect to the model outcomes. As such, the potential impacts of uncertainty within the model can only be adequately addressed through a process of model validation. The purpose of the validation process is to determine whether all parameters and model forms that are essential for describing the modelled pharmacokinetic behaviour have been adequately identified and characterized. One approach used by many researchers is to compare the model output with the experimental observations. The greater the commonality between the simulated and experimental data, the greater the confidence one will have in the overall model (assuming the data used for validating the results is not the same as that used to parameterize the model). The standard statistical techniques frequently used for the validation of models include: tests of means, analysis of variance, goodness-of-fit testing, regression and correlation analysis, Cook's statistics, confidence interval comparisons, the chi-squared test, the Kolmogorov-Smirnov test, factor analysis, and a variety of

nonparametric tests (Wen *et al.*, 1999). However, this process can be made more difficult due to a lack of sufficient data (either experimental or modelled), resulting in insufficient predictive baselines to properly evaluate the underlying scientific hypotheses. While model validation is a partly subjective process and there are no absolute criteria for model "correctness", it is important to use standardized criteria to determine the appropriateness of the model (Wen *et al.*, 1999).

The following are other criteria by which one can evaluate the overall appropriateness of the model in question:

- Generalizability of the model (*i.e.*, not locked into one specific application or use due to "custom" fitting parameters);
- Internal consistency (*e.g.*, blood volumes in each compartment add up to the total organism-based blood volume; Kd values for enzymatic activity the same in all compartments);
- Computational correctness (*i.e.*, model does not contain any mathematical mis-specifications or oversights);
- Model form is correct (*i.e.*, overall structure and equations, regardless of parameter values, accurately reflects model objectives);
- Robustness to changing input parameters (*i.e.*, model does not break down under differing input and exposure scenarios);
- Sensitivity to changing input parameters (*i.e.*, changes to key input parameters results in biologically appropriate changes to model outcomes);
- Biological realism and relevance (*i.e*, correctly specifies or approximates the underlying biological mechanism);
- Agreement between different models characterizing the same process (*i.e.*, does the equilibrium-based model duplicate the results produced by the steady-state model, under similar conditions);
- Heuristic value (*i.e.*, provides usable indicator variables, such as receptor occupancy, induction fold, liver-to-fat ratio, *etc.*);
- Capacity to deal with dose-dependent biological responses;
- Parsimony in the model (*i.e.*, the model is not over-parameterized or unduly complex);

- Absence of numerical (computational) artifacts (*i.e.*, outcome oscillations at low dose), and;
- Useful in extrapolations to other conditions (*e.g.*, route, dose, dose-rate, *etc.*).

4.0 METHODOLOGY

The following methodological approaches were used to attempt to answer the individual questions raised in the objectives of the current research project.

4.1 Gathering of Field Monitoring Data

4.1.1 Objective Overview

One objective of the current research project is to compare estimated whole body TCDD concentrations for a theoretical vole receptor to those measured as part of the long-term environmental monitoring programme conducted at the SHTC. Thus, the environmental concentrations of PCDD/Fs detected in sampled red-backed voles, as well as plant species such as Labrador tea and moss, were gathered from the SHTC environmental monitoring database for the key monitoring sites with the highest detected concentrations (*i.e.*, sites 11, 107, and 114).

For the current research, environmental ambient concentrations were represented by those concentrations detected on the leaves of the Labrador tea or moss. Concentrations from site 107 (closest to the facility) were used as the primary source, with data from the other near-site sampling locations (*e.g.*, sites 11 or 114) used for the purposes of cross-validation and comparative analysis. To maximize potential ambient environmental PCDD/F concentrations, temporal data sampled just prior and following the accidental release event in October 1996 were selected.

4.1.2 Environmental Sampling of PCDD/F Concentrations

Two primary objectives of the SHTC wildlife monitoring program were to monitor the concentrations in the tissues of red-backed voles of various chemicals in emissions from the Treatment Centre, and to monitor the demographic characteristics of the red-backed vole (*e.g.* abundance, sex ratios, reproduction) in the vicinity of the Treatment Centre (Westworth, 1998).

Voles sacrificed for the analysis of chemicals in their body tissues were collected through the use of snap traps by SHTC contractors. They were placed in sealed glass jars, which were labelled with the following information: species, date of capture, location, specimen number, sex and body weight. The collected samples were then stored on ice until sent to an accredited laboratory for detailed congener-specific chemical analyses of their whole-body tissues (Westworth, 1998).

Further details of the sampling program, as well as a field study conducted by this author involving a statistical evaluation of potential impacts of the SHTC on surrounding vole populations, can be found in a research practicum conducted by this author (Ferguson, 1999).

4.1.3 Collation and Selection of SHTC Monitoring Data

All sampling data used in the current project were obtained from the Swan Hills Treatment Centre environmental monitoring database, developed by CanTox Inc. for BOVAR Waste Management Limited, and later supplemented as part of this research project. The current research database contains sampling analytical results on a chemical-specific basis for all analyzed environmental media from June 1990 to February 1998.

Distribution of Bodyweights for SHTC-Sampled Voles

A variety of external physiological parameters were recorded as part of the ongoing SHTC biological monitoring program, including species, sex, bodyweight, reproductive condition and general external condition (Westworth, 1998). Table 4.1 provides an overview of bodyweights of the red-backed voles sampled between June 1995 and 1998.

Table 4.1 Overview of Red-Backed Voles Bodyweights Sampled as part of the SHTC Monitoring Program between June 1995 and June1998.

Sampling Time	Body Weights[1] (grams) Male	Female	Combined
June 1995	21.8 ± 3.7 (n=97)	22.3 ± 5.5 (n=70)	22.0 ± 4.5 (n=167)
September 1995	16.1 ± 3.0 (n=96)	15.4 ± 3.9 (n=157)	15.6 ± 3.6 (n=253)
June 1996	20.8 ± 2.7 (n=38)	21.7 ± 4.5 (n=32)	21.2 ± 3.6 (n=70)
September 1996	14.4 ± 5.0 (n=54)	14.8 ± 5.2 (n=48)	14.6 ± 5.1 (n=102)
June 1997	21.6 ± 2.3 (n=35)	25.3 ± 2.7 (n=23)	23.1 ± 3.1 (n=58)
September 1997	16.1 ± 3.0 (n=146)	16.5 ± 3.6 (n=122)	16.3 ± 3.3 (n=268)
June 1998	24.8 ± 3.8 (n=101)	26.3 ± 5.9 (n=82)	25.5 ± 4.9 (n=183)
June 1995-1998	**22.7 ± 3.8 (n=271)**	**24.1 ± 5.6 (n=207)**	**23.3 ± 4.7 (n=478)**
September 1995-1997	**15.8 ± 3.5 (n=296)**	**15.7 ± 4.1 (n=327)**	**15.8 ± 3.8 (n=623)**
All Sampling Times	**19.1 ± 5.0 (n=567)**	**19.0 ± 6.3 (n=534)**	**19.1 ± 5.7 (n=1101)**

[1] Includes trapped voles from juvenile to adult life-stages.

No detailed bodyweights were available for February monitoring, however, bodyweights were typically between 8 and 12 grams (D. Skinner, Westworth and Associates, personal communication). This is in line with the observations and conclusions in the scientific literature indicating that voles substantially decrease their body mass during the months preceding winter (Dark and Zucker, 1986).

Measured Congener-Specific PCDD/F Concentrations

To achieve the aims of the current research project, dioxin and furan concentrations from various biological species were evaluated at three sampling locations directly surrounding the facility (*i.e.*, sites 11, 107, and 114). A detailed map providing specific plot locations is provided in Figure 2.3. These three sites have the largest amount of historical dioxin/furan congener-specific data for the primary biological monitoring species (*i.e.*, voles, Labrador tea, and moss), when compared to other monitoring programme sampling locations. Tables 4.2 through 4.4 demonstrate the available historical sampling data on voles, Labrador tea, and moss at these sites, respectively.

Table 4.2 Available PCDD/F Congener-Specific Data in Vole Receptors for Specific Exposure Impact Periods.

	Pre-Incident													Incident Impact	Post-Incident Impact		
Site	6/90	9/90	6/91	2/92	6/92	2/93	6/93	2/94	6/94	2/95	6/95	2/96	6/96	9/96	2/97	6/97	9/97	2/98
11			✔		✔		✔		✔		✔		✔	✔	✔	✔	✔	✔
107	✔	✔	✔	✔	✔	✔	✔	✔	✔	✔	✔	✔	✔		✔	✔	✔	✔
114							✔		✔		✔		✔	✔	✔	✔	✔	✔

Table 4.3 Available PCDD/F Congener-Specific Data in Labrador Tea for Specific Exposure Periods.

	Pre-Incident						Incident Impact		Post-Incident Impact	
Site	9/92	9/93	9/94	9/95	5/96	9/96	11/96	2/97	9/97	2/98
11	✔	✔	✔	✔	✔	✔	✔	✔	✔	✔
107	✔	✔	✔	✔	✔	✔	✔	✔	✔	✔
114		✔	✔	✔	✔	✔	✔	✔	✔	✔

Table 4.4 Available PCDD/F Congener-Specific Data in Moss Samples for Specific Exposure Periods.

	Pre-Incident						Incident Impact		Post-Incident Impact	
Site	9/92	9/93	9/94	9/95	5/96	9/96	11/96	2/97	9/97	2/98
11						✔	✔		✔	
107							✔		✔	
114						✔	✔			

All dioxin/furan congener-specific laboratory results for the key biological monitoring species were extracted from the SHTC environmental monitoring database for the three key monitoring locations (*i.e.*, 11, 107, and 114) in time-series for the sampling events immediately prior to and following the accidental release incident in October 1996. Actual sampling dates were dependent upon the particular sampling teams involved, sampling site initiation, receptor availability and life-cycle issues, and seasonal site access restrictions. In certain specific cases, sampling could not be conducted at the scheduled time (*e.g.*, vole sampling at site 107 in

September 1996), while in other cases, additional unscheduled sampling was conducted for specific reasons (*i.e.*, vegetation sampling during November 1996 to evaluate potential deposition following the October 1996 release incident).

4.1.4 Data Cleanup and Quality Assurance/Quality Control

The initial methodological step involved a complete quality assurance/quality control (QA/QC) evaluation of the extracted SHTC dataset to identify and attempt to fill existing data gaps with supplementary information from BOVAR or CanTox Inc. QA/QC datastamps and surrogate recovery rates for the laboratory chemical extractions of each sample set were evaluated to ensure the quality of the data being used.

4.2 Development of TCDD PBPK Prototype Models

To evaluate the potential efficacy and validity of the use of physiologically-based pharmacokinetic models as a appropriate tool in the assessment of health risks related to environmental exposure to POPs, a thorough review of the scientific literature was conducted to select the most appropriate PBPK model methodology for absorption, disposition, metabolism, and excretion (ADME) of PCDD/Fs. A steady-state (time-dependent) PBPK model, proposed by Wang *et al.* (1997) was selected as the prototype analysis model for the current research.

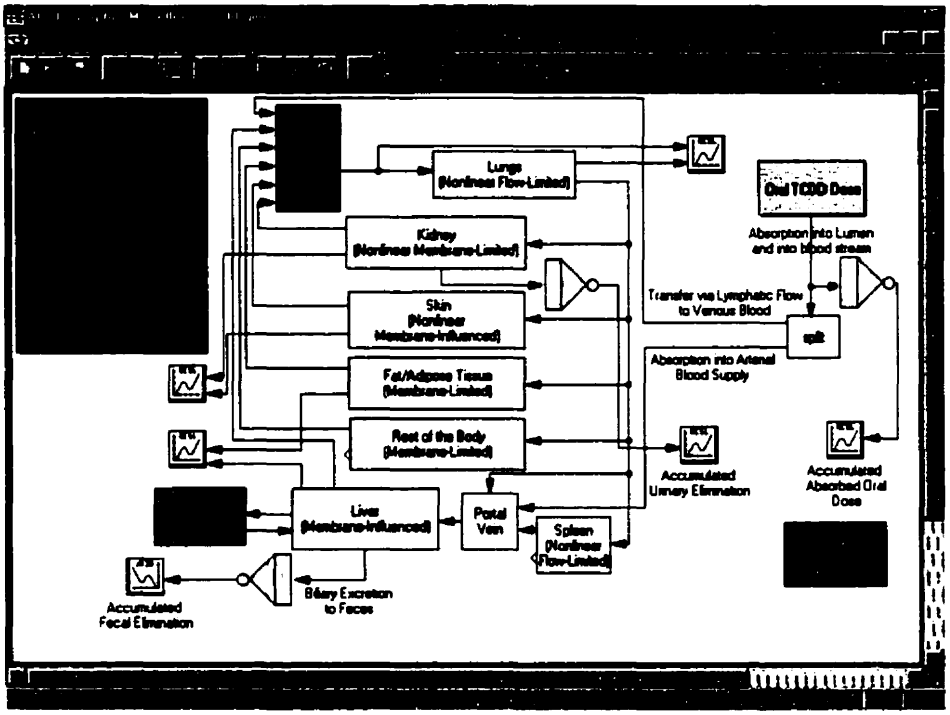
To evaluate potential "over-parameterization" of existing steady-state based models (*i.e.*, Wang *et al.*, 1997), an additional less-complex, equilibrium-based model, described by Evans and Andersen (2000), was also evaluated.

4.2.1 Steady- State PBPK Model

The Wang *et al.* (1997) was selected as the prototype steady state-based (time-dependent) PBPK model to evaluate the absorption, disposition, metabolism, and excretion (ADME) of TCDD for the current research project. A complete overview of the methodology and mathematical equations used in this model is provided in Section A-1 of the Appendix. The model was programmed in the *Advanced Continuous Simulation Language* (ACSL) PBPK programming system, based upon the methodology published in Wang *et al.* (1997). The ACSL Tox software suite, which includes the ACSL Model (PBPK model design), ACSL Optimize (PBPK parameter estimation, optimization, and sensitivity analysis) and ACSL Math (Monte Carlo routines, transformations, graphing, *etc.*), was licensed from the Pharsight Corporation (product support and distributor for developer, AEgis software). The model system was run on a Pentium-II 200 MHz computer (with 128 MB of RAM) running the Windows NT 4.0 operating system.

Figure 4.1 shows a graphical representation of the developed PBPK model within the ACSL modelling system.

Figure 4.1 Screenshot of TCDD PBPK Model developed in the ACSL Modelling System



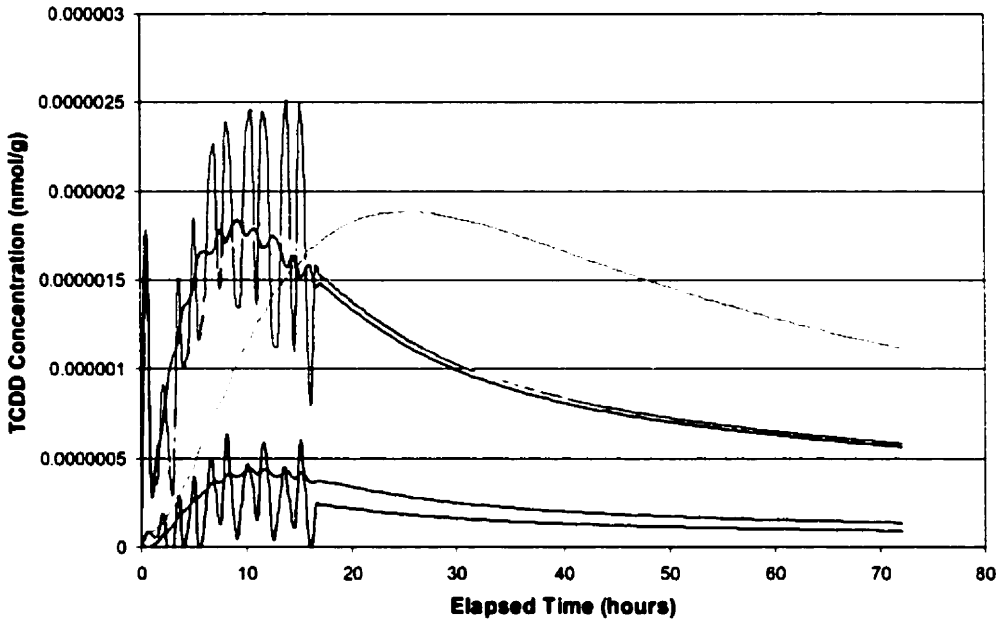
4.2.1.1 Revisions to Prototype PBPK Model

Inaccuracies and gaps within the published methodologies were noted during the development of the model and corrected by incorporation of methodologies from other original source literature (*i.e.*, source material referenced within Wang *et al.*, 1997) and more recent publications by these and other authors (*i.e.*, Wang *et al.*, 2000, DeVito *et al.*, 1997; Santostefano *et al.*, 1998; Evans and Anderson, 2000). These inaccuracies included incorrectly transcribed formulas for certain tissue groups, as well as incomplete descriptions of certain formula steps with the model methodology (particularly with respect to binding interactions between the liver and CYP1A2 compartments, and related physiological induction delays).

This initial model was also demonstrated to be highly unstable at low administered doses. Given the need to evaluate the extremely low concentration levels typically found within environment and tissue of biota, this posed a definite impediment to its use as a suitable model to evaluate potential toxicity and risk. An extensive breakdown and evaluation of the model methodology

indicated that low ligand concentrations resulted in numerical artifacts in the nonlinear Ah-TCDD binding term. These numerical difficulties appear to be related to the inability of the model (or modelling software) to properly calculate implicit differential equations at very low doses, resulting in oscillations in predicted compartment-specific TCDD concentrations. Figure 4.2 demonstrates the fluctuations present in the model's ability to calculate various tissue concentrations in a Sprague-Dawley rat at an administered dose of 0.001 μg/kg bodyweight.

Figure 4.2 Example of TCDD Tissue Concentration Fluctuations in Model Predictions at Low Administered Doses



Further research and brief discussions with the model's original author (X. Wang, personal communication, 2001) indicated that at low doses, where the amount of available TCDD ligand is significantly less than the Ah receptor binding coefficient (K_d), TCDD sequestration related to the nonlinear binding term (*i.e.*, binding to the Ah receptor) could be essentially eliminated. This can be confirmed by an evaluation of the underlying Michaelis-Menton kinetics, where at very low concentrations ligand (*i.e.* $[L] << K_d$), receptor occupancy occurs but may be trivial (*i.e.*, the curve approaches 0% occupancy of receptors) (Lucier *et al.*, 1993).

Further testing also indicated that these mathematical resolution issues could also be alleviated by greatly reducing the size of the iterative timestep within each ACSL model run (*i.e.*, from the model's typical timestep of one hour to as low as measurements every 5 minutes). Reduction of the iterative timestep allowed for improved mathematical resolution of the differential equations used within certain compartments, but resulted in an extended run time of computer simulations.

Other modifications/improvements made to the base model for the current project included: i) the ability to provide the administered dose as a one-time bolus (*i.e.*, acute exposure) or as a constant dose spread over time (*i.e.*, chronic exposure); ii) the ability to either maintain the initial bodyweight or allow growth of the test organism, and; iii) the ability to better control the proportion of administered dose that is transferred *via* lymphatic flow into the venous blood supply and that which is directly absorbed into the arterial blood supply. Finally, to evaluate the potential impacts of CYP1A2 ligand binding on overall disposition patterns (*i.e.*, liver *versus* adipose sequestration ratios), the ability to diminish or completely disable binding to CYP1A2 was incorporated into the developmental PBPK model.

4.2.1.2 Development of a Multi-scenario Managing Interface

While the ACSL Tox modelling system provides an excellent design and programming environment in which to develop a complex PBPK model, it is not well suited for detailed evaluations under multiple scenario, chemical, and species designs.

To bridge this gap, and allow for the necessary output and statistical analyses required for the current research project, an interactive interface was created in Microsoft Excel™ (version 7.0, Microsoft Corporation) using underlying Windows DDE (direct data exchange) systems to link the spreadsheet with the underlying ACSL model system. This shell spreadsheet allowed for easy transition between test organisms (*i.e.*, Sprague-Dawley rats, C57BL/6J mice, and red-backed voles), test chemicals (*i.e.*, 2,3,7,8-TCDD, 2,3,7,8-TCDF, 1,2,3,7,8-PeCDF, 2,3,4,7,8-PeCDF) and exposure scenarios (*i.e.*, differing exposure concentrations, durations, *etc.*) by passing the representative PBPK data to the underlying model based upon the user's selection. Upon model run completion, all relevant compartment- and run-specific data was automatically

displayed and analysed by the shell system. Figures 4.3 through 4.5 provide screenshots of the developed Excel-based model interface, while Figures 4.6 through 4.8 provide screenshots of both tissue-specific and receptor binding results from a completed model run. It should be noted that Windows DDE support appears to have degraded badly from Windows NT version 4.0 (the operating system on which the model was run) to more current versions of the Windows platform (*i.e.*, Windows 98 and Windows ME). Considerable frustration was incurred by this researcher when he attempted to upgrade to a research machine using an operating system other than Windows NT.

Monte-Carlo simulations and uncertainty/sensitivity analyses were conducted using the Crystal Ball (Decisioneering Limited) simulation add-on (version 4.0c) to the MS Excel environment.

Figure 4.3 **Scenario-specific Data Entry for Excel-Based Interface to the Prototype PBPK Model.**

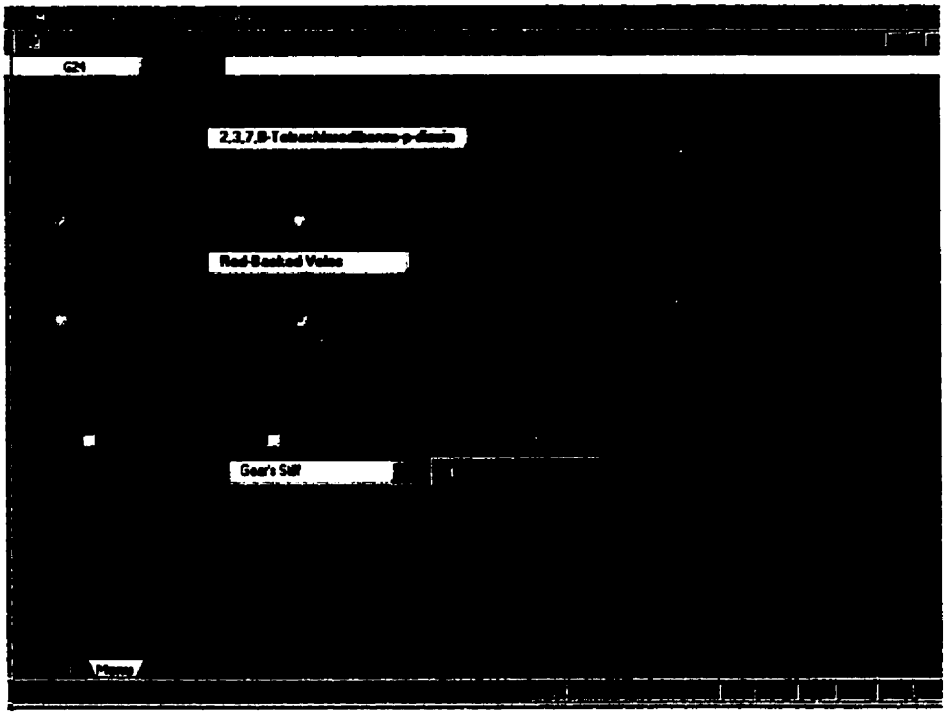
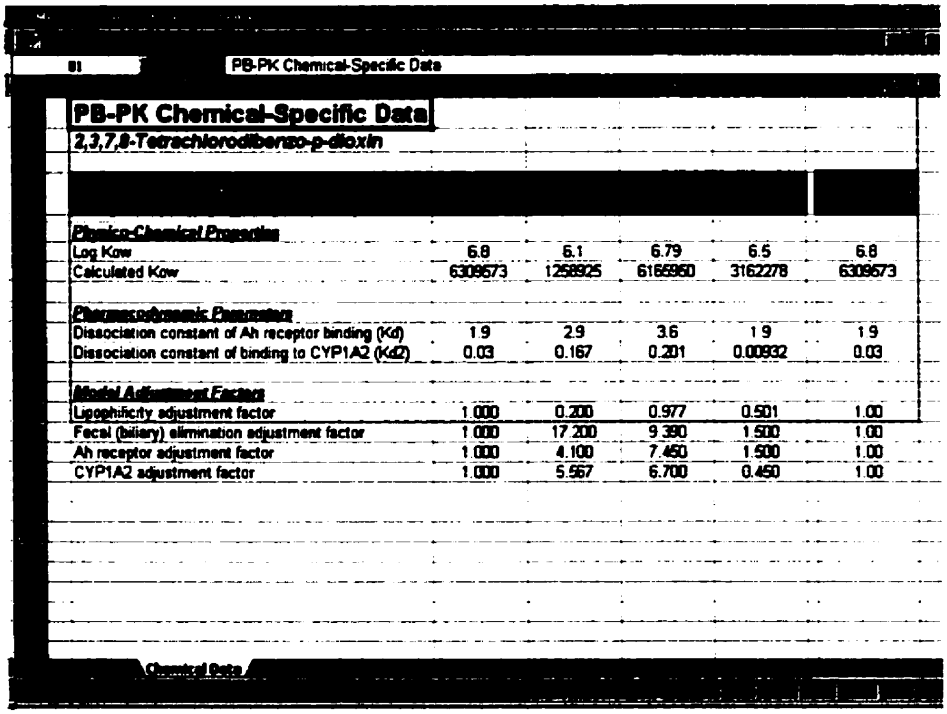


Figure 4.4 **Chemical-specific Data Entry for Excel-Based Interface to the Prototype PBPK Model.**

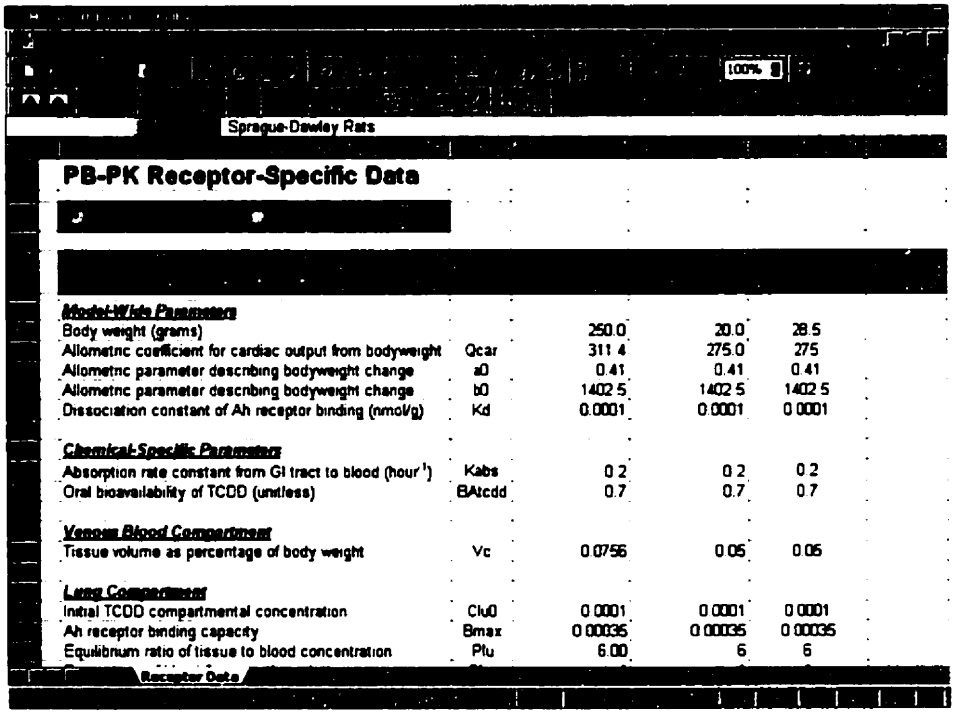


PB-PK Chemical-Specific Data

2,3,7,8-Tetrachlorodibenzo-p-dioxin

Physico-Chemical Properties					
Log Kow	6.8	6.1	6.79	6.5	6.8
Calculated Kow	6309573	1258925	6165950	3162278	6309573
Pharmacodynamic Parameters					
Dissociation constant of Ah receptor binding (Kd)	1.9	2.9	3.6	1.9	1.9
Dissociation constant of binding to CYP1A2 (Kd2)	0.03	0.167	0.201	0.00932	0.03
Model Adjustment Factors					
Lipophilicity adjustment factor	1.000	0.200	0.977	0.501	1.00
Fecal (biliary) elimination adjustment factor	1.000	17.200	9.390	1.500	1.00
Ah receptor adjustment factor	1.000	4.100	7.460	1.500	1.00
CYP1A2 adjustment factor	1.000	5.567	6.700	0.450	1.00

Figure 4.5 Species-Specific Data Entry for Excel-Based Interface to Prototype PBPK Model



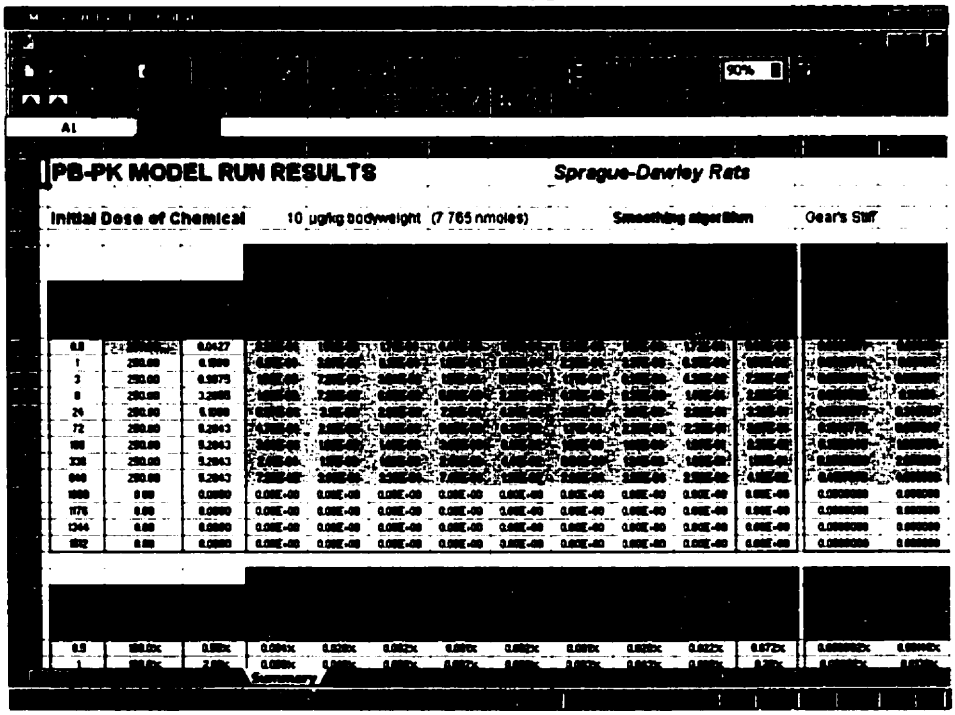
Sprague-Dawley Rats

PB-PK Receptor-Specific Data

Model-Wide Parameters				
Body weight (grams)		250.0	20.0	28.5
Allometric coefficient for cardiac output from bodyweight	Qcar	311.4	275.0	275
Allometric parameter describing bodyweight change	a0	0.41	0.41	0.41
Allometric parameter describing bodyweight change	b0	1402.5	1402.5	1402.5
Dissociation constant of Ah receptor binding (nmol/g)	Kd	0.0001	0.0001	0.0001
Chemical-Specific Parameters				
Absorption rate constant from GI tract to blood (hour^{-1})	Kabs	0.2	0.2	0.2
Oral bioavailability of TCDD (unitless)	BAtcdd	0.7	0.7	0.7
Venous Blood Compartment				
Tissue volume as percentage of body weight	Vc	0.0756	0.05	0.05
Lung Compartment				
Initial TCDD compartmental concentration	Clu0	0.0001	0.0001	0.0001
Ah receptor binding capacity	Bmax	0.00035	0.00035	0.00035
Equilibrium ratio of tissue to blood concentration	Plu	6.00	6	6

Receptor Data

Figure 4.6 Interactive Model Run Results Displayed in Excel-Based Interface to Prototype PBPK Model



PB-PK MODEL RUN RESULTS — *Sprague-Dawley Rats*

Initial Dose of Chemical: 10 ug/kg bodyweight (7.765 nmoles) — Smoothing algorithm: Gear's Stiff

Summary

Figure 4.7 Overview of PBPK Model Results Displayed in Excel-Based Interface to Prototype PBPK Model.

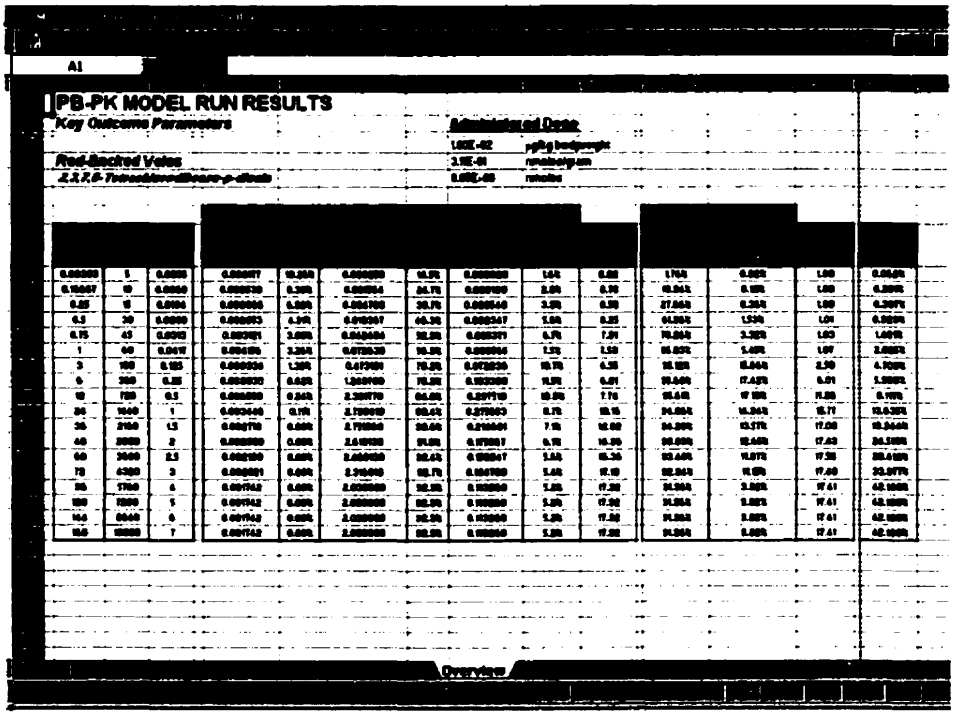
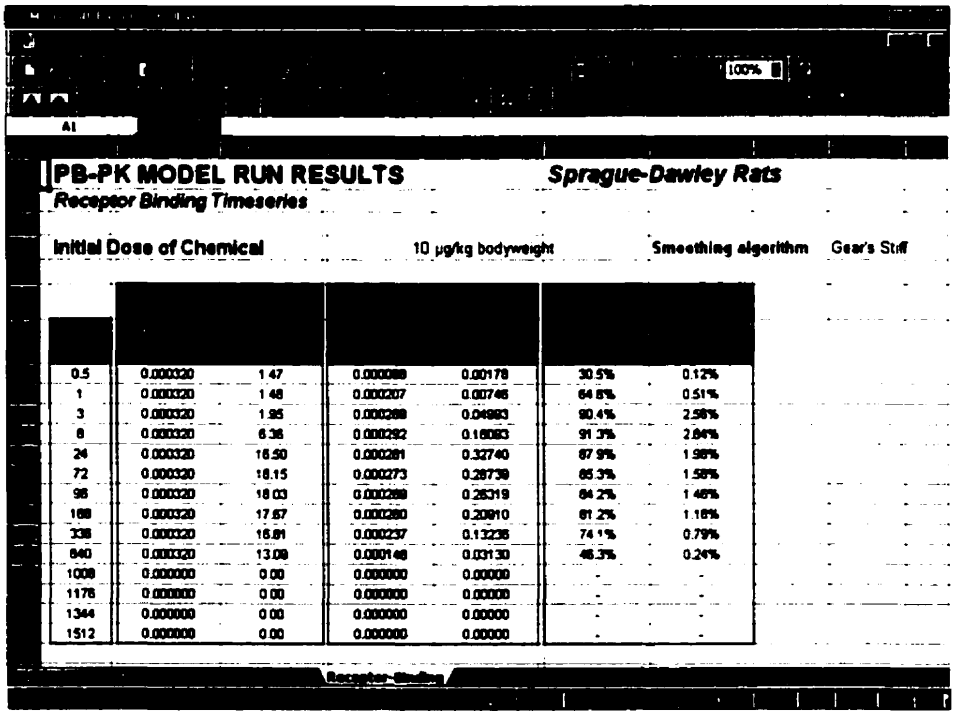


Figure 4.8 Receptor Binding Run Results Displayed in Excel-Based Interface to Prototype PBPK Model.



0.5	0.000320	1.47	0.000088	0.00178	30.5%	0.12%
1	0.000320	1.48	0.000207	0.00746	64.8%	0.51%
3	0.000320	1.95	0.000288	0.04983	90.4%	2.56%
8	0.000320	6.38	0.000292	0.18083	91.3%	2.84%
24	0.000320	16.50	0.000281	0.32740	87.9%	1.98%
72	0.000320	16.15	0.000273	0.28739	85.3%	1.78%
96	0.000320	18.03	0.000269	0.26319	84.2%	1.46%
168	0.000320	17.67	0.000260	0.20910	81.2%	1.18%
336	0.000320	16.81	0.000237	0.13236	74.1%	0.79%
840	0.000320	13.09	0.000148	0.03130	46.3%	0.24%
1008	0.000000	0.00	0.000000	0.00000	-	-
1176	0.000000	0.00	0.000000	0.00000	-	-
1344	0.000000	0.00	0.000000	0.00000	-	-
1512	0.000000	0.00	0.000000	0.00000	-	-

4.1.2.3 Species-Specific Physiological Data

Three distinct species of rodents, the Sprague-Dawley rat, the C57BL/6J mouse, and the red-backed vole, were selected as test organisms to evaluate the efficacy and validity of the selected equilibrium-based PBPK methodology for assessing the disposition of TCDD within living organisms. While there are similarities in the pharmacokinetics of TCDD between various test species, there are also subtle differences between species that must be incorporated into the proposed PBPK methodology.

Sprague-Dawley Rat

The initial model, based upon the Wang *et al.* (1997) methodology, was developed using the Sprague-Dawley rat as the test organism. Biological and physiological parameters for this rat strain were obtained from the Wang *et al.* (1997) source paper.

C57BL/6J Mouse

As a mid step between the rat and vole specific PBPK models, physiological parameters for the C57BL/6J mice were gathered. The C57BL/6J mouse is a hybrid mouse strain (based on the C57 black laboratory mouse), weighing approximately 20 grams, and was selected due to its general similarities to those physiological parameters found in the red-backed vole sentinel species. Biological and physiological parameters for this mouse strain were obtained from the research presented by Wang *et al.* (2000), or modified allometrically as a function of bodyweight from data presented in Wang *et al.* (1997).

To evaluate the appropriateness of these parameters, experimental data provided by Diliberto *et al.* (1999) were compared to the results of the PBPK model run under similar exposure conditions (*i.e.*, 25 μg TCDD/kg bodyweight). Results of this comparison indicated that both the urinary and fecal excretion rates provided in Wang *et al.* (2000) were too low and under-estimated the contribution of TCDD elimination at the earlier exposure periods (*i.e.*, ≤4 days). In a study involving TCDD-treated mice, fecal excretion of TCDD-derived radioactivity ranged from 18% to 28% of administered dose by 4 days (Diliberto *et al.*, 1999). Results of multiple test

runs indicated that values of 1.5 and 6 hour^{-1} provided better matches to the presented time-series results for urinary and fecal excretion, respectively.

Wang *et al.* (2000) also recommended that 1.5 nmoles/gram of liver tissue be selected as the basal level of CYP1A2 with the liver. However, modelling analysis indicated that this value resulted in an underestimation in the level of CYP1A2 within the liver, and a related lower calculated liver-to-fat ratio when compared to the Diliberto *et al.* (1999) experimental results. Testing of the revised model indicated that using a value of 1.6 nmoles/gram (as specified for the Sprague-Dawley rats) resulted in sequestration patterns which more accurately reflected the experimental data. Fit between experimental data and model results were further improved by reducing the CYP1A2 physiological delay period to 1 hour from the value of 1.5 hours suggested in Wang *et al.* (2000).

Table 4.5, below, provides a summary of the parameter revisions made to the prototype PBPK model to better fit the experimental results observed for C57BL/6J mice.

Table 4.5 Summary of Parameter Revisions made to Better Fit the Prototype PBPK Model to C57BL/6J Mice Experimental Results (Diliberto *et al.*, 1999).

Parameter	Original Value	Revised Value
Urinary excretion rate (hour^{-1})	1	1.5
Fecal excretion rate (hour^{-1})	2.2	6
Basal level of CYP1A2 in liver (nmoles/gram)	1.5	1.6
CYP1A2 physiological delay period (hours)	1.5	1

Gapper's Red-backed Vole

Vole biological and physiological parameters was gathered from researchers using voles as their investigative species, and the scientific literature. Any remaining data gaps were filled using allometrically adjusted data obtained from Wang *et al.* (1997) or other relevant studies (Andersen *et al.*, 1997a; Diliberto *et al.*, 1996; Kedderis *et al.*, 1991; Webber *et al.*, 1993). Given the minimal amount of data available for voles (particularly related to liver-based metabolism), many of the parameters were assumed to be equivalent to those used to characterize the C57BL/6J mouse, given the similar sizes and organ weights.

Tissue-specific organ weights for red-backed voles were obtained from an extensive database of small mammal and bird sampling measurements (Mallory, 2001) and are presented below in Table 4.6.

Table 4.6 Red-backed Vole Summary Organ Weights (Mallory, 2001). [a]

Parameter	Weight (grams)				
	Total	Liver	Lungs	Kidneys	Spleen
Both Sexes					
Count (n)	421	420	419	418	389
Mean	28.5	1.7	0.364	0.264	0.164
Standard Deviation	7.2	0.985	0.164	0.0785	0.187
Male Voles					
Count (n)	247	246	246	246	233
Mean	28.6	1.66	0.362	0.268	0.187
Standard Deviation	6.65	1.17	0.143	0.0761	0.212
Female Voles					
Count (n)	174	174	173	172	165
Mean	28.4	1.77	0.366	0.257	0.131
Standard Deviation	7.94	0.634	0.191	0.0814	0.14

[a] Confidential red-backed vole data was provided by Dr. Frank Mallory of Laurentian University. This data is not to be used without the express permission of Dr. Mallory (fmallory@nickel.laurentian.ca).

Using a daily consumption rate of 0.31 g/g/d for the Gapper's red-backed vole (McManus, 1974), daily consumption rates of congener-specific PCDD/F concentrations in environmental media can be estimated from the PCDD/F concentrations detected in surrounding biota (*i.e.*, Labrador tea and moss).

Table 4.7 provides a list of the species-specific physiological parameters used in the TCDD PBPK model, for each of the three test species.

Table 4.7 PBPK Physiological Parameters Selected for each Test Species.

Parameters	Abbr.	Sprague-Dawley Rats [a]	C57BL/6J Mice [b]	Red-Backed Voles [c]
Model-Wide Parameters				
Body weight (grams)		250	20	28.5 [f]
Allometric coefficient for cardiac output from bodyweight	Qcar	311.4	275 [e]	275 [f]
Allometric parameter describing bodyweight change	a0	0.41	0.41 [a]	0.41 [a]
Allometric parameter describing bodyweight change	b0	1402.5	1402.5 [a]	1402.5 [a]
Dissociation constant of Ah receptor binding (nmole/g)	Kd	0.0001	0.0001	0.0001
Chemical-Specific Parameters				
Absorption rate constant from GI tract to blood (hour^{-1})	Kabs	0.2	0.2 [a]	0.2 [a]
Oral bioavailability of TCDD (unitless)	BAtcdd	0.7	0.7 [a]	0.7 [a]
Venous Blood Compartment				
Tissue volume as percentage of body weight	Vc	0.0756	0.05 [e]	0.05
Lung Compartment				
Initial TCDD compartmental concentration	Clu0	0.0001	0.0001	0.0001
Ah receptor binding capacity	Bmax	0.00035	0.00035	0.00035
Equilibrium ratio of tissue to blood concentration	Plu	6	6	6
Percentage of blood flow rate through tissue	Qluc	1	1	1
Fraction of overall tissue volume composed of blood	Vbc	0.568	0.568 [d]	0.568 [d]
Tissue volume as percentage of body weight	Vluc	0.00324	0.0073 [e]	0.00553 [f]
Kidney Compartment				
Initial TCDD compartmental concentration	Clu0	0.0001	0.0001	0.0001
Ah receptor binding capacity	Bmax	0.00025	0.00025	0.00025
Urinary excretion rate (hour^{-1})	Kk	1.0	1.5 [g]	1.5
Membrane permeability*area / blood flow rate	PAc	0.010	0.01	0.01
Equilibrium ratio of tissue to blood concentration	Pk	6	10	10
Percentage of blood flow rate through tissue	Qkc	0.141	0.141 [d]	0.141 [d]
Fraction of overall tissue volume composed of blood	Vbc	0.189	0.189 [d]	0.189 [d]
Tissue volume as percentage of body weight	Vkc	0.00656	0.0167 [e]	0.0075 [f]
Skin Compartment				
Initial TCDD compartmental concentration	Clu0	0.0001	0.0001	0.0001
Ah receptor binding capacity	Bmax	0.00005	0.00005	0.00005
Membrane permeability*area / blood flow rate	PAc	0.09	0.07	0.07
Equilibrium ratio of tissue to blood concentration	Ps	10	20	20
Percentage of blood flow rate through tissue	Qsc	0.058	0.058 [d]	0.058 [d]
Fraction of overall tissue volume composed of blood	Vbc	0.0201	0.0201 [d]	0.0201 [d]
Tissue volume as percentage of body weight	Vsc	0.183	0.1653 [e]	0.1653
Adipose Tissue Compartment				
Membrane permeability*area / blood flow rate	PAc	0.08	0.12	0.12
Equilibrium ratio of tissue to blood concentration	Pf	100	125 [g]	125
Percentage of blood flow rate through tissue	Qfc	0.0699	0.0699 [d]	0.0699 [d]
Fraction of overall tissue volume composed of blood	Vbc	0.0503	0.0503 [d]	0.0503 [d]
Tissue volume as percentage of body weight	Vfc	0.0692	0.068 [e]	0.068

Table 4.7 PBPK Physiological Parameters Selected for each Test Species.

Parameters	Abbr.	Sprague-Dawley Rats [a]	C57BL/6J Mice [b]	Red-Backed Voles [c]
Rest of the Body Compartment				
Membrane permeability*area / blood flow rate	PAc	0.030	0.03	0.03
Equilibrium ratio of tissue to blood concentration	Pre	1.5	3	3
Percentage of blood flow rate through tissue	Qrec	0.548	0.548 [d]	0.548 [d]
Fraction of overall tissue volume composed of blood	Vbc	0.0298	0.0298 [d]	0.0298 [d]
Tissue volume as percentage of body weight	Vrec	0.470	0.512 [e]	0.512
Spleen Compartment				
Initial TCDD compartmental concentration	Clu0	0.0001	0.0001	0.0001
Ah receptor binding capacity	Bmax	0.0001	0.0001	0.0001
Equilibrium ratio of tissue to blood concentration	Psp	5	5	5
Percentage of blood flow rate through tissue	Qspc	0.017	0.017 [d]	0.017 [d]
Fraction of overall tissue volume composed of blood	Vbc	0.273	0.273 [d]	0.273 [d]
Tissue volume as percentage of body weight	Vspc	0.00176	0.0035 [e]	0.00418 [f]
Liver Compartment				
Initial TCDD compartmental concentration	Clu0	0.0001	0.0001	0.0001
Ah receptor binding capacity	Bmax	0.00035	0.00035	0.00035
Dissociation constant of binding to CYP1A2	Kdcyp	0.030	0.035	0.035
Biliary elimination rate (hour^{-1})	Kli	2.20	6 [g]	6
Membrane permeability*area / blood flow rate	PAc	0.35	0.35	0.35
Equilibrium ratio of tissue to blood concentration	Pli	6	6	6
Percentage of blood flow rate through tissue	Qc	0.183	0.183 [d]	0.183 [d]
Fraction of overall tissue volume composed of blood	Vbc	0.266	0.266 [d]	0.266 [d]
Tissue volume as percentage of body weight	Vc	0.0362	0.0549 [e]	0.0438 [f]
CYP1A2 Compartment				
Basal level of CYP1A2 within the liver (nmole/gram)	Ccyp0	1.6	1.6 [g]	1.6
Hill coefficient (unitless)	h	0.6	0.6 [d]	0.6 [d]
Value to cause half of the maximum induction folds	ICa2	0.13	0.13 [d]	0.13 [d]
Maximum induction folds over the basal induction rate	INa2	600	600 [d]	600 [d]
First-order degradation rate constant of binding (1/hour)	K2	0.1	0.1	0.1
CYP1A2 physiological holding time (hours)	tau	0.25	1.0 [g]	1

[a] Data obtained from Wang *et al.* (1997), unless otherwise specified.
[b] Data obtained from Wang *et al.* (2000), unless otherwise specified.
[c] Assumed based upon C57BL/6J mouse data, unless otherwise specified.
[d] Assumed based upon Wang *et al.* (1997).
[e] Obtained from ILSI PBPK database information presented in Brown *et al.* (1997).
[f] Data obtained from red-backed vole sampling database (Mallory, 2001).
[g] Data obtained based upon fitting model results to experimental results (Diliberto *et al.*, 1999).

The chemical-specific parameters used in the evaluation of gastrointestinal absorption of TCDD (*i.e.*, absorption rate constant and oral bioavailability) were assumed equivalent across the various species. Research has indicated that no interspecies differences have been observed for the absorption of PCDDs and PCDFs from the gastrointestinal (GI) tract. This is thought to be due to molecular size and solubility being the rate limiting factors for GI tract absorption (Van den Berg *et al.*, 1994).

Where species-specific data were unavailable, data from the better characterized Sprague-Dawley rat or C57BL/6J mouse were substituted. This was viewed as a reasonable approach given that most of these parameters were allometrically-linked to the tissue volume of the specific compartment, and species-specific tissue volumes were available for all compartments in almost every case.

An extensive review of the scientific literature, as well as discussions with various laboratories conducting research with voles, failed to provide any suitable information on which to base ligand-receptor parameter selection (*i.e.*, for either the Ah or CYP1A2 receptor systems) for the vole sentinel receptor. Given this lack of information, data from the physiologically-similar C57BL/6J mouse receptor were used to represent the necessary ligand-receptor data in the vole receptor.

4.1.2.4 Chemical-Specific Physiological Data

The initial prototype PBPK model was developed to evaluation the pharmacokinetic disposition of TCDD within the Sprague-Dawley rat. However, while TCDD is the most toxic of the PCDD/F congeners and is commonly the primary focus of environmental risk assessments, chemical analyses of environmental media and biotic receptors have indicated that TCDD typically makes up a very minor component (approximately 0.8%) of the total PCDD/F mass (Czuczwa and Hites, 1995; Rappe *et al.*, 1987). This trend has also been observed in the chemical analyses conducted on environmental biota sampled as part of the SHTC long-term monitoring program, with results indicating very low or non-detect TCDD biotic concentrations in most cases (presented in Results section). This pattern is primarily due to the congener-specific pattern, or "fingerprint", typically associated with the combustion releases from an incineration process (*i.e.*, furans, particularly the PeCDFs, tend to dominate). A more detailed discussion of this pattern and congener-specific fingerprinting can be viewed in this researcher's Masters thesis project (Ferguson, 1998).

Given the particular congener-specific fingerprint associated with incineration facility emissions and the very low levels of TCDD detected in the biota sampled as part of the SHTC monitoring program, it was necessary to attempt to evaluate other congeners of interest, in addition to TCDD. Based upon the typical fingerprint demonstrated in chemical samples, three additional congeners were selected for evaluation: i) 2,3,7,8-tetrachlorodibenzofuran (TCDF); ii) 1,2,3,7,8-pentachlorodibenzofuran (1-PeCDF), and; iii) 2,3,4,7,8-pentachlorodibenzofuran(4-PeCDF). To adapt the current TCDD-based model for these structurally-related congeners, the shell interface was designed to allow for the adjustment of key pharmacokinetic and pharmacodynamic parameters.

Given that the current PBPK model was developed for TCDD and that many of its parameters were "fitted" to experimental data derived from exposures to TCDD, ratio-based adjustments to the existing TCDD-derived parameters are more appropriate than simply substituting values obtained for each parameter from the literature (S. Safe, personal communication, 2001).

As noted previously, the disposition (and ultimate toxicity) of the PCDD/F congeners is controlled by four key chemical-specific factors: 1) the lipophilicity of the chemical; 2) the Ah receptor ligand-specific affinity; 3) CYP1A2 sequestration affinity, and; 4) metabolism of the chemical.

Lipophilicity of the Chemical

To account for differing pharmacokinetic disposition due to the chemical's lipophilicity, a lipophilicity adjustment factor was calculated for each congener based upon the ratio of its octanol-water partition coefficient (K_{ow}) to that of TCDD. This lipophilicity adjustment factor was then used to update the equilibrium ratio of tissue to blood concentration for each compartment (*e.g.*, the equilibrium ratio for the lung compartment of 6 was adjusted by 0.2 for TCDF to provide a TCDF-specific equilibrium ratio of 1.2). The chemical-specific K_{ow} values were calculated from the respective log K_{ow} values presented in USEPA (2000). Table 4.8, below, provides the specific calculation parameters and calculated lipophilicity adjustment factor, for each of the assessed congeners.

Table 4.8 Specific parameters used in the calculation of congener-specific lipophilicity adjustments.

Chemical	Log K_{ow} [a]	Estimated K_{ow}	Lipophilicity Adjustment Factor
2,3,7,8-TCDD	6.8	6310000	1
2,3,7,8-TCDF	6.1	1260000	0.2
1,2,3,7,8-PeCDF	6.79	6170000	0.977
2,3,4,7,8-PeCDF	6.5	3160000	0.501

[a] U.S. EPA (2000)

Following an oral dose, TCDD and related lipophilic compounds are delivered to the blood circulation *via* the lymphatic system as well as *via* the GI tract (Lakshmanan *et al.*, 1986). As noted in Wang *et al.* (1997), the process of absorption for lipophilic compounds by the GI tract and delivery into the blood circulation *via* the lymphatic system were analyzed in detail by Roth *et al.* (1993), and were simplified in the current model through the use of specific empirical parameters K_{abs} and K_{st}. The emptying rate of the stomach (K_{st}) is an organism-specific value, and

would not differ with the particular congener under study. The fraction of total dose absorbed (K_{abs}) was estimated for TCDD by Wang *et al.* (1997) by fitting the model to the tissue distribution. Given that research has demonstrated that plasma lipoproteins act as carriers for extremely hydrophobic chemicals (Roth *et al.*, 1993) and that the chemicals being assessed have very similar lipophilicity, it was assumed that the K_{abs} value for TCDD absorption would be suitably representative for the other assessed congeners. This assumption is strengthened by studies into PeCDF absorption and elimination by Brewster and Birnbaum (1987) which showed that more than 70% of the administered dose was absorbed from the gut, independent of the amount of PeCDF administered in the dose range studied.

The potency of the ligand for eliciting a response (*i.e.*, the dose-response relationship) is dependent upon the properties of *affinity* and *efficacy*. Affinity refers to the strength of the interaction, or binding, with the receptor, and is a property of the ligand and receptor. Efficacy, on the other hand, is the ability of that ligand-receptor complex to ultimately produce a response and is influenced by both ligand- and tissue-specific properties (Hestermann *et al.*, 2000). While separation of receptor-ligand action into the properties of affinity and efficacy allows for improved prediction of the behaviour of complex mixtures of ligands, as well as mechanistic comparison across species and toxic endpoints (Hestermann *et al.*, 2000), the current PBPK models only attempt to address the impacts of ligand-receptor affinity when evaluating ligand binding to the Ah and CYP1A2 receptor systems.

Chemical-specific variations in ligand affinity to both the Ah and CYP1A2 receptor systems are primarily governed by the dissociation constants (K_D) for each of the receptors. There is considerable uncertainty with respect to the methodology used to calculate these ligand-specific K_D values. The K_D values are dependent on ligand, the source of the cytosol preparation, and the assay procedures (Safe, 1988). Absolute values for ligand-receptor binding affinities are typically calculated from studies of competitive displace of ^{3}H-TCDD or saturation binding studies using Woolf or Scatchard plot analysis (a graph used to study molecular interaction in a mixed population of molecules in which different types of molecules are bound reversibly to one another). However, research has demonstrated that the rat cytosolic Ah receptor is thermally unstable, and therefore the results obtained from Scatchard plots are inaccurate and tend to

significantly overestimate the true value of K_D (Brown *et al.*, 1992; Rosengren *et al.*, 1992). Furthermore, due to these issues some researchers question the accuracy of using Kd developed based upon these types of studies (Santostefano *et al.*, 1994).

Ah Receptor Ligand-Specific Affinity

To account for differences in the chemical-specific K_D values, in comparison to TCDD, pharmacodynamic adjustment factors for each receptor were calculated for each of the chemicals. The receptor-specific K_D values (to which the TCDD-based model was originally "calibrated") were then adjusted by these receptor-specific adjustment factors. Given the considerable variability in K_D values presented in the literature, largely due to the type of assay and the conditions under which it was conducted (*e.g.*, temperature, dose, *etc.*), it is likely that absolute K_D values are a lot less reliable than calculated adjustment factor ratios which are self-calibrating assuming similar assay conditions or estimation methodology.

A considerable amount of research in the past decade has been directed at the derivation of predictive ***Quantitative Structural-Activity Relationships*** (QSAR) and ***Quantitative Structure-Property Relationships*** (QSPR) models. Previous QSAR analyses suggest that steric, electrostatic, hydrophobic, hydrogen bonding and dispersion properties may all be important for Ah receptor binding affinity (Tuppurainen and Ruuskanen, 2000). A number of recent QSAR studies have indicated that the methodology appears to provide a reasonable estimate of Ah receptor binding affinity for a large number of biphenyls, dibenzofurans, and dibenzo-*p*-dioxins (Tuppurainen and Ruuskanen, 2000; So and Karplus, 1997; Waller and McKinney, 1995). Given the considerable uncertainty inherent in the use of experimentally derived Kd values, and the complete lack of Kd information on the 2,3,4,7,8-PeCDF congener in the scientific literature, it was decided that the development of pharmacodynamic adjustment factors, based upon the differences in QSAR-estimated binding affinities for each congener compared to that of TCDD, would be the more prudent methodology for the current investigation.

Using structure and affinity data, QSAR models developed by Tuppurainen and Ruuskanen (2000) predicted EC_{50} values of 10, 41.0, 74.5, and 15.0 nM (calculated by taking the -antilog

value of the pEC_{50} values: 8.000, 7.387, 7.128, and 7.824 M) for TCDD, TCDF, 1-PeCDF, and 4-PeCDF, respectively. The EC_{50} values are one representation of the ligand's affinity to the Ah receptor, and typically indicating the concentration of the ligand required to elicit half-maximal response expression (typically CYP1A *via* quantification of EROD activity) (Hestermann *et al.*, 2000). As such, as the receptor-ligand affinity (or EC_{50}) increases, the related K_D value will correlationally decrease.

Table 4.9 provides the chemical-specific EC_{50} values and calculated receptor adjustment factors for both receptor sets, used to produce revised K_D values for the other assessed congeners. For example, the species-specific Ah receptor K_D value assumed for TCDD in the prototype steady-state model (*i.e.*, 0.1 nM for the Sprague-Dawley rat) was multiplied by the calculated adjustment factor to produce a revised, chemical-specific Ah receptor K_D value for that particular species.

Table 4.9 Chemical-specific dissociation constants and calculated adjustment factors for Ah receptor affinity.

Chemical	Ah Receptor Affinity	
	EC_{50} (nM)	Adjustment Factor [a]
2,3,7,8-TCDD	10	1
2,3,7,8-TCDF	41	4.1
1,2,3,7,8-PeCDF	74.5	7.45
2,3,4,7,8-PeCDF	15	1.5

[a] As the adjustment factors will be applied to the species-specific Ah receptor K_D value, these factors represent an inverse function of the affinity (*i.e.*, as K_D increases, the ligand-receptor affinity decreases).

CYP1A2 Binding Affinity

Unfortunately, there is very little information in the scientific literature for the estimation of chemical-specific CYP1A2 dissociation constants, and conservative assumptions are typically used to estimate appropriate values. While quantification of enzyme induction, such as ACOH activity for CYP1A2, provides a good indication of relative potencies for the various congeners (DeVito *et al.*, 1997), they are indicators which combine the impacts of both Ah and CYP1A2 receptor binding events. As such, it would be difficult to estimate either the Ah or CYP1A2 ligand-receptor binding Kd based upon ACOH induction. There are a number of likely methods

to get around this difficulty (*e.g.*, mRNA expression assays, immuno-assays, extraction of CYP1A2 to an *in vitro* system for quantification of ligand binding, *etc.*). However, much of this research has been conducted on the CYP1A1 isozyme, with less focus being placed on its 1A2 counterpart.

The CYP1A2 dissociation constant (K_{D2}) for TCDD was estimated by fitting the parameter based upon experimental time course tissue distributions (Wang *et al.*, 1997). Research conducted by DeVito *et al.* (1998) provided disposition, in % dose/gram units, of various PCDDs and PCDFs over a range of doses, following a 13-week subchronic gavage study. Given the close similarities in the pharmacokinetics of TCDD and the other assessed congeners, at oral exposure doses sufficiently elevated as to result in maximal Ah receptor occupancy, one would expect any differences in congener-specific liver concentrations would be a result of differing CYP1A2 binding affinities. DeVito *et al.* (1998) reported liver-specific concentrations of 6.62, 1.19, 0.99, and 21.32 % dose/gram tissue for TCDD, TCDF, 1-PeCDF, and 4-PeCDF, respectively, at the highest administered dose level. Given these relative concentrations, the ratio of K_{D2} for CYP1A2 binding of each particular congener to that of TCDD was calculated as 5.56, 6.69, and 0.311 for TCDF, 1-PeCDF, and 4-PeCDF, respectively (*e.g.*, 6.62 / 1.19 = 5.56-fold for TCDF, *etc.*). This results in a calculated K_{D2} for CYP1A2 binding of 0.167, 0.201, and 0.00932 for TCDF, 1-PeCDF, and 4-PeCDF, respectively (*e.g.*, 0.03 nmole/gram * 5.56 = 0.167 nmole/gram tissue for TCDF, *etc.*). Given the lack of other suitable data, these chemical-specific values were used as initial values in the assessment of CYP1A2 ligand binding in the current study (see Table 4.10).

Model run results based upon these assumptions were compared to tissue distribution data for 4-PeCDF dosed C57BL/6N mice (Diliberto *et al.*, 1999). Based upon a 300 μg 4-PeCDF/kg bodyweight dose, model results indicated that the initial CYP1A2 K_{D2} estimated was over-estimating sequestration of 4-PeCDF in the liver. A more accurate reflection of the tissue distribution presented in Diliberto *et al.* (1999) was obtained when an adjustment factor of 0.45 (rather than previously estimated value of 0.311) was used.

Table 4.10 Chemical-specific dissociation constants and calculated adjustment factors for CYP1A2 receptor affinity.

Chemical	CYP1A2 Receptor Affinity	
	Dissociation Constant (K_{D2})	Adjustment Factor
2,3,7,8-TCDD	0.03 [a]	1
2,3,7,8-TCDF	0.167 [b]	5.56
1,2,3,7,8-PeCDF	0.201 [b]	6.69
2,3,4,7,8-PeCDF		
Initial	0.00932 [b]	0.311
Revised	-	0.45

[a] Wang *et al.* (1997).
[b] Calculated (see discussion above).

The Hill coefficient (h), which describes the interaction between the ligand-Ah receptor complex and the binding sites on DNA, was obtained for TCDD by Wang *et al.* (1997) by fitting their model with both time course and Day 3 tissue concentration data. Given this term represents the interaction between a bound Ah receptor and DNA binding sites at the DRE, and is biologically meant to loosely reflect the number of available DNA binding sites with cooperative binding interactions, the value calculated for TCDD by Wang *et al.* (1997) was assumed representative for the other assessed congeners (*i.e.*, species-specific, rather than chemical-specific). However, it is important to remember that this is ultimately a "fitted" parameter, based upon TCDD time-series data, and as such would have a degree of uncertainty associated with it when used for circumstances outside of the scenario for which the base model was designed. As it is a fitted parameter, the default value specified by Wang *et al.* (1997) of 0.6 was assumed for other assessed congeners.

Metabolism and Elimination of the Chemical

Finally, differing rates of metabolic breakdown of the individual congeners can play a significant role in disposition and excretion patterns within biological species. Although the relative rate of metabolism of TCDD and related compounds can be roughly estimated from tissue and excretion half-life data of the metabolic breakdown products, other factors such as relative body composition (*e.g.*, amount of adipose tissue), hepatic and extrahepatic binding proteins (*i.e.*, CYP1A1 and CYP1A2), and direct intestinal elimination of the parent compound can also

regulate excretion (mOlson *et al.*, 1994). In the current steady-state model, the biliary elimination of TCDD from the liver was assumed to follow first-order kinetics, since research has demonstrated that very little TCDD is subject to metabolic breakdown in the liver (Wang *et al.*, 1997). In addition, the excretion of TCDD parent compound and its metabolites from the liver *via* bile was also assumed to follow first-order kinetics. Given this, Wang *et al.* (1997) used on "lumped" empirical parameter to represent the unknown parameters of the metabolic and excretion rate constants. Research has also demonstrated that the amount of TCDD and its metabolites eliminated *via* urinary excretion is fairly small (Allen *et al.*, 1975; Diliberto *et al.*, 1996). It is believed that the excretion of metabolites from the kidney may be controlled by the metabolic rate in the liver or the membrane transfer process (Wang *et al.*, 1997). As such, the current model assumes first-order kinetics of urinary excretion, as shown previously by Birnbaum (1986). To calculate the chemical-specific excretion rates, a ratio of half-lives for each congener to that of TCDD was used to create congener-specific adjustment factors.

The elimination constants of TCDD from both kidney and liver were calculated by Wang *et al.* (1997) based on the kidney and liver time course data, as well as elimination data (Allen *et al.*, 1975; Diliberto *et al.*, 1996). As for TCDD (< 1.5%), studies have demonstrated that urinary excretion plays a very minor role in the clearance of TCDF (< 3%) and the PeCDFs (< 0.2%) from rodent species (Diliberto *et al.*, 1996; King *et al.*, 1983; Brewster and Birnbaum, 1987). As such, the urinary elimination constant for TCDD was assumed for the remaining assessed congeners.

Fecal elimination is the primary route of excretion for TCDD and the other assessed congeners. Three days after an oral dosing of TCDD in rats, fecal excretion of percentage administered dose was 32.2%, with an overall calculated biliary linear elimination constant of 2.2 ($hour^{-1}$) (Diliberto *et al.*, 1996). In studies on TCDD-treated C57BL/6N mice, fecal excretion was determined to be 28% of administered dose by 4 days, while in 4-PeCDF-treated C57BL/6N mice, fecal excretion was approximately 31% of administered dose by 4 days (Diliberto *et al.*, 1999). Rates of fecal excretion of TCDF, on the other hand, are considerably higher than those viewed in TCDD or the PeCDFs. Studies have demonstrated that the rat excretes 63 to 70% of an oral dose of TCDF in feces in 3 days (Birnbaum *et al.*, 1980).

As previously noted, model run results based upon these assumptions were compared to tissue distribution data for 4-PeCDF dosed C57BL/6N mice (Diliberto *et al.*, 1999). Based upon a 300 μg 4-PeCDF/kg bodyweight dose, model results indicated that the initial estimated fecal elimination adjustment factor was under-estimating the excretion rate of 4-PeCDF. A more accurate reflection of the tissue distribution presented in Diliberto *et al.* (1999) was obtained when an fecal elimination adjustment factor of 1.5 (rather than previously estimated value of 0.278) was used. This revised elimination adjustment factor appears to be more in line with the results of the experimental excretion data, where TCDD-treated C57BL/6N mice demonstrated fecal excretion of 28% of administered dose by 4 days, while in 4-PeCDF-treated C57BL/6N mice demonstrated fecal excretion of 31% of administered dose by 4 days (Diliberto *et al.*, 1999).

Table 4.11 provides the half-lives reported in a variety of studies for each congener, and the associated calculated excretion adjustment factor (*i.e.*, TCDD half-life divided by the congener-specific half-life).

Table 4.11 Congener-Specific Fecal Excretion Half-Lives and Calculated Adjustment Factor.

PCDD/F Congener	Half-Life (days)	Calculated Adjustment Factor	Reference
2,3,7,8-TCDD	31 [a]	1	Rose *et al.*, 1976
2,3,7,8-TCDF	1.8 [b]	17.2	Birnbaum *et al.*, 1980
1,2,3,7,8-PeCDF	3.3 [c]	9.39	Van den Berg *et al.*, 1989
2,3,4,7,8-PeCDF			
Initial	108 [d]	0.287	Van den Berg *et al.*, 1989
Revised	-	1.5 [e]	Estimated (see above)

[a] Calculated based upon an orally administered dose of 1.0 μg TCDD/kg to male and female Sprague-Dawley rats.
[b] Calculated based upon an iv administered dose of 0.1 μmol/kg to male Fischer 344 rats.
[c] Calculated based upon an orally administered dose of 4.0 μg 1-PeCDF/kg to female Sprague-Dawley rats.
[d] Calculated based upon an orally administered dose of 5.6 μg 4-PeCDF/kg to female Sprague-Dawley rats.
[e] Calculated by fitting PBPK model results to experimental data presented in Diliberto *et al.* (1999).

Due to inherent dose-dependencies in TCDF excretion, caution should be taken selecting one value for the elimination rate constant. In control, uninduced rat liver, the rate of TCDF metabolism was shown to be 2- to 7-fold greater than that of TCDD at dose rates between 0.01 and 0.1 μM, depending on the degree of CYP1A1 induction (Olson *et al.*, 1994). *In vitro* results suggest that TCDF is far more persistent in the rat at very low exposures due to little or no

induction of CYP1A1 and CYP1A2. However, as the current PBPK model does not have a sub-module for assessing the potential impacts of CYP1A1 metabolism and ultimate elimination *via* urinary and fecal excretion, it was conservatively assumed to be included in the fecal elimination term (*i.e.*, it is likely underestimating excretion and overestimating body burden TCDF concentrations at elevated exposure doses which highly induce CYP1A1).

4.1.2.5 Validation of Model Outcomes

Compartment-specific model outcomes were compared visually to those outcomes graphed in the Wang *et al.* (1997) paper to demonstrate an accurate reproduction of the published methodology. Model results were also compared to experimental time-series results provided by Wang *et al.* (1997) both visually, and by residual sums of squares analyses to demonstrate the applicability of predicted model results to those shown under experimental conditions.

Unfortunately, due to the lack of detailed compartment-specific data (*i.e.*, actual data, rather than the summaries available in the source literature), it is difficult to conduct any further detailed statistical analyses of the model's predictive accuracy (*i.e.*, *F*-test, *PRESS* statistic, *etc.*) and produce conclusions which themselves have statistical validity and meaning. A request was made to the primary author of Wang *et al.* (1997) for the actual raw data for the TCDD time-series experimental study to allow for a more detailed statistical analysis. Unfortunately, this data was no longer available (X. Wang, personal communication, 2001).

4.1.2.6 Sensitivity Analysis of Model Parameters

Limitations in the available data for adequately estimating PBPK model parameters results in the unintentional introduction of uncertainty into overall model predictions. Uncertainty typically refers to the lack of knowledge about specific factors, parameters, or models.

In order to evaluate the level of confidence that could be given to the calculations performed with the PBPK model, a series of quantitative and qualitative analyses were performed to characterize the uncertainty in the model structure, parameterization, and dose metric selection. A sensitivity

analysis was conducted on the current developed TCDD PBPK model based upon 5,000 MonteCarlo iterations, to determine which variables pose the largest influence on the ultimate outcome of the model (*i.e.*, overall body sequestration of TCDD). Extensive testing of model run performance at multiple doses and iteration counts indicated that at least 5,000 iterations were required to ensure proper model stability and that model outcomes were not being skewed by extreme selections from the distributional tails of model parameters.

Standardized probabilistic distributions were applied to each of the key compartmental parameters. Typically, where parameter-specific information was not available, a default standard deviation reflecting 10% of the mean was used. A normal distribution was applied to those "macro-biological" parameters thought to demonstrate natural variability within a given strain or species, while a triangular distribution was applied to those "micro-biological" parameters thought to demonstrate variance due to uncertainty in quantification or measurement of the underlying processes. As such, all mass transport parameters (*e.g.*, percentage of blood flow through the tissue, tissue volumes, membrane permeability, *etc.*) were assumed normally distributed, while all ligand-receptor parameters (*e.g.*, Ah receptor binding capacity, dissociation constant of binding to CYP1A2, hill coefficient, *etc.*) were assumed to be triangularly distributed.

Briefly, the normal distribution is typically used to describe many natural phenomena such as IQ's, people's heights, or the inflation rate. The parameters for the normal distribution are the mean and standard deviation, and typically adhere to the following three conditions: i) some value of the unknown variable is the most likely (the mean of the distribution); ii) the unknown variable could as likely be above or below the mean (symmetrical about the mean), and; iii) the unknown variable is more likely to be close to the mean than far away (*i.e.*, of the values of a normal distribution, approximately 68% are within one standard deviation of the mean.) (Morgan and Henrion, 1990).

The triangular distribution, on the other hand, demonstrates the distributional selection pattern when one knows the minimum, maximum, and most likely values. This distributional form is typically used in circumstances where a range of values are possible, but the underlying mechanism for the dispersal is unknown. The parameters for the triangular distribution are the

minimum, maximum, and likeliest values, and it typically follows the following three conditions: i) the minimum number of items is fixed; ii) the maximum number of items is fixed, and; iii) the most likely number of items falls between the minimum and maximum values, forming a triangular shaped distribution (Morgan and Henrion, 1990).

The PBPK model was run stochastically (*i.e.*, using Monte Carlo methods) for 5,000 iterations, and a quantification of the sensitivity of each parameter was achieved by computing rank correlation coefficients between each key variable and the distribution of outcomes describing the overall body sequestration of TCDD under these varying parameters. Each variable was then assessed to evaluate their overall contribution to the total variance observed in the outcome measure. Essentially this statistical evaluation answers the question "what percentage of the variance or uncertainty in the outcome is due to the each model variable?". The contribution to variance calculations are achieved by squaring the rank correlation coefficients and normalizing them to 100%. This process was conducted for each of the following dose levels: 10, 3.16, 1.0, 0.316, and 0.1 μg/kg bodyweight. This will allow for the evaluation of the effect any apparent dose-dependencies may have on the key model leverage parameters. These doses were selected based upon a log scale from the original 10 μg/kg bodyweight dose (*i.e.*, 10^{1}, $10^{0.5}$, 10^{0}, $10^{-0.5}$, and 10^{-1}).

4.2.2 Equilibrium-Based Model

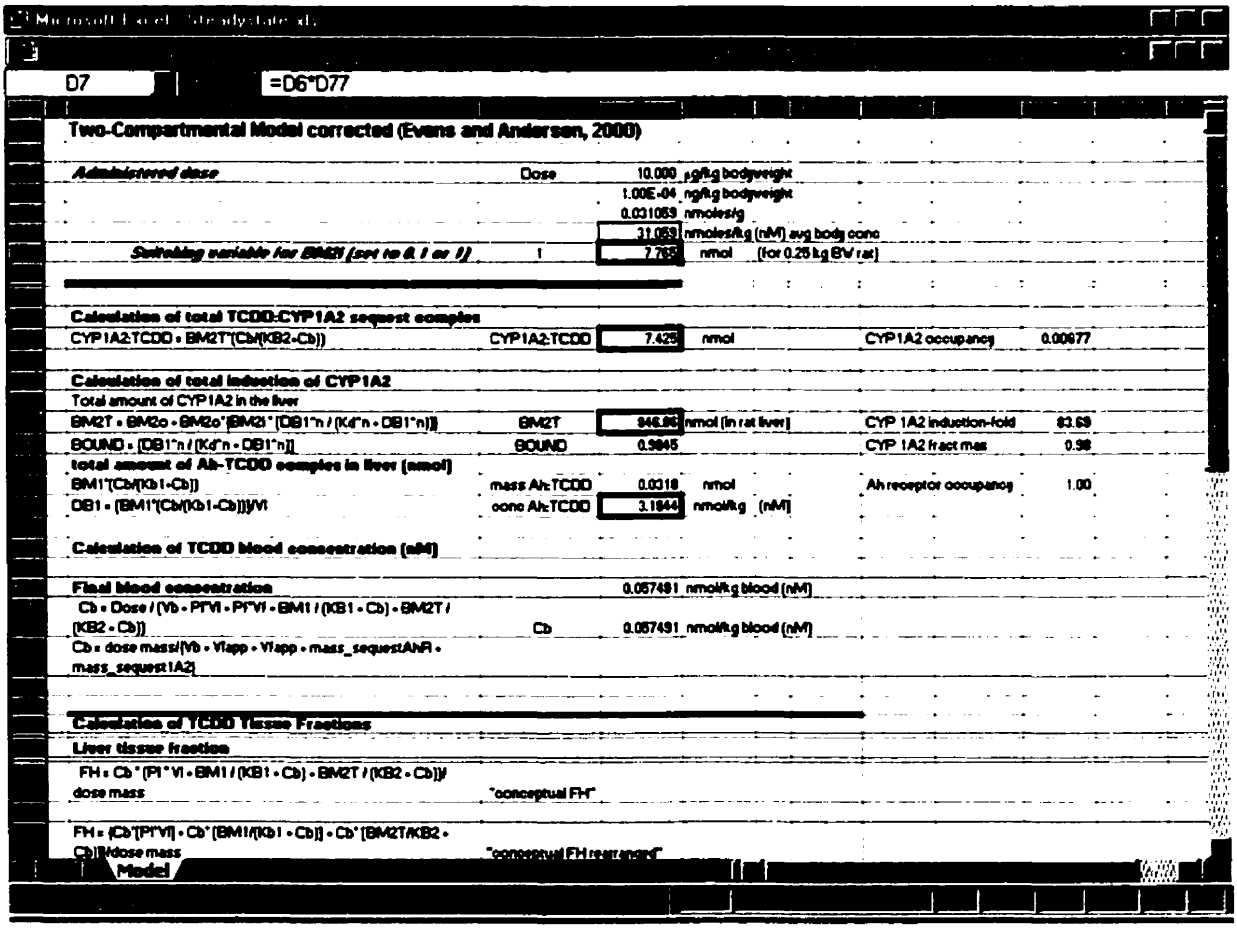
Evans and Andersen (2000) was selected as the prototype equilibrium-based model to provide an alternate comparison methodology with which to evaluate the parameterization of the prototype steady state-based model. It should be noted that, while the authors have identified this model as a "steady-state" PBPK model, this would be an incorrect specification given there are no time-dependencies within the overall model methodology, and no mass balance of flow between the modelled compartments.

A complete overview of the methodology and mathematical equations used in this model is provided in Section A-2 of the Appendix. The model was programmed in the Microsoft Excel™, version 7.0, based upon methodology presented in the source paper (Evans and

Andersen, 2000) and the Simulsolv™ source code received in communication with the primary author (M. Evans, personal communication, 2001). This source code is presented in Section A-3 of the Appendix.

Figure 4.9, below, provides a screenshot of the Excel-based model design. Empirical solving of the implicit equation (*i.e.*, the equation is iterative in nature with the variable in question is on both sides of the equation) used to calculate compartmental blood concentrations was conducted using the built-in Excel Solver tool (this system uses the Generalized Reduced Gradient [GRG2] nonlinear optimization code) or through manual adjustment if the convergence is not difficult to achieve by hand.

Figure 4.9 Screenshot of equilibrium-based model developed based upon Evans and Andersen (2000).



4.2.2.1 Revisions to Base Equilibrium Model

Inaccuracies and gaps within the published methodologies were also noted during the development of this steady-state model, and were corrected through detailed evaluation of the underlying PK or PD processes. These inaccuracies included incomplete descriptions of certain formula steps with the model methodology (particularly with respect to Ah receptor and CYP1A2 binding interactions in the liver compartment). Significant discrepancies were also noted in the methodology published in the Evans and Andersen (2000) article when compared to the actual model source code provided by the primary author. The model methodology presented in the source paper assumed compartment interactions were on a concentration basis (*i.e*, nM), while the methodology presented in the model source code methodology used mass-based approach (nmoles).

In the methodology presented in the model source code, potential impacts of blood volume on overall TCDD blood concentration levels were ignored. While this particular variable was accounted for in the methodology presented in the Evans and Andersen (2000) source paper, the impacts of this variable would be negligible in comparison to the much larger impacts of liver and adipose volumes. While not significant in the model output, to ensure methodological completeness, the blood volume term was included in the prototype equilibrium model developed for this research project.

Of particular concern is a mis-specification present within the calculation of CYP1A2 induction provided in the model source code. Both the Evans and Andersen (2000) paper and the Simulsolv source code specify the total induction of CYP1A2 in the liver, BM2T, as follows:

$$BM_{2T} = BM_{2o} + BM_{2i} \times \frac{Ah{:}TCDD^{n}}{Kd^{n} + Ah{:}TCDD^{n}} \qquad \text{Eq. 1}$$

The total induction of CYP1A2 in the liver can be calculated by adding the basal (initial) level of CYP1A2 available in the liver to the additional amount induced by the binding of TCDD to the Ah receptor. However, a problem is noted when one breaks down the Evans and Andersen methodology. The BM_{2i} variable is a dimensionless parameter that is the factor by which BM_{20}

(a concentration) is increased. The remaining term is a Michaelis-Menton kinetics relationship providing a quantification of the Ah receptor occupancy fraction (also a unitless parameter). By combining the two, a quantification of the induction fold increase over the basal level of CYP1A2, based upon the current Ah receptor occupancy level, is achieved. However, for this value to properly quantify the amount of CYP1A2 induced as a result of this Ah receptor occupancy, the modified induction fold increase value **must** be multiplied by the basal level of CYP1A2 in the liver (as it is the induction fold increase over the basal level).

Thus, the above equation should be modified to read:

$$BM_{2T} = BM_{20} + BM_{20} \times BM_{2i} \times \frac{Ah{:}TCDD^n}{Kd^n + Ah{:}TCDD^n} \quad \text{Eq. 2}$$

or perhaps more clearly as:

$$BM_{2T} = BM_{20} \times \left[1 + BM_{2i} \times \frac{Ah{:}TCDD^n}{Kd^n + Ah{:}TCDD^n}\right] \quad \text{Eq. 3}$$

By failing to include BM20 in the induction fold increase calculation, the model (as depicted in Eq. 1) proposed by Evans and Andersen (2000) would incorrectly limit the impact of CYP1A2 induction on overall CYP1A2 levels in the liver . The case of the parameter set used for the default model (a BM20 of 10 nmoles/liver), this would result in a 10-fold under-estimation of induced CYP1A2 concentrations at higher ligand (TCDD) concentration levels.

This error would not be apparent at the low doses demonstrated by the authors due to the lower expected induction rates at these concentrations. However, if dose regimes outside these values were used (particularly in the higher dose range), the model would not accurately calculate the correct degree of CYP1A2 induction, and thus under-estimate potential hepatic sequestration of TCDD at these higher doses. To illustrate this problem, analysis results using the equilibrium-based model were presented using both the original, mis-specified methodology, as well as the corrected version.

4.2.2.2 Species-Specific Physiological Data

Table 4.12, below, provides a list of the species-specific physiological data used to assess TCDD disposition within the Sprague-Dawley equilibrium-based model (Evans and Andersen, 2000). A majority of the parameters appear to have been estimated through curve-fitting simulations conducted by the Simusolv modelling package. As such, the independent output variables of the model are specifically tied to the assumptions and equations on which the model is built. Given this fact, it is likely that the assumed variables would not be applicable to the corrected model methodology, due to the considerable impact of the revised CYP1A2 induction and binding capacity.

Table 4.12 Default physiological parameters specified for the equilibrium-based model by Evans and Andersen (2000).

Physiological Parameter	Abbreviation	Value	Reference
Liver-to-blood partition coefficient	Pl	10	Estimated
Fat-to-blood partition coefficient	Pf	350	Estimated
Percent liver volume/body volume	Vlc	4%	Andersen *et al.*, 1993
Percent fat volume/body volume	Vfc	6%	Andersen *et al.*, 1993
Ah receptor availability	BM1	0.054 nmole/liver	Gasiewicz *et al.*, 1984
Ah receptor binding constant	KB1	0.04 nM	Estimated
Ah receptor/DNA receptor binding constant	Kd	0.05 nM	Estimated
CYP1A2 basal levels	BM20	10 nmole/liver	Estimated
CYP1A2 induction fold increase	BM2i	85 fold	Estimated
CYP1A2 binding constant to TCDD	KB2	6.5 nM	Estimated
Hill coefficient	N	1	Estimated

4.2.2.3 Comparisons of Steady-State *versus* Equilibrium-Based Model Methodologies

Comparisons were conducted between the steady-state and equilibrium-based models for the predictions of compartment-specific TCDD concentrations in the blood, liver, and adipose tissue. The relative fractions present in both liver and adipose, as well as the overall liver-to-fat disposition ratio, were also evaluated. Doses of 0.001, 0.01, 0.1, 1.0, 10, 100, 1000, and 10000

ng/kg bodyweight (a range of 0.000001 to 10 μg/kg bodyweight) were used to illustrate any inherent dose-dependencies present within the model outcomes.

To allow for an accurate comparison of these parameters following an initial dose, all excretionary processes (*i.e.*, urinary and biliary excretion) in the PBPK model were eliminated. This allowed the PBPK model to achieve a "quasi" steady-state condition, and allow for comparisons on the same footing as the equilibrium-based model.

4.3 Congener-Specific PBPK Modelling of Test Organisms

Once characterized and corrected (for problems such as low-dose instability), the prototype PBPK model was used to evaluate the compartment-specific disposition pattern of each of the assessed PCDD/F congeners (*i.e.*, TCDD, TCDF, 1-PeCDF, and 4-PeCDF) for the two primary test organisms. The Sprague-Dawley rat was selected due to its use as the primary test species for the original development of the PBPK, and its common use in laboratory studies on which many of the PCDD/F TEQ values were derived. The Gapper's red-backed vole was selected to determine whether it is an adequate sentinel species for use in long-term environmental monitoring programs, and if a PBPK model can be designed to approximate the pharmacokinetic and pharmacodynamic properties controlling PCDD/F disposition within such a sentinel species.

4.3.1 Time-Series Modelling of Congener-Specific Deposition Patterns

As the current PBPK model is designed to assess PCDD/F disposition and elimination patterns based upon a single acute dose, it is most important to evaluate the various congener-specific pharmacokinetic and pharmacodynamic impacts at early time points following administration. For this reason, all PBPK modelling specifically focused on the first 96 hours (*i.e.*, 4 days) following administration.

To evaluate the dose-dependent impacts of congener-specific PCDD/F administration, time-series modelling was conducted for the Sprague-Dawley rat and the Gapper's red-backed vole for a multiple dose levels (*i.e.*, 0.001, 0.01, 0.1, 1, 10, 100 μg/kg bodyweight). This allows for an evaluation of the potential impacts of ligand-specific CYP1A2 sequestration within the liver on overall compartment-specific depositional patterns, for a wide range of potential doses. Research has indicated that the lower dose levels (*i.e.*, 0.001 to 0.1 μg/kg bodyweight), more typical of those observed in the environment, are unlikely to result in significant CYP1A2 induction and ligand-specific sequestration within the liver, while the higher doses (*i.e.*, 1 to 100 μg/kg bodyweight) represent elevated ambient concentrations which would likely stimulate considerable induction and sequestration, in those congeners which demonstrate a high affinity to CYP1A2.

To evaluate the congener-specific impacts on each test species (*i.e.*, Sprague-Dawley rat and red-backed vole), the following congener-specific parameters were estimated for each dose level at 1, 24, 48, 72, and 96 hours following administration for TCDD, TCDF, 1-PeCDF, 4-PeCDF, and the TCDD-TEQ group:

- Mass (pmoles) in the liver, adipose tissue, and whole body;
- Concentration (pmoles/gram wet weight) in the liver, adipose tissue, and whole body;
- Percent of administered dose/gram in the liver and adipose tissue;
- Percentage of overall Ah and CYP1A2 receptor occupancy;
- CYP1A2 fold induction, and;
- Percentage of administered dose excreted.

The overall time-series curve data for both whole body concentration and liver-to-fat ratio was also gathered for each congener at the various assessed dose levels. This data allows for an indication of dose-dependency in the overall body burden and deposition patterns in each of the congeners, over time.

The same process was then repeated for the red-backed vole using administered doses corresponding to the maximum plant concentration measured as part of the SHTC monitoring program at site 107 following the incident (*i.e.*, Winter 1996). This data was then used to calculate vole-to-plant BAF values for each of the congeners, for comparison with the vole-to-plant BAF values calculated based upon environmental sampling data.

5.0 RESULTS

5.1 Summary of Field-Monitoring Results

5.1.1 Temporal Congener-Specific Biota Concentrations

Temporal data for each of the biological species were grouped into five discrete seasonal sets: i) Summer 1996 (prior to incident); ii) Fall 1996 (prior to incident); iii) Winter 1996 (after the incident); iv) Summer 1997 (after the incident), and; v) Fall 1997 (after the incident). Tables 5.1 through 5.3 provide the results of the biological sampling conducted during these specified temporal periods for sites 11, 107, and 114, respectively.

Of particular interest when evaluating the potential impacts of pharmacokinetics on the disposition of the PCDD/Fs within living organisms is the congener-specific pattern of concentrations (*i.e.*, congener "fingerprint"). Figures 5.1 through 5.6 provide graphs depicting the congener-specific fingerprint breakdown for each of the sampled biological organisms (*i.e.*, red-backed voles, Labrador tea, and moss) sampled prior to and following the October 1996 release incident, for sites 11, 107, and 114, respectively. The data demonstrate that the congener-specific fingerprint in all sampled biota, before and after the release incident, is dominated by TCDF and the two PeCDF congeners, with the HxCDF congeners providing a smaller but significant portion of the profile.

A congener-specific breakdown of the PCDD/F mass and TEF-adjusted concentrations, as well as their relative overall percentages, for both vole and Labrador tea samples taken at each key monitoring site (*i.e.*, sites 11, 107, and 114) during summer and winter 1996 (*i.e.*, immediately pre- and post-incident) are provided in Table 5.4 and Figures 5.7 and 5.8.

Table 5.1 PCDD/F Congener Concentrations (ppt) in Various Environmental Media at Monitoring Site 11.

PCDD/F Congeners	Summer 1996		Fall 1996				Winter 1996						Summer 1997	Fall 1997				
	Vole [a]	Tea	Vole	Tea	Moss		Vole		Tea		Moss		Vole	Vole	Tea	Moss	Browse	Berries
2378-TCDD	0.4	nd [b]	0.4	nd	nd		4.3	nd	nd	nd	nd	nd	0.8	nd	nd	nd	nd	nd
12378-PECDD	1.6	nd	1.2	nd	nd		nd	15	0.6	0.6	nd	nd	5.1	1	nd	nd	nd	nd
123478-HXCDD	nd	nd	0.9	nd	nd		nd	9.1	nd	nd	0.3	nd	4.6	1.1	nd	nd	nd	nd
123678-HXCDD	1.8	nd	1.3	nd	1.2		10	nd	nd	nd	0.6	nd	3.8	1.1	nd	nd	nd	nd
123789-HXCDD	0.7	nd	0.4	nd	0.8		1.7	nd	nd	nd	0.7	nd	1.3	nd	nd	nd	nd	nd
1234678-HPCDD	6.4	1.2	2.9	0.5	14		28	17	1.4	0.9	13	0.4	12	3.6	2	13	1.1	4
OCDD	5.1	8.7	2.6	2.1	80		nd	23	7.4	4.6	85	4.2	5.6	4.1	15	71	11	nd
2378-TCDF	97	25	120	93	8.3		640	870	450	330	36	170	270	34	20	27	6.9	nd
12378-PECDF	29	2.5	34	11	2.9		290	380	57	39	5.5	17	140	13	2	6.1	nd	nd
23478-PECDF	820	4.8	460	18	5.7		33000	24000	180	130	16	39	12000	3100	5.8	12	1.5	6.3
123478-HXCDF	88	1.2	93	3.5	4.7		2500	2100	30	27	5.6	5.2	1100	380	nd	5.2	nd	4.8
123678-HXCDF	59	0.5	59	1.3	1.4		1700	1400	9.9	8.6	2.4	1.7	550	280	nd	1.5	nd	3.7
234678-HXCDF	nd	0.6	110	1.7	2.1		23	nd	16	13	2.9	1.7	9.1	nd	nd	2.9	0.7	3.8
123789-HXCDF	130	nd	3.7	nd	nd		2700	2300	1.3	1	nd	nd	1500	640	nd	nd	nd	nd
1234678-HPCDF	22	0.9	18	1.9	8.7		220	280	5.6	4.7	5.7	1.5	160	30	1.1	8.6	nd	11
1234789-HPCDF	2.6	nd	2.1	nd	nd		31	34	nd	nd	0.6	nd	18	4.3	nd	1.3	nd	3.1
OCDF	2.3	1	2.1	0.6	12		nd	10	1.6	1	8.5	1	4.2	2.3	nd	9.7	nd	3.3
TCDD TEQ	**451**	**5.3**	**272**	**19.5**	**5.1**		**17279**	**12705**	**144**	**106**	**13.3**	**38.2**	**6359**	**1686**	**5**	**10.2**	**1.5**	**4.6**

RELEASE INCIDENT

[a] Whole body wet-weight concentrations.

[b] nd = non-detect

Table 5.2 PCDD/F Congener Concentrations (ppt) in Various Environmental Media at Monitoring Site 107.

PCDD/F Congeners	Summer 1996		Fall 1996		Winter 1996						Summer 1997	Fall 1997			
	Vole [a]	Tea	Tea		Vole		Tea		Moss	Browse	Vole	Vole	Tea	Moss	Browse
2378-TCDD	4.5	1	nd [b]		45	57	1.1	0.5	0.6	nd	6.6	1.2	nd	nd	nd
12378-PECDD	14	1.2	1.4		110	98	2.1	1	4.2	nd	17	5.2	nd	2.6	nd
123478-HXCDD	5.8	1	nd		50	47	1	0.6	7.2	nd	5.1	5.7	nd	5	nd
123678-HXCDD	9.3	1.5	nd		43	52	1.1	0.6	16	0.3	5.4	6.2	nd	12	nd
123789-HXCDD	3.4	1.6	nd		13	12	1.5	0.5	18	nd	2.1	2.4	nd	13	nd
1234678-HPCDD	25	18	8.3		90	120	16	8.8	320	5.2	14	40	2.4	250	14
OCDD	24	100	54		72	91	100	52	2300	40	15	39	18	1500	29
2378-TCDF	270	850	560		2600	4600	1500	970	440	380	580	190	43	350	18
12378-PECDF	220	120	64		1400	1800	190	110	80	33	350	120	nd	69	nd
23478-PECDF	7600	290	170		100000	100000	540	290	230	68	8200	3900	8.6	170	5.8
123478-HXCDF	670	93	44		6400	7100	100	53	97	9.9	480	380	3.2	77	1.1
123678-HXCDF	520	33	14		5500	4500	37	21	35	3.9	290	230	nd	29	1.2
123789-HXCDF	14	0.8	0.8		120	120	1.9	nd	1.9	nd	12	4	nd	2.4	nd
234678-HXCDF	1200	55	24		7800	6700	60	30	45	5.5	780	380	nd	37	nd
1234678-HPCDF	130	33	19		840	890	27	15	120	6.6	65	96	4.8	110	3.5
1234789-HPCDF	13	2.5	1.4		120	140	2.8	1.3	14	1	7.8	11	nd	16	nd
OCDF	9.7	15	19		40	49	24	7.9	260	7.9	5.5	10	3	180	nd
TCDD-TEQ	**4100**	**257**	**154**		**52488**	**52570**	**453**	**260**	**195**	**76**	**4357**	**2084**	**9**	**148**	**5.1**

RELEASE INCIDENT

[a] Whole body wet-weight concentrations.

[b] nd = non-detect

Table 5.3 PCDD/F Congener Concentrations (ppt) in Various Environmental Media at Monitoring Site 114.

PCDD/F Congeners	Summer 1996 Vole [a]	Summer 1996 Tea	Fall 1996 Vole	Fall 1996 Tea	Fall 1996 Moss	RELEASE INCIDENT	Winter 1996 Vole			Winter 1996 Tea		Winter 1996 Moss	Winter 1996 Browse	Summer 1997 Vole	Fall 1997 Vole	Fall 1997 Tea	Fall 1997 Browse	Fall 1997 Litter
2378-TCDD	1.5	0.3	nd	nd	nd		5	4.4	nd	nd	nd	nd	nd	0.6	nd	nd	nd	nd
12378-PECDD	3.3	0.4	0.2	nd	nd		13	9.5	8.8	0.3	nd	nd	nd	2	0.3	nd	nd	nd
123478-HXCDD	2.8	0.3	nd	nd	0.7		nd	5.4	nd	nd	nd	0.7	nd	1.3	0.5	nd	nd	nd
123678-HXCDD	3.2	0.4	nd	nd	1.2		nd	5.9	nd	0.4	nd	1.4	nd	2	0.4	nd	nd	1
123789-HXCDD	0.5	0.5	nd	nd	1.6		nd	nd	1.3	nd	nd	2	nd	0.6	0.5	nd	nd	1.6
1234678-HPCDD	9.9	4.9	1	nd	28		25	18	18	1.5	1.1	30	0.9	17	2	1.3	1.3	21
OCDD	8.9	25	1.6	8	160		19	18	21	6.8	6.1	160	7	16	2.6	10	11	110
2378-TCDF	110	200	13	120	41		590	890	1100	280	160	66	140	160	24	16	2.9	76
12378-PECDF	52	32	4	11	6.8		270	220	190	31	18	14	18	69	9.4	1.6	nd	20
23478-PECDF	6100	48	300	24	14		8200	8300	9300	69	36	28	31	1500	350	2.2	nd	26
123478-HXCDF	600	15	42	2.6	5.4		920	790	820	13	7.4	9.2	5.4	500	81	0.6	nd	10
123678-HXCDF	370	5.2	37	1	2		580	680	500	5.2	3.1	3.1	2	300	32	nd	nd	3.3
123789-HXCDF	nd [b]	0.2	nd	nd	0.2		11	nd	nd	0.2	nd	0.5	nd	nd	nd	nd	nd	nd
234678-HXCDF	660	6.7	180	2.3	3.1		910	790	780	7.3	2.3	4.6	2.2	590	65	0.5	0.7	5.7
1234678-HPCDF	89	0.8	7.3	1.2	7.1		120	150	110	3.6	nd	8.6	nd	7.5	11	nd	0.6	17
1234789-HPCDF	9.3	6.4	0.6	nd	1		18	14	22	nd	4.7	1.3	2.5	nd	nd	nd	nd	3.2
OCDF	5.5	4.7	0.7	0.6	16		8.7	nd	nd	2	1.4	18	1.6	nd	1	0.9	nd	28
TCDD TEQ	3233	49.3	178	25.2	13.2		4434	4493	4990	67	36.2	23.9	31.4	912	196	2.9	0.4	24.2

[a] Whole body wet-weight concentrations.

[b] nd = non-detect

Figure 5.1 SHTC Congener-Specific PCDD/F Disposition Pattern in Biological Samples from Fall 1996 at Site 11

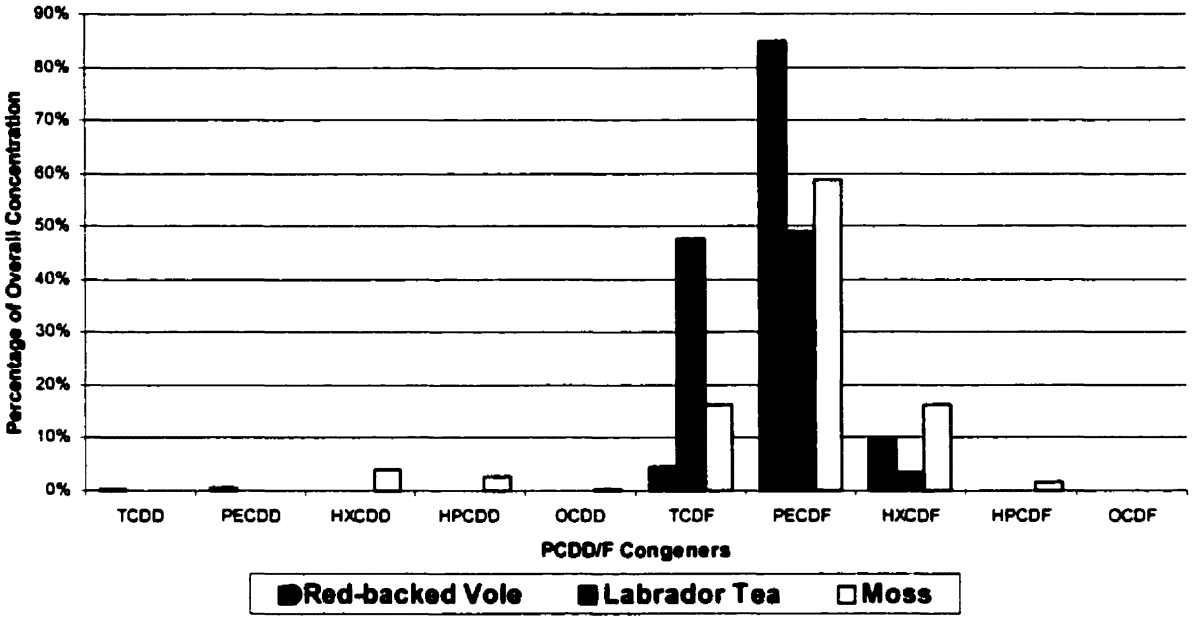


Figure 5.2 SHTC Congener-Specific PCDD/F Disposition Pattern in Biological Samples from Winter 1996 at Site 11

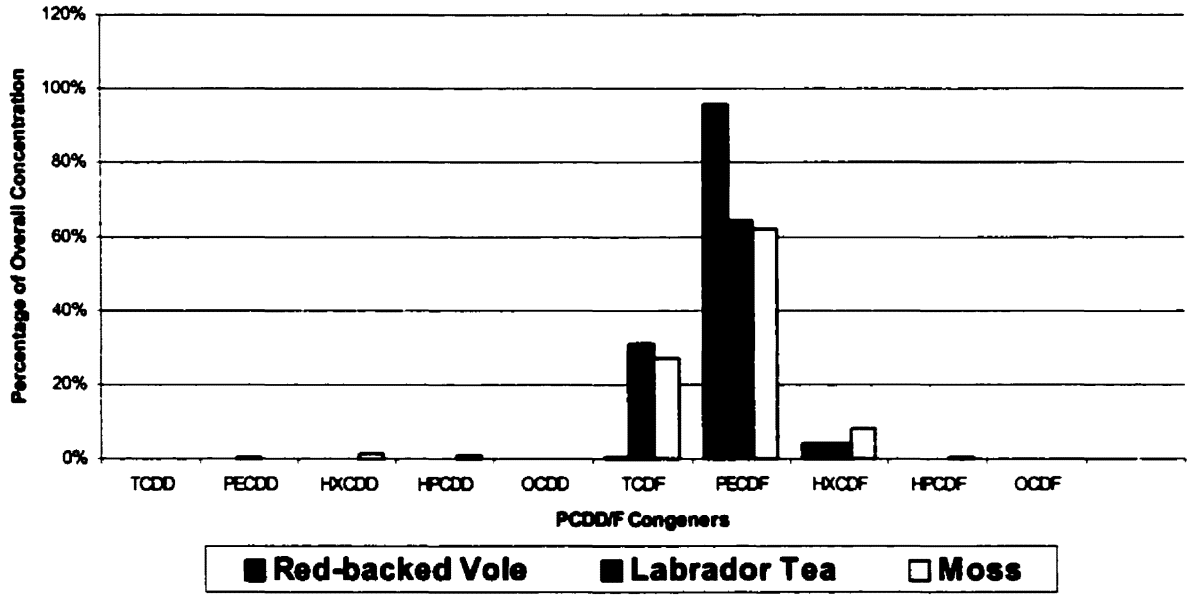


Figure 5.3 SHTC Congener-Specific PCDD/F Disposition Pattern in Biological Samples from Summer 1996 at Site 107

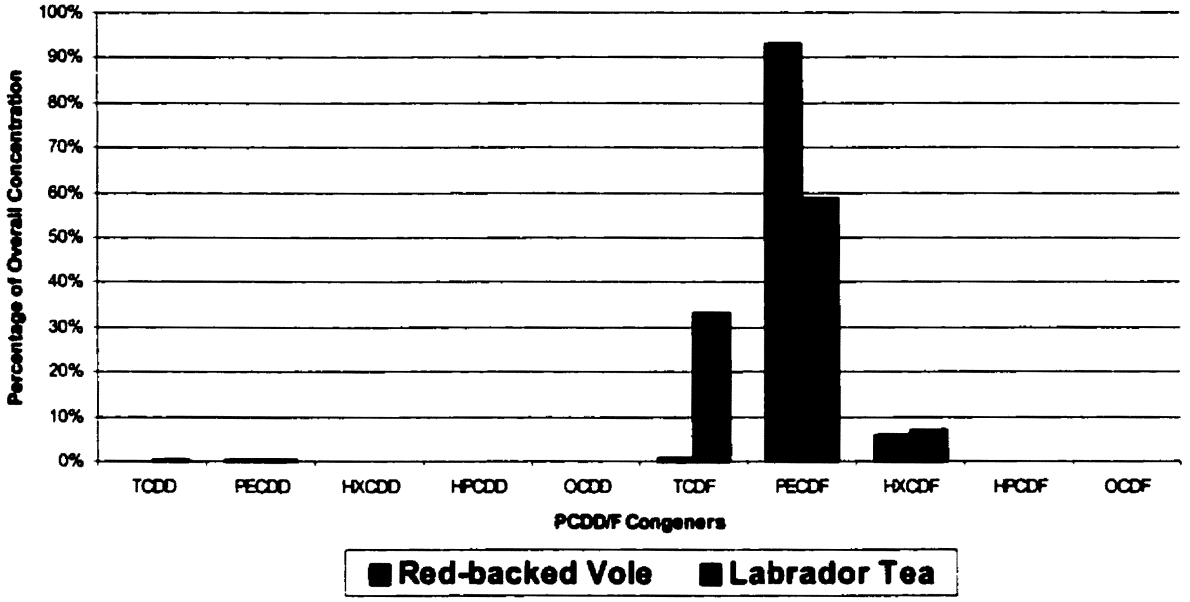


Figure 5.4 SHTC Congener-Specific PCDD/F Disposition Pattern in Biological Samples from Winter 1996 at Site 107

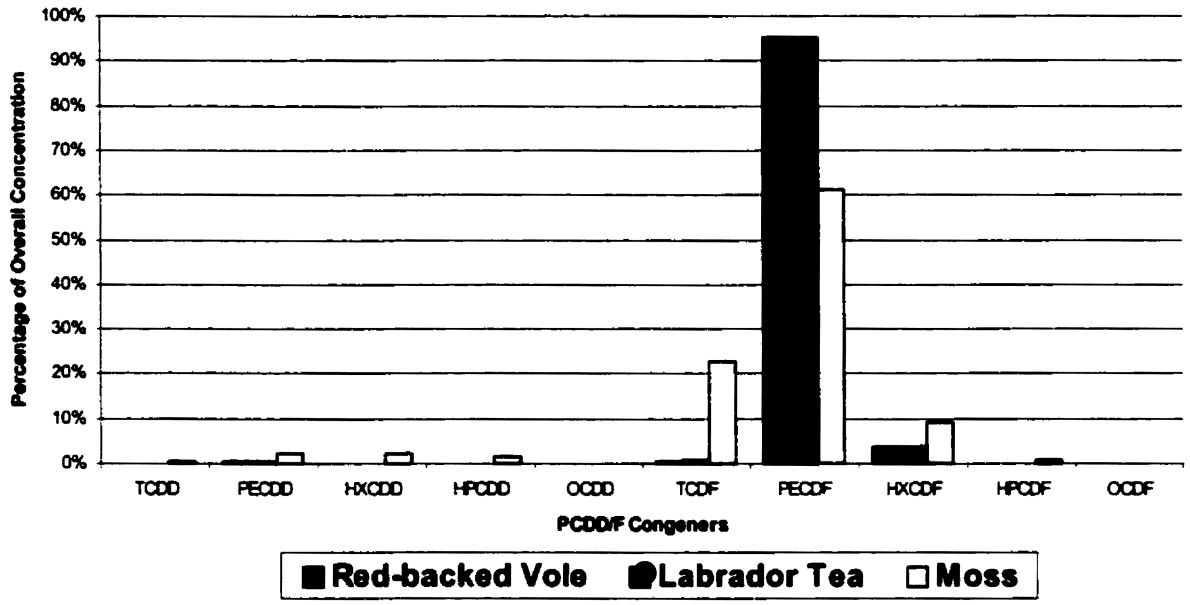


Figure 5.5 SHTC Congener-Specific PCDD/F Disposition Pattern in Biological Samples from Fall 1996 at Site 114

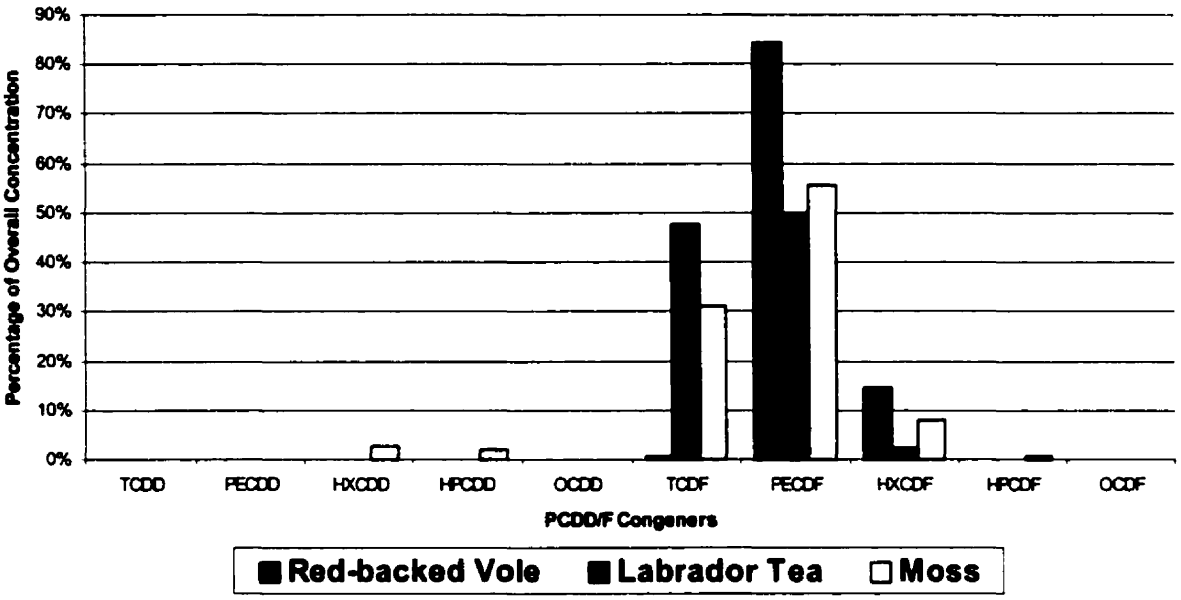


Figure 5.6 SHTC Congener-Specific PCDD/F Disposition Pattern in Biological Samples from Winter 1996 at Site 114

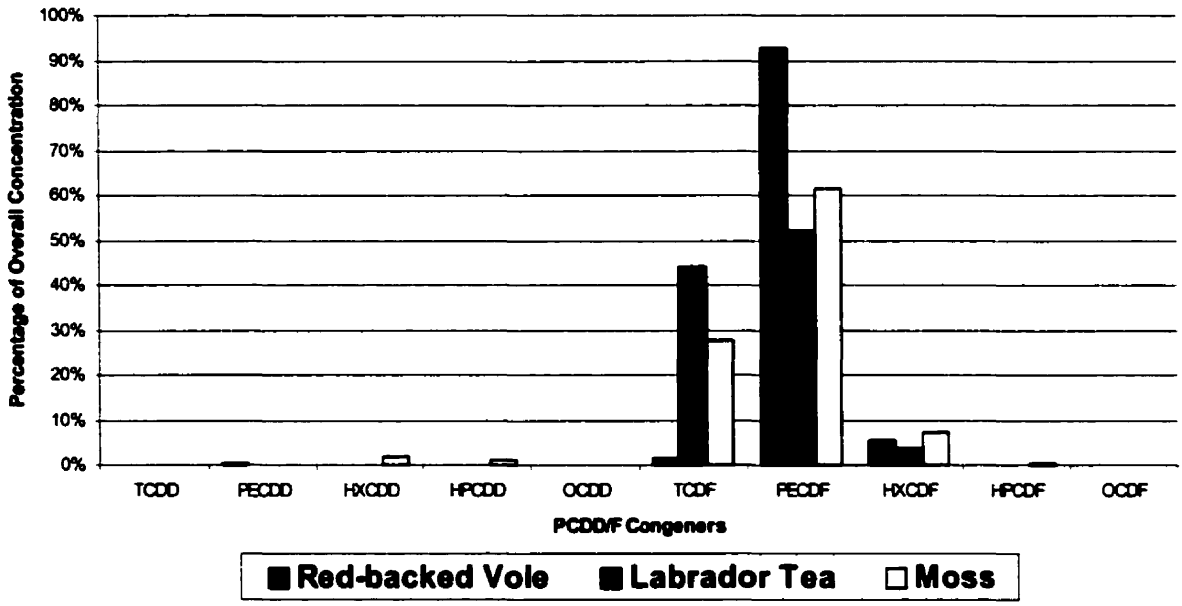


Table 5.4 Congener-Specific PCDD/F Mass and TEF-Adjusted[a] Concentrations (ppt) and their Relative Overall Percentages for the Vole and Labrador Tea Samples taken at each Key Monitoring Site during Summer and Winter 1996.

Congener	Summer 1996 (pre-incident)								Winter 1996 (post-incident)							
	Vole				Labrador Tea				Vole				Labrador Tea			
	Mass		TEQ-Eq		Mass		TEQ-Eq		Mass		TEQ-Eq		Mass		TEQ-Eq	
	Conc. (ppt)	Percent	Conc. (ppt)	Percent	Conc. (ppt)	Percent	Conc. (ppt)	Percent	Conc. (ppt)	Percent	Conc. (ppt)	Percent	Conc. (ppt)	Percent	Conc. (ppt)	Percent
Site 11																
2,3,7,8-TetraCDD	0.4	0.032%	0.4	0.089%	nd	~0%	nd	~0%	2.15	0.00592%	2.15	0.014%	nd	~0%	nd	~0%
1,2,3,7,8-PentaCDD	1.6	0.126%	1.6	0.354%	nd	~0%	nd	~0%	7.5	0.0207%	7.5	0.05%	0.6	0.091%	0.6	0.480%
1,2,3,4,7,8-HexaCDD	nd[a]	0%	nd	~0%	nd	~0%	nd	~0%	4.55	0.0125%	0.455	0.003%	nd	~0%	nd	~0%
1,2,3,6,7,8-HexaCDD	1.8	0.142%	0.18	0.04%	nd	~0%	nd	~0%	5	0.0138%	0.5	0.003%	nd	~0%	nd	~0%
1,2,3,7,8,9-HexaCDD	0.7	0.055%	0.07	0.016%	nd	~0%	nd	~0%	0.85	0.00234%	0.085	0.001%	nd	~0%	nd	~0%
1,2,3,4,6,7,8-HeptaCDD	6.4	0.506%	0.064	0.014%	1.2	2.59%	0.012	0.227%	22.5	0.0620%	0.225	0.002%	1.15	0.174%	0.0115	0.009%
OctaCDD	5.1	0.403%	0	~0%	8.7	18.8%	0.001	0.016%	11.5	0.0317%	0.001	~0%	6	0.908%	0.001	~0%
2,3,7,8-TetraCDF	97	7.66%	9.7	2.15%	25	53.9%	2.5	47.4%	755	2.08%	75.5	0.504%	390	59.0%	39	31.2%
1,2,3,7,8-PentaCDF	29	2.29%	1.45	0.321%	2.5	5.39%	0.125	2.37%	335	0.923%	16.8	0.112%	48	7.27%	2.4	1.92%
2,3,4,7,8-PentaCDF	820	64.8%	410	90.8%	4.8	10.3%	2.4	45.5%	28500	78.5%	14250	95.1%	155	23.5%	77.5	62.0%
1,2,3,4,7,8-HexaCDF	88	6.95%	8.8	1.95%	1.2	2.59%	0.12	2.27%	2300	6.34%	230	1.53%	28.5	4.31%	2.85	2.28%
1,2,3,6,7,8-HexaCDF	59	4.66%	5.9	1.31%	0.5	1.08%	0.05	0.948%	1550	4.27%	155	1.03%	9.25	1.40%	0.925	0.741%
1,2,3,7,8,9-HexaCDF	nd	0%	nd	~0%	0.6	1.29%	0.06	1.14%	11.5	0.0317%	1.15	0.008%	14.5	2.20%	1.45	1.16%
2,3,4,6,7,8-HexaCDF	130	10.3%	13	2.88%	nd	~0%	nd	~0%	2500	6.89%	250	1.67%	1.15	0.174%	0.115	0.092%
1,2,3,4,6,7,8-HeptaCDF	22	1.74%	0.22	0.049%	0.9	1.94%	0.009	0.171%	250	0.689%	2.5	0.017%	5.15	0.780%	0.0515	0.041%
1,2,3,4,7,8,9-HeptaCDF	2.6	0.205%	0.026	0.006%	nd	~0%	nd	~0%	32.5	0.0896%	0.325	0.002%	nd	~0%	nd	~0%
OctaCDF	2.3	0.182%	0	~0%	1	2.16%	0	0.002%	5	0.0138%	0.001	~0%	1.3	0.197%	0	~0%

Table 5.4 Congener-Specific PCDD/F Mass and TEF-Adjusted[a] Concentrations (ppt) and their Relative Overall Percentages for the Vole and Labrador Tea Samples taken at each Key Monitoring Site during Summer and Winter 1996.

Congener	Summer 1996 (pre-incident)								Winter 1996 (post-incident)							
	Vole				Labrador Tea				Vole				Labrador Tea			
	Mass		TEQ-Eq		Mass		TEQ-Eq		Mass		TEQ-Eq		Mass		TEQ-Eq	
	Conc. (ppt)	Percent	Conc. (ppt)	Percent	Conc. (ppt)	Percent	Conc. (ppt)	Percent	Conc. (ppt)	Percent	Conc. (ppt)	Percent	Conc. (ppt)	Percent	Conc. (ppt)	Percent
Site 107																
2,3,7,8-TetraCDD	4.5	0.0419%	4.5	0.11%	1	0.0619%	1	0.389%	51	0.041%	51	0.097%	0.8	0.0384%	0.8	0.224%
1,2,3,7,8-PentaCDD	14	0.130%	14	0.341%	1.2	0.0742%	1.2	0.466%	104	0.083%	104	0.198%	1.55	0.0744%	1.55	0.435%
1,2,3,4,7,8-HexaCDD	5.8	0.054%	0.58	0.014%	1	0.0619%	0.1	0.039%	48.5	0.039%	4.85	0.009%	0.8	0.0384%	0.08	0.022%
1,2,3,6,7,8-HexaCDD	9.3	0.0867%	0.93	0.023%	1.5	0.0928%	0.15	0.058%	47.5	0.038%	4.75	0.009%	0.85	0.0408%	0.085	0.024%
1,2,3,7,8,9-HexaCDD	3.4	0.0317%	0.34	0.008%	1.6	0.099%	0.16	0.062%	12.5	0.010%	1.25	0.002%	1	0.0480%	0.1	0.028%
1,2,3,4,6,7,8-HeptaCDD	25	0.233%	0.25	0.006%	18	1.11%	0.18	0.070%	105	0.083%	1.05	0.002%	12.4	0.595%	0.124	0.035%
OctaCDD	24	0.224%	0.002	~0%	100	6.19%	0.01	0.004%	81.5	0.065%	0.0082	~0%	76	3.65%	0.008	0.002%
2,3,7,8-TetraCDF	270	2.52%	27	0.658%	850	52.8%	85	33.0%	3600	2.86%	360	0.685%	1235	59.3%	123.5	34.6%
1,2,3,7,8-PentaCDF	220	2.05%	11	0.268%	120	7.42%	6	2.33%	1600	1.27%	80	0.152%	150	7.20%	7.5	2.10%
2,3,4,7,8-PentaCDF	7600	70.8%	3800	92.7%	290	17.9%	145	56.3%	100000	79.5%	50000	95.2%	415	19.9%	207.5	58.2%
1,2,3,4,7,8-HexaCDF	670	6.24%	67	1.63%	93	5.75%	9.3	3.61%	6750	5.37%	675	1.29%	76.5	3.67%	7.65	2.15%
1,2,3,6,7,8-HexaCDF	520	4.85%	52	1.27%	33	2.04%	3.3	1.28%	5000	3.97%	500	0.952%	29	1.39%	2.9	0.813%
1,2,3,7,8,9-HexaCDF	14	0.130%	1.4	0.034%	0.8	0.0495%	0.08	0.031%	120	0.095%	12	0.023%	0.95	0.0456%	0.095	0.027%
2,3,4,6,7,8-HexaCDF	1200	11.2%	120	2.93%	55	3.40%	6	2.14%	7250	5.76%	725	1.38%	45	2.16%	4.5	1.26%
1,2,3,4,6,7,8-HeptaCDF	130	1.21%	1.3	0.032%	33	2.04%	0.33	0.128%	865	0.688%	8.65	0.016%	21	1.01%	0.21	0.059%
1,2,3,4,7,8,9-HeptaCDF	13	0.121%	0.13	0.003%	2.5	0.155%	0.025	0.010%	130	0.103%	1.3	0.002%	2.05	0.0984%	0.021	0.006%
OctaCDF	9.7	0.0904%	0	~0%	15	0.928%	0.0015	0.001%	44.5	0.035%	0.0045	~0%	15.95	0.765%	0.002	~0%

Table 5.4 Congener-Specific PCDD/F Mass and TEF-Adjusted[a] Concentrations (ppt) and their Relative Overall Percentages for the Vole and Labrador Tea Samples taken at each Key Monitoring Site during Summer and Winter 1996.

Congener	Summer 1996 (pre-incident)								Winter 1996 (post-incident)							
	Vole				Labrador Tea				Vole				Labrador Tea			
	Mass		TEQ-Eq		Mass		TEQ-Eq		Mass		TEQ-Eq		Mass		TEQ-Eq	
	Conc. (ppt)	Percent	Conc. (ppt)	Percent	Conc. (ppt)	Percent	Conc. (ppt)	Percent	Conc. (ppt)	Percent	Conc. (ppt)	Percent	Conc. (ppt)	Percent	Conc. (ppt)	Percent
Site 114																
2,3,7,8-TetraCDD	1.5	0.019%	1.5	0.046%	0.3	0.0855%	0.3	0.609%	2.2	0.0178%	2.2	0.046%	nd	~0%	nd	~0%
1,2,3,7,8-PentaCDD	3.3	0.041%	3.3	0.102%	0.4	0.114%	0.4	0.812%	9.15	0.0739%	9.15	0.193%	0.15	0.045%	0.15	0.291%
1,2,3,4,7,8-HexaCDD	2.8	0.035%	0.28	0.009%	0.3	0.0855%	0.03	0.061%	2.7	0.0218%	0.27	0.006%	nd	~0%	nd	~0%
1,2,3,6,7,8-HexaCDD	3.2	0.040%	0.32	0.010%	0.4	0.114%	0.04	0.081%	2.95	0.0238%	0.295	0.006%	0.2	0.061%	0.02	0.039%
1,2,3,7,8,9-HexaCDD	0.5	0.006%	0.05	0.002%	0.5	0.143%	0.05	0.102%	0.65	0.0052%	0.065	0.001%	nd	~0%	nd	~0%
1,2,3,4,6,7,8-HeptaCDD	9.9	0.123%	0.099	0.003%	4.9	1.40%	0.049	0.099%	18	0.145%	0.18	0.004%	1.3	0.394%	0.013	0.025%
OctaCDD	8.9	0.111%	0	~0%	25	7.13%	0.0025	0.005%	19.5	0.158%	0.002	~0%	6.45	1.95%	0.001	0.001%
2,3,7,8-TetraCDF	110	1.37%	11	0.340%	200	57.0%	20	40.6%	995	8.04%	99.5	2.10%	220	66.6%	22	42.6%
1,2,3,7,8-PentaCDF	52	0.648%	2.6	0.080%	32	9.12%	1.6	3.25%	205	1.66%	10.25	0.216%	24.5	7.42%	1.23	2.37%
2,3,4,7,8-PentaCDF	6100	76.0%	3050	94.3%	48	13.7%	24	48.7%	8800	71.1%	4400	92.8%	52.5	15.9%	26.3	50.8%
1,2,3,4,7,8-HexaCDF	600	7.48%	60	1.86%	15	4.28%	1.5	3.05%	805	6.50%	80.5	1.70%	10.2	3.09%	1.02	1.98%
1,2,3,6,7,8-HexaCDF	370	4.61%	37	1.14%	5.2	1.48%	0.52	1.06%	590	4.76%	59	1.24%	4.15	1.26%	0.415	0.804%
1,2,3,7,8,9-HexaCDF	nd	~0%	nd	~0%	0.2	0.057%	0.02	0.041%	nd	~0%	nd	~0%	0.1	0.030%	0.01	0.019%
2,3,4,6,7,8-HexaCDF	660	8.22%	66	2.04%	6.7	1.91%	0.67	1.36%	785	6.34%	78.5	1.66%	4.8	1.45%	0.48	0.930%
1,2,3,4,6,7,8-HeptaCDF	89	1.11%	0.89	0.028%	0.8	0.228%	0.008	0.016%	130	1.05%	1.3	0.027%	1.8	0.545%	0.018	0.035%
1,2,3,4,7,8,9-HeptaCDF	9.3	0.116%	0.093	0.003%	6.4	1.82%	0.064	0.130%	18	0.145%	0.18	0.004%	2.35	0.712%	0.0235	0.046%
OctaCDF	5.5	0.069%	0	~0%	4.7	1.34%	0	0.001	nd	~0%	nd	~0%	1.7	0.515%	0	~0%

[a] Congener-specific mass concentrations were multiplied by their respective TEF value (Van den Berg *et al.*, 1998) to obtain a TCDD-TEQ concentration.

[b] nd = non detect

Figure 5.7 **Congener-Specific PCDD/F Mass and TEF-Adjusted Percentages for Red-backed Voles and Labrador Tea sampled at Site 107 during Summer 1996 (Pre-Incident).**

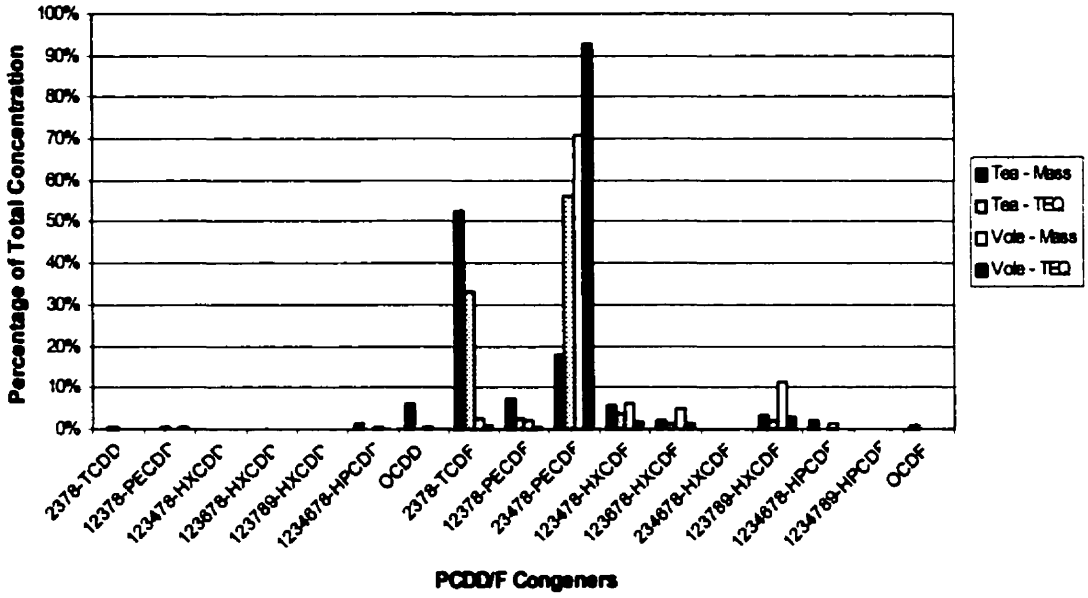
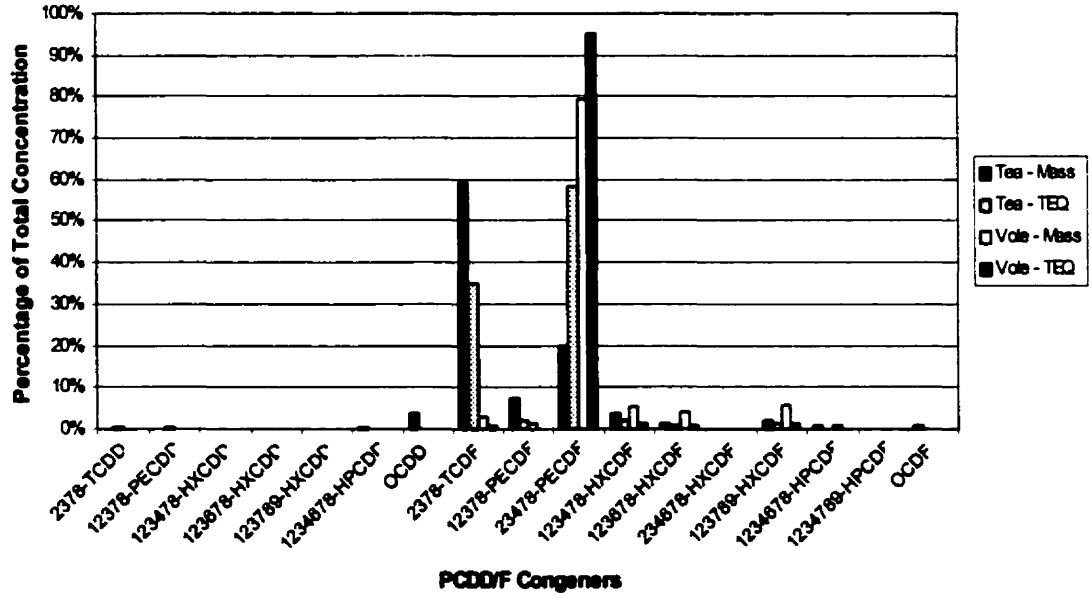


Figure 5.8 **Congener-Specific PCDD/F Mass and TEF-Adjusted Percentages for Red-backed Voles and Labrador Tea sampled at Site 107 during Winter 1996 (Post-Incident).**



Plant-to-Vole bioaccumulation factors (BAFs) were also calculated for each of the PCDD/F congeners at each temporal sampling period (*i.e.*, Summer 1996, Fall 1996, Winter 1996, Summer 1997, and Fall 1997, where sampling data were available). Tables 5.5 through 5.7 provide the congener-specific BAF values representing sites 11, 107, and 114, respectively. Interestingly, this data demonstrates that, in addition to having the highest environmental concentrations, the highest plant-to-vole BAF values are observed in the PeCDF and HxCDF congeners.

Table 5.5 Calculated Vole-to-Plant Bioaccumulation Factors (BAFs) for Site 11.

Congener	Summer 1996	Fall 1996		Winter 1996		Fall 1997	
	Vole:Tea	*Vole:Tea*	*Vole:Moss*	*Vole:Tea*	*Vole:Moss*	*Vole:Tea*	*Vole:Moss*
2378-TCDD	-	-	-	-	-	0	0
12378-PECDD	-	-	-	12.50	-	-	-
123478-HXCDD	0	-	-	-	30.33	-	-
123678-HXCDD	-	-	1.08	-	16.67	-	-
123789-HXCDD	-	-	0.50	-	2.43	0	0
1234678-HPCDD	5.33	5.8	0.21	19.57	3.36	1.80	0.28
OCDD	0.59	1.24	0.03	1.92	0.26	0.27	0.06
2378-TCDF	3.88	1.29	14.46	1.94	7.33	1.70	1.26
12378-PECDF	11.60	3.09	11.72	6.98	29.78	6.50	2.13
23478-PECDF	170.83	25.56	80.7	183.87	1036.36	534.48	258.33
123478-HXCDF	73.33	26.57	19.79	80.7	425.93	-	73.08
123678-HXCDF	118.00	45.38	42.14	167.57	756.1	-	186.67
234678-HXCDF	0	64.71	52.38	0.79	5.00	0	0
123789-HXCDF	-	-	-	2173.91	-	-	-
1234678-HPCDF	24.44	9.47	2.07	48.54	69.44	27.27	3.49
1234789-HPCDF	-	-	-	-	108.33	-	3.31
OCDF	2.3	3.5	0.18	3.85	1.05	-	0.24
TCDD-TEQ	105.8	26.9	54	348	645.9	268	155.4

Table 5.6 Calculated Vole-to-Plant Bioaccumulation Factors (BAFs) for Site 107.

Congeners	Summer 1996	Winter 1996		Fall 1997	
	Vole:Tea	*Vole:Tea*	*Vole:Moss*	*Vole:Tea*	*Vole:Moss*
2378-TCDD	4.50	63.75	85.00	-	-
12378-PECDD	11.67	67.10	24.76	-	2.00
123478-HXCDD	5.80	60.63	6.74	-	1.14
123678-HXCDD	6.20	55.88	2.97	-	0.52
123789-HXCDD	2.13	12.50	0.69	-	0.18
1234678-HPCDD	1.39	8.47	0.33	16.67	0.16
OCDD	0.24	1.07	0.04	2.17	0.03
2378-TCDF	0.32	2.91	8.18	4.42	0.54
12378-PECDF	1.83	10.67	20.00	-	1.74
23478-PECDF	26.21	240.96	434.78	453.49	22.94
123478-HXCDF	7.20	88.24	69.59	118.75	4.94
123678-HXCDF	15.76	172.41	142.86	-	7.93
234678-HXCDF	17.50	126.32	63.16	-	1.67
123789-HXCDF	21.82	161.11	161.11	-	10.27
1234678-HPCDF	3.94	41.19	7.21	20.00	0.87
1234789-HPCDF	5.20	63.41	9.29	-	0.69
OCDF	0.65	2.79	0.17	3.33	0.06
TCDD-TEQ	37.1	321	373.8	239.4	16.3

Table 5.7 Calculated Vole-to-Plant Bioaccumulation Factors (BAFs) for Site 114.

Congeners	Summer 1996	Fall 1996		Winter 1996		Fall 1997
	Vole:Tea	*Vole:Tea*	*Vole:Moss*	*Vole:Tea*	*Vole:Moss*	*Vole:Tea*
2378-TCDD	5.00	0	0	-	-	0
12378-PECDD	8.25	-	-	61.00	-	-
123478-HXCDD	9.33	0	0	-	3.86	-
123678-HXCDD	8.00	0	0	14.75	2.11	-
123789-HXCDD	1	0	0	-	0.33	-
1234678-HPCDD	2.02	-	0.04	13.85	0.60	1.54
OCDD	0.36	0.20	0.01	3.02	0.12	0.26
2378-TCDF	0.55	0.11	0.32	4.52	15.08	1.50
12378-PECDF	1.63	0.36	0.59	8.37	14.64	5.88
23478-PECDF	127.08	12.5	21.43	167.62	314.29	159.09
123478-HXCDF	40.00	16.15	7.78	78.92	87.50	135.00
123678-HXCDF	71.15	37	18.50	142.17	190.32	-
234678-HXCDF	0	0	0	0	0	0
123789-HXCDF	98.51	78.26	58.06	163.54	170.65	130.00
1234678-HPCDF	111.25	6.08	1.03	72.22	15.12	-
1234789-HPCDF	1.45	-	0.60	7.66	13.85	0
OCDF	1.17	1.17	0.04	0	0	1.11
TCDD-TEQ	100.9	19.5	19.2	186.6	205.2	106.5

It is important to note the significant differences in BAF values prior to and after the accidental release incident in October 1996.

5.1.2 Estimated Congener-Specific Consumption Rates for Red-Backed Voles

Given their typical diet of the red-backed vole and the absorptive nature of the sampled plants (*i.e.*, Labrador tea and moss), detected concentrations of PCDD/Fs on sampled plant material can be viewed as a suitable surrogate for the calculation dietary intakes for the vole sentinel species. Based upon a typical daily consumption rate of 0.31 g/g/d for Gapper's red-backed voles (McManus, 1974), estimated daily intakes were calculated for each of the key assessed congeners for monitoring sites 11, 107, and 114. Table 5.8 provides a summary of the highest biota concentrations measured during Winter 1996 and the related estimated daily intakes. The Winter 1996 sampling set was selected due to the elevated ambient PCDD/F concentrations arising from the October 1996 SHTC facility release incident and short-term acute nature of the ambient increase in PCDD/F concentrations.

Table 5.8 Summary of Highest Biota Concentrations Measured during Winter 1996 for the Key Congeners, and Related Estimated Daily Intakes. [a]

Congener	Site 11			Site 107			Site 114		
	Plant (pg/g)	Vole (pg/g)	Estimated Daily Intake (pg/g)	Plant (pg/g)	Vole (pg/g)	Estimated Daily Intake (pg/g)	Plant (pg/g)	Vole (pg/g)	Estimated Daily Intake (pg/g)
TCDD	nd[b]	4.3	nd	0.6	57	0.186	nd	5	nd
TCDF	170	870	52.7	440	4600	136.4	280	1100	86.8
1-PeCDF	17	380	5.27	80	1800	24.8	31	270	9.61
4-PeCDF	39	33000	12.1	230	100000	71.3	69	9300	21.4
TCDD-TEQ	38.2	17279	11.8	195	52570	60.5	67	4990	20.8

[a] Estimated daily intake calculations were based upon a daily food consumption rate of 0.31 g/g/d for Gapper's red-backed voles (McManus, 1974).
[b] nd = non-detect

5.2 Validation of Prototype Steady-State PBPK Model

Following construction of the prototype steady-state PBPK model, it was essential to validate the model against both the graphical output presented in the Wang *et al.* (1997) source paper, as well as the actual time course tissue distribution data presented in the Wang *et al.* (1997) paper. This step ensures an accurate replication of the Wang *et al.* methodology was used in the development of the base steady-state PBPK model used in this research project.

5.2.1 Comparison of Modelled Results versus Wang et al. (1997) Graphs

The initial TCDD PBPK model described by Wang *et al.* (1997) was developed with the time course tissue distribution data obtained following a single oral dose of 10 μg [^{3}H]TCDD/kg to female Sprague-Dawley rats. Various time points were selected by the authors to demonstrate the importance of early time points in accurately assigning unique parameter values such as permeability (Wang *et al.*, 1997). Based upon these time points, the authors provided graphs of experimental results compared to the results predicted in their model simulations, for the key accumulative and non-accumulative compartmental tissue groups (Figures 5.9 and 5.10). This experimental design was duplicated using the current prototype steady-state model to demonstrate consistency between the results depicted in Wang *et al.* (1997) and the reproduced model, based upon the Wang *et al.* (1997) methodology. Figures 5.11 and 5.12 provide graphical

comparisons of experimental data *versus* the predicted TCDD time series tissue concentrations in accumulative and non-accumulate tissue compartments, respectively, using the reproduced model. Visual comparisons of the two sets of model outputs indicate that the current prototype steady-state model appears to have accurately duplicated the results described in Wang *et al.* (1997).

Tissue disposition at early time points (*i.e.*, within the first 24 hours) following the TCDD dose administration is of particular importance when evaluating the ability of the current developmental model to reproduce the results presented in Wang *et al.* (1997). Figures 5.13 and 5.14 provide the early time point results presented in the Wang *et al.* (1997) paper, and Figures 5.15 and 5.16 provide the corresponding results produced by the current development model. Again, visual comparisons of the two sets of model outputs indicate that the current prototype steady-state model appears to have accurately duplicated the results described in Wang *et al.* (1997).

Figure 5.9 **Experimentally-derived TCDD concentrations in rats compared to curves describing model simulation results in accumulative tissue compartments (Wang *et al.*, 1997).**

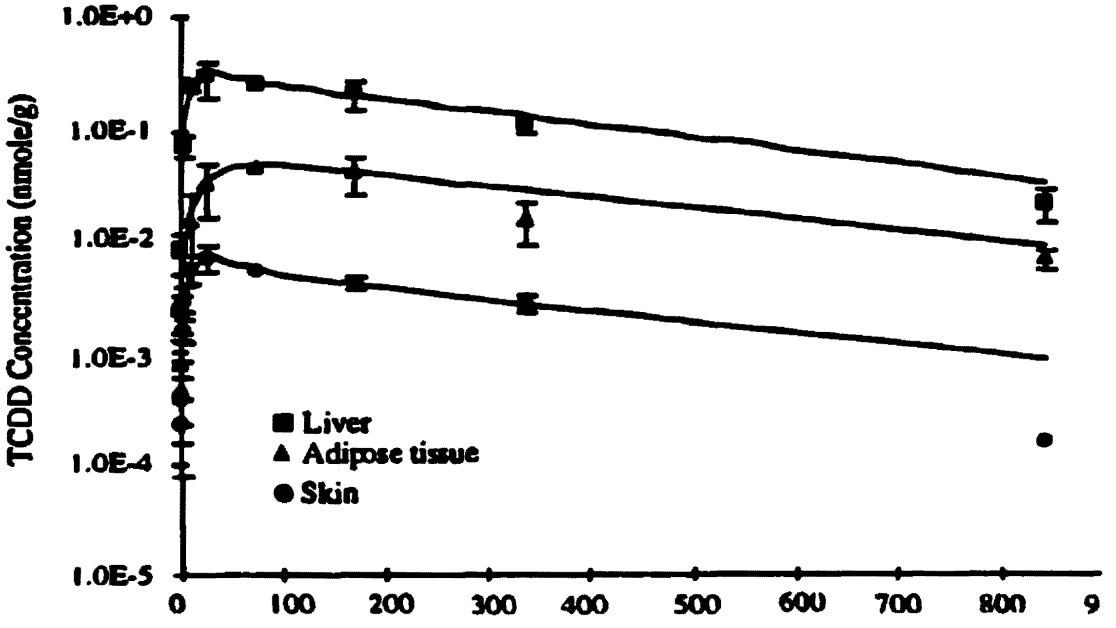


Figure 5.10 **Comparison of experimental (Wang et al., 1997) *versus* predicted (with reproduced model) TCDD timeseries tissue concentrations in various accumulative tissue compartments.**

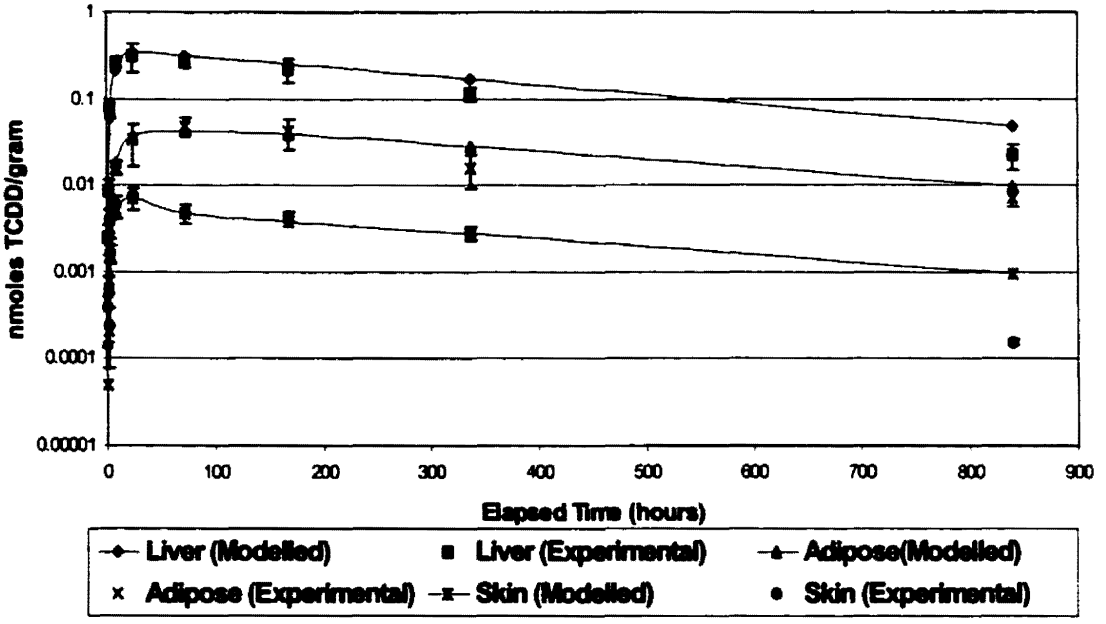


Figure 5.11 **Experimentally-derived TCDD concentrations in rats compared to curves describing model simulation results in non-accumulative tissue compartments (Wang *et al.*, 1997).**

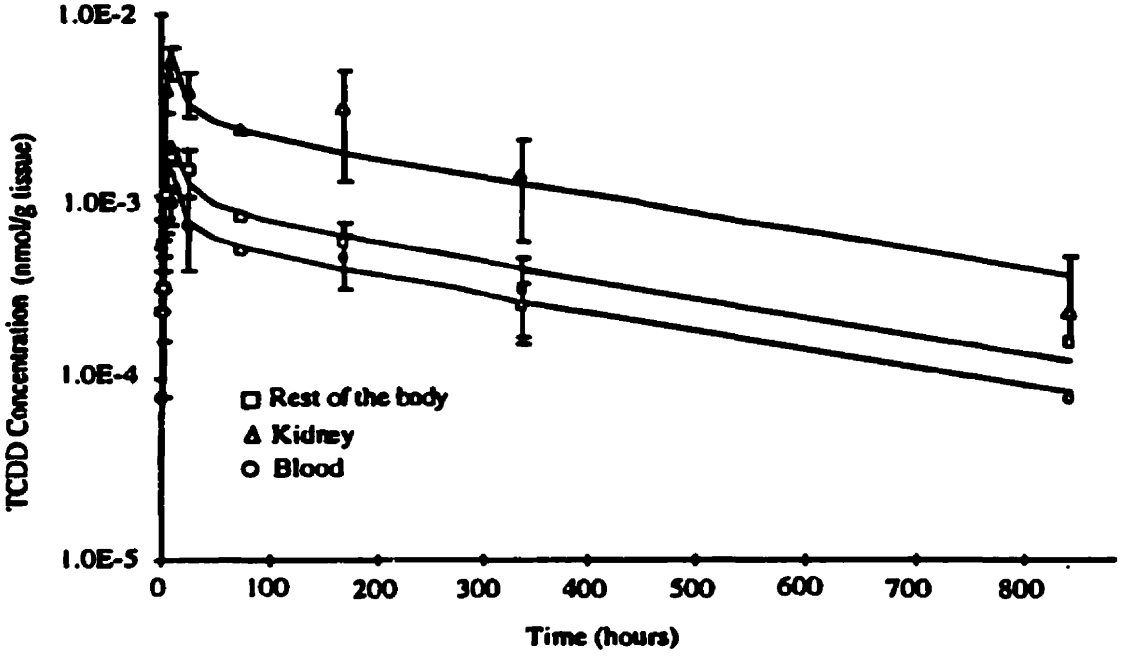


Figure 5.12 **Comparison of experimental (Wang et al., 1997) versus predicted (with reproduced model) TCDD timeseries tissue concentrations in various non-accumulative tissue compartments.**

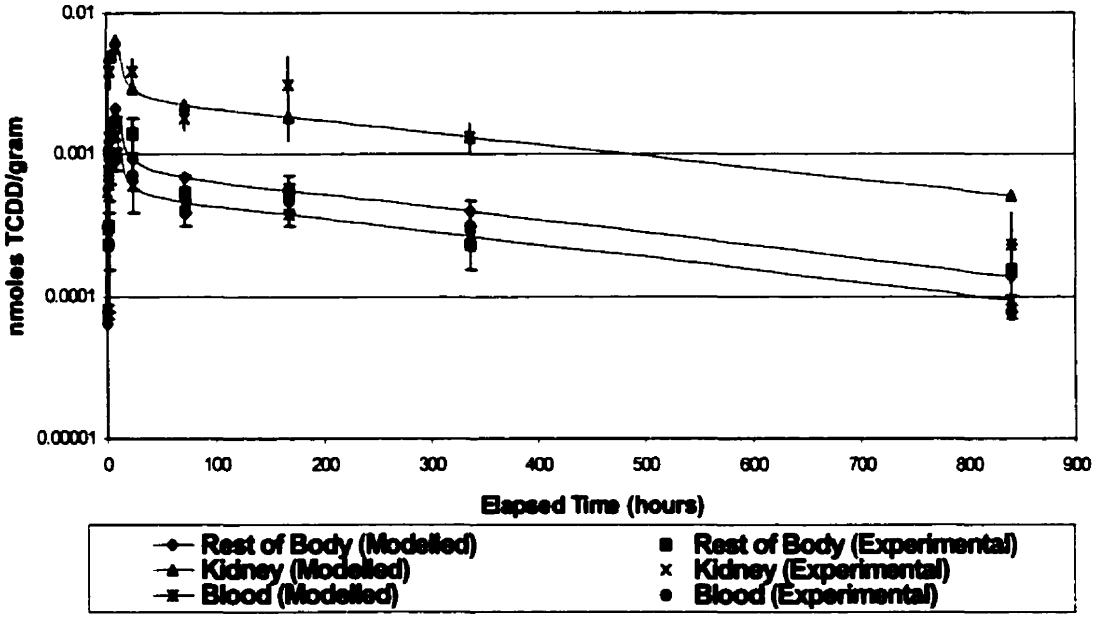


Figure 5.13 **Experimentally-derived TCDD concentrations in rats compared to curves describing model simulation results in accumulative tissue compartments, at early time points (Wang *et al.*, 1997).**

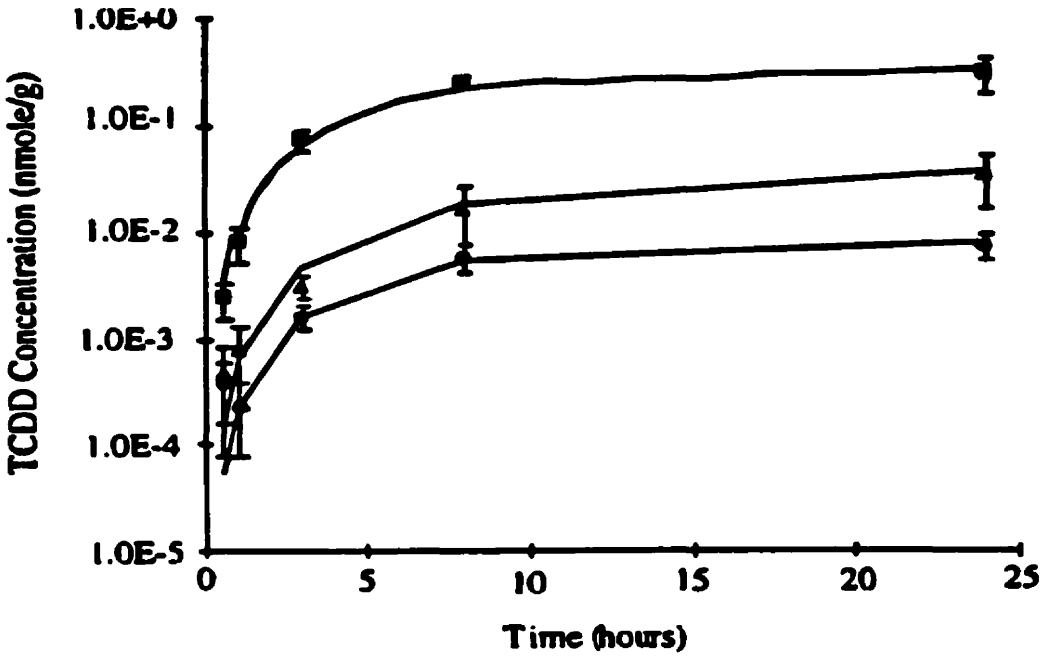


Figure 5.14 **Comparison of experimental (Wang et al., 1997) *versus* predicted (with reproduced model) TCDD timeseries tissue concentrations in various accumulative tissue compartments, at early time points.**

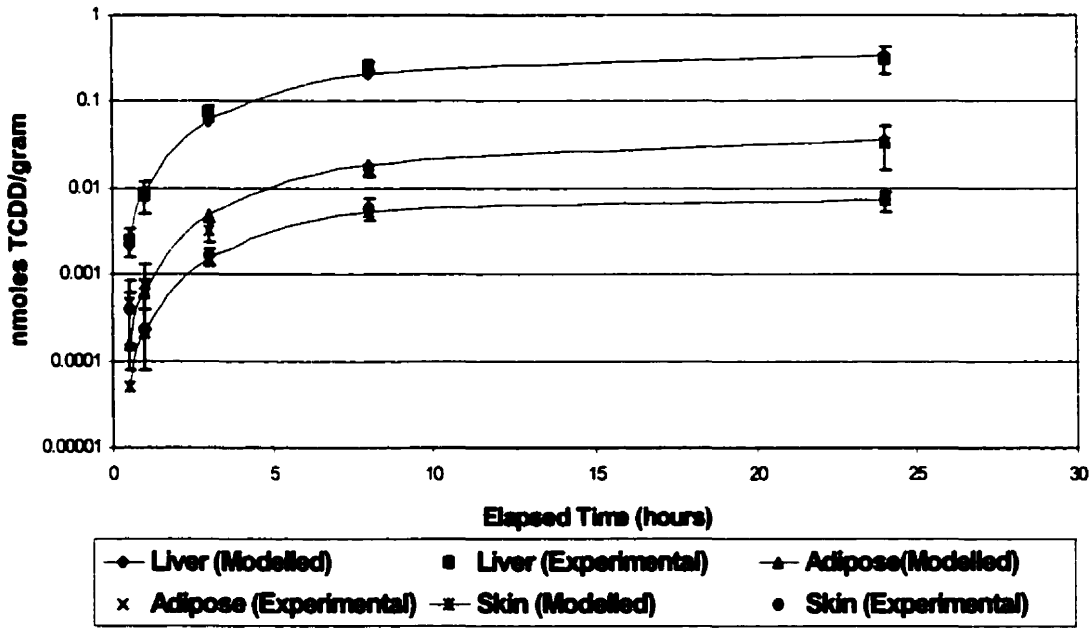


Figure 5.15 **Experimentally-derived TCDD concentrations in rats compared to curves describing model simulation results in non-accumulative tissue compartments, at early time points (Wang *et al.*, 1997).**

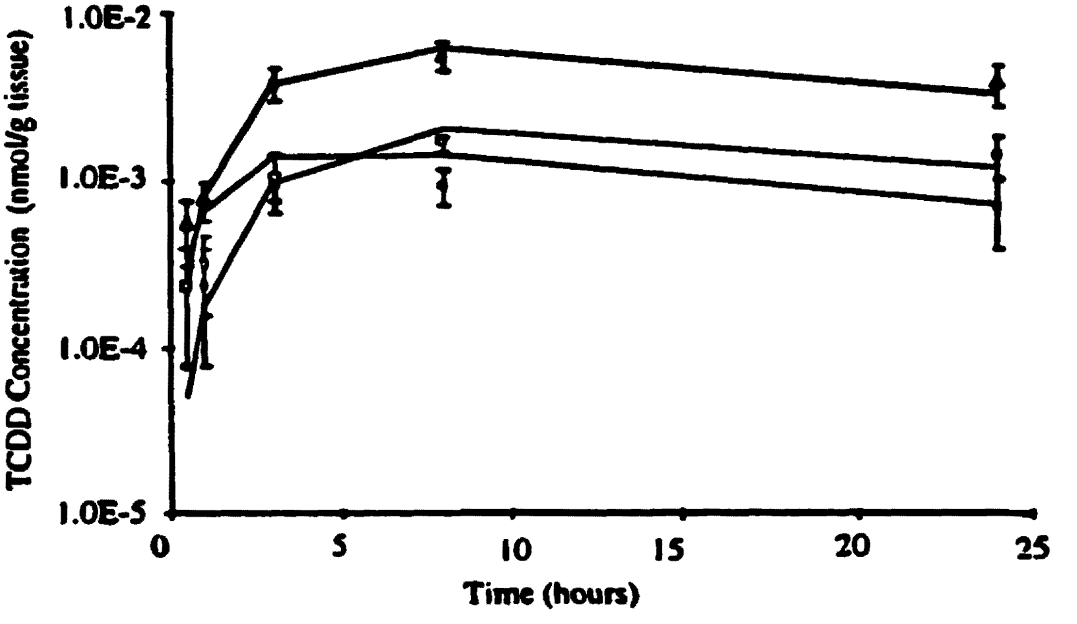
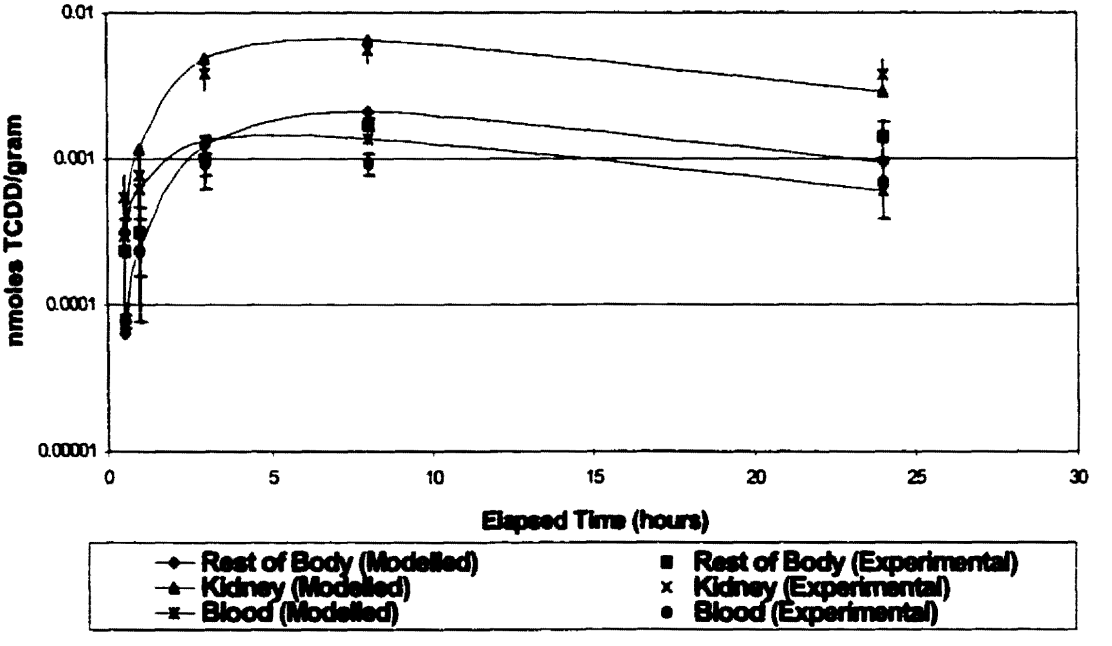


Figure 5.16 **Comparison of experimental (Wang et al., 1997) *versus* modelled TCDD timeseries tissue concentrations in various non-accumulative tissue compartments, at early time points.**



5.2.2 Comparison of Experimental versus Modelled Disposition Results

Comparative evaluations were conducted to determine if the developed steady-state PBPK model accurately reflected the results of experimental studies conducted with Sprague-Dawley rats (Wang *et al.*, 1997) and C57BL/6J mice (Diliberto *et al.*, 1999).

Sprague-Dawley Rat

The experimental results (Wang *et al.*, 1997) of the time course of TCDD distribution in all relevant tissue compartments (*i.e.*, the blood, liver, lungs, kidneys, spleen, skin, muscle, and adipose tissues) after an oral administration of 10 μg [^{3}H]TCDD/kg to Sprague-Dawley rats, and similar compartment-specific estimates calculated by the steady-state PBPK model, are provided in Table 5.9.

Table 5.9 Comparison of experimental [a] and modelled compartment-specific time course distribution of TCDD (% administered dose/g) after oral administration to Sprague-Dawley rats.

Time after dosing (hours)	Blood		Lungs		Spleen		Rest of the Body	
	Experimental	Modelled	Experimental	Modelled	Experimental	Modelled	Experimental	Modelled
0.5	0.001 ± 0.000	0.004	0.004 ± 0.001	0.019	0.016 ± 0.025	0.02	0.003 ± 0.002	0.001
1	0.003 ± 0.002	0.008	0.016 ± 0.005	0.036	0.016 ± 0.008	0.041	0.004 ± 0.002	0.003
3	0.012 ± 0.002	0.017	0.094 ± 0.019	0.075	0.073 ± 0.025	0.091	0.013 ± 0.005	0.016
8	0.012 ± 0.002	0.018	0.077 ± 0.012	0.077	0.037 ± 0.008	0.094	0.022 ± 0.002	0.027
24	0.009 ± 0.004	0.008	0.053 ± 0.015	0.035	0.023 ± 0.004	0.042	0.018 ± 0.005	0.012
72	0.005 ± 0.001	0.006	0.024 ± 0.003	0.027	0.013 ± 0.001	0.032	0.007 ± 0.002	0.009
168	0.006 ± 0.002	0.005	0.022 ± 0.007	0.022	0.011 ± 0.002	0.026	0.007 ± 0.002	0.007
336	0.004 ± 0.002	0.003	0.013 ± 0.003	0.016	0.010 ± 0.004	0.019	0.003 ± 0.001	0.005
840	0.001 ± 0.000	0.001	0.003 ± 0.001	0.006	0.002 ± 0.003	0.007	0.002 ± 0.001	0.002
	Adipose Tissue		Kidneys		Liver		Skin	
	Experimental	Modelled	Experimental	Modelled	Experimental	Modelled	Experimental	Modelled
0.5	0.006 ± 0.005	0.002	0.007 ± 0.003	0.004	0.032 ± 0.012	0.028	0.005 ± 0.003	0.001
1	0.010 ± 0.007	0.008	0.010 ± 0.004	0.015	0.108 ± 0.042	0.11	0.003 ± 0.002	0.003
3	0.041 ± 0.010	0.062	0.050 ± 0.012	0.063	0.958 ± 0.184	0.76	0.021 ± 0.005	0.02
8	0.206 ± 0.034	0.237	0.072 ± 0.014	0.084	3.321 ± 0.376	2.715	0.075 ± 0.021	0.068
24	0.435 ± 0.225	0.472	0.049 ± 0.013	0.038	4.046 ± 1.416	4.443	0.093 ± 0.025	0.092
72	0.626 ± 0.137	0.553	0.023 ± 0.004	0.028	3.502 ± 0.541	4.014	0.061 ± 0.014	0.062
168	0.547 ± 0.209	0.498	0.040 ± 0.024	0.023	2.824 ± 0.852	3.19	0.056 ± 0.008	0.049
336	0.204 ± 0.083	0.36	0.017 ± 0.004	0.017	1.461 ± 0.277	2.175	0.036 ± 0.006	0.035
840	0.091 ± 0.017	0.127	0.003 ± 0.000	0.007	0.288 ± 0.091	0.61	0.002 ± 0.000	0.012

[a] Time course tissue distribution of TCDD after oral administration of 10 μg [^{3}H]TCDD/kg to Sprague-Dawley rats; mean ± standard deviation (n = 3-5 animals/group) (Wang *et al.*, 1997).

To assess whether the compartment-specific TCDD concentrations provide an accurate surrogate for experimentally-derived concentrations reported in Wang *et al.* (1997), modelled concentrations were evaluated as to whether they fall within the 95% confidence intervals (represented by 2.575-times the standard deviation for 5 observations) of the experimental results. Table 5.10, below, provides the results of this analyses, and indicates that the modelled concentrations fell within the 95% confidence interval approximately 80% of the time with most of the excursions occurring at later time points (*i.e.*, > 14 days following exposure). Furthermore, the vast majority of the excursions were observed in the lung and spleen compartments, with the important disposition compartments (*i.e.*, the skin, liver, and adipose tissue) demonstrating a high degree of correlation between experimental and modelled data (falling within the 95% confidence interval approximately 89% of the time).

Figure 5.17 provides a snapshot comparison of the experimental data, including the 95% confidence intervals, and the modelled TCDD concentrations in the liver and adipose tissue compartments over time. As indicated in Table 5.10, the figure demonstrates the high degree of consistency between the experimental results and modelled TCDD compartmental concentration predictions.

Table 5.10 Evaluation of Time Course Compartment-Specific Concentration (% Administered Dose/Gram) for Modelled *versus* Experimental Data.

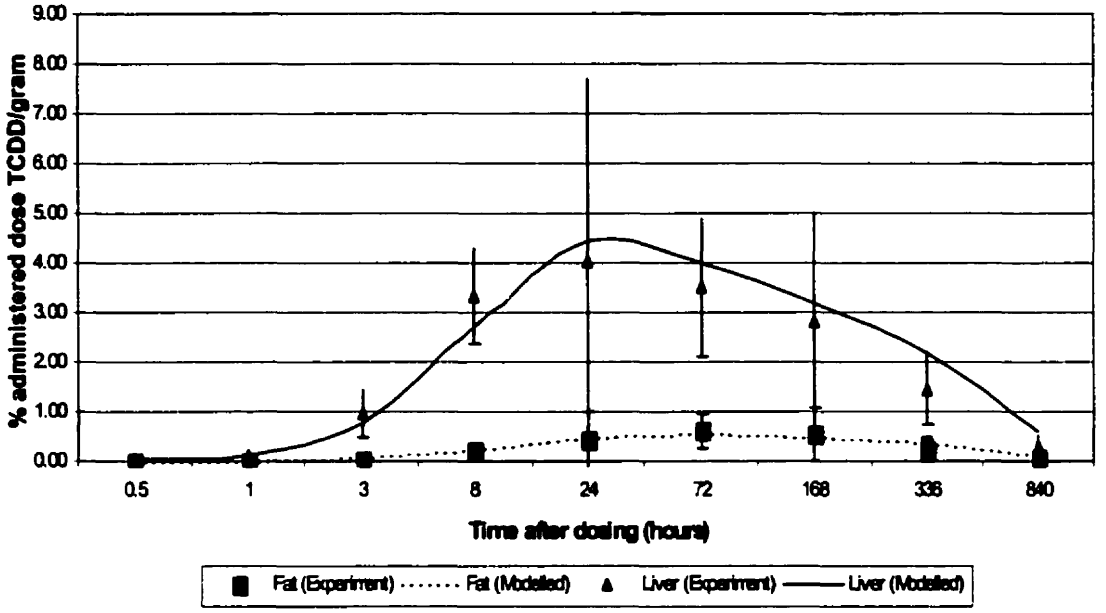
Time (hrs)	Experiment [a]	SD	95% CI bound	5% CI	95% CI	Modelled	Match [b]	Difference	Diff *vs.* Exp
Blood									
0.5	0.001	0	0.0005	0.0005	0.0015	0.004		0.00250	250%
1	0.003	0.002	0.00515	0.0001	0.00815	0.008	✓		
3	0.012	0.002	0.00515	0.00685	0.0172	0.017	✓		
8	0.012	0.002	0.00515	0.00685	0.0172	0.018		0.000850	7%
24	0.009	0.004	0.0103	0.0001	0.0193	0.008	✓		
72	0.005	0.001	0.00258	0.00243	0.00758	0.006	✓		
168	0.006	0.002	0.00515	0.00085	0.0112	0.005	✓		
336	0.004	0.002	0.00515	0.0001	0.00915	0.003	✓		
840	0.001	0	0.0005	0.0005	0.0015	0.001	✓		
							77.8%		
Lungs									
0.5	0.004	0.001	0.00258	0.00143	0.00658	0.019		0.0124	311%
1	0.016	0.005	0.0129	0.00313	0.0289	0.036		0.00713	45%
3	0.094	0.019	0.0489	0.0451	0.143	0.075	✓		
8	0.077	0.012	0.0309	0.0461	0.108	0.0777	✓		
24	0.053	0.015	0.0386	0.0144	0.0916	0.035	✓		
72	0.024	0.003	0.00773	0.0163	0.0317	0.027	✓		
168	0.022	0.007	0.0180	0.00398	0.0400	0.022	✓		
336	0.013	0.003	0.00773	0.00528	0.0207	0.016	✓		
840	0.003	0.001	0.00258	0.000425	0.00558	0.006		0.000425	14%
							66.7%		
Spleen									
0.5	0.016	0.025	0.0644	0.0001	0.0804	0.02	✓		
1	0.016	0.008	0.0206	0.0001	0.0366	0.041		0.00440	28%
3	0.073	0.025	0.0644	0.00862	0.137	0.091	✓		
8	0.037	0.008	0.0206	0.0164	0.0576	0.094		0.0364	98%
24	0.023	0.004	0.0103	0.0127	0.0333	0.042		0.00870	38%
72	0.013	0.001	0.00258	0.0104	0.0156	0.032		0.0164	126%
168	0.011	0.002	0.00515	0.00585	0.0162	0.026		0.00985	90%
336	0.01	0.004	0.0103	0.0001	0.0203	0.019	✓		
840	0.002	0.003	0.00773	0.0001	0.00973	0.007	✓		
							44.4%		
Rest of the Body									
0.5	0.003	0.002	0.00515	0.0001	0.00815	0.001	✓		
1	0.004	0.002	0.00515	0.0001	0.00915	0.003	✓		
3	0.013	0.005	0.0129	0.000125	0.0259	0.016	✓		
8	0.022	0.002	0.00515	0.0169	0.0272	0.027	✓		
24	0.018	0.005	0.0129	0.00513	0.0309	0.012	✓		
72	0.007	0.002	0.00515	0.00185	0.0122	0.009	✓		
168	0.007	0.002	0.00515	0.00185	0.0122	0.007	✓		
336	0.003	0.001	0.00258	0.000425	0.00558	0.005	✓		
840	0.002	0.001	0.00258	0.0001	0.00458	0.002	✓		
							100.0%		

Table 5.10 Evaluation of Time Course Compartment-Specific Concentration (% Administered Dose/Gram) for Modelled *versus* Experimental Data.

Time (hrs)	Experiment [a]	SD	95% CI bound	5% CI	95% CI	Modelled	Match [b]	Difference	Diff *vs.* Exp
Fat									
0.5	0.006	0.005	0.0129	0.0001	0.0189	0.002	✓		
1	0.01	0.007	0.0180	0.0001	0.0280	0.008	✓		
3	0.041	0.01	0.0258	0.0153	0.0668	0.062	✓		
8	0.206	0.034	0.0876	0.118	0.294	0.237	✓		
24	0.435	0.225	0.579	0.0001	1.01	0.472	✓		
72	0.626	0.137	0.353	0.273	0.979	0.553	✓		
168	0.547	0.209	0.538	0.00882	1.09	0.498	✓		
336	0.204	0.083	0.214	0.0001	0.418	0.36	✓		
840	0.091	0.017	0.0438	0.0472	0.135	0.127	✓		
							100.0%		
Kidneys									
0.5	0.007	0.003	0.00773	0.0001	0.0147	0.004	✓		
1	0.01	0.004	0.0103	0.0001	0.0203	0.015	✓		
3	0.05	0.012	0.0309	0.0191	0.0809	0.063	✓		
8	0.072	0.014	0.0361	0.0360	0.108	0.084	✓		
24	0.049	0.013	0.0335	0.0155	0.0825	0.038	✓		
72	0.023	0.004	0.0103	0.0127	0.0333	0.028	✓		
168	0.04	0.024	0.0618	0.0001	0.102	0.023	✓		
336	0.017	0.004	0.0103	0.0067	0.0273	0.017	✓		
840	0.003	0	0.0005	0.0025	0.0035	0.007		0.00350	117%
							88.9%		
Liver									
0.5	0.032	0.012	0.0309	0.0011	0.0629	0.028	✓		
1	0.108	0.042	0.108	0.0001	0.216	0.11	✓		
3	0.958	0.184	0.474	0.484	1.43	0.76	✓		
8	3.321	0.376	0.968	2.35	4.29	2.715	✓		
24	4.046	1.416	3.65	0.400	7.69	4.443	✓		
72	3.502	0.541	1.39	2.11	4.90	4.014	✓		
168	2.824	0.852	2.19	0.630	5.02	3.19	✓		
336	1.461	0.277	0.713	0.748	2.17	2.175	• [c]	0.000725	0.0496%
840	0.288	0.091	0.234	0.0537	0.522	0.61		0.0877	30.4%
							77.8%		
Skin									
0.5	0.005	0.003	0.00773	0.0001	0.0127	0.001	✓		
1	0.003	0.002	0.00515	0.0001	0.00815	0.003	✓		
3	0.021	0.005	0.0129	0.00813	0.0339	0.02	✓		
8	0.075	0.021	0.0541	0.0209	0.129	0.068	✓		
24	0.093	0.025	0.0644	0.0286	0.157	0.092	✓		
72	0.061	0.014	0.0361	0.0250	0.0971	0.062	✓		
168	0.056	0.008	0.0206	0.0354	0.0766	0.049	✓		
336	0.036	0.006	0.0155	0.0206	0.0515	0.035	✓		
840	0.002	0	0.0005	0.0015	0.0025	0.012		0.00950	475%
							88.9%		
OVERALL							**80.6%**	**0.014**	**116%**

[a] Time course tissue distribution of TCDD after oral administration (Wang *et al.*, 1997).
[b] Does modelled results fall within the 95% confidence interval (2.575x SD for 5 observations)?
[c] Predicted value was marginally outside of the 95% confidence interval, with only a 0.05% difference between the predicted value and the upper CI limit value.

Figure 5.17 Comparison of experimental (with 95% confidence intervals) *versus* modelled liver and adipose tissue compartmental TCDD distribution.



A statistical analysis of the sums of squares variance between the experimental and modelled disposition results was also conducted, based upon the percentage of administered dose per gram tissue in each compartment and time point. The sums of squares was 51.9 and 60.2 for the experimental and modelled mean values, respectively. This results in a residual Sums of Squares of 1.66, indicating that the modelled data effectively represented the experimental data 96.8% of the time, based upon its residual sums of squares error.

Based upon the above evaluations, it was concluded that the Sprague-Dawley TCDD PBPK model appears to accurately duplicate the output of the model presented in Wang *et al.* (1997). Furthermore, it also appears to accurately represent the experimentally-derived data presented in Wang *et al.* (1997).

C57BL/6J Mice

The experimental results (Diliberto *et al.*, 1999) of the time course of TCDD distribution in all relevant tissue compartments (*i.e.*, the blood, liver, lungs, kidneys, spleen, skin, muscle, and adipose tissues) after an oral administration of 25 μg [^{3}H]TCDD/kg to C57BL/6J mice, and similar compartment-specific estimates calculated by the steady-state PBPK model are provided in Table 5.11. Unfortunately, experimental results were only provided at 4 days post-treatment, and as such it is difficult to determine whether the model accurately reflects the experimental results at differing time points.

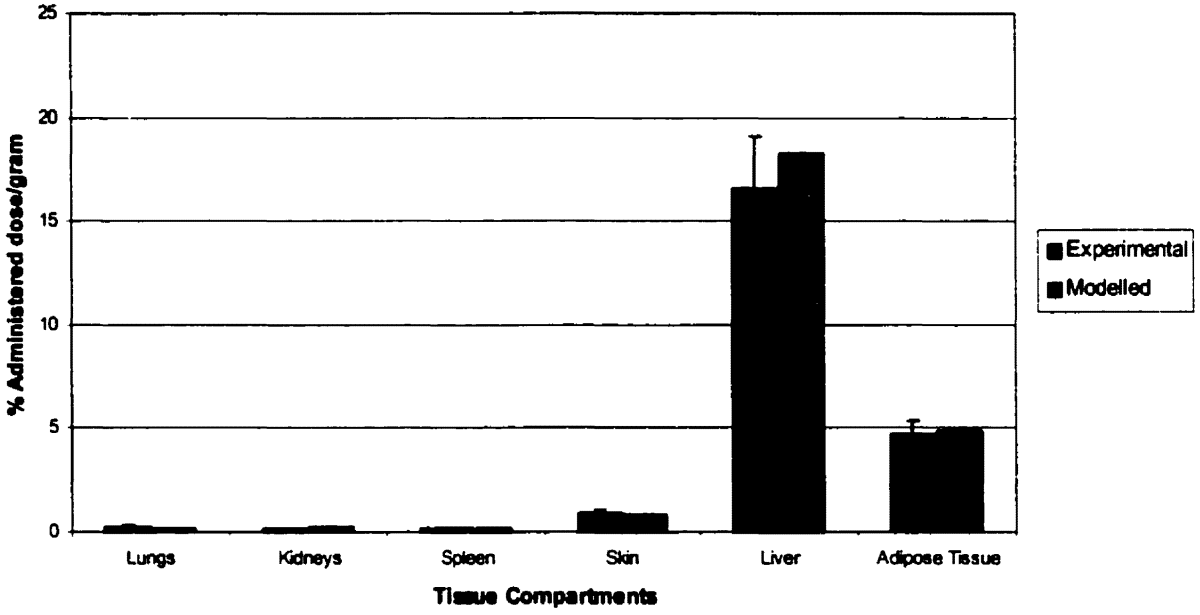
Table 5.11 Comparison of experimental * and modelled compartment-specific time course distribution of TCDD (% administered dose/g) after oral administration to C57BL/6J mice, 4-days Post-treatment.

Parameter	Experimental	Modelled
Lungs	0.27 ± 0.07	0.144
Kidneys	0.17 ± 0.02	0.213
Spleen	0.14 ± 0.02	0.178
Skin	0.89 ● 0.19	0.79
Liver	16.52 ± 2.58	18.27
Adipose Tissue	4.67 ± 0.70	4.91
Liver/Fat Ratio	3.55 ± 0.41	3.72

* Time course tissue distribution (expressed as means ± SD) of TCDD after oral administration of 25 μg [^{3}H]TCDD/kg to C57BL/6J mice, 4-days post-treatment (Diliberto *et al.*, 1999).

While the modelled results slightly overestimated disposition in most of the assessed compartments, they were generally within one standard deviation of the experimental mean concentration (see Figure 5.18), and well within the 95% confidence interval of the experimental results. Given the agreement between experimental and modelled results in most compartments, as well as with the liver-to-fat ratios, it was concluded (based upon the minimal experimental data available) that the modified model provided a reasonable estimation of TCDD disposition, based upon the Diliberto *et al.* (1999) data.

Figure 5.18 Comparison of experimental and modelled compartment-specific TCDD concentrations (% administered dose/gram) after oral administration of 25 μg/kg to C57BL/6J mice, 4-days post-treatment.



Diliberto *et al.* (1999) also conducted a time course study of 4-PeCDF distribution in all relevant compartments after an oral administration of 300 μg [^{3}H]4-PeCDF/kg to C57BL/6J mice. Table 5.12, below, provides the results of this study compared to the similar compartment-specific estimates calculated by the research steady-state model, after 4-days of exposure.

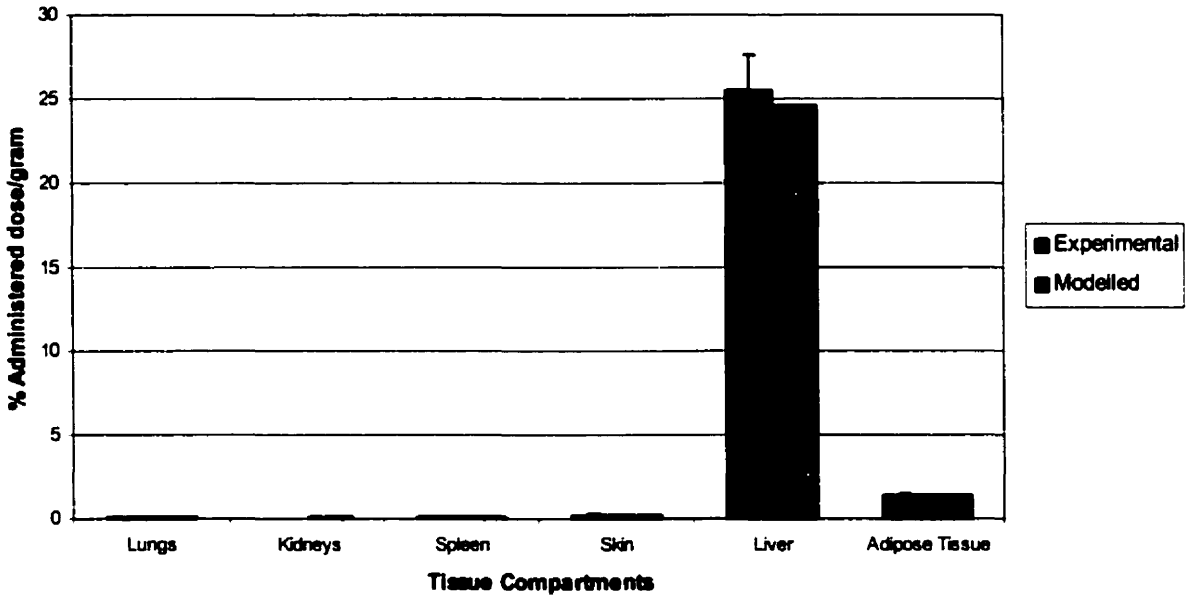
Table 5.12 Comparison of experimental [a] and modelled compartment-specific time course distribution of 4-PeCDF (% administered dose/g) after oral administration to C57BL/6J mice, 4-days Post-treatment.

Parameter	Experimental	Modelled
Lungs	0.09 ± 0.03	0.093
Kidneys	0.028 ± 0.002	0.07
Spleen	0.06 ± 0.01	0.06
Skin	0.22 ± 0.09	0.233
Liver	25.44 ± 2.13	24.6
Adipose Tissue	1.38 ± 0.14	1.43
Liver/Fat Ratio	18.68 ± 2.96	17.2

[a] Time course tissue distribution (expressed as means ± SD) of 4-PeCDF after oral administration of 300 μg [^{3}H]4-PeCDF/kg to C57BL/6J mice, 4-days post-treatment (Diliberto *et al.*, 1999).

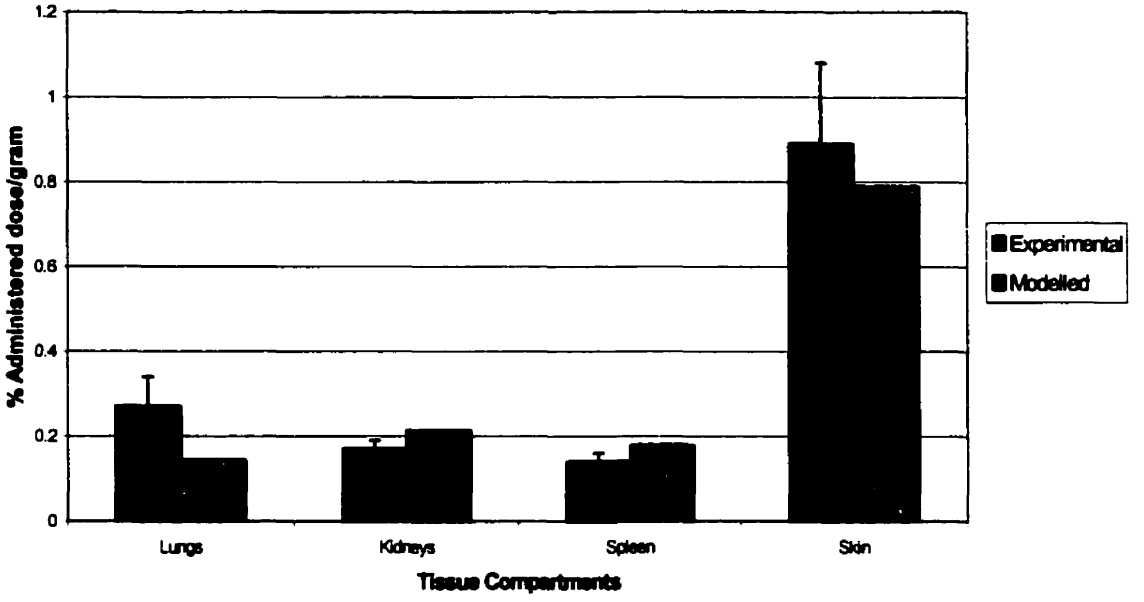
While the modelled results slightly overestimated disposition in most of the assessed compartments, the modelled results were generally within one standard deviation of the experimental mean concentration (see Figure 5.19), and well within the 95% confidence interval of the experimental results. Given the agreement between experimental and modelled results in most compartments, as well as with the liver-to-fat ratios, it was concluded (based upon the minimal experimental data available) that the modified model provided a reasonable estimation of 4-PeCDF disposition, based upon the Diliberto *et al.* (1999) data.

Figure 5.19 Comparison of experimental and modelled compartment-specific 4-PeCDF concentrations (% administered dose/gram) after oral administration of 300 µg/kg to C57BL/6J mice, 4-days post-treatment.



Given the low % administered dose/gram found in the lungs, kidneys, spleen, and skin compartments, Figure 5.20, below, provides a closer evaluation of these particular compartmental tissue groups.

Figure 5.20 Comparison of experimental and modelled compartment-specific 4-PeCDF concentrations (% administered dose/gram) after oral administration of 300 μg/kg to C57BL/6J mice, 4-days post-treatment (only lungs, kidneys, spleen, and skin).



5.2.3 Sensitivity Analysis of Prototype Steady-State PBPK Model

A sensitivity/uncertainty analysis was conducted on the steady-state PBPK model based upon 5,000 Monte Carlo iterations, to determine which variables pose the largest influence on the ultimate outcome of the model (*i.e.*, overall body sequestration of TCDD). Table 5.13 provides the contribution to variance (by percentage) of each parameter group, over a range of administered dose levels, at 8-, 24-, and 48-hours after exposure, for the Sprague-Dawley rat. A complete breakdown of the contribution to variance of each individual parameter is provided in Table B-1.0 of Appendix B.

Table 5.13 Sensitivity Analysis of Contribution to Variance between TCDD PBPK Model Variables and Sequestration Outcome for Specific Parameter Groups[a] the Sprague-Dawley Rat.

Parameter Groups	Administered Dose of TCDD (μg/kg)				
	0.1	0.316	1	3.16	10
8-Hours after Exposure					
General Physiological Parameters	19.6%	2.7%	2.2%	1.6%	4.3%
Equilibrium Distribution Ratio	26.3%	9.1%	12.3%	25.0%	13.2%
Permeability	7.0%	10.6%	10.8%	13.9%	25.4%
Compartment Volumes	13.1%	13.1%	15.0%	27.0%	11.1%
Absorption and Elimination	18.5%	12.7%	14.6%	5.4%	26.1%
Ah Receptor Pharmacodynamics	4.2%	18.8%	35.7%	9.6%	5.6%
CYP1A2 Receptor Pharmacodynamics	11.3%	33.1%	9.4%	17.5%	14.4%
24-Hours after Exposure					
General Physiological Parameters	17.6%	1.6%	5.7%	1.8%	3.4%
Equilibrium Distribution Ratio	21.9%	8.2%	11.0%	22.3%	13.3%
Permeability	7.3%	12.2%	16.2%	14.5%	27.2%
Compartment Volumes	12.5%	17.0%	14.1%	29.4%	12.8%
Absorption and Elimination	19.6%	18.1%	11.5%	5.5%	23.5%
Ah Receptor Pharmacodynamics	5.4%	9.8%	32.3%	10.6%	6.2%
CYP1A2 Receptor Pharmacodynamics	15.6%	33.1%	9.2%	16.0%	13.6%
72-Hours after Exposure					
General Physiological Parameters	9.1%	3.7%	6.1%	2.3%	2.4%
Equilibrium Distribution Ratio	16.8%	11.2%	14.4%	20.5%	13.4%
Permeability	7.2%	19.7%	10.4%	14.8%	26.0%
Compartment Volumes	19.0%	15.0%	14.7%	29.9%	14.5%
Absorption and Elimination	22.1%	11.6%	14.5%	6.1%	20.2%
Ah Receptor Pharmacodynamics	4.6%	11.0%	27.6%	12.0%	8.9%
CYP1A2 Receptor Pharmacodynamics	21.2%	27.7%	12.3%	14.4%	14.5%

[a] Applicable parameters were added to produce an overall total contribution to variance percentage for each parameter group. A detailed list of the specific parameters combined to form each group can be found in Table B-2.0 of Appendix B.

Graphical comparisons of the contribution of variance for each of the parameter groups at various administered dose levels are presented in Figure 5.21 through 5.23 at 8-, 24-, and 48-hours following exposure, respectively.

Figure 5.21 Comparison of contribution of variance (%) for key parameter groups at each administered dose level, 8-hours after exposure.

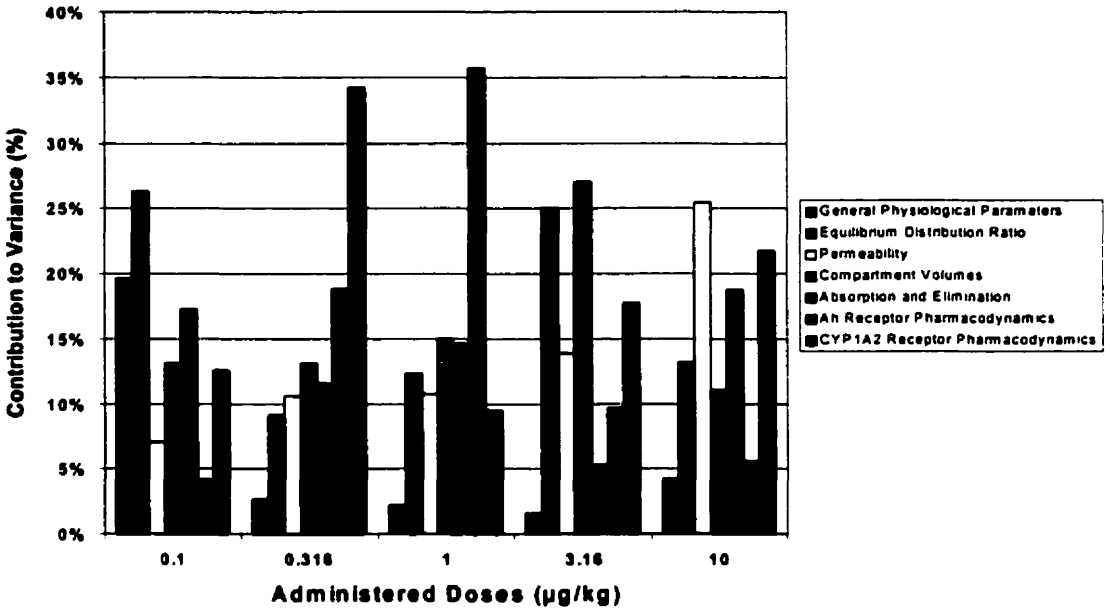


Figure 5.22 Comparison of contribution of variance (%) for key parameter groups at each administered dose level, 24-hours after exposure.

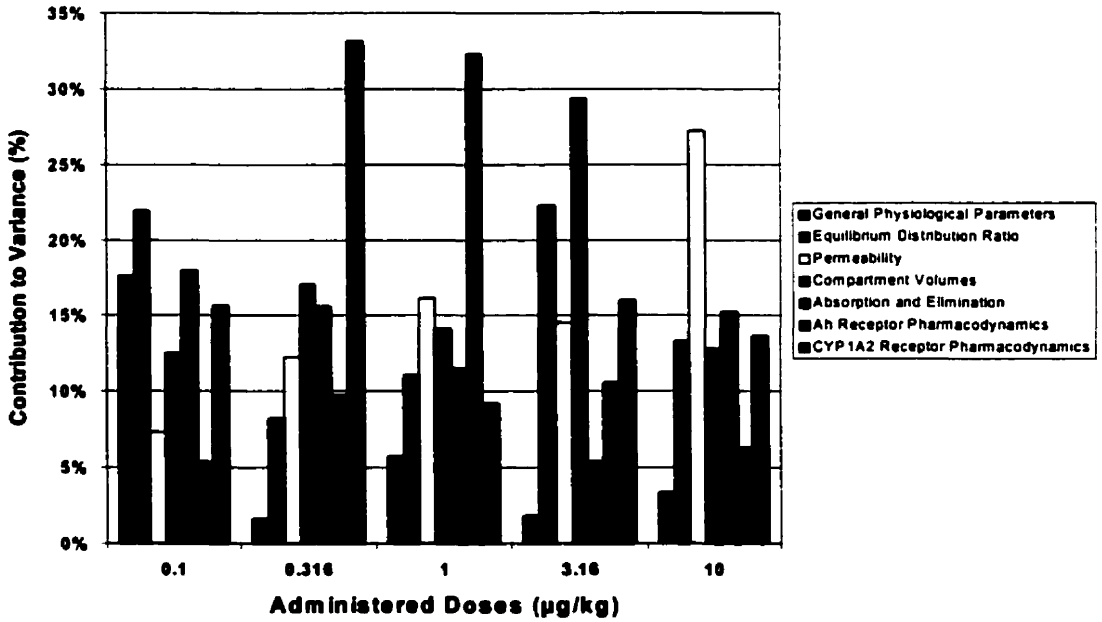
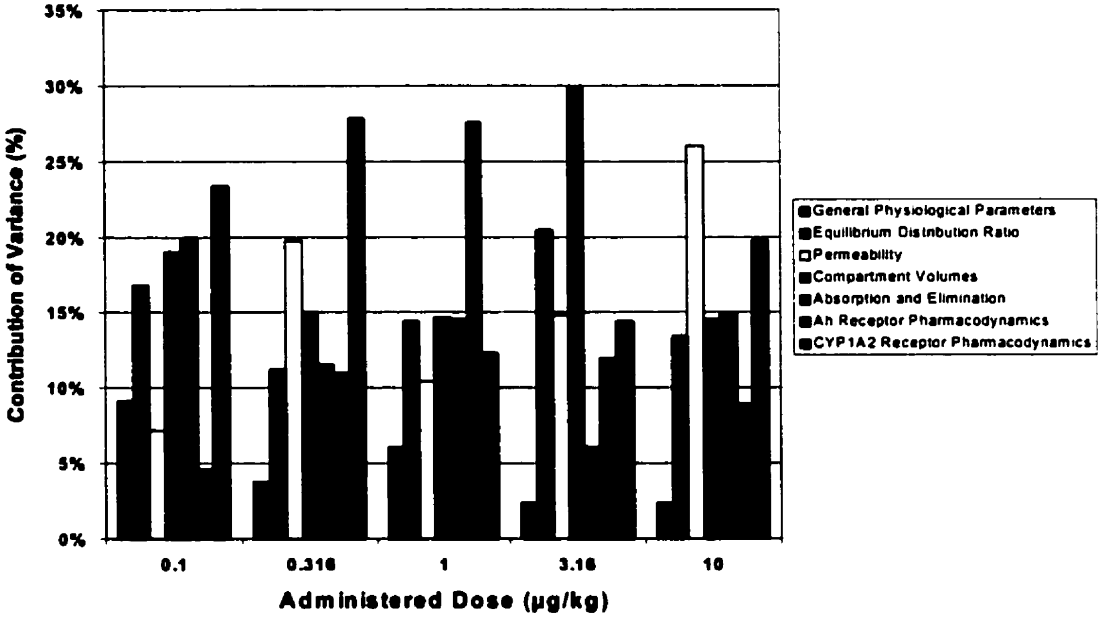


Figure 5.23 Comparison of contribution of variance (%) for key parameter groups at each administered dose level, 72-hours after exposure.



Results of the sensitivity analysis indicate that while individual parameters within the set parameter groups do vary as to their relative impacts on overall contribution to variance, there appears to be very little difference in overall group variance patterns between the three exposure times (*i.e.*, 8-, 24-, and 48-hours following dose exposure).

Unlike the relative lack of variance at differing time points after exposure, results of the sensitivity analyses indicates a definite dose-dependancy in those variable groups showing the highest contribution of variance. In addition to the overall parameter group evaluations, Table 5.14 provides the top 15 individual parameters demonstrating the largest contribution to variance in TCDD disposition for each dose level, 24-hours following initial exposure.

At low administered doses (*i.e.*, below the 0.1 µg/kg bodyweight level), the compartment-specific equilibrium ratios and general physiological parameters dominated the contribution to variance in TCDD disposition kinetics (*i.e.*, > 45%), with ligand-receptor pharmacodynamics typically playing a very minor role. The receptor body weight, biliary excretion rate, and equilibrium ratio of skin tissue to blood concentration appear to be the key leverage parameters at

this particular dose level. However, as the exposure dose increases, these roles become reversed with pharmacodynamic impacts dominating the overall contribution to variance.

For example, at the 0.316 μg/kg bodyweight dose, CYP1A2 binding kinetic parameters (primarily the concentration resulting in half maximum induction folds) have the largest contribution to variance, with Ah receptor related parameters playing a lesser (though still elevated) role. However, at the 1 μg/kg bodyweight dose, the contribution of Ah receptor binding parameters (primarily the Ah receptor binding capacity in the large compartments such as the skin and lungs) to overall variance in TCDD disposition is elevated, with CYP1A2-related parameters having a greatly reduced role.

It is interesting to note that the oral bioavailability of TCDD appears to be a significant leverage variable at the 0.316 μg/kg bodyweight dose level, while playing a very minor role at the 1 μg/kg bodyweight level. Conversely, the compartmental permeability of the liver is important at the higher dose rate, while not even in the top 15 list of parameters at lower dose exposures.

As the administered dose increases beyond the 3.16 μg/kg bodyweight level, the contribution to variance from ligand-receptor parameters return to the levels observed at the very low doses (*i.e.*, ≤0.1 μg/kg bodyweight), while parameters related to compartmental permeability, as well as TCDD absorption and elimination, play key roles in the ultimate disposition of the contaminant. At the 3.16 μg/kg bodyweight dose level, the equilibrium ratio of liver tissue to blood concentration and the rest of the body volume as a percentage of body weight appear to be the dominant parameters, while at the higher 10 μg/kg bodyweight dose, the compartmental permeability of the adipose tissue and liver compartments contribute more than 20% of the overall variance in TCDD disposition.

Table 5.14 Top 15 Physiological Parameters by Contribution to Variance to TCDD Disposition, 24-Hours at each Administered Dose Level.

Physiological Parameter	Contribution to Variance
0.1 μg TCDD/kg Dose	
Body weight of the receptor	11.6%
Biliary excretion rate	8.6%
Equilibrium ratio of skin tissue to blood concentration	7.8%
Allometric parameter for cardiac output from bodyweight	6.1%
Absorption rate constant from GI tract to blood	5.5%
Equilibrium ratio of kidney tissue to blood concentration	5.4%
Lung volume as a percentage of body weight	4.8%
Basal level of CYP1A2 within the liver	4.4%
Compartmental permeability of the skin	3.9%
Urinary excretion rate	3.8%
Dissociation constant of CYP1A2 binding	3.7%
Equilibrium ratio of spleen tissue to blood concentration	3.6%
Equilibrium ratio of tissue in the rest of the body to blood concentration	3.3%
Hill coefficient	2.9%
CYP1A2 physiological delay time	2.8%
0.316 μg TCDD/kg Dose	
Concentration to cause half of the maximum induction folds	15.7%
Oral bioavailability of TCDD	12.3%
Maximum induction folds over the basal induction rate	7.1%
Compartmental permeability of the skin	6.2%
Equilibrium ratio of adipose tissue to blood concentration	5.5%
CYP1A2 physiological delay time	5.3%
Skin volume as a percentage of body weight	5.1%
Hill coefficient	4.6%
Compartmental permeability of the rest of the body	4.4%
Kidney volume as a percentage of body weight	4.1%
Venous blood volume as a percentage of body weight	3.0%
Ah receptor binding capacity in the liver	2.8%
Ah receptor binding capacity in the spleen	2.7%
First-order degradation rate constant of CYP1A2 binding	2.5%
Ah receptor binding capacity in the skin	2.3%
1 μg TCDD/kg Dose	
Ah receptor binding capacity in the skin	19.4%
Compartmental permeability of the liver	11.2%
Ah receptor binding capacity in the lungs	7.1%
Equilibrium ratio of adipose tissue to blood concentration	7.0%
Urinary excretion rate	6.2%
Allometric parameter for cardiac output from bodyweight	4.4%
Compartmental permeability of the adipose tissue	4.0%
Lung volume as a percentage of body weight	3.8%
Kidney volume as a percentage of body weight	3.7%
Skin volume as a percentage of body weight	3.6%
Oral bioavailability of TCDD	2.9%
Basal level of CYP1A2 within the liver	2.6%
Dissociation constant of Ah receptor binding	2.6%
Hill coefficient	2.6%
Ah receptor binding capacity in the spleen	2.3%

3.16 μg TCDD/kg Dose

Table 5.14 Top 15 Physiological Parameters by Contribution to Variance to TCDD Disposition, 24-Hours at each Administered Dose Level.

Physiological Parameter	Contribution to Variance
Equilibrium ratio of liver tissue to blood concentration	13.0%
Rest of the body volume as a percentage of body weight	12.5%
Maximum induction folds over the basal induction rate	7.5%
Compartmental permeability of the skin	7.1%
Kidney volume as a percentage of body weight	6.4%
Compartmental permeability of the kidneys	5.6%
Basal level of CYP1A2 within the liver	5.2%
Ah receptor binding capacity in the skin	4.6%
Ah receptor binding capacity in the liver	4.3%
Spleen volume as a percentage of body weight	3.8%
Equilibrium ratio of kidney tissue to blood concentration	3.0%
Lung volume as a percentage of body weight	2.9%
Adipose tissue volume as a percentage of body weight	2.4%
Urinary excretion rate	2.3%
Equilibrium ratio of lung tissue to blood concentration	1.8%
10 μg TCDD/kg Dose	
Compartmental permeability of the adipose tissue	11.6%
Compartmental permeability of the liver	9.7%
First-order degradation rate constant of CYP1A2 binding	8.3%
Absorption rate constant from GI tract to blood	8.1%
Maximum induction folds over the basal induction rate	7.4%
Equilibrium ratio of tissue in the rest of the body to blood concentration	5.7%
Concentration to cause half of the maximum induction folds	4.5%
Equilibrium ratio of liver tissue to blood concentration	4.3%
Biliary excretion rate	4.1%
Compartmental permeability of the kidneys	4.0%
Skin volume as a percentage of body weight	3.9%
Dissociation constant of Ah receptor binding	3.8%
Kidney volume as a percentage of body weight	2.7%
Lung volume as a percentage of body weight	2.7%
Equilibrium ratio of adipose tissue to blood concentration	2.1%

5.3 Validation of Prototype Equilibrium-based Model

Following construction of the prototype equilibrium-based model, it is useful to validate the model against both the graphical output presented in the Evans and Andersen (2000) source paper. This step ensures that an accurate duplication of the Evans and Andersen methodology was used in the development of the base equilibrium-based model used in this research project.

5.2.1 Comparison of Modelled Results versus Evans and Andersen (2000) Graph

Evans and Andersen (2000) conducted an analysis of liver fraction (FH) fluctuations with respect to changing average body concentrations, and presented a plot of the resulting curve (see the default FH curve in Figure 5.24, below). To demonstrate an accurate reproduction of the published Evans and Andersen (2000) results, the equilibrium-based methodology and described analysis was recreated in an Excel spreadsheet. The resulting curve is provided in Figure 5.25. Based upon a visual comparison of the two figures, it appears that the based equilibrium model correctly reproduces the results presented by Evans and Andersen.

A similar analysis was conducted using the corrected version of the Evans and Andersen (2000) methodology, and the resulting curve is plotted along with the previous curve in Figure 5.26. As outlined in the methodology section, the mis-specification in the Evans and Andersen (2000) model results in a lower ceiling value for the liver fraction due to the 10-fold restriction in the maximum CYP1A2 induction fold increase. As noted previously, this impact is not immediately evident at lower exposure doses (*i.e.*, < 0.01 ng/kg), and only becomes apparent when Ah receptor occupancy is sufficient to result in an induction fold increase in microsomal CYP1A2 levels.

Figure 5.24 **Simulation results for the liver fraction (FH) presented in Evans and Andersen (2000).**

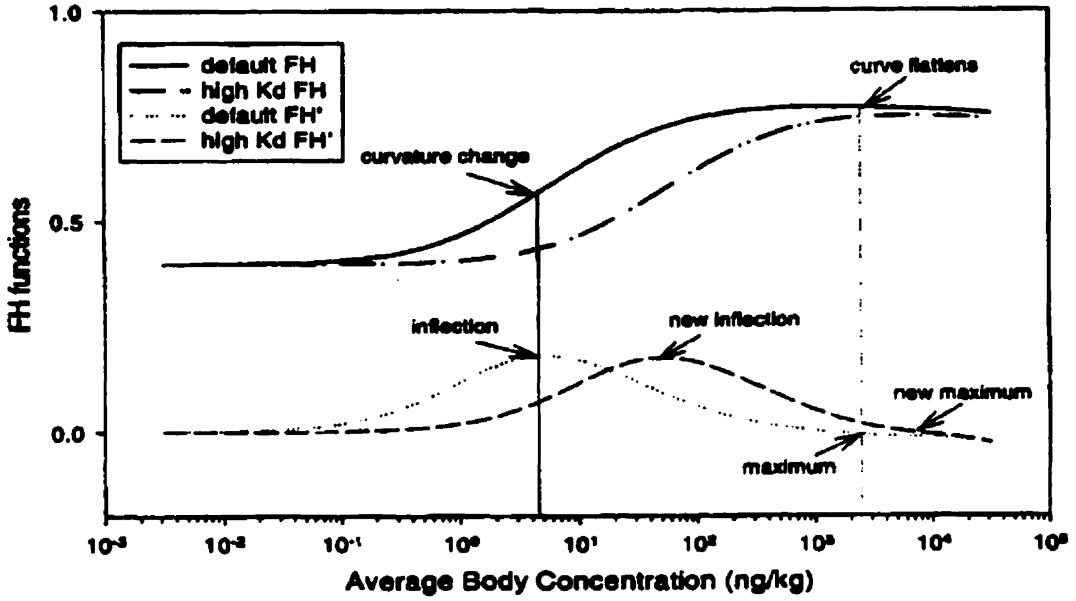


Figure 5.25 **Reproduction of dose-dependency curve based on original Evans and Andersen (2000) methodology.**

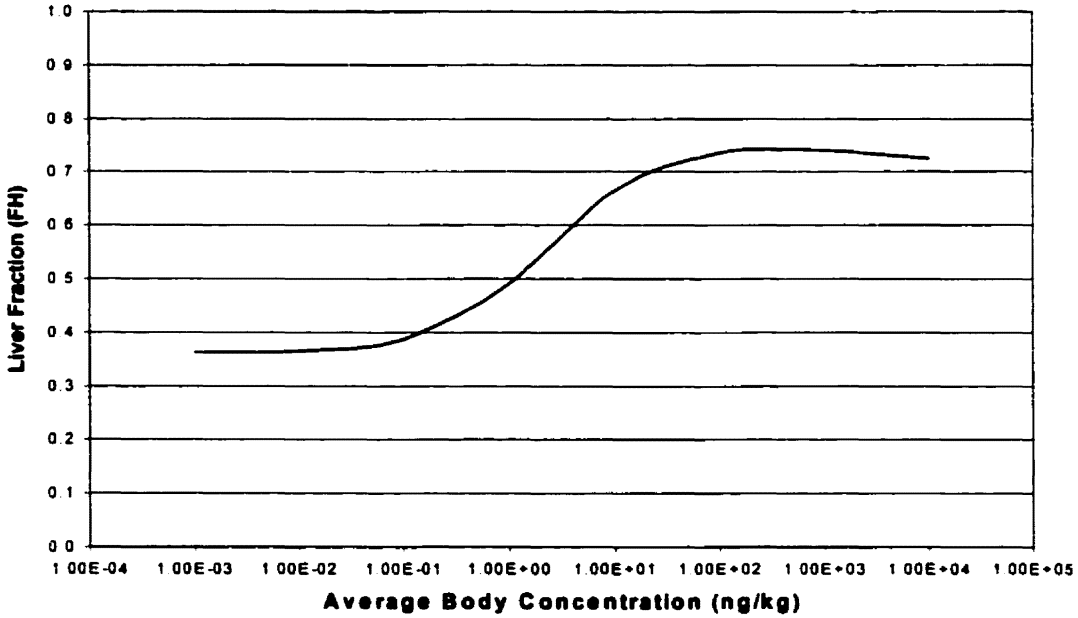
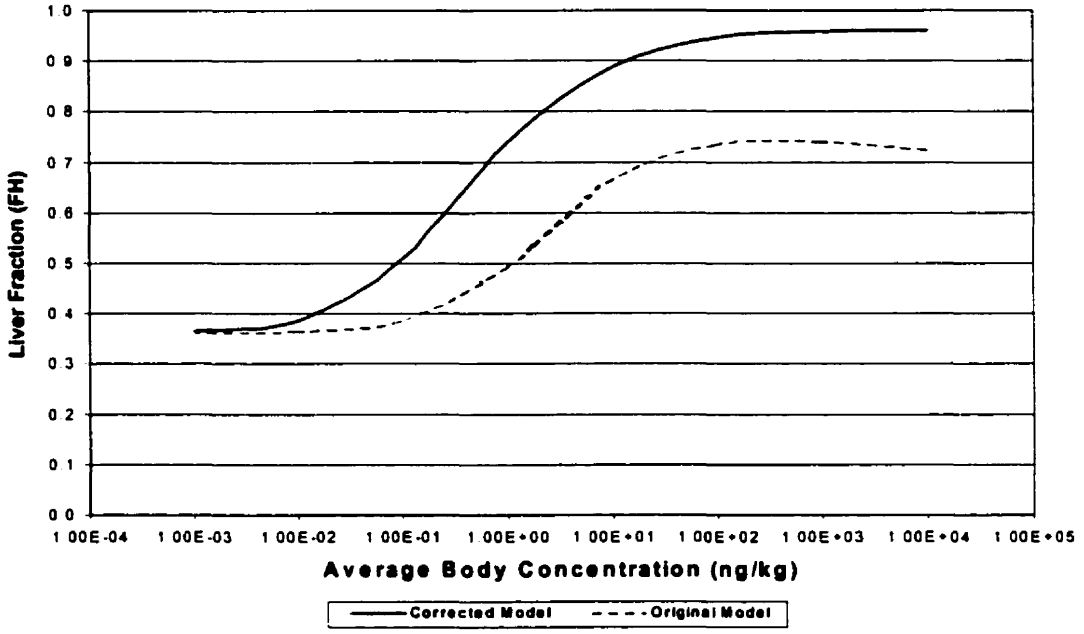


Figure 5.26 Reproduction of dose-dependency curves using both the original and corrected Evans and Andersen (2000) methodology.



5.2.2 Comparison of Steady-State versus Equilibrium-based Model

A comparison of the three assessed model methodologies (*i.e.*, steady-state PBPK model, original equilibrium-based model, and corrected equilibrium-based model) was conducted to determine if a two-compartment equilibrium-based model could adequately estimate the disposition pattern of TCDD in the Sprague-Dawley rat. This would allow one to determine whether the more complex, steady-state PBPK model is over-parameterized in its simulation of the physiological process involved.

To achieve this comparison, the excretion pathway was eliminated from the Wang *et al.* model to allow compartmental concentrations to reach a "pseudo" steady-state. As indicated in Figure 5.27, this pseudo steady-state level appeared to occur 24-hours following exposure to an administered dose of 10 μg/kg bodyweight. As such, comparisons with the equilibrium-based models were conducted using the data estimated at 24-hours following exposure. Interestingly enough, pseudo steady-state was not achieved until the 96-hour point at dose exposures less than 0.01 μg/kg bodyweight (see Figure 5.28) as a further physiological delay was required while initial liver and fat compartmental concentrations equilibrated. As such, comparisons with the

equilibrium-based models were conducted using the data estimated at 96-hours following exposure, for doses at and below 0.01 μg/kg bodyweight.

Figure 5.27 Graphical plot of time-series chemical concentrations in the liver and fat compartments following a 10 μg/kg bodyweight dose, using the steady-state PBPK model with excretion eliminated.

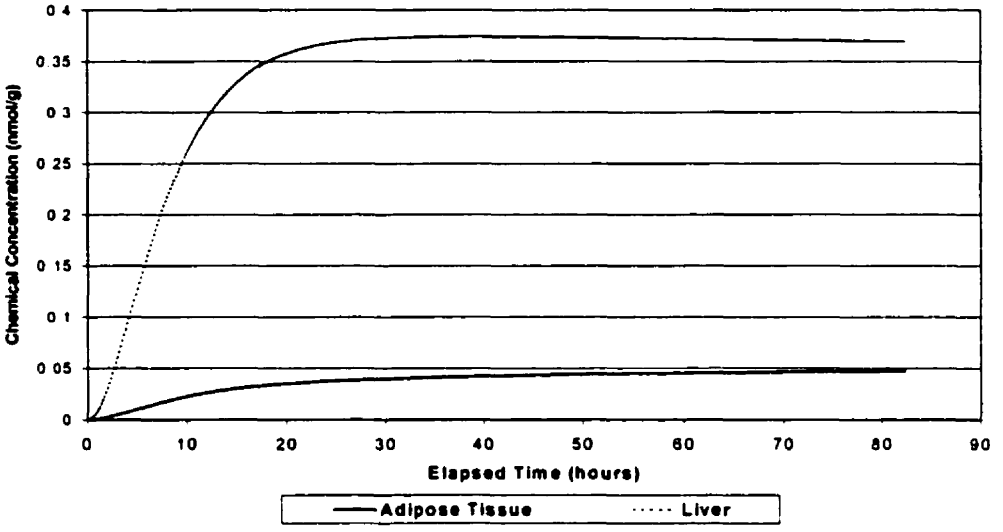


Figure 5.28 Graphical plot of time-series chemical concentrations in the liver and fat compartments following a 0.01 μg/kg bodyweight dose, using the steady-state PBPK model with excretion eliminated.

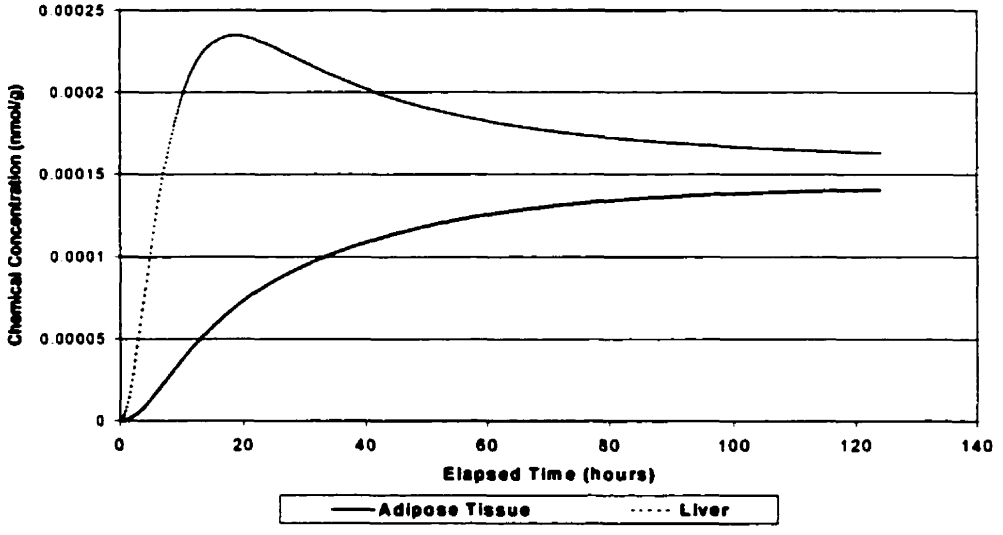


Table 5.15 provides the dose-specific liver-to-fat ratios, Ah and CYP1A2 receptor occupancy, and CYP1A2 fold induction estimates for the steady-state PBPK model (model A), the original equilibrium-based model (model B), and the corrected equilibrium-based model (model C).

Table 5.15 Comparison of steady-state results of the three assessed models of TCDD disposition in the Sprague-Dawley rat.

Dose (ng/kg)	Liver-to-Fat Ratio			Receptor Occupancy						CYP1A2 Fold Induction		
				Ah			CYP1A2					
	A[a]	B[b]	C[c]	A	B	C	A	B	C	A	B	C
0.001	0.5	0.86	0.86	0.0002%	0.008%	0.008%	0%	0%	0%	1	0.002	0.022
0.01	0.5	0.86	0.94	0.002%	0.08%	0.08%	0%	0%	0%	1	0.02	0.21
0.1	0.6	0.94	1.57	0.018%	1%	1%	0%	0%	0%	1.1	0.2	1.63
1	0.7	1.45	4.31	0.2%	7%	7%	0.001%	0.0001%	0.001%	1.4	1.41	7.9
10	1.2	2.99	12.18	1.5%	44%	44%	0.005%	0.008%	0.002%	2.4	4.84	25.8
100	4.9	4.2	26.12	11.5%	89%	89%	0.043%	0.060%	0.012%	5.3	7.7	57.7
1000	7.9	4.31	35.42	43.8%	99%	99%	0.259%	0.58%	0.092%	10.5	8.34	79.3
10000	9.8	3.95	37.24	85.4%	100%	100%	1.91%	5.88%	0.8%	15.1	8.41	83.7

[a] Model results at pseudo steady-state from Wang *et al.* (1997) PBPK model with excretion eliminated.
[b] Model results from equilibrium-based model derived from **original** Evans and Andersen (2000) methodology.
[c] Model results from equilibrium-based model derived from **corrected** Evans and Andersen (2000) methodology.

Results of the comparison indicate that neither the original nor corrected equilibrium-based model adequately reflected the results estimated by the modified steady-state PBPK model. While the original equilibrium-based model (model B) provided an accurate reflection of the steady-state results (model A) at moderate to low dose levels (*i.e.*, ≤ 1.0 ng/kg), due to the mis-specification in the CYP1A2 indiction and binding calculations it failed to adequately predict potentially elevated exposure doses. Unfortunately, as some of the parameters specified by Evans and Andersen (2000) appear to have been selected to ensure the modelled outcome accurately reflect the desired dose-dependency curves of compartmental disposition, correction of the mis-specification (model C) produces even less-accurate results at elevated exposures doses.

In an attempt to correct this over-specification in the selected receptor-ligand parameters, the following three parameters (Table 5.16) were systematically adjusted until the corrected equilibrium-based model provided a reasonably accurate prediction of the results produced by the steady-state model (model A) at all dose levels.

Table 5.16 Revised parameters used in the updated equilibrium-based model.

Physiological Parameter	Abbreviation	Original Value	Revised Value
Ah receptor binding constant	KB1	0.04 nM	5 nM
Ah receptor/DNA receptor binding constant	Kd	0.05 nM	0.005 nM
CYP1A2 induction fold increase	BM2i	85 fold	16 fold

A comparison of steady-state results to those predicted using the updated version of the equilibrium-based model (Model D) are presented in Table 5.17. Using these revised receptor-ligand based parameters, the updated model appears to adequately reflect the results estimated by the steady-state PBPK model.

Table 5.17 Comparison of steady-state results with an updated version of the equilibrium-based model of TCDD disposition in the Sprague-Dawley rat.

Dose (ng/kg)	Liver-to-Fat Ratio		Receptor Occupancy				CYP1A2 Fold Induction	
			Ah		CYP1A2			
	A [a]	D [c]	A	D	A	D	A	D
0	0.5	0.46	0.0002%	0.0001%	0%	0%	1	0.0004
0.01	0.5	0.46	0.002%	0.0006%	0%	0%	1	0.004
0.1	0.6	0.48	0.018%	0.006%	0%	0%	1.1	0.038
1	0.7	0.62	0.2%	0.062%	0.001%	0.002%	1.4	0.352
10	1.2	1.45	1.5%	0.62%	0.005%	0.012%	2.4	2.2
100	4.9	3.9	11.5%	5.8%	0.043%	0.063%	5.3	7.6
1000	7.9	6.43	43.8%	38.3%	0.259%	0.4%	10.5	13.7
10000	9.8	7.1	85.4%	86.1%	1.91%	3.8%	15.1	15.7

[a] Model results at pseudo steady-state from Wang *et al.* (1997) PBPK model with excretion eliminated.
[d] Model results from equilibrium-based model derived from the updated **corrected** Evans and Andersen (2000) methodology.

While this updated version of the equilibrium-based model appears to provide a reasonable representation of the results produced by the steady-state PBPK model, the biological validity of the updated values for the parameters selected to "correct" model outcomes (particularly the KB1 value which represents the K_D for Ah receptor binding) is questionable.

5.3 Dose-Dependent Application of PBPK Model

A range of administered doses (*i.e.*, 0.001, 0.01, 0.1, 1, 10, and 100 μg/kg bodyweight) was used to model a time-series of chemical disposition for each of the assessed PCDD/Fs (*i.e.*, TCDD, TCDF, 1-PeCDF, and 4-PeCDF) for both the Sprague-Dawley rat and the Gapper's red-backed vole. The results of these simulations are presented in Tables 5.18 through 5.21 and Tables 5.22 through 5.25 for the Sprague-Dawley rat and red-backed vole, respectively. Based upon the estimated daily dietary intake of PCDD/Fs (see Table 5.8), the time-series deposition of each assessed congener was also modelled for the Gapper's red-backed vole at site 107 and presented in Table 5.26.

To provide a better reflection of the overall deposition patterns predicted for the red-backed voles over time, whole body concentration and liver-to-fat ratio curves are presented in Figures 5.29 through 5.40 for each of the administered dose levels (*i.e.*, 0.001, 0.01, 0.1, 1, 10, and 100 μg/kg bodyweight, respectively). Results of the time-series modelling indicates that the highest whole body concentration appears to occur near the 15 hour mark for the lower doses, yet shifts towards the 24 hour mark as the dose levels increase. Liver-to-fat ratios are demonstrated to start high (approximately 8-fold) regardless of the dose level, but drops rapidly as the model begins to equilibrate based upon the overall lipophilicity of each of the tissue compartments. The impacts of ligand binding to CYP1A2, in both whole body concentrations and liver-to-fat ratios, begin to become evident at administered doses of 1 μg/kg and higher (see Figures 5.35 through 5.40).

Based upon an overview of each modelled dose level, maximal impacts appear to be in full effect at 24-hours following initial administration. This delay is likely due to the time required for CYP1A2 induction to occur. These impacts can be better viewed, on an administered dose basis, in comparisons of congener-specific liver-to-fat ratios presented in Figures 5.41 and 5.42 for the Sprague-Dawley rat and red-backed vole, respectively. Results of the analyses indicate that while liver-to-fat ratios follow a similar inter-congener pattern at each of the dose levels, liver-to-fat ratios for the Sprague-Dawley rat are typically nearly 2-fold higher than those in the red-backed vole. While this pattern is due to species-specific differences in ligand binding to CYP1A2 within the liver, there are also significant inter-congener differences between the two

modelled species. As indicated in Table 5.27, a comparison of TCDF : TCDD and 1-PeCDF : TCDD liver-to-fat ratios indicates a similar pattern between the two modelled species. However, a comparison 4-PeCDF : TCDD indicates that the 4-PeCDF liver-to-fat ratios tend to be 1.5 to 2-fold higher than TCDD liver-to-fat ratios in the Sprague-Dawley rat, and 2.2 to 2.9-fold higher for the red-backed vole. This indicates, when compared against the TCDD benchmark, that the red-backed vole appears to sequester more 4-PeCDF in the liver than the Sprague-Dawley rat (based upon the chemical-specific assumptions outlined in Tables 4.8 through 4.11).

These differences would likely have large implications on the apparent toxicity of 4-PeCDF when comparing the red-backed vole to the Sprague-Dawley rat. Studies have indicated that the relative potency of 4-PeCDF is dramatically different when determined based on administered dose or tissue dose. For example, in a mouse study conducted by DeVito *et al.* (1998), the relative potency of 4-PeCDF for inducing skin EROD activity based on administered dose was 0.08, similar to that noted for hepatic EROD induction. However, when estimated based upon tissue dose, the relative potency of 4-PeCDF to induce skin EROD activity increased to 1.25, while the relative potency to induce hepatic EROD activity decreased to 0.04 when estimated based upon tissue dose. The authors concluded that for some compounds, the difference in hepatic sequestration (as reflected in liver-to-fat ratio) compared to TCDD may impact their relative potencies depending on which dose metric is used to estimate the relative potency (DeVito *et al.*, 1998), as is inherent in the selection of model parameters for the current study.

These differences in congener-specific sequestration in the liver are also apparent in the congener-specific difference in CYP1A2 fold induction between the two species (see Figures 5.43 and 5.44). As expected, minimal CYP1A2 induction was viewed at the low administered doses for each of the evaluated congeners. However, as the administered dose increased beyond the 1 μg/kg bodyweight level, the difference in TCDD and 4-PeCDF CYP1A2 induction, when compared to the comparable induction rates for TCDF and 1-PeCDF, is much greater in the red-backed vole than observed in the Sprague-Dawley rat. Again, these differences in congener-specific CYP1A2 induction between the two modelled species, would have significant implications in the overall sequestration of each congener in the liver, and species-specific apparent toxicity. These implications will be discussed in depth in Section 6.0.

Table 5.18 Time-Series Dose-Dependent Modelled Disposition of TCDD for the Sprague-Dawley Rat.

Elapsed Time (hours)	Mass of TCDD (pmoles)			Concentration of TCDD (pmoles/g)			Percent of Administered Dose/Gram		Liver-to-Fat Ratio	Receptor Occupancy		CYP1A2 Fold Induction	Percent of Administered Dose Excreted
	Liver	Adipose Tissue	Whole Body	Liver	Adipose Tissue	Whole Body	Liver	Adipose Tissue		Ah	CYP1A2		
0.001 μg TCDD/kg bodyweight (0.000776 nmoles)													
1	0.00751	0.00107	0.00859	0.0008	<0.0001	0.0009	0.107%	0.008%	13.4	0.0165%	0.00005%	1	0.260%
24	0.116	0.152	0.152	0.0128	0.00879	0.0216	1.65%	1.13%	1.46	0.192%	0.00064%	1.39	17.1%
48	0.0656	0.185	0.251	0.00724	0.0107	0.0179	0.933%	1.38%	0.678	0.114%	0.00038%	1.33	25.9%
72	0.0484	0.178	0.226	0.00535	0.0103	0.0156	0.689%	1.32%	0.521	0.0873%	0.00029%	1.27	32.0%
96	0.0392	0.161	0.2	0.00433	0.00929	0.0136	0.558%	1.20%	0.466	0.0724%	0.00024%	1.24	36.9%
0.01 μg TCDD/kg bodyweight (0.00776 nmoles)													
1	0.0751	0.0107	0.0859	0.0083	0.0006	0.00893	0.107%	0.008%	13.5	0.164%	0.00055%	1	0.700%
24	1.62	1.31	2.93	0.179	0.0758	0.254	2.30%	0.976%	2.36	1.63%	0.00551%	2.38	16.3%
48	1.05	1.65	2.7	0.116	0.0956	0.211	1.49%	1.23%	1.21	1.12%	0.00376%	2.25	28.7%
72	0.77	1.66	2.43	0.0851	0.0958	0.181	1.10%	1.23%	0.889	0.887%	0.00298%	2.07	38.1%
96	0.61	1.55	2.16	0.0674	0.0893	0.157	0.868%	1.15%	0.755	0.743%	0.00250%	1.95	45.8%
0.1 μg TCDD/kg bodyweight (0.0776 nmoles)													
1	0.752	0.107	0.86	0.0831	0.0062	0.0894	0.107%	0.008%	13.4	1.60%	0.00542%	1.02	0.731%
24	23.2	9.94	33.2	2.56	0.575	3.14	3.29%	0.740%	4.45	10.3%	0.0384%	5.09	11.2%
48	18.6	12.6	31.2	2.06	0.728	2.79	2.65%	0.937%	2.83	8.52%	0.0310%	5.07	20.6%
72	15.3	13.2	28.5	1.69	0.765	2.45	2.17%	0.984%	2.2	7.48%	0.0270%	4.76	28.8%
96	12.8	13	25.8	1.41	0.75	2.16	1.82%	0.965%	1.88	6.68%	0.0239%	4.5	36.0%
1.0 μg TCDD/kg bodyweight (0.776 nmoles)													
1	7.57	1.08	865	0.837	0.0622	0.9	0.108%	0.008%	13.5	13.5%	0.0521%	1.08	0.717%
24	289	74.1	363	31.9	4.28	36.2	4.11%	0.551%	7.45	42.0%	0.241%	10.3	7.04%
48	266	88.6	354	29.4	5.12	34.5	3.78%	0.659%	5.73	38.58%	0.211%	10.8	13.2%
72	240	93	334	26.6	5.38	31.9	3.42%	0.692%	4.94	37.0%	0.195%	10.6	19.0%
96	219	93.1	312	24.2	5.38	29.6	3.11%	0.693%	4.5	35.4%	0.182%	10.3	24.3%

Table 5.18 Time-Series Dose-Dependent Modelled Disposition of TCDD for the Sprague-Dawley Rat.

Elapsed Time (hours)	Mass of TCDD (pmoles)			Concentration of TCDD (pmoles/g)			Percent of Administered Dose/Gram		Liver-to-Fat Ratio	Receptor Occupancy		CYP1A2 Fold Induction	Percent of Administered Dose Excreted
	Liver	Adipose Tissue	Whole Body	Liver	Adipose Tissue	Whole Body	Liver	Adipose Tissue		Ah	CYP1A2		
10 μg TCDD/kg bodyweight (7.76 nmoles)													
1	76.6	10.8	87.5	8.47	0.624	9.1	0.109%	0.00806%	13.6	58.5%	0.468%	1.27	0.698%
24	3127	63.5	3762	346	36.7	382	4.45%	0.473%	9.41	84.6%	1.80%	15	5.29%
48	3006	72.4	3730	332	41.8	374	4.28%	0.539%	7.94	83.0%	1.60%	16.3	10.0%
72	2824	74.4	3569	312	43	355	4.02%	0.554%	7.26	82.1%	1.50%	16.3	14.5%
96	2659	73.9	3398	294	42.7	337	3.78%	0.550%	6.88	81.2%	1.42%	16.2	18.6%
100 μg TCDD/kg bodyweight (77.6 nmoles)													
1	773	10.8	881	85.4	6.22	91.7	0.110%	0.00801%	13.7	92.5%	3.97%	1.56	0.661%
24	30920	6506	37430	3417	376	3793	4.40%	0.484%	9.08	98.3%	16.4%	16.4	5.52%
48	29580	7482	37070	3268	433	3701	4.21%	0.557%	7.56	98.1%	14.4%	17.9	10.5%
72	27780	7664	35440	3069	443	3512	3.95%	0.570%	6.93	97.9%	13.4%	18	15.0%
96	26180	7560	33740	2893	437	3330	3.72%	0.563%	6.62	97.7%	12.6%	17.8	19.3%

Table 5.19 Time-Series Dose-Dependent Modelled Disposition of TCDF for the Sprague-Dawley Rat.

Elapsed Time (hours)	Mass of TCDF (pmoles)			Concentration of TCDF (pmoles/g)			Percent of Administered Dose/Gram		Liver-to-Fat Ratio	Receptor Occupancy		CYP1A2 Fold Induction	Percent of Administered Dose Excreted
	Liver	Adipose Tissue	Whole Body	Liver	Adipose Tissue	Whole Body	Liver	Adipose Tissue		Ah	CYP1A2		
0.001 μg TCDF/kg bodyweight (0.000776 nmoles)													
1	0.00332	0.00136	0.00469	0.0004	<0.000001	0.0004	0.0472%	0.0101%	4.66	0.00927%	0.0000228%	1	32.1%
24	0.00118	0.024	0.0252	0.0001	0.00139	0.00152	0.0168%	0.179%	0.0937	0.00317%	0.0000078%	1.06	93.9%
48	0	0.00347	0.00356	<0.000001	0.0002	0.0002	0.00128%	0.0258%	0.0496	0.00025%	0.0000006%	1.02	98.9%
72	0.0001	0.0004	0.0005	<0.000001	<0.000001	<0.000001	0.000152%	0.00327%	0.0465	0.00003%	0.0000001%	1	99.5%
96	<0.0000001	<0.0000001	<0.0000001	<0.000001	<0.000001	<0.000001	0.0000190%	0.000410%	0.0462	0.000004%	<0.0000001%	1	99.7%
0.01 μg TCDF/kg bodyweight (0.00776 nmoles)													
1	0.0333	0.0136	0.0469	0.00368	0.0008	0.00447	0.0473%	0.0101%	4.67	0.0925%	0.000227%	1	32.1%
24	0.0135	0.241	0.254	0.00149	0.0139	0.0154	0.0192%	0.179%	0.107	0.0319%	0.0000784%	1.24	93.9%
48	0.0009	0.0348	0.0357	0.0001	0.00201	0.00211	0.00134%	0.0259%	0.0517	0.00251%	0.0000062%	1.07	98.9%
72	0.0001	0.0044	0.00451	<0.000001	0.0003	0.0003	0.000265%	0.00328%	0.047	0.000301%	0.0000007%	1.02	99.5%
96	<0.000001	0.0006	0.0006	<0.000001	<0.000001	<0.000001	0.0000191%	0.000412%	0.0463	0.000038%	0.0000001%	1.01	99.6%
0.1 μg TCDF/kg bodyweight (0.0776 nmoles)													
1	0.335	0.136	0.471	0.037	0.00786	0.0449	0.0476%	0.0101%	4.7	0.914%	0.00226%	1.02	32.0%
24	0.206	2.42	2.62	0.0228	0.14	0.163	0.0290%	0.180%	0.161	0.328%	0.000807%	1.94	93.7%
48	0.0111	0.351	0.362	0.00122	0.0203	0.0215	0.00157%	0.0261%	0.0601	0.0255%	0.0000625%	1.28	98.9%
72	0.00114	0.0445	0.0456	0.0001	0.00257	0.0027	0.000162%	0.00331%	0.0491	0.00304%	0.0000075%	1.07	99.5%
96	0.0001	0.00558	0.00571	<0.000001	0.0003	0.0003	0.0000195%	0.000415%	0.0469	0.000379%	0.0000009%	1.02	99.6%
1.0 μg TCDF/kg bodyweight (0.776 nmoles)													
1	3.42	1.37	4.79	0.378	0.079	0.458	0.0486%	0.0102%	4.77	8.33%	0.0223%	1.07	32.0%
24	5.18	24.5	29.7	0.573	1.42	1.99	0.0737%	0.182%	0.404	3.60%	0.00916%	4.69	92.8%
48	0.184	3.63	3.82	0.0203	0.21	0.23	0.00261%	0.0270%	0.0966	0.272%	0.000670%	2.13	98.9%
72	0.0141	0.462	0.476	0.00155	0.0267	0.0283	0.000200%	0.00344%	0.0581	0.0319%	0.0000783%	1.31	99.5%
96	0.0015	0.058	0.0595	0.0002	0.00336	0.00352	0.0000213%	0.000433%	0.0493	0.00396%	0.0000097%	1.09	99.6%

Table 5.19 Time-Series Dose-Dependent Modelled Disposition of TCDF for the Sprague-Dawley Rat.

Elapsed Time (hours)	Mass of TCDF (pmoles)			Concentration of TCDF (pmoles/g)			Percent of Administered Dose/Gram		Liver-to-Fat Ratio	Receptor Occupancy		CYP1A2 Fold Induction	Percent of Administered Dose Excreted
	Liver	Adipose Tissue	Whole Body	Liver	Adipose Tissue	Whole Body	Liver	Adipose Tissue		Ah	CYP1A2		
10 μg TCDF/kg bodyweight (7.76 nmoles)													
1	36	13.7	49.8	3.98	0.793	4.78	0.0513%	0.0103%	5	46.3%	0.211%	1.25	31.5%
24	148	248	396	16.3	14.4	30.7	0.210%	0.185%	1.14	31.6%	0.113%	11.2	90.4%
48	5.32	39.4	44.7	0.588	2.28	2.86	0.00757%	0.0293%	0.258	3.26%	0.00827%	5.37	98.7%
72	0.261	5.1	5.36	0.0288	0.295	0.324	0.000371%	0.00380%	0.0975	0.364%	0.000896%	2.28	99.5%
96	0.0202	0.643	0.664	0.00224	0.0372	0.0394	0.0000288%	0.000480%	0.06	0.0443%	0.0000109%	1.36	99.6%
100 μg TCDF/kg bodyweight (77.6 nmoles)													
1	386	136	522	42.6	7.88	50.6	0.0549%	0.0101%	5.41	88.9%	1.92%	1.55	30.3%
24	2110	2480	4590	233	143	377	0.300%	0.184%	1.63	82.8%	1.17%	15.6	89.0%
48	155	413	568	17.1	23.9	41	0.0221%	0.0307%	0.718	30.5%	0.107%	12.4	98.4%
72	7.92	56.3	64.2	0.875	3.25	4.13	0.00113%	0.00419%	0.269	4.41%	0.0113%	5.87	99.5%
96	0.408	7.24	7.65	0.0451	0.419	0.464	0.0000580%	0.000540%	0.107	0.519%	0.00128%	2.53	99.6%

Table 5.20 Time-Series Dose-Dependent Modelled Disposition of 1-PeCDF for the Sprague-Dawley Rat.

Elapsed Time (hours)	Mass of 1-PeCDF (pmoles)			Concentration of 1-PeCDF (pmoles/g)			Percent of Administered Dose/Gram		Liver-to-Fat Ratio	Receptor Occupancy		CYP1A2 Fold Induction	Percent of Administered Dose Excreted
	Liver	Adipose Tissue	Whole Body	Liver	Adipose Tissue	Whole Body	Liver	Adipose Tissue		Ah	CYP1A2		
0.001 μg 1-PeCDF/kg bodyweight (0.000776 nmoles)													
1	0.00429	0.00128	0.00557	0.0005	<0.000001	0.0005	0.0610%	0.00958%	6.37	0.00544%	0.0000202%	1	17.9%
24	0.00286	0.0818	0.0847	0.0003	0.00473	0.00505	0.0407%	0.608%	0.0669	0.00355%	0.0000132%	1.06	74.8%
48	0.0009	0.062	0.0629	0	0.00359	0.00368	0.0125%	0.461%	0.0272	0.00111%	0.0000041%	1.03	85.1%
72	0.0005	0.0431	0.0436	0	0.00249	0.00254	0.00705%	0.320%	0.022	0.000628%	0.0000023%	1.02	90.3%
96	0.0003	0.0293	0.0296	0	0.00169	0.00173	0.00442%	0.218%	0.0203	0.000395%	0.0000015%	1.01	93.4%
0.01 μg 1-PeCDF/kg bodyweight (0.00776 nmoles)													
1	0.0429	0.0128	0.0557	0.00474	0.0007	0.00549	0.0610%	0.00960%	6.36	0.0543%	0.000201%	1	19.9%
24	0.0314	0.818	0.85	0.00346	0.0473	0.0508	0.0448%	0.608%	0.0733	0.0357%	0.000133%	1.22	74.8%
48	0.0092	0.621	0.63	0.00102	0.0359	0.0369	0.0131%	0.461%	0.0284	0.0111%	0.0000413%	1.1	85.1%
72	0.00509	0.431	0.436	0.0006	0.0249	0.0255	0.00723%	0.320%	0.0226	0.00629%	0.0000233%	1.06	90.3%
96	0.00317	0.293	0.296	0.0004	0.0169	0.0173	0.00450%	0.218%	0.0207	0.00395%	0.0000147%	1.04	93.4%
0.1 μg 1-PeCDF/kg bodyweight (0.0776 nmoles)													
1	0.43	0.128	0.559	0.0475	0.0074	0.055	0.0612%	0.00960%	6.38	0.539%	0.00201%	1.01	17.9%
24	0.427	8.17	8.598	0.0472	0.472	0.519	0.0607%	0.607%	0.1	0.367%	0.00136%	1.89	74.5%
48	0.107	6.21	6.32	0.0119	0.359	0.371	0.0152%	0.462%	0.033	0.112%	0.000417%	1.4	85.0%
72	0.0561	4.31	4.37	0.0062	0.249	0.256	0.00797%	0.321%	0.0249	0.0632%	0.000234%	1.25	90.3%
96	0.0341	2.94	2.97	0.00377	0.17	0.174	0.00484%	0.218%	0.0222	0.0397%	0.000147%	1.18	93.4%
1.0 μg 1-PeCDF/kg bodyweight (0.776 nmoles)													
1	4.35	1.29	5.64	0.48	0.0743	0.556	0.0618%	0.00958%	6.46	5.10%	0.0199%	1.05	17.7%
24	9.15	81.1	90.3	1.01	4.69	5.7	0.130%	0.603%	0.216	3.93%	0.0152%	4.44	73.3%
48	1.71	62.4	64.1	0.189	3.61	3.8	0.0244%	0.464%	0.0525	1.15%	0.00432%	2.63	84.8%
72	0.777	43.4	44.2	0.0858	2.51	2.6	0.0110%	0.323%	0.0342	0.641%	0.00239%	2	90.2%
96	0.438	29.6	30	0.0484	1.71	1.76	0.00622%	0.220%	0.0283	0.401%	0.00149%	1.72	93.3%

Table 5.20 Time-Series Dose-Dependent Modelled Disposition of 1-PeCDF for the Sprague-Dawley Rat.

Elapsed Time (hours)	Mass of 1-PeCDF (pmoles)			Concentration of 1-PeCDF (pmoles/g)			Percent of Administered Dose/Gram		Liver-to-Fat Ratio	Receptor Occupancy		CYP1A2 Fold Induction	Percent of Administered Dose Excreted
	Liver	Adipose Tissue	Whole Body	Liver	Adipose Tissue	Whole Body	Liver	Adipose Tissue		Ah	CYP1A2		
10 μg 1-PeCDF/kg bodyweight (7.76 nmoles)													
1	44.5	12.9	57.5	4.92	0.746	5.67	0.0633%	0.00961%	6.59	34.2%	0.192%	1.18	17.6%
24	239	79.3	1032	26.4	45.8	72.2	0.339%	0.590%	0.575	32.7%	0.180%	10.8	70.1%
48	43.3	62.8	672	4.79	36.3	41.1	0.0616%	0.467%	0.132	11.5%	0.0480%	7.05	84.0%
72	16.7	44	457	1.85	25.5	27.3	0.0238%	0.328%	0.0726	6.40%	0.0254%	4.92	89.8%
96	8.4	30.1	309	0.928	17.4	18.3	0.0119%	0.224%	0.0533	4.04%	0.0156%	3.86	93.1%
100 μg 1-PeCDF/kg bodyweight (77.6 nmoles)													
1	461	128	590	509	7.41	58.5	0.0656%	0.00955%	6.87	82.4%	1.76%	1.46	16.9%
24	3385	7805	1120	374	451	825	0.482%	0.581%	0.829	83.3%	1.82%	15.5	68.0%
48	905	6263	7169	100	362	462	0.129%	0.466%	0.276	58.4%	0.517%	14.5	82.8%
72	407	4424	4832	45	256	301	0.0579%	0.329%	0.176	42.5%	0.273%	12.2	89.1%
96	213	3041	3254	23.5	176	199	0.0303%	0.226%	0.134	31.1%	0.167%	10.3	92.7%

Table 5.21 Time-Series Dose-Dependent Modelled Disposition of 4-PeCDF for the Sprague-Dawley Rat.

Elapsed Time (hours)	Mass of 4-PeCDF (pmoles)			Concentration of 4-PeCDF (pmoles/g)			Percent of Administered Dose/Gram		Liver-to-Fat Ratio	Receptor Occupancy		CYP1A2 Fold Induction	Percent of Administered Dose Excreted
	Liver	Adipose Tissue	Whole Body	Liver	Adipose Tissue	Whole Body	Liver	Adipose Tissue		Ah	CYP1A2		
0.001 μg 4-PeCDF/kg bodyweight (0.000776 nmoles)													
1	0.00806	0.00105	0.00911	0.0009	0.0001	0.001	0.115%	0.00782%	14.7	0.00599%	0.0000666%	1	0.638%
24	0.192	0.104	0.297	0.0212	0.00604	0.0273	2.73%	0.777%	2.41	0.115%	0.00128%	1.27	22.2%
48	0.127	0.11	0.237	0.014	0.006.38	0.0204	1.80%	0.821%	2.2	0.0766%	0.000852%	1.25	41.1%
72	0.0905	0.00924	0.183	0.01	0.00534	0.0153	1.29%	0.687%	1.87	0.0566%	0.000629%	1.21	54.8%
96	0.0669	0.0731	0.14	0.00739	0.00423	0.0116	0.951%	0.544%	1.75	0.0429%	0.000477%	1.18	65.0%
0.01 μg 4-PeCDF/kg bodyweight (0.00776 nmoles)													
1	0.0806	0.0105	0.0911	0.00891	0.0006	0.00952	0.0115%	0.000782%	14.7	0.00599%	0.0000666%	1	0.638%
24	2.31	0.89	3.2	0.256	0.0514	0.307	0.273%	0.0777%	3.52	0.115%	0.00128%	1.27	22.2%
48	1.74	0.944	2.68	0.192	0.0546	0.247	0.180%	0.0821%	2.2	0.0766%	0.000852%	1.25	41.1%
72	1.32	0.836	2.16	0.146	0.0483	0.194	0.129%	0.0687%	1.87	0.0466%	0.000629%	1.21	54.8%
96	1.01	0.704	1.72	0.112	0.0407	0.153	0.0951%	0.0544%	1.75	0.0429%	0.000477%	1.18	65.0%
0.1 μg 4-PeCDF/kg bodyweight (0.0776 nmoles)													
1	0.807	0.105	0.912	0.0891	0.00606	0.0953	0.115%	0.00781%	14.7	0.590%	0.00659%	1.01	0.626%
24	28.8	6.68	35.4	3.18	0.386	3.56	4.09%	0.497%	8.23	5.59%	0.0658%	3.77	12.0%
48	25.3	6.75	32	2.79	0.39	3.18	3.59%	0.502%	7.16	4.84%	0.0565%	3.86	23.1%
72	21.6	6.24	27.8	2.38	0.361	2.74	3.07%	0.464%	6.61	4.34%	0.0504%	3.7	33.0%
96	18.4	5.65	24	2.03	0.327	2.35	2.61%	0.420%	6.21	3.88%	0.0449%	3.53	41.9%
1.0 μg 4-PeCDF/kg bodyweight (0.776 nmoles)													
1	8.11	1.05	9.16	0.896	0.0608	0.957	0.115%	0.00783%	14.7	5.47%	0.0642%	1.05	0.623%
24	333	49	382	36.8	2.83	39.6	4.74%	0.364%	13	25.1%	0.371%	7.8	7.04%
48	322	43.8	366	35.6	2.53	38.1	4.58%	0.326%	14	23.5%	0.339%	8.25	13.5%
72	299	39.5	339	33.1	2.28	35.4	4.26%	0.294%	14.5	22.5%	0.321%	8.11	19.7%
96	277	36.6	313	20.6	2.11	32.7	3.94%	0.0272%	14.5	21.5%	0.303%	7.93	25.5%

Table 5.21 Time-Series Dose-Dependent Modelled Disposition of 4-PeCDF for the Sprague-Dawley Rat.

Elapsed Time (hours)	Mass of 4-PeCDF (pmoles)			Concentration of 4-PeCDF (pmoles/g)			Percent of Administered Dose/Gram		Liver-to-Fat Ratio	Receptor Occupancy		CYP1A2 Fold Induction	Percent of Administered Dose Excreted
	Liver	Adipose Tissue	Whole Body	Liver	Adipose Tissue	Whole Body	Liver	Adipose Tissue		Ah	CYP1A2		
10 μg 4-PeCDF/kg bodyweight (7.76 nmoles)													
1	81.8	10.6	92.4	9.04	0.612	9.66	0.116%	0.00788%	14.8	34.7%	0.586%	1.17	0.615%
24	3554	404	3958	393	23.3	416	5.05%	0.300%	16.8	68.2%	2.33%	13.3	4.60%
48	3566	320	3886	394	18.5	413	5.07%	0.238%	21.3	66.5%	216%	14.4	8.77%
72	3435	272	3706	380	15.7	395	4.88%	0.202%	24.2	65.6%	2.08%	14.4	12.8%
96	3287	247	3534	363	14.3	378	4.67%	0.184%	25.4	64.8%	2.00%	14.3	16.7%
100 μg 4-PeCDF/kg bodyweight (77.6 nmoles)													
1	823	106	929	90.9	6.11	97.1	0.117%	0.00787%	14.9	82.2%	4.87%	1.43	0.591%
24	35610	4012	39630	3935	232	4167	5.07%	0.299%	17	95.6%	19.3%	16.1	4.50%
48	35770	3171	38940	3952	183	4136	5.09%	0.236%	21.6	95.1%	17.8%	17.6	8.64%
72	34530	2669	37190	3815	154	3969	4.91%	0.199%	24.7	94.9%	17.0%	17.7	12.6%
96	33410	2399	35540	3661	139	3800	4.71%	0.179%	26.4	94.6%	16.4%	17.7	16.3%

Table 5.22 Time-Series Dose-Dependent Modelled Disposition of TCDD for the Gapper's Red-Backed Vole.

Elapsed Time (hours)	Mass of TCDD (pmoles)			Concentration of TCDD (pmoles/g)			Percent of Administered Dose/Gram		Liver-to-Fat Ratio	Receptor Occupancy		CYP1A2 Fold Induction	Percent of Administered Dose Excreted
	Liver	Adipose Tissue	Whole Body	Liver	Adipose Tissue	Whole Body	Liver	Adipose Tissue		Ah	CYP1A2		
0.001 µg TCDD/kg bodyweight (0.0000885 nmoles)													
1	0.0008	0.0002	0.00101	0.0007	0.0001	0.0008	0.697%	0.122%	5.69	0.0149%	0.0000425%	1	3.24%
24	0.00547	0.0189	0.0244	0.00438	0.00976	0.0142	4.94%	11.0%	0.449	0.0861%	0.000246%	1.27	36.8%
48	0.0003	0.0161	0.0188	0.00218	0.00931	0.0105	2.46%	9.37%	0.262	0.0450%	0.000129%	1.2	54.1%
72	0.00191	0.0121	0.0141	0.00153	0.00626	0.00779	1.75%	7.07%	0.244	0.0326%	0.0000932%	1.15	65.7%
96	0.00138	0.00905	0.0104	0.00111	0.00467	0.00578	1.25%	5.27%	0.237	0.0241%	0.0000689%	1.13	74.2%
0.01 µg TCDD/kg bodyweight (0.000885 nmoles)													
1	0.00821	0.00192	0.0101	0.00658	0.001	0.00757	0.738%	0.114%	6.49	0.156%	0.000445%	1	2.36%
24	0.0816	0.178	0.26	0.0654	0.092	0.157	7.38%	10.4%	0.711	0.847%	0.00244%	2.03	34.1%
48	0.0403	0.158	0.199	0.0323	0.0816	0.114	3.64%	9.21%	0.395	0.467%	0.00134%	1.8	52.0%
72	0.0266	0.122	0.149	0.0213	0.0629	0.0842	2.40%	7.10%	0.338	0.337%	0.000966%	1.63	64.0%
96	0.0186	0.0921	0.111	0.0149	0.0475	0.0624	1.68%	5.36%	0.313	0.251%	0.000718%	1.52	72.8%
0.1 µg TCDD/kg bodyweight (0.00885 nmoles)													
1	0.0821	0.0192	0.101	0.0658	0.00992	0.0758	0.758%	0.112%	6.77	1.57%	0.00457%	1	2.27%
24	1.49	1.51	3	1.19	0.781	1.97	13.5%	8.82%	1.53	7.03%	0.0216%	4.43	27.4%
48	0.981	1.45	2.34	0.714	0.746	1.46	8.05%	8.42%	0.957	4.70%	0.0141%	4.04	45.1%
72	0.587	1.19	1.78	0.47	0.615	1.09	5.30%	6.93%	0.765	3.56%	0.0105%	3.54	57.9%
96	0.404	0.946	1.35	0.323	0.488	0.812	3.65%	5.51%	0.662	2.74%	0.00805%	3.16	67.9%
1.0 µg TCDD/kg bodyweight (0.0885 nmoles)													
1	0.823	0.193	1.02	0.66	0.0995	0.76	0.746%	0.113%	6.62	13.6%	0.0449%	1.01	2.28%
24	23.2	11.9	35.1	18.6	6.14	24.7	21.0%	6.93%	3.03	35.9%	0.160%	9.61	19.3%
48	18.1	11.6	29.6	14.5	5.96	20.4	16.3%	6.74%	2.42	30.2%	0.123%	9.7	33.6%
72	14	10.2	24.2	11.2	5.25	16.5	12.7%	5.93%	2.14	26.4%	0.102%	9.06	45.5%
96	10.9	8.72	19.7	8.75	4.5	13.3	9.89%	5.08%	1.94	23.0%	0.0854%	8.44	55.3%

Table 5.22 Time-Series Dose-Dependent Modelled Disposition of TCDD for the Gapper's Red-Backed Vole.

Elapsed Time (hours)	Mass of TCDD (pmoles)			Concentration of TCDD (pmoles/g)			Percent of Administered Dose/Gram		Liver-to-Fat Ratio	Receptor Occupancy		CYP1A2 Fold Induction	Percent of Administered Dose Excreted
	Liver	Adipose Tissue	Whole Body	Liver	Adipose Tissue	Whole Body	Liver	Adipose Tissue		Ah	CYP1A2		
10 μg TCDD/kg bodyweight (0.885 nmoles)													
1	8.26	1.95	10.2	6.62	1.01	7.63	0.748%	0.114%	6.59	61.4%	0.453%	1.04	2.32%
24	275	102	377	220	52.8	273	24.9%	5.96%	4.19	81.7%	1.26%	14.6	15.1%
48	239	96.6	335	191	49.9	241	21.6%	5.63%	3.83	78.1%	1.01%	15.9	26.7%
72	204	85.3	289	163	44	207	18.4%	4.97%	3.71	75.4%	0.870%	15.7	36.7%
96	174	74.6	249	140	38.5	178	15.8%	4.35%	3.62	72.8%	0.757%	15.4	45.3%
100 μg TCDD/kg bodyweight (8.85 nmoles)													
1	82.5	19.6	102	66.1	10.1	76.3	0.747%	0.114%	6.54	94.2%	4.40%	1.1	2.39%
24	273	1031	3765	2190	532	2722	24.7%	6.01%	4.12	97.8%	11.4%	16.1	15.3%
48	2391	964	3355	1915	497	2413	21.6%	5.62%	3.85	97.2%	9.01%	17.8	26.8%
72	2076	838	2915	1663	433	2096	18.8%	4.88%	3.84	96.7%	7.78%	17.9	36.4%
96	1805	724	2530	1446	374	1820	16.3%	4.22%	3.87	96.2%	6.78%	17.8	44.6%

Table 5.23 Time-Series Dose-Dependent Modelled Disposition of TCDF for the Gapper's Red-Backed Vole.

Elapsed Time (hours)	Mass of TCDF (pmoles)			Concentration of TCDF (pmoles/g)			Percent of Administered Dose/Gram		Liver-to-Fat Ratio	Receptor Occupancy		CYP1A2 Fold Induction	Percent of Administered Dose Excreted
	Liver	Adipose Tissue	Whole Body	Liver	Adipose Tissue	Whole Body	Liver	Adipose Tissue		Ah	CYP1A2		
0.001 μg TCDF/kg bodyweight (0.0000885 nmoles)													
1	0.0002	0.0002	0.0004	0.0001	0.0001	0.0002	0.150%	0.125%	1.21	0.00389%	0.0000082%	1	51.5%
24	0	0.00119	0.00123	0.0003	0.0006	0.0006	0.0323%	0.695%	0.0464	0.000823%	0.0000017%	1.03	96.8%
48	9.13×10^{-7}	<0.0000001	9.14×10^{-7}	7.31×10^{-7}	<0.0000001	7.32×10^{-7}	0.000826%	0.0278%	0.0297	0.0000214%	0.00000045%	1.01	99.6%
72	2.37×10^{-8}	1.40×10^{-6}	1.43×10^{-6}	1.90×10^{-8}	7.23×10^{-7}	7.42×10^{-7}	0.0000214%	0.000817%	0.0263	0.0000006%	<0.0000001%	1	99.7%
96	6.20×10^{-10}	3.81×10^{-8}	3.87×10^{-8}	4.97×10^{-10}	1.96×10^{-8}	2.01×10^{-8}	0.0000006%	0.000022%	0.0253	<0.0000001%	<0.0000001%	1	99.7%
0.01 μg TCDF/kg bodyweight (0.000885 nmoles)													
1	0.00166	0.00212	0.00378	0.00133	0.00109	0.00243	0.150%	0.124%	1.22	0.0389%	0.0000819%	1	51.5%
24	0.0004	0.0119	0.0123	0.0003	0.00616	0.00646	0.0345%	0.695%	0.0496	0.00824%	0.0000173%	1.12	96.8%
48	9.28×10^{-6}	0.0005	0.0005	7.43×10^{-6}	0.0002	0.0003	0.000840%	0.0278%	0.0302	0.000214%	0.00000451%	1.03	99.6%
72	2.38×10^{-7}	<0.0000001	2.39×10^{-7}	1.90×10^{-7}	7.23×10^{-6}	7.42×10^{-6}	0.0000215%	0.000817%	0.0263	0.0000056%	0.00000012%	1	99.7%
96	6.21×10^{-9}	3.81×10^{-7}	3.87×10^{-7}	4.97×10^{-9}	1.97×10^{-7}	2.02×10^{-7}	0.0000006%	0.000022%	0.0253	0.00000015%	<0.0000001%	1	99.7%
0.1 μg TCDF/kg bodyweight (0.00885 nmoles)													
1	0.0166	0.0212	0.0379	0.0133	0.0109	0.0243	0.150%	0.124%	1.22	0.388%	0.000820%	1	51.5%
24	0.00478	0.119	0.124	0.00383	0.0616	0.0655	0.0433%	0.696%	0.0622	0.0828%	0.000174%	1.49	96.8%
48	0.0001	0.00478	0.00488	0.0007	0.00247	0.00255	0.000895%	0.0279%	0.0321	0.00215%	0.0000045%	1.12	99.6%
72	2.41×10^{-6}	0.0001	0.0001	1.93×10^{-6}	0.0001	2.93×10^{-5}	0.0000218%	0.000818%	0.0266	0.000056%	0.00000012%	1.02	99.7%
96	6.23×10^{-8}	3.82×10^{-6}	3.88×10^{-6}	4.99×10^{-8}	1.97×10^{-6}	2.02×10^{-6}	0.0000006%	0.000022%	0.0253	0.00000147%	<0.0000001%	1	99.7%
1.0 μg TCDF/kg bodyweight (0.0885 nmoles)													
1	0.167	0.213	0.38	0.134	0.11	0.244	0.151%	0.1224%	1.22	3.75%	0.00821%	1.01	51.7%
24	0.0866	1.2	1.29	0.0694	0.618	0.688	0.0784%	0.698%	0.112	0.839%	0.00178%	2.93	96.7%
48	0.00123	0.0481	0.00494	0.001	0.0248	0.0258	0.00112%	0.0280%	0.0398	0.0217%	0.0000457%	1.46	99.6%
72	0	0.00141	0.00144	0	0.0007	0.0007	0.0000228%	0.000823%	0.0277	0.000564%	0.00000187%	1.07	99.7%
96	6.30×10^{-7}	0	0	5.05×10^{-7}	0	0	0.0000006%	0.000022%	0.0255	0.0000148%	<0.0000001%	1.01	99.7%

Table 5.23 Time-Series Dose-Dependent Modelled Disposition of TCDF for the Gapper's Red-Backed Vole.

Elapsed Time (hours)	Mass of TCDF (pmoles)			Concentration of TCDF (pmoles/g)			Percent of Administered Dose/Gram		Liver-to-Fat Ratio	Receptor Occupancy		CYP1A2 Fold Induction	Percent of Administered Dose Excreted
	Liver	Adipose Tissue	Whole Body	Liver	Adipose Tissue	Whole Body	Liver	Adipose Tissue		Ah	CYP1A2		
10 µg TCDF/kg bodyweight (0.885 nmoles)													
1	1.66	2.14	3.81	1.33	1.11	2.44	0.151%	0.125%	1.21	28.1%	0.0821	1.03	52.0%
24	2.18	12.1	14.3	1.75	6.23	7.98	0.197%	0.704%	0.28	8.25%	0.0189	7.45	96.5%
48	0.0217	0.489	0.511	0.0174	0.253	0.27	0.00196%	0.0285%	0.0689	0.224%	0.000473	2.74	99.6%
72	0.0003	0.0144	0.0147	0.0002	0.00742	0.00765	0.0000267%	0.000838%	0.0319	0.00575%	0.00001	1.29	99.7%
96	6.55×10^{-6}	0.0004	0.0004	5.25×10^{-6}	0.0002	0.0002	0.0000006%	0.000023%	0.0261	0.000150%	<0.0000001	1.04	99.7%
100 µg TCDF/kg bodyweight (8.85 nmoles)													
1	16.4	21.5	38	13.2	11.1	24.3	0.149%	0.125%	1.19	79.5%	0.811%	1.09	52.3%
24	41.3	122	163	33.1	62.7	95.9	0.374%	0.709%	0.528	48.8%	0.200%	13.7	96.0%
48	0.509	5.02	5.54	0.408	2.59	3	0.00460%	0.0293%	0.157	2.37%	0.00510%	6.39	99.6%
72	0.00443	0.148	0.153	0.00355	0.0764	0.08	0.0000401%	0.000863%	0.0465	0.0598%	0.000126%	2.02	99.7%
96	0	0.00402	0.0041	0	0.00208	0.00214	0.0000007%	0.000023%	0.0281	0.00155%	0.00000326%	1.15	99.7%

Table 5.24 Time-Series Dose-Dependent Modelled Disposition of 1-PeCDF for the Gapper's Red-Backed Vole.

Elapsed Time (hours)	Mass of 1-PeCDF (pmoles)			Concentration of 1-PeCDF (pmoles/g)			Percent of Administered Dose/Gram		Liver-to-Fat Ratio	Receptor Occupancy		CYP1A2 Fold Induction	Percent of Administered Dose Excreted
	Liver	Adipose Tissue	Whole Body	Liver	Adipose Tissue	Whole Body	Liver	Adipose Tissue		Ah	CYP1A2		
0.001 µg 1-PeCDF/kg bodyweight (0.0000885 nmoles)													
1	0.0003	0.0002	0.0005	0.0002	0.0001	0.0003	0.252%	0.125%	2.02	0.00285%	0.00000905%	1	35.2%
24	0.0001	0.00748	0.00759	0	0.00386	0.00394	0.0930%	4.36%	0.0213	0.00104%	0.00000331%	1.03	81.0%
48	0	0.00399	0.00403	0	0.00206	0.00209	0.0280%	2.33%	0.012	0.000316%	0.00000101%	1.01	90.6%
72	0	0.00202	0.00203	0..00001	0.00104	0.00105	0.0136%	1.18%	0.0116	0.000154%	0.00000049%	1.01	95.2%
96	7.39×10^{-6}	0.00101	0.00102	5.92×10^{-6}	0.0005	0.0005	0.00668%	0.589%	0.0113	0.0000757%	0.00000024%	1	97.5%
0.01 µg 1-PeCDF/kg bodyweight (0.000885 nmoles)													
1	0.00279	0.00214	0.00493	0.00223	0.0011	0.00334	0.252%	0.125%	2.02	0.0285%	0.0000905%	1	35.2%
24	0.00107	0.0748	0.0759	0.0009	0.0386	0.0395	0.0969%	4.36%	0.0222	0.0104%	0.0000331%	1.12	81.0%
48	0.0003	0.04	0.0403	0.0003	0.0206	0.0209	0.0285%	1022%	0.0123	0.00316%	0.0000101%	1.05	90.6%
72	0.0002	0.0202	0.0203	0.0001	0.0104	0.0105	0.0137%	1.18%	0.0117	0.00154%	0.00000489%	1.03	95.2%
96	0..00001	0.0101	0.0101	0	0.00522	0.00528	0.00673%	0.589%	0.0114	0.000758%	0.00000241%	1.02	97.5%
0.1 µg 1-PeCDF/kg bodyweight (0.00885 nmoles)													
1	0.0279	0.0214	0.0493	0.0223	0.011	0.0334	0.252%	0.125%	2.02	0.284%	0.000905%	1	35.2%
24	0.0125	0.748	0.761	0.00999	0.386	0.396	0.113%	4.36%	0.0259	0.105%	0.000333%	1.46	80.9%
48	0.00338	0.4	0.403	0.00271	0.206	0.209	0.0306%	2.33%	0.0131	0.0317%	0.000101%	1.2	90.6%
72	0.00158	0.202	0.203	0.00127	0.104	0.105	0.0143%	1.18%	0.0122	0.0154%	0.0000489%	1.11	95.2%
96	0.0008	0.101	0.102	0.0006	0.0522	0.0528	0.00691%	0.589%	0.0117	0.00758%	0.0000241%	1.07	97.5%
1.0 µg 1-PeCDF/kg bodyweight (0.0885 nmoles)													
1	0.279	0.215	0.495	0.224	0.111	0.335	0.253%	0.125%	2.02	2.77%	0.00906%	1.01	35.3%
24	0.195	7.48	7.68	0.156	3.86	4.02	0.176%	4.36%	0.0404	1.05%	0.00338%	2.82	80.8%
48	0.0429	4	4.05	0.0344	2.06	2.1	0.0388%	2.33%	0.0167	0.317%	0.00101%	1.8	90.6%
72	0.0183	2.02	2.04	0.0147	1.04	1.06	0.0166%	1.18%	0.0141	0.154%	0.000491%	1.46	95.2%
96	0.00844	1.01	1.02	0.00676	0.553	0.529	0.00764%	0.590%	0.0129	0.0759%	0.000241%	1.29	97.5%

Table 5.24 Time-Series Dose-Dependent Modelled Disposition of 1-PeCDF for the Gapper's Red-Backed Vole.

Elapsed Time (hours)	Mass of 1-PeCDF (pmoles)			Concentration of 1-PeCDF (pmoles/g)			Percent of Administered Dose/Gram		Liver-to-Fat Ratio	Receptor Occupancy		CYP1A2 Fold Induction	Percent of Administered Dose Excreted
	Liver	Adipose Tissue	Whole Body	Liver	Adipose Tissue	Whole Body	Liver	Adipose Tissue		Ah	CYP1A2		
10 µg 1-PeCDF/kg bodyweight (0.885 nmoles)													
1	2.8	2.16	5	2.24	1.11	3.36	0.254%	0.126%	2.02	22.2%	0.0906%	1.02	35.5%
24	4.36	74.8	79.2	3.5	38.6	42.1	0.395%	4.36%	0.0906	10.1%	0.0357%	7.21	80.3%
48	0.779	40.1	40.9	0.624	20.7	21.3	0.0705%	2.34%	0.0301	3.14%	0.0103%	4.05	90.5%
72	0.284	20.3	20.6	0.228	10.5	10.7	0.0257%	1.18%	0.0217	1.54%	0.00496%	2.8	95.2%
96	0.117	10.2	10.3	0.0933	5.25	5.35	0.0105%	0.593%	0.0178	0.761%	0.00244%	2.16	97.4%
100 µg 1-PeCDF/kg bodyweight (8.85 nmoles)													
1	27.9	21.6	49.6	22.4	11.2	33.6	0.253%	0.126%	2	74.0%	0.895%	1.07	35.6%
24	80.5	746	827	64.5	385	449	0.728%	4.35%	0.168	54.1%	0.373%	13.6	79.5%
48	17.7	403	421	14.2	208	222	0.160%	2.35%	0.0681	25.1%	0.106%	10.2	90.2%
72	6.35	204	211	5.09	105	110	0.0575%	1.19%	0.0483	13.8%	0.0509%	7.38	95.1%
96	2.38	103	105	1.91	52.9	54.8	0.0215%	0.598%	0.036	7.27%	0.0249%	5.4	97.4%

Table 5.25 Time-Series Dose-Dependent Modelled Disposition of 4-PeCDF for the Gapper's Red-Backed Vole.

Elapsed Time (hours)	Mass of 4-PeCDF (pmoles)			Concentration of 4-PeCDF (pmoles/g)			Percent of Administered Dose/Gram		Liver-to-Fat Ratio	Receptor Occupancy		CYP1A2 Fold Induction	Percent of Administered Dose Excreted
	Liver	Adipose Tissue	Whole Body	Liver	Adipose Tissue	Whole Body	Liver	Adipose Tissue		Ah	CYP1A2		
0.001 μg 4-PeCDF/kg bodyweight (0.0000885 nmoles)													
1	0.0009	0.0002	0.00108	0.0007	0.0001	0.0008	0.813%	0.107%	7.63	0.00597%	0.0000569%	1	1.95%
24	0.0102	0.0122	0.0224	0.00816	0.0063	0.0145	9.21%	7.12%	1.29	0.0574%	0.000547%	1.2	46.6%
48	0.00448	0.0075	0.012	0.00359	0.00387	0.00746	4.06%	4.37%	0.928	0.0263%	0.000250%	1.15	71.8%
72	0.00224	0.00404	0.00628	0.0018	0.00208	0.00388	2.03%	2.35%	0.862	0.0137%	0.000130%	1.1	84.7%
96	0.00114	0.00214	0.00328	0.0009	0.0011	0.00202	1.03%	1.24%	0.829	0.00717%	0.0000683%	1.07	91.5%
0.01 μg 4-PeCDF/kg bodyweight (0.000885 nmoles)													
1	0.009	0.00183	0.0108	0.0072	0.0009	0.00815	0.813%	0.107%	7.63	0.0597%	0.000569%	1	1.95%
24	0.137	0.112	0.249	0.109	0.0579	0.167	12.4%	6.54%	1.89	0.536%	0.00513%	1.74	41.9%
48	0.0665	0.0742	0.141	0.0533	0.0383	0.0916	6.02%	4.32%	1.39	0.283%	0.00270%	1.61	67.5%
72	0.033	0.0431	0.0762	0.0265	0.0223	0.0487	2.99%	2.51%	1.19	0.157%	0.00150%	1.43	81.8%
96	0.0164	0.0242	0.0406	0.0132	0.0125	0.0257	1.49%	1.41%	1.06	0.0856%	0.000816%	1.3	89.8%
0.1 μg 4-PeCDF/kg bodyweight (0.00885 nmoles)													
1	0.0899	0.0183	0.108	0.072	0.00944	0.0815	0.814%	0.107%	7.63	0.593%	0.00568%	1	1.95%
24	2.11	0.913	3.02	1.69	0.471	2.16	19.1%	5.32%	3.59	4.13%	0.0410%	3.42	32.0%
48	1.36	0.662	2.02	1.09	0.341	1.43	12.3%	3.86%	3.18	2.84%	0.0278%	3.24	55.2%
72	0.804	0.457	1.26	0.644	0.236	0.88	7.27%	2.66%	2.73	1.94%	0.0189%	2.82	71.5%
96	0.452	0.306	0.758	0.362	0.158	0.52	4.09%	1.79%	2.29	1.27%	0.0123%	2.43	82.3%
1.0 μg 4-PeCDF/kg bodyweight (0.0885 nmoles)													
1	0.901	0.183	1.09	0.722	0.0946	0.817	0.816%	0.107%	7.63	5.63%	0.0567%	1.01	1.95%
24	29.6	6.78	36.4	23.7	3.5	27.2	26.8%	3.95%	6.77	22.1%	0.269%	7.39	20.8%
48	24.5	4.86	29.4	19.6	2.51	22.1	22.2%	2.83%	7.82	18.7%	0.218%	7.52	37.4%
72	18.8	3.82	22.6	15.1	1.97	17	17.0%	2.22%	7.66	15.9%	0.180%	7	51.4%
96	14	3.08	17.1	11.3	1.59	12.8	12.7%	1.80%	7.07	13.3%	0.146%	6.43	62.8%

Table 5.25 Time-Series Dose-Dependent Modelled Disposition of 4-PeCDF for the Gapper's Red-Backed Vole.

Elapsed Time (hours)	Mass of 4-PeCDF (pmoles)			Concentration of 4-PeCDF (pmoles/g)			Percent of Administered Dose/Gram		Liver-to-Fat Ratio	Receptor Occupancy		CYP1A2 Fold Induction	Percent of Administered Dose Excreted
	Liver	Adipose Tissue	Whole Body	Liver	Adipose Tissue	Whole Body	Liver	Adipose Tissue		Ah	CYP1A2		
10 μg 4-PeCDF/kg bodyweight (0.885 nmoles)													
1	9.06	1.85	10.9	7.26	0.952	8.22	0.820%	0.108%	7.62	37.3%	0.564%	1.03	1.97%
24	346	54.3	400	277	28	305	31.3%	3.17%	9.87	65.7%	1.79%	13	14.2%
48	319	35.5	355	256	18.3	274	28.9%	2.07%	13.9	62.1%	1.54%	14	25.7%
72	277	28.2	305	222	14.5	236	25.0%	1.64%	15.2	59.1%	1.36%	13.7	36.0%
96	237	24.1	261	190	12.4	202	21.4%	1.41%	15.2	55.9%	1.19%	13.4	45.0%
100 μg 4-PeCDF/kg bodyweight (8.85 nmoles)													
1	90.7	18.5	109	72.6	9.57	82.3	0.821%	0.108%	7.59	85.8%	5.45%	1.07	2.03%
24	3495	534	4029	2799	276	3075	31.6%	3.11%	10.2	94.9%	14.9%	15.8	13.6%
48	3269	339	3609	2619	175	2794	29.6%	1.98%	15	93.8%	12.7%	17.4	24.5%
72	2891	261	3152	2316	135	2451	26.2%	1.52%	17.2	92.9%	11.1%	17.5	34.0%
96	2534	220	2754	2030	113	2143	22.9%	1.28%	17.9	92.0%	9.82%	17.4	42.2%

Table 5.26 Time-Series Modelled Disposition of each Assessed PCDD/F Congener for the Gapper's Red-Backed Vole, based upon Intake Rates at Site 107 following Emission Incident. [a]

Elapsed Time (hours)	Mass of Assessed PCDD/F (pmoles)			Concentration of Assessed PCDD/F (pmoles/g)			Percent of Administered Dose/Gram		Liver-to-Fat Ratio	Receptor Occupancy		CYP1A2 Fold Induction	Percent of Administered Dose Excreted
	Liver	Adipose Tissue	Whole Body	Liver	Adipose Tissue	Whole Body	Liver	Adipose Tissue		Ah	CYP1A2		
0.000186 µg TCDD/kg bodyweight (0.0000165 nmoles)													
1	0.0002	<0.000001	0.0002	0.0001	<0.000001	0.0001	0.743%	0.112%	6.63	0.00292%	0.0000083%	1	2.26%
24	0.0009	0.00357	0.00447	0.0007	0.00184	0.00256	4.36%	11.2%	0.39	0.0160%	0.0000456%	1.1	37.5%
48	0.0005	0.003	0.00346	0.0004	0.00155	0.00192	2.22%	9.41%	0.236	0.00830%	0.0000237%	1.07	54.6%
72	0.0003	0.00225	0.00258	0.0003	0.00116	0.00143	1.59%	7.06%	0.225	0.00602%	0.0000172%	1.06	66.1%
96	0.0002	0.00168	0.00192	0.0002	0.0009	0.00106	1.17%	5.25%	0.222	0.00445%	0.0000127%	1.05	74.5%
0.136 µg TCDF/kg bodyweight (0.0120 nmoles)													
1	0.0226	0.0288	0.0515	0.0181	0.0149	0.0331	0.150%	0124%	1.22	0.527%	0.00111%	1	51.5%
24	0.00687	0.162	0.169	0.0055	0.0838	0.0893	0.0457%	0.696%	0.0656	0.113%	0.000237%	1.59	96.8%
48	0.0001	0.00651	0.00665	0.0001	0.00336	0.0347	0.000910%	0.0279%	0.0326	0.00293%	0.000006%	1.14	99.6%
72	<0.000001	0.0002	0.0002	2.63×10^{-6}	0.0001	0.0001	0.000022%	0.000819%	0.0267	0.0000762%	<0.000001%	1.02	99.7%
96	8.48×10^{-8}	5.19×10^{-6}	5.28×10^{-6}	6.79×10^{-8}	2.68×10^{-6}	2.75×10^{-6}	<0.000001%	0.000022%	0.0254	<0.000001%	<0.000001%	1	99.7%
0.0248 µg 1-PeCDF/kg bodyweight (0.00220 nmoles)													
1	0.00691	0.00531	0.0122	0.00553	0.00274	0.00829	0.252%	0.125%	2.02	0.0706%	0.000224%	1	35.2%
24	0.00276	0.186	0.188	0.00221	0.0957	0.098	0.101%	4.36%	0.0231	0.0259%	0.000082%	1.2	81.0%
48	0.0008	0.0991	0.0999	0.0006	0.0511	0.0518	0.0290%	2.33%	0.0125	0.00785%	0.000025%	1.09	90.6%
72	0.0004	0.05	0.0504	0.0003	0.0258	0.0261	0.0139%	1.18%	0.0118	0.00381%	0.000012%	1.05	95.2%
96	0.0002	0.0251	0.0253	0.0001	0.0129	0.0131	0.00677%	0.589%	0.0115	0.00188%	0.000006%	1.03	97.5%
0.0713 µg 4-PeCDF/kg bodyweight (0.00631 nmoles)													
1	0.0641	0.013	0.0772	0.0514	0.00673	0.0581	0.814%	0.107%	7.63	0.424%	0.00405%	1	1.95%
24	1.41	0.677	2.09	1.13	0.349	1.48	19.9%	5.53%	3.24	3.12%	0.0307%	3.05	33.8%
48	0.867	0.486	1.35	0.695	0.251	0.945	11.0%	3.97%	2.77	2.06%	0.0200%	2.87	57.6%
72	0.493	0.326	0.82	0.395	0.168	0.564	6.26%	2.67%	2.35	1.36%	0.0131%	2.49	73.7%
96	0.267	0.212	0.479	0.214	0.109	0.323	3.39%	1.73%	1.96	0.853%	0.00820%	2.14	84.1%

Table 5.26 Time-Series Modelled Disposition of each Assessed PCDD/F Congener for the Gapper's Red-Backed Vole, based upon Intake Rates at Site 107 following Emission Incident. [a]

Elapsed Time (hours)	Mass of Assessed PCDD/F (pmoles)			Concentration of Assessed PCDD/F (pmoles/g)			Percent of Administered Dose/Gram		Liver-to-Fat Ratio	Receptor Occupancy		CYP1A2 Fold Induction	Percent of Administered Dose Excreted
	Liver	Adipose Tissue	Whole Body	Liver	Adipose Tissue	Whole Body	Liver	Adipose Tissue		Ah	CYP1A2		
0.0605 µg TCDD TEQ-equiv./kg bodyweight (0.00536 nmoles)													
1	0.0497	0.0116	0.0613	0.0398	0.006	0.0458	0.743%	0.112%	6.63	0.939%	0.00271%	1	2.26%
24	0.791	0.96	1.75	0.634	0.495	1.13	11.8%	9.25%	1.28	4.57%	0.0137%	3.69	29.2%
48	0.445	0.902	1.35	0.357	0.466	0.823	6.66%	8.70%	0.766	2.90%	0.00852%	3.31	47.1%
72	0.288	0.73	1.02	0.231	0.377	0.607	4.31%	7.03%	0.613	2.14%	0.00626%	2.89	59.9%
96	0.197	0.571	0.768	0.158	0.294	0.452	2.94%	5.50%	0.535	1.63%	0.00473%	2.59	69.4%

[a] Administered doses were calculated based upon ambient congener-specific concentrations measured on sampled Labrador tea at site 107 in winter 1996 (post-incident), and the typical daily food consumption rate for Gapper's red-backed voles of 0.31 g/g/day (McManus, 1979).

Figure 5.29 **Modelled red-backed vole time-series whole body concentration results for each assessed PCDD/F congener for an administered dose of 0.001 μg/kg.**

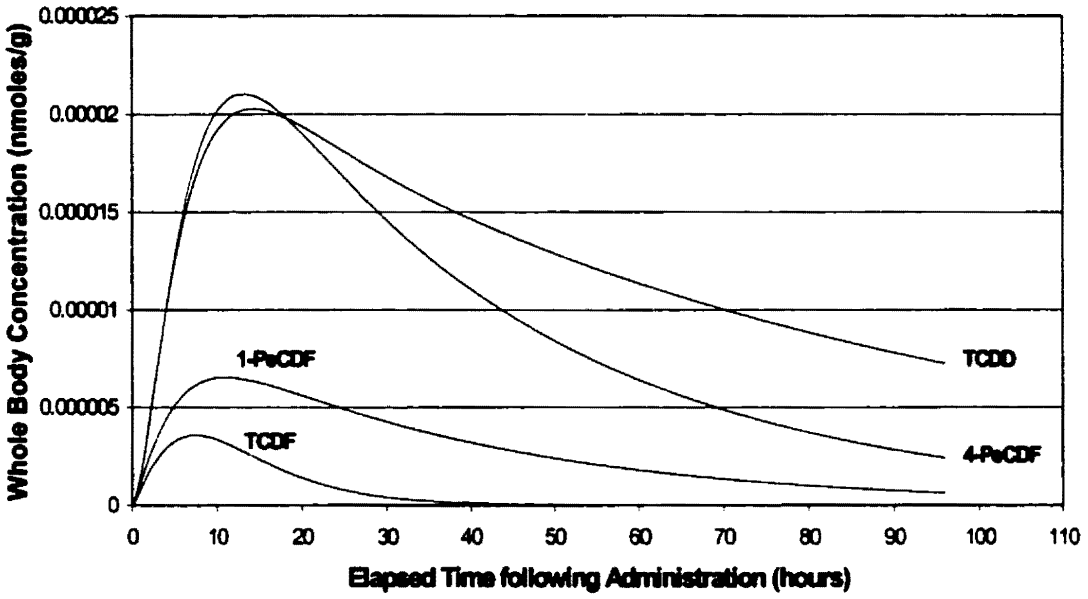


Figure 5.30 **Modelled red-backed vole time-series liver-to-fat ratios for each assessed PCDD/F congener for an administered dose of 0.001 μg/kg.**

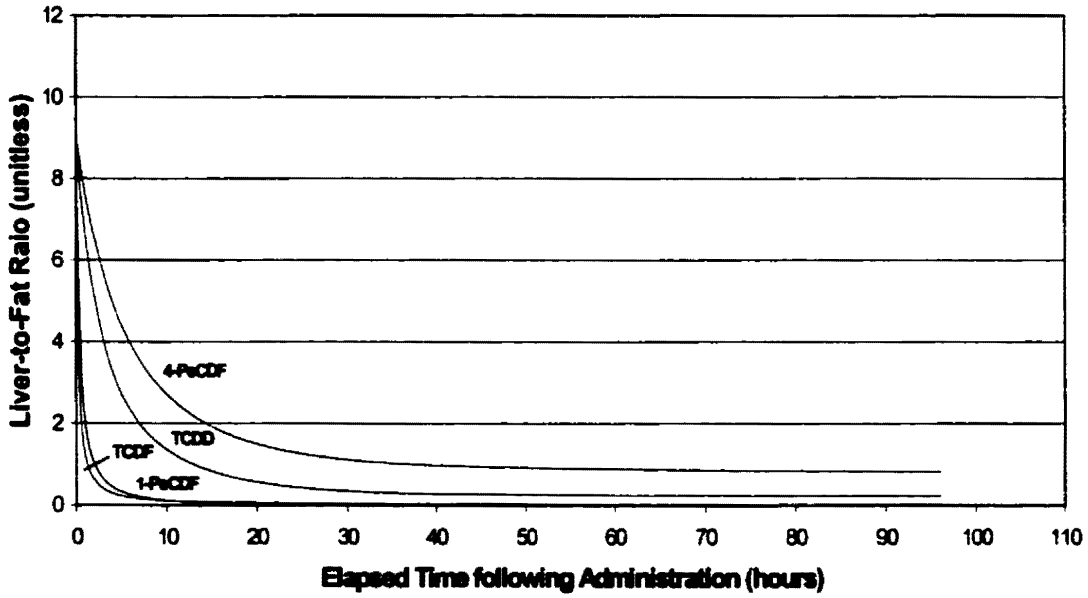


Figure 5.31 **Modelled red-backed vole time-series whole body concentration results for each assessed PCDD/F congener for an administered dose of 0.01 μ/kg.**

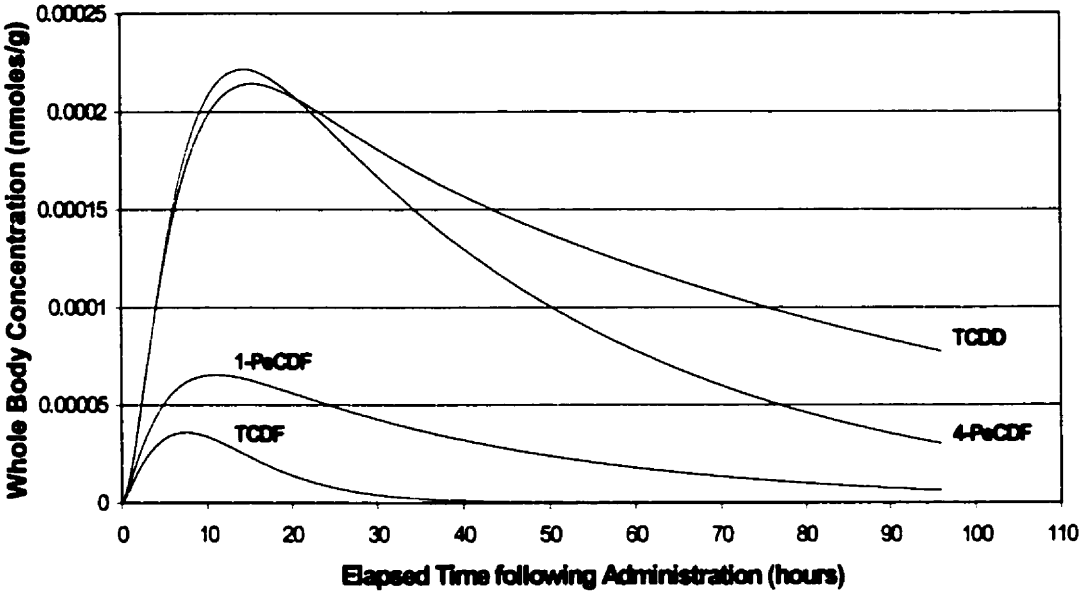


Figure 5.32 **Modelled red-backed vole time-series liver-to-fat ratios for each assessed PCDD/F congener for an administered dose of 0.01 μg/kg.**

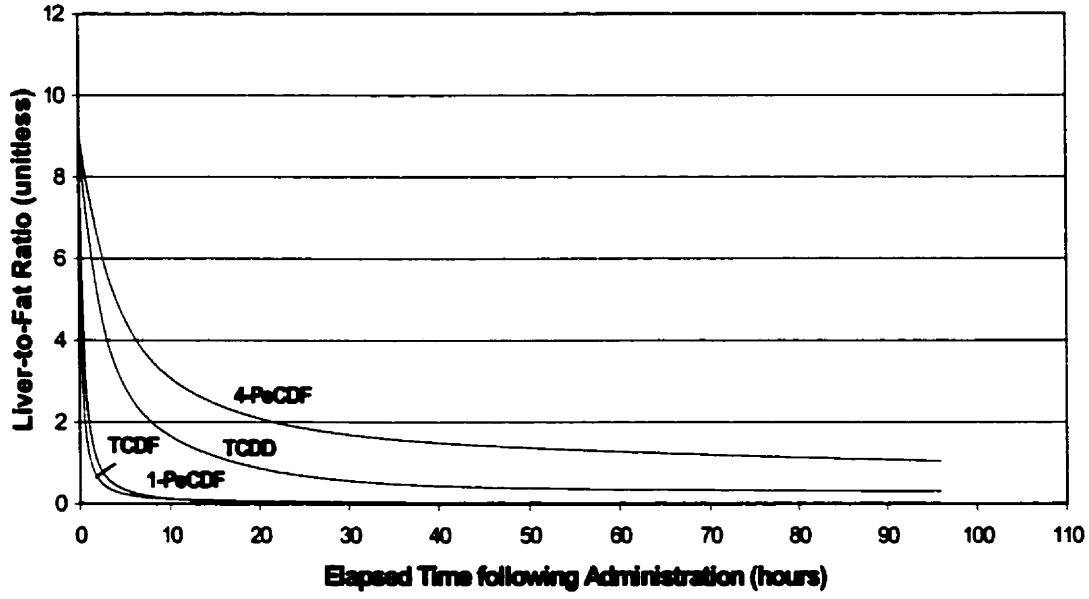


Figure 5.33 **Modelled red-backed vole time-series whole body concentration results for each assessed PCDD/F congener for an administered dose of 0.1 μg/kg**

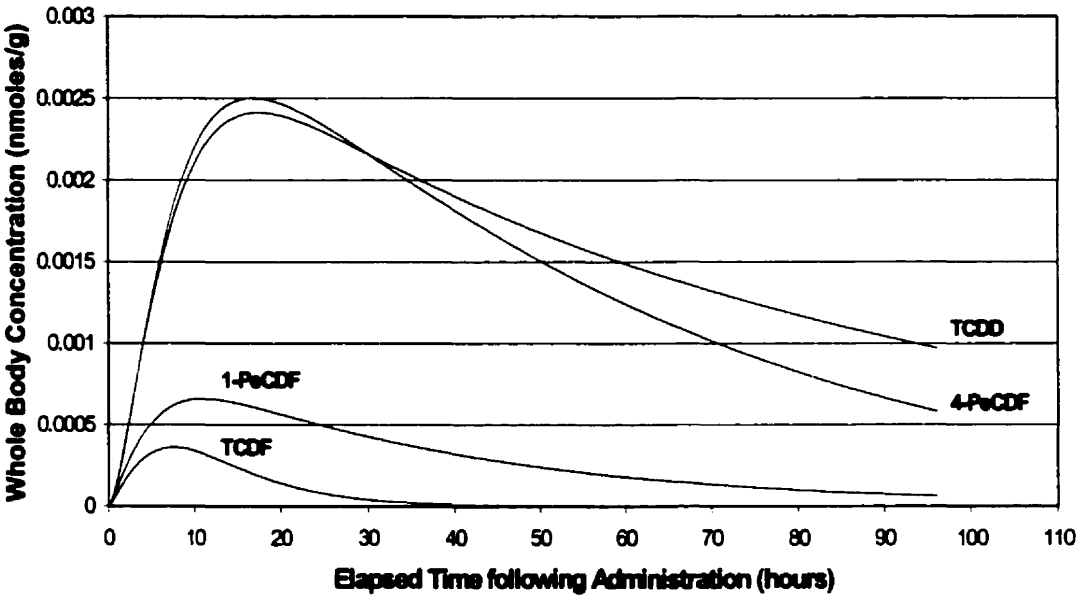


Figure 5.34 **Modelled red-backed vole time-series liver-to-fat ratios for each assessed PCDD/F congener for an administered dose of 0.1 μg/kg.**

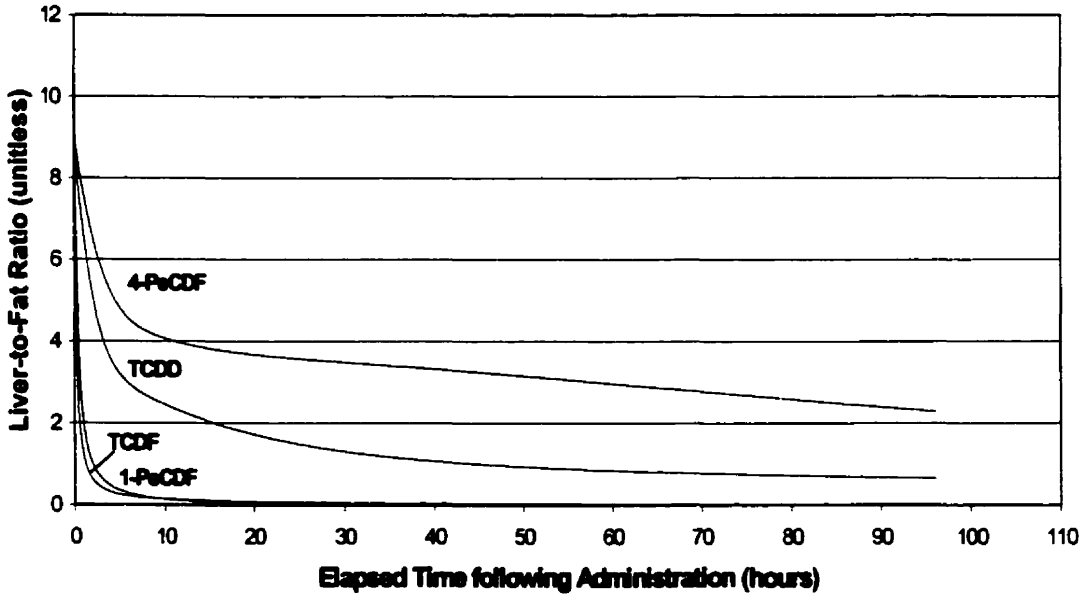


Figure 5.35 **Modelled red-backed vole time-series whole body concentration results for each assessed PCDD/F congener for an administered dose of 1 μg/kg.**

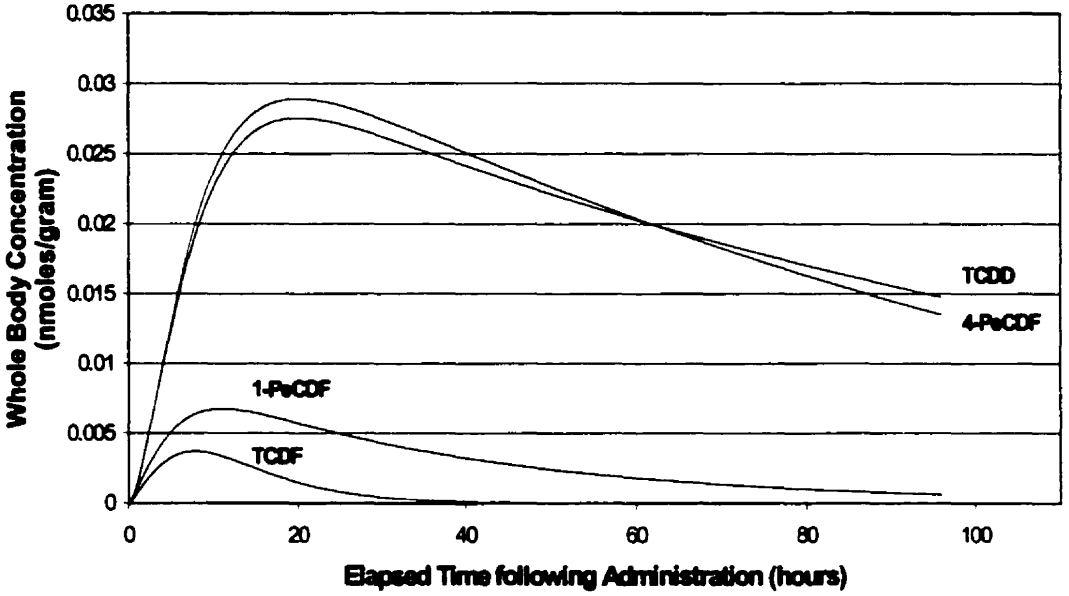


Figure 5.36 **Modelled red-backed vole time-series liver-to-fat ratios for each assessed PCDD/F congener for an administered dose of 1 μg/kg.**

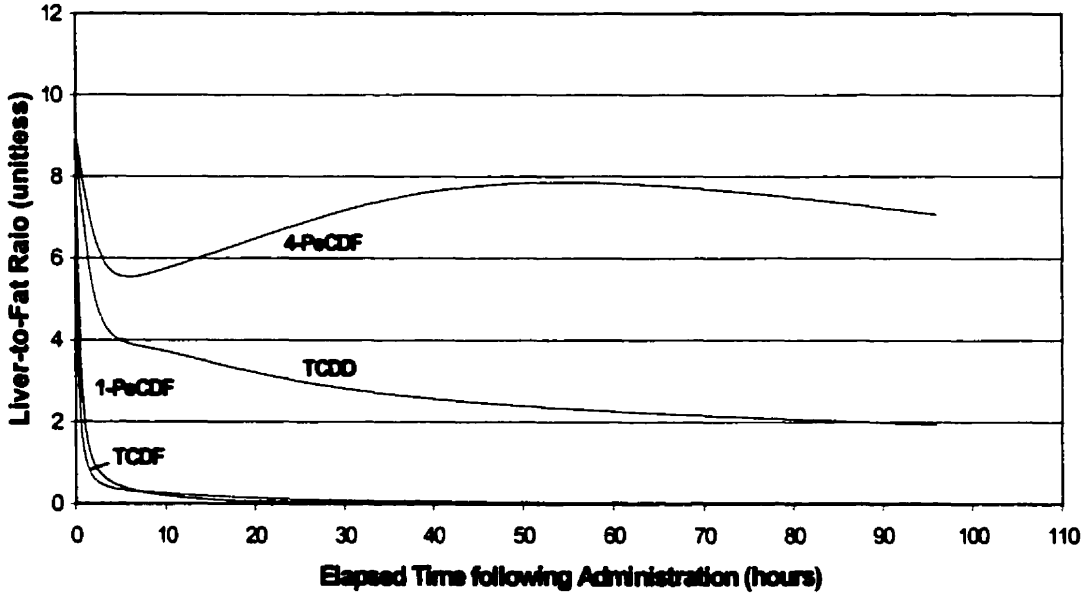


Figure 5.37 **Modelled red-backed vole time-series whole body concentration results for each assessed PCDD/F congener for an administered dose of 10 µg/kg.**

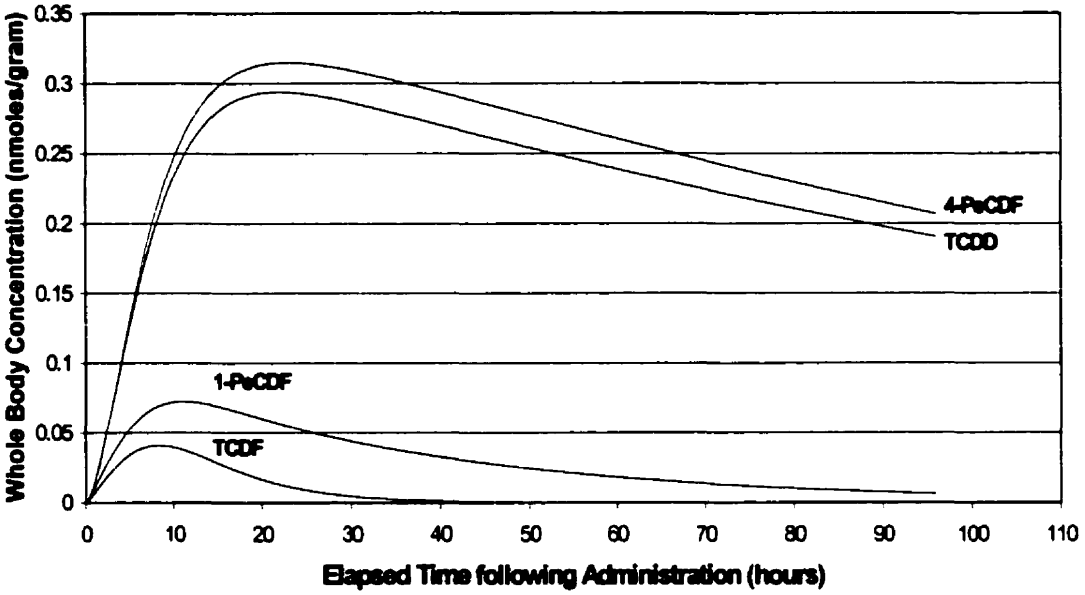


Figure 5.38 **Modelled red-backed vole time-series liver-to-fat ratios for each assessed PCDD/F congener for an administered dose of 10 µg/kg.**

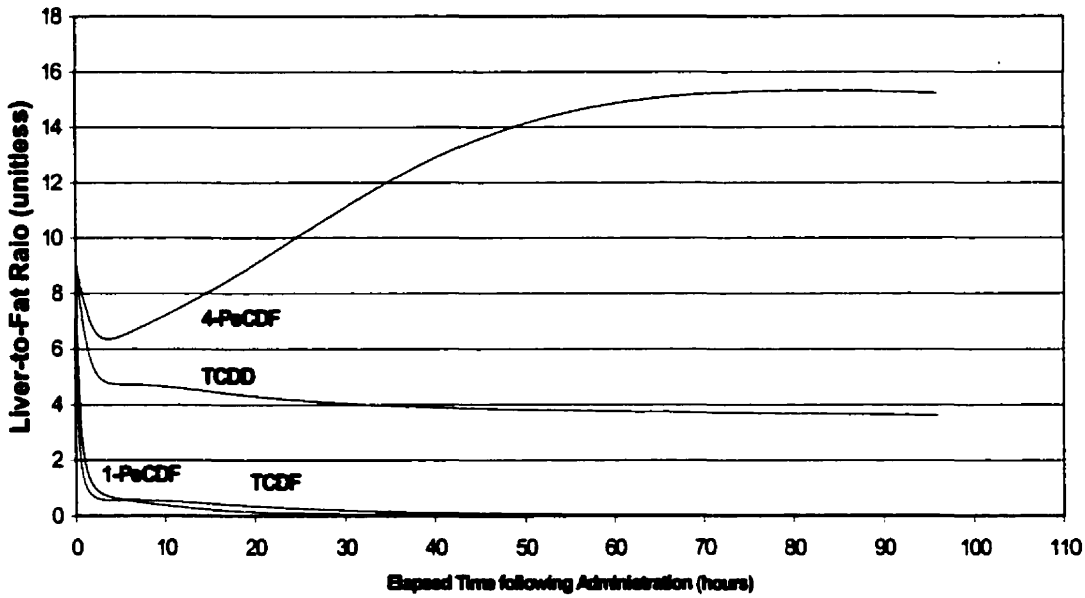


Figure 5.39 **Modelled red-backed vole time-series whole body concentration results for each assessed PCDD/F congener for an administered dose of 100 µg/kg.**

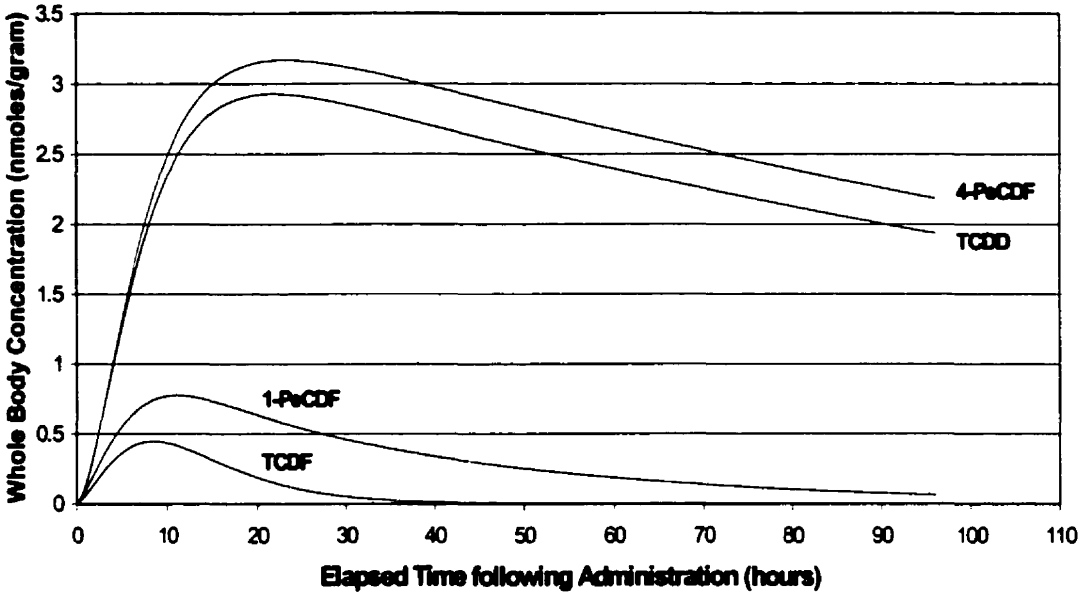


Figure 5.40 **Modelled red-backed vole time-series liver-to-fat ratios for each assessed PCDD/F congener for an administered dose of 100 µg/kg.**

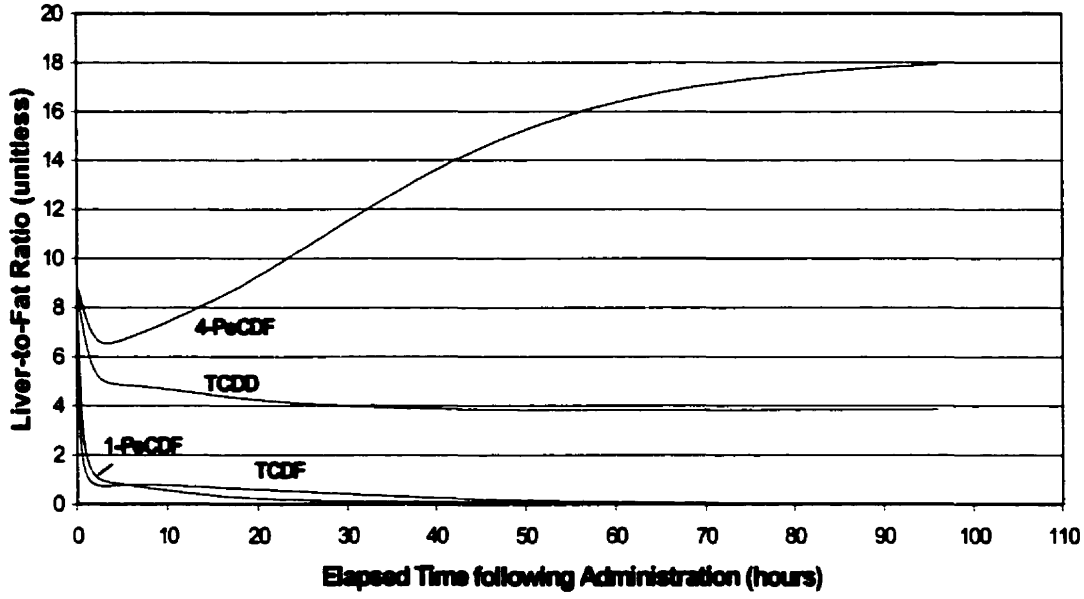


Figure 5.41 Congener-specific liver-to-fat ratios for various administered doses (µg/kg bodyweight) for the Sprague-Dawley rat after 24 hours.

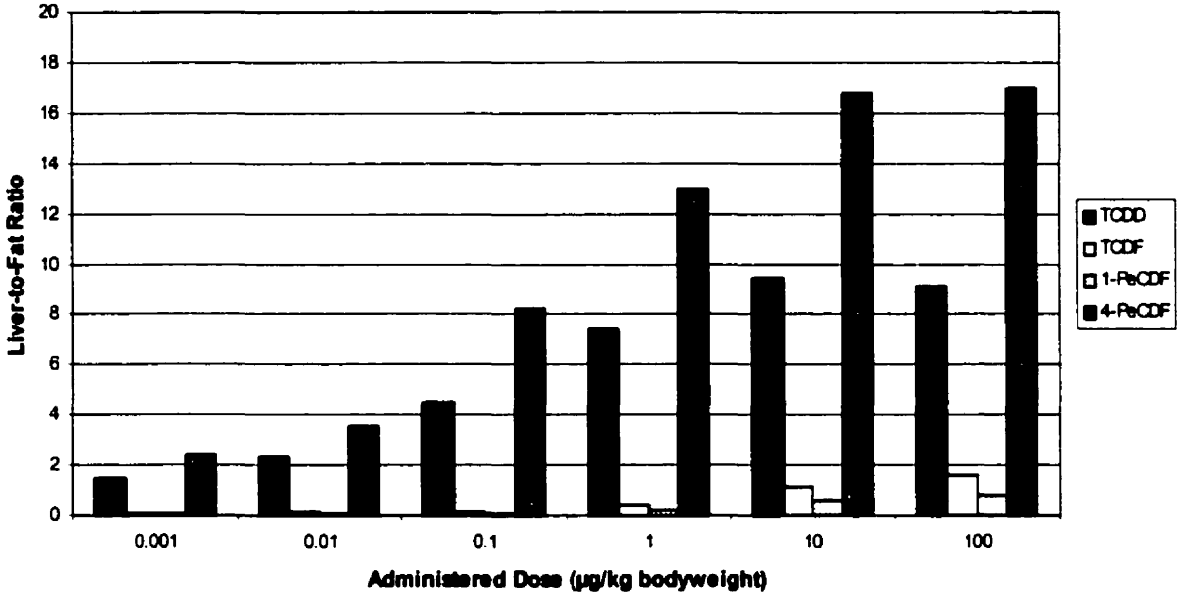


Figure 5.42 Congener-specific liver-to-fat ratios for various administered doses (µg/kg bodyweight) for the red-backed vole after 24 hours.

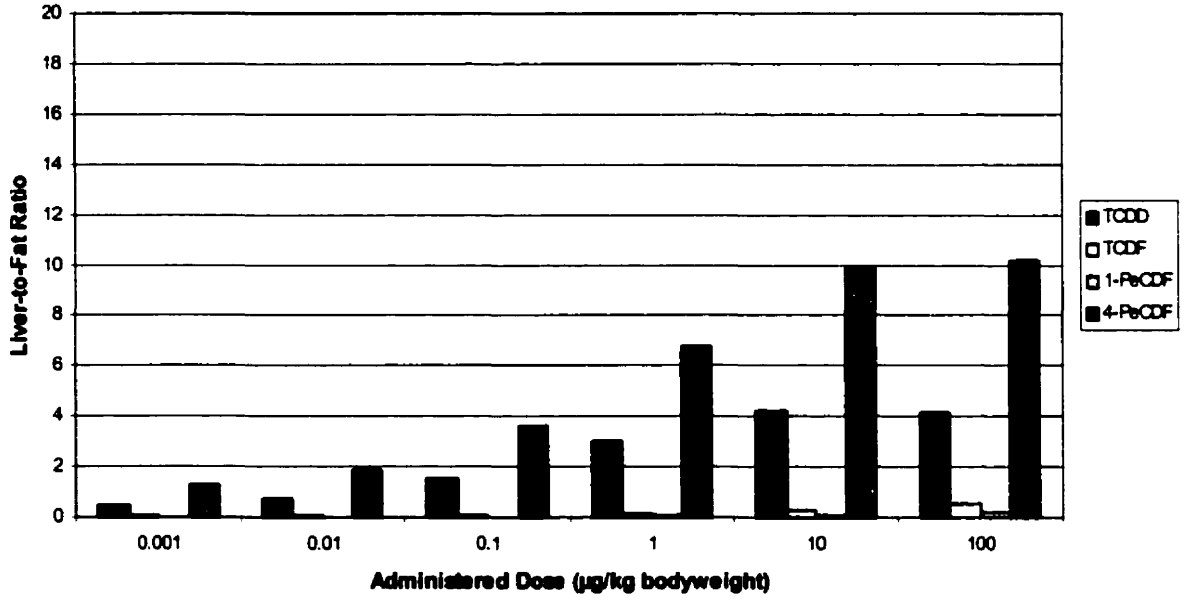


Figure 5.43 Congener-Specific CYP1A2 fold induction for various administered doses (μg/kg bodyweight) for the Sprague-Dawley rat after 24 hours.

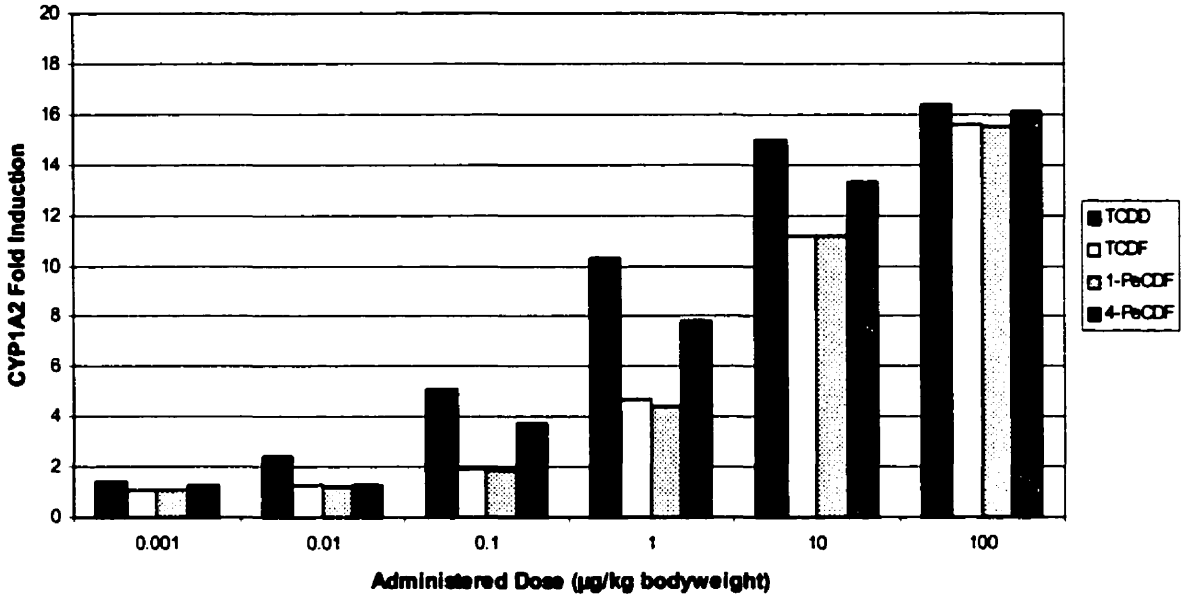


Figure 5.44 Congener-Specific CYP1A2 fold induction for various administered doses (μg/kg bodyweight) for the red-backed vole after 24 hours.

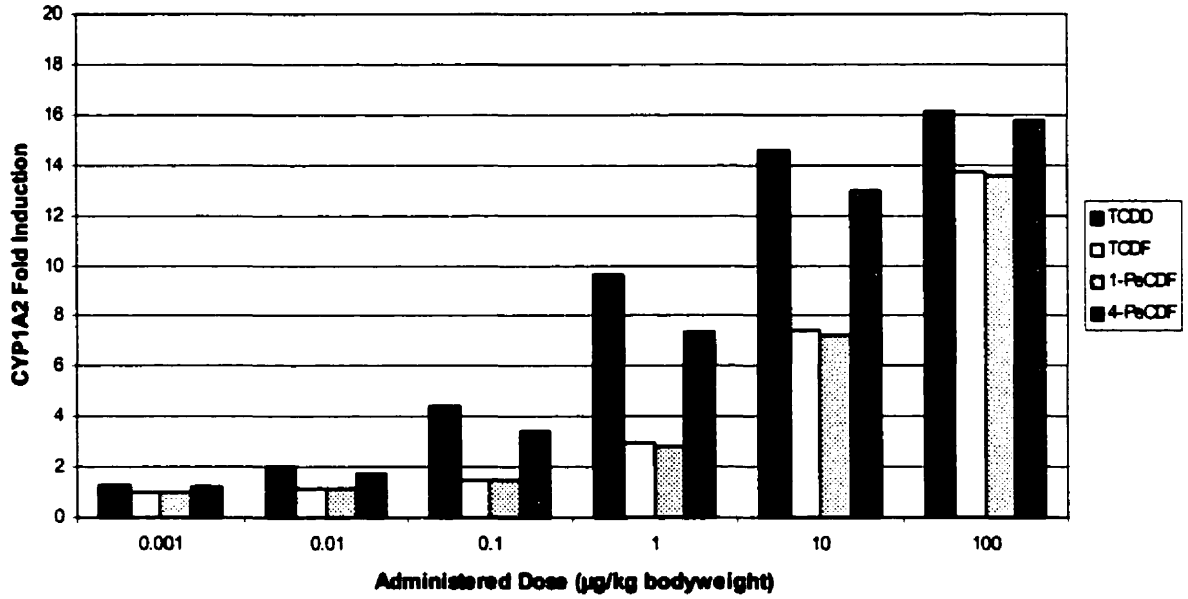


Table 5.27 Comparison of Liver-To-Fat Ratios between TCDF, 1-PeCDF, and 4-PeCDF to that of TCDD for the Sprague-Dawley Rat and Gapper's Red-Backed Vole.

Administered Dose (μg/kg)	TCDF : TCDD Ratio		1-PeCDF : TCDD Ratio		4-PeCDF : TCDD Ratio	
	Sprague-Dawley Rat	Red-Backed Vole	Sprague-Dawley Rat	Red-Backed Vole	Sprague-Dawley Rat	Red-Backed Vole
0.001	0.064	0.103	0.046	0.047	1.65	2.87
0.01	0.045	0.07	0.031	0.031	1.49	2.66
0.1	0.036	0.041	0.022	0.017	1.85	2.35
1	0.054	0.037	0.029	0.013	1.75	2.23
10	0.121	0.067	0.061	0.022	1.79	2.36
100	0.18	0.128	0.091	0.041	1.87	2.48

Note: The TCDF:TCDD, 1-PeCDF:TCDD, and 4-PeCDF:TCDD ratio values were calculated by dividing the Liver-to-Fat ratio value for each of the congeners by that of TCDD, for each dose group.

Based upon the predicted red-backed vole whole body concentrations, congener-specific vole-to-plant BAF values can be calculated and compared to similar values observed in the actual environmental data (see the calculated vole-to-plant BAF values for site 107 provided in Table 5.6). A dose-specific comparison of the modelled *versus* measured vole-to-plant BAF values for each assessed PCDD/F congener and the TCDD-TEQ is provided in Table 5.28. Results of this comparison indicate that the modelled results under-estimate the vole-to-plant BAF for all congeners, when compared to the comparable BAFs calculated based upon environmental sampling data. However, given the current PBPK model is designed to only simulate the congener-specific deposition based upon a single acute dose, rather than chronic exposures, whole body concentrations arising from bioaccumulation of specific congeners over time would be greatly underestimated (development of a chronic administration submodule was attempted but could not be effectively integrated into the existing model methodology). Accordingly, it would likely be useful to observe the BAF values of various congeners to that of TCDD to determine whether similar congener-specific patterns are evident between modelled and measured BAF data. As indicated in Table 5.29, the congener-specific BAF pattern observed in the modelled data closely approximates that observed in the environmentally sampled data for the TCDF and 1-PeCDF congeners. However, this similarity breaks down when one compares the congener-specific BAF patterns for the 4-PeCDF congener and the TCDD-TEQ group. Again, this is not unexpected, given the acute dosing nature of the PBPK model, which would ultimately result in underestimation of chronic whole body concentrations for the more

bioaccumulative PCDD/F congeners (*i.e.*, 4-PeCDF and the TCDD-TEQ group) over an extended period of time.

Table 5.28 Dose-Specific Comparison of Modelled *versus* Measured Vole-to-Plant BAF values for each Assessed PCDD/F Congener.

Elapsed Time (hours)	Vole Whole Body Concentration		Plant Concentration	Modelled Vole-to-Plant BAF	Measured Vole-to-Plant BAF
	pmoles/gram	ppt	ppt		
0.000186 µg TCDD/kg bodyweight (0.0000165 nmoles)					
1	0.000141	0.0454		0.244	
24	0.00256	0.824		4.43	
48	0.00192	0.618	0.186	3.32	63.75
72	0.00143	0.46		2.48	
96	0.00106	0.341		1.84	
0.136 µg TCDF/kg bodyweight (0.0120 nmoles)					
1	0.0331	10.1		0.0743	
24	0.0893	27.3		0.2	
48	0.0347	10.6	136.4	0.0778	2.91
72	0.000101	0.0309		0.000227	
96	0.000003	0.000842		0.000006	
0.0248 µg 1-PeCDF/kg bodyweight (0.00220 nmoles)					
1	0.00829	2.82		0.114	
24	0.098	33.4		1.35	
48	0.0518	17.6	24.8	0.711	10.67
72	0.0261	8.88		0.358	
96	0.0131	4.46		0.18	
0.0713 µg 4-PeCDF/kg bodyweight (0.00631 nmoles)					
1	0.0581	19.8		0.277	
24	1.48	504		7.07	
48	0.945	322	71.3	4.51	240.96
72	0.564	192		2.69	
96	0.323	110		1.54	
0.0605 µg TCDD TEQ-equiv./kg bodyweight (0.00536 nmoles)					
1	0.458	14.7		0.244	
24	1.13	364		6.01	
48	0.823	265	60.5	4.38	320.99
72	0.607	195		3.23	
96	0.452	146		2.41	

Table 5.29 Comparison of Congener-Specific to TCDD BAF values in based on Modelled and Environmental Data.

Congener	Modelled Data		Environmental Data	
	Vole-to-Plant BAF	Ratio to TCDD [a]	Vole-to-Plant BAF	Ratio to TCDD
TCDD	4.43	-	63.75	-
TCDF	0.2	0.0451	2.91	0.0456
1-PeCDF	1.35	0.305	10.67	0.167
4-PeCDF	7.07	1.6	240.96	3.78
TCDD-TEQ	6.01	1.36	320.99	5.04

[a] BAF ratios for each congeners to TCDD (*i.e.*, TCDF-to-TCDD, 1-PeCDF-to-TCDD, 4-PeCDF-to-TCDD, and TCDD-TEQ-to-TCDD).

6.0 DISCUSSION

The principal objectives of the current research involved: (1) the empirical characterization and preliminary validation of computer-based models used for exposure and toxicological (*i.e.*, PBPK modeling) assessment; (2) characterization of the potential health consequences related to environmental exposure to bioaccumulative chemicals; and (3) improved scientific support for risk management decisions concerning industrial activities, such as incineration.

As indicated in the methodological overview, there were three key research aims and questions stressed, which follow a chronological order of implementation: a) modelling issues; b) empirical issues, and; c) application issues.

6.1 Modelling Issues

1. *Evaluation of relative merits of simple (i.e., two-compartment or equilibrium-based) pharmacokinetic models versus complex (i.e., multi-compartmental) PBPK models for the assessment of health risks related to environmental exposures to dioxins and furans.*

Detailed multi-compartmental PBPK models, such as the prototype steady-state model used in this research, provide an excellent framework by which to estimate the effects of absorption, disposition, metabolism, and excretion on the tissue-specific distribution and ultimate toxicity of contaminants. This is particularly the case when non-linear ligand-receptor binding kinetics alter the natural lipophilicity-driven tissue disposition of the chemical. For example, TCDD typically partitions primarily according to its lipophilic nature at low doses, while higher doses result in binding to CYP1A2, leading to preferential accumulation in the liver. However, extension of the model to very high doses predicts that, as specific hepatic binding sites become saturated, TCDD concentrations in liver will plateau, and TCDD will again preferentially accumulate in adipose tissue.

While these multi-compartmental models appear to adequately reflect the disposition of POPs, such as the PCDD/Fs, across a wide variety of exposure doses, there is always some concern that these large, complex models may be over-parameterized. This becomes pertinent as the inherent

uncertainty within the model invariably increases with incorporation of each additional variable into its framework, especially given the inherent difficulty in quantifying many of these parameters. As such, there is considerable interest in determining whether less complex models, such as the equilibrium-based model proposed by Evans and Andersen (2000), can adequately simulate the disposition kinetics of TCDD, using far fewer model parameters.

To evaluate the significance of this concern, the steady-state PBPK model was adjusted to approximate the equilibrium-based conditions of the Evans and Andersen model, by disabling both urinary and biliary/fecal excretion. With the two models being evaluated on an "even playing field", if the two-compartment equilibrium-based model could accurately duplicate the key indicator variables (*i.e.*, liver-to-fat ratio, receptor occupancy, and CYP1A2 induction fold), then the more complex, steady-state model may be deemed as "over-parameterized".

This investigation indicated that the TCDD disposition following a variety of exposure doses did not result in close agreement between the equilibrium-based model and the prototype PBPK model. Results were even more divergent after the equilibrium-based model was corrected for a mis-specification in its methodology (*i.e.*, incorrect calculation of CYP1A2 fold induction). As with the more complex steady-state PBPK model, many of the parameters used in the equilibrium-based model were "fitted" to allow the model outcome to correctly duplicate a set of experimental data. While this allows for the accurate prediction of TCDD disposition under these particular exposure conditions, the use of fitted parameters to represent biological functions makes it very difficult to generalize model predictions outside of a particular set of exposure scenarios (*i.e.*, impacts of high *versus* low exposure doses).

This is particularly the case when parameters were fitted to a mis-specified model methodology, as viewed in the biologically impossible results predicted by the "corrected" Evans and Andersen model using the originally defined parameters. For example, the "corrected" model predicted a CYP1A2 induction increase exceeding 80-fold, when research studies have indicated that the maximum induction fold increase, at high TCDD exposure doses, is approximately 20-fold in rats (Xu *et al.*, 2000). Given the amount of leverage the CYP1A2 induction fold parameter has on the ultimate outcome (see results of the sensitivity analysis in Section 5.2.3), a four-fold

difference in this parameter would have serious implications on the empirical validity of the model results.

The equilibrium-based model was able to closely duplicate the results predicted by the more complex PBPK model with the adjustment of the Ah receptor binding constant (KB1) to 5 nM (125-fold higher than the original value of 0.04 nM), the Ah receptor/DNA binding constant (Kd) to 0.005 nM (10-fold less than the original value of 0.05 nM), and the CYP1A2 induction fold increase to 16-fold (approximately 5-times less than the original value of 85-fold). While this updated version of the equilibrium-based model appeared to provide a reasonable representation of the results produced by the steady-state PBPK model, the biological reality of the updated values for the parameters selected to "correct" model outcomes is questionable. Many studies into TCDD-Ah receptor binding kinetics have indicated that the binding constant (Kd) for Sprague-Dawley rats is less than 1 nM, if not 0.1 or 0.01 nM, depending on the particular type of study (Sloop and Lucier, 1987; Tukey *et al.*, 1982; Gasiewicz and Rucci, 1984; Safe, 1988). Wang *et al.* (1997) indicated that, as the reported values of the Ah receptor concentration in each tissue and the dissociation constant of TCDD bound to the Ah receptor from different studies were different, those values were selected as initial seed values and the final results (*e.g.*, a Kd of 0.1 nM) were obtained by fitting the model to an experimental TCDD tissue distribution. While certainly possible, it is likely that a value of 5 nM would over-estimate the degree of TCDD disassociation from the Ah receptor. It is difficult to determine whether the values selected for the Ah receptor/DNA binding constant and CYP1A2 induction fold increase are biologically unlikely given the considerable amount of uncertainty surrounding these types of pharmacodynamic parameters.

While the modified equilibrium-based model may be able to provide a reasonable estimation of TCDD disposition, it is likely that the inherent uncertainty in its methodology outweighs any benefits gained by its simplicity. Furthermore, this methodology is only appropriate when exposure conditions have reached a "quasi" steady-state, and body burden concentrations have reached an equilibrium plateau. However, given that the elimination half-life of TCDD, based upon a single dose, can range from 10 to 43 days depending on the rodent species being tested, it may take some time to reach a steady-state body burden plateau (Delzell *et al.*, 1994). Moreover,

as the elimination half-life of TCDD in humans is least 5 years, it could conceivably take well over 15 years to reach 90% of steady state, and over 30 years to reach 99% of steady state levels in human populations (U.S. EPA, 1994). As such, it is questionable as to whether an equilibrium-based model could ever adequately estimate the complex dispositional patterns of TCDD, arising from typical environmental exposure conditions over an extended period of time. Based upon these arguments, it is likely that the steady-state PBPK model provides a more appropriate methodology to address potentially complex exposure conditions, despite the increased level of uncertainty arising from the higher degree of inherent parameterization. However, one must be aware that the model assumptions play a dominant role in determining the predicted model outcomes, and that any uncertainty associated with these assumptions will ultimately affect the overall validity of the predicted PBPK model results.

2. *Evaluation of the feasibility of using a PBPK model developed using laboratory rodents for use with the vole sentinel species (i.e., availability of detailed physiological data for the vole receptors or adequate allometric methodologies to produce equivalent data for the appropriate biological receptor).*

Results of the application of the PBPK model developed using laboratory rodents for use with the vole sentinel species has indicated that this model methodology appears to provide a reasonably accurate estimation of chemical-specific disposition and elimination patterns within the vole sentinel species. Thus, it appears that the vole is a useful and relevant sentinel species to evaluate the pharmacokinetic and pharmacodynamic issues surrounding the environmental impacts of PCDD/Fs released as a result of anthropogenic activities. PBPK model systems, such as the one developed based upon the Wang *et al.* (1997) methodology, provide valuable tools for use in long-term environmental monitoring programs such as that in place at the Swan Hills Treatment Centre.

Uncertainties surroudning the use of this methodology can be attributed to the lack of species-specific pharmacokinetic and pharmacodynamic parameter information for the vole sentinel species. While some tissue-specific physiological data, primarily tissue volumes, are available from the scientific literature and field researchers, there are still significant data gaps in the physiological data available for voles. In this work, allometric equations developed for similar rodent species (*i.e.*, the C57BL/6J mouse) were used. However, experimental values of the parameters related to the ligand-receptor binding (both Ah and CYP1A2) are required to reduce the inherent uncertainty present within the model outcomes. A number of research labs which work with Gapper's red-backed voles were contacted for such information. Unfortunately, none of them performed this type of detailed analyses. Nor was any of the information discovered during an extensive review of the scientific literature on the *Microtus* and *Clethrionomys* vole families.

While not currently available, it is likely that this type of information could be obtained for future expansion of the current research. It would likely require the capture of a number of live red-backed voles as part of the ongoing monitoring program (or from other stock sources), and

immediate transport of the live specimens or extracted liver tissues (properly packed for transport) to a laboratory capable of performing this type of analyses. Obviously, the transport of live specimens would be preferable (especially given the Ah receptor is notoriously unstable), as it would allow a more complete characterization of the necessary physiological parameters (*e.g.*, tissue weights, fraction of overall tissue volume composed of blood, tissue permeability, *etc.*), in addition to the required pharmacodynamic information.

Unfortunately, research has indicated that the vole species are notoriously difficult to maintain long-term under laboratory conditions, and tend to react detrimentally to extended contact or captivity (D. Skinner, personal communication, 2000). As such, it would be difficult to do an extended time-series study of the impacts of TCDD (or other congeners) on voles, so that the current PBPK models may be better calibrated for this use. However, until this type of information is obtained, there will still be considerable uncertainty expressed within the outcome of any PBPK model-based assessment of PCDD/F environmental exposure.

3. *Discussion of the relative strengths and weaknesses of the selected PBPK model for dioxins and furans. Objective measures of model strength and weakness such as i) robustness, ii) sensitivity, iii) parsimony, and iv) explanatory value will be evaluated to provide a better indication of the potential uncertainty related to the application of this particular model design.*

Various model methodologies used to describe the pharmacokinetics of PCDD/Fs within a biological system each have their own relative strengths and weaknesses, depending on the exposure scenario. For the current research, a PBPK model and an equilibrium-base model were evaluated to determine their relative effectiveness in predicting the disposition of PCDD/Fs. The following criteria, provided in Table 6.1, were used to evaluate the overall appropriateness of each model in addressing the research objectives. Refer back to Section 3.2.4 for a more detailed description of each criterion.

Table 6.1 Comparison of Prototype Models based upon Several Validity Criteria.

Criteria	Steady-State Model (Wang *et al.*, 1997)	Equilibrium-Based Model (Evans and Andersen, 2000)
Generalizability	With the modification of a few parameters, this model is able to accurately predict the disposition of various PCDD/F congeners in a number of biological test species.	The use of "custom" fitted parameters has greatly reduced the applicability of this model methodology outside of the specific scenario it was designed in.
Internal consistency	Internal diagnostic routines ensure consistency in variables such as total organism-based blood volumes. The designed shell system also ensure consistency for other variables across compartments (*i.e.*, consistency in Ah receptor Kd value between tissue groups).	The lower number of assumed parameters allows for easier maintenance of internal consistency. However, the original model methodology had very few "consistency" checks, resulting in the mis-specification not being caught by any QA/QC processes.
Computational correctness	The original Wang *et al.* (1997) model contained numerous gaps and inaccuracies in the published methodology. These were corrected through research into its original source papers and logical adjustments for biological validity.	The original Evans and Andersen (2000) model contained a serious mis-specification in the CYP1A2 fold induction calculation.
Model form is correct	Once properly developed, the overall model structure accurately reflected the methodological objectives.	Once the mis-specification in the original methodology was corrected, the overall model structure accurately reflected the methodological objectives.
Robustness	While the model did initially show significant instabilities at low exposure doses, this was corrected through reduction of the model time step. Once rectified, the model has demonstrated considerable robustness across doses, chemicals, and species.	Due to the large number of fitted parameters, this model had considerable difficulty under differing input and exposure scenarios.

Table 6.1 Comparison of Prototype Models based upon Several Validity Criteria.

Criteria	Steady-State Model (Wang *et al.*, 1997)	Equilibrium-Based Model (Evans and Andersen, 2000)
Sensitivity	Analyses of model results indicate that changes to input variables appear to have biologically appropriate changes to model outcomes.	While appearing to follow the correct induction curve pattern (*i.e.*, inflection point), the magnitude of CYP1A2 induction fold is incorrectly calculated.
Biological realism and relevance	The multi-compartmental nature of this PBPK methodology allows for a biologically realistic and relevant depiction of PCDD/F pharmacokinetics. The biological realism does not completely extend to detailed pharmacodynamic and metabolic processes, which are assumed "lumped" in with excretion.	This equilibrium-based methodology lacks detailed biological realism (*e.g.*, only two compartments, no modelled movement between compartments *via* the blood, *etc*). Furthermore, the impacts of absorption, metabolism, and excretion are ignored.
Agreement between different models describing the same process	Considerable amount of manipulation of the fitted parameters within the equilibrium-based model was required to achieve a reasonable duplication of the disposition outcomes predicted by the steady-state PBPK model. However, it is questionable as to whether these adjusted parameters are biologically realistic.	
Heuristic value	A full suite of excellent indicator variables is available at each significant point in the post-treatment time series.	A full suite of excellent indicator variables is available for the one equilibrium state.
Capacity to deal with dose-dependent behaviour	The model is fully capable of estimating disposition kinetics under dose-dependent conditions.	Using the original methodology, this model showed a significant lack of capacity to estimate disposition outside of the limited dose levels on which it was built. However, once "corrected" and modified, this model was able to estimate disposition kinetics under dose-dependent conditions.
Absence of numerical artifacts	While the model did initially show significant instabilities at low exposure doses, this was corrected through reduction of the model time step.	Due to the more simplistic nature of the model (as compared to the full PBPK model), it appears to be generally free of numerical artifacts. While not necessarily an artifact or error, the inefficiencies of using the implicit equation solver to determine blood concentrations does pose problems (particularly when attempting Monte Carlo simulations or sensitivity analyses).
Useful in extrapolation to other conditions	This model can adequately evaluate relative absorption, disposition and elimination kinetics across a variety of exposure routes, doses, and dose-rates, with very minor adjustments to its underlying methodology (many of which were added during this research project).	Given the equilibrium-based nature of this methodology, it is very limited in its ability to extrapolate to conditions outside of those for which it was originally designed. As it handles dose as an internal dose at equilibrium, external calculations would be required to allow for assessments using alternative exposure routes or dose rates.

Based upon this evaluation of the relative strengths and weaknesses of each model methodology, it would appear that the steady-state PBPK model provides the more robust, sensitive, and parsimonious methodology for predicting PCDD/F disposition kinetics in a variety of biological species.

6.2 Empirical Issues

1. Evaluate the apparent empirical relationship between the octanol-water partitioning coefficient (log K_{ow}) and Bioaccumulation Factor (BAF) or Bioconcentration Factor (BCF) of dioxins and furans in the vole sentinel receptor.

The octanol-water partitioning coefficient, also referred to as the K_{ow}, provides an empirical or experimental representation of the distribution of a particular organic chemical between water and an organic liquid phase. All organic compounds have an inherent level of lipophilicity, which is indicative of their general affinity for lipids (or fats). The more lipophilic (or hydrophobic) the compound, the larger the K_{ow} that would be assigned. Given the large range in potential K_{ow} values (*i.e.*, 0 to > 1 x 10^8), the lipophilicity of a compound is typically presented as the log of the K_{ow}. Table 6.2, below, provides an overview of the log K_{ow} values for each of the dioxin and furan congener groups.

Table 6.2 Overview of Log Octanol-Water Partition Coefficient Values for the key Dioxin and Furan Congeners.

Congener	Log K_{ow} [a]
Dioxins	
TCDD	6.8 (6.1 to 7.1)
PeCDD	6.64 (6.2 to 7.4)
HxCDD	7.8 (6.85 to 7.8)
HpCDD	8
OctaCDD	8.2
Furans	
TCDF	6.1 (5.6 to 6.79)
PeCDF	6.5 (6.19 to 6.92)
HxCDF	7
HpCDF	7.4
OctaCDF	8

[a] Summarized in U.S. EPA (2000).

Physico-chemical properties have demonstrated that the log K_{ow} of an organic compound increases with the compound's propensity to accumulate within the tissues of biological organisms (*i.e.*, due to storage within fats or tissues, the concentrations of the compound within the organism are greater than the ambient concentrations found in the environment of the

organism). Based upon this behaviour, compounds with log K_{ow} values which exceed 3 are generally viewed as "bioaccumulative" in nature. Bioaccumulate compounds, such as the PCDD/Fs, are of particular concern as they concentrate the compound within the organism, greatly increasing the opportunity for a potentially toxic exposure dose to occur over an extended period of time (sometimes well after the initial environmental release).

As indicated by Table 6.2, as the degree of chlorination increases, the log K_{ow} and lipophilic tendencies of a particular congener also increase (if one ignores the potential impacts of solubility and gastric absorption on congener-specific bioavailability). Based upon this pattern, one would expect the degree to which a particular congener bioaccumulates within an organism would also increase with degree of chlorination (*e.g.*, one would expect the OCDD/Fs to be more bioaccumulative than the TCDD/Fs). However, if one evaluates the vole-to-plant bioaccumulation factors (BAFs) calculated based upon the SHTC environmental monitoring data (refer to Tables 5.4 through 5.6), it becomes quite evident that the PeCDD/Fs and HxCDD/Fs are far more bioaccumulative than their HPCDD/F and OCDD/F counterparts. As this behaviour would typically be counter-intuitive, obviously there are other factors in addition to the lipophilicity of the compound which impact upon the disposition and rate of elimination of these congeners.

As previously discussed, research has demonstrated that the variable ligand-receptor binding of the PCDD/F congeners to CYP1A2 results in a significant sequestration/accumulation of the compound within the liver. This sequestration temporarily prevents the metabolism (if applicable) and excretion of a large portion of the internal congener dose; thus leading to a much greater degree of bioaccumulation within the organism than would be expected through lipophilicity partitioning to adipose tissue depots alone.

Of all the congeners, the PeCDFs and the HxCDFs appear to have the greatest affinity to CYP1A2, resulting in a much larger degree of sequestration and accumulation, than their weakly binding, higher-chlorinated counterparts. This makes the weaker binding, higher-chlorinated congeners relatively more susceptible to metabolic breakdown and/or excretion in mammalian systems, typically leading to a much lower degree of bioaccumulation once the congener has

been mobilized from adipose tissue stores (*i.e.*, through stress or elevated activity). Other issues, such as the gastric bioavailability (or lack thereof) of the higher-chlorinated congeners (*i.e.*, OCDD/Fs), also impact upon the degree to which a particular congener will accumulate with a particular biological organism.

As such, the apparent toxicity of compounds such as PCDD/Fs (*i.e.*, a biological endpoint) can never be simply related to their inherent lipophilicity as described by its log K_{ow} (a physio-chemical parameter), but requires a more significant evaluation of the toxicokinetics and toxicodynamics of the particular congener being assessed (*i.e.*, through the use of PBPK modelling).

2. *Evaluate whether the Toxic Equivalency Factors (TEFs) for dioxins and furans provide a suitable surrogate for toxicity in the vole species, considering such parameters as chemical bioavailability, pharmacokinetic factors, and toxicodynamic equivalency.*

Based upon the current research, it is likely that pharmacokinetic and pharmacodynamic differences between the vole and the Sprague-Dawley rate may result in significant implications on PCDD/F toxicodynamic equivalency in an environmental setting. For example, a larger proportion of the persistent 4-PeCDF congener appears to become sequestered in the liver of the vole, than observed in its rat counterpart, when scaled on a species-specific basis to the TCDD benchmark (see Table 5.21). While the adipose tissue can be viewed as a temporary depot for PCDD/F concentrations (easily mobilized under stress or elevated activity), 4-PeCDF appears to bind tightly to the CYP1A2 in the liver, causing the liver to serve as a ligand sink, binding and effectively removing free 4-PeCDF from the general body circulation until CYP1A2 protein turnover and/or slow ligand disassociation occurs. The same pattern is observable with TCDD and the other Ah-responsive congeners, though to a lesser extent.

As noted previously, the overt signs of toxicity in animals from exposures to chlorinated dioxins and furans are characterized by a general wasting syndrome, with an overall loss in body weight, even though food consumption is normal. These effects are typically accompanied by wide-ranging impacts upon the functions of the immune, reproductive, adrenocortical, and thyroid endocrine systems. These toxic outcomes have been largely traced back to ligand-receptor interactions between the PCDD/Fs and the Ah receptor, resulting in a cascade series of systemic impacts (*e.g.*, inhibition of glucocorticoid-regulated enzymes, abnormal impacts on levels of growth factor receptors, antiestrogenic impacts mediated through receptor-based "cross-talk", *etc.*).

As these toxic outcomes appear to be mediated by Ah receptor ligand interactions principally within extrahepatic tissues (*e.g.*, thyroid, adrenal cortex, reproductive organs, thymus, spleen, *etc.*), it is likely that a high degree of ligand sequestration within the liver (as denoted by a high liver-to-fat ratio) would result in less "free" ligand available in the body circulation to bind to Ah receptors in these tissue organs. Accordingly, the lower number of ligand-receptor binding

events would result in fewer AhR-mediated toxic outcomes, decreasing the overall apparent systemic toxicity of the administered congener dose.

This variability in inter-species (and even inter-strain) toxicity has been observed in a number of toxicity studies. For example, the acute LD_{50} values of PCDDs in guinea pig and various rat strains have been shown to follow the typical order (and accordingly, potency) predicted by their TEF values. However, in the resistant Hann-Wistar rat strain for example, the order of potency for male and female rats was 1,2,3,4,7,8-hexaCDD > 1,2,3,4,6,7,8-heptaCDD > 1,2,3,7,8-pentaCDD > TCDD. The data from these studies indicate that 1,2,3,4,6,7,8-heptaCDD was slightly more acutely toxic than TCDD in Hann-Wistar rats, whereas in other rat strains and the guinea pig, TCDD is at least 100 times more toxic than 1,2,3,4,6,7,8-heptaCDD (Safe, 1998b). For example, acute LD_{50} values for TCDD in guinea pigs, the most sensitive species tested, ranged from 0.6 to 2.1 μg/kg bodyweight (Schwetz *et al.*, 1973; McConnell *et al.*, 1978), while an LD_{50} value for the hamster, the least sensitive species tested, was determined to be 5000 μg/kg bodyweight (Olson *et al.*, 1980; Henck *et al.*, 1981). In addition to differences in relative adiposity, research has demonstrated that differences in ligand-receptor binding affinity to the Ah receptor (Poland and Glover, 1990; Poland *et al.*, 1994), as well the degree to which the congener is sequestered in the liver through binding to CYP1A2 protein, can result in significant species- and strain-specific differences in potency.

This hypothesis has considerable implications on the selection of representative TEFs for specific PCDD/F congeners for environmental sentinel species, such as the red-backed vole. For the most part, TEF values are established based upon *in vivo* and/or *in vitro* laboratory assays using species such as the Sprague-Dawley rat. Therefore, if the red-backed vole is less sensitive to the 4-PeCDF congener than the rat, due to its higher degree of hepatic sequestration or more rapid metabolism and excretion, it is likely that the established TEF would also overestimate the toxic potential of 4-PeCDF in the vole sentinel species. Given the 4-PeCDF congener represents the vast majority of both the mass- and TEF-based concentration of PCDD/F measured in biota surrounding facilities such as the SHTC (see Table 5.4), a systemic over-estimation of the TEF for the 4-PeCDF congener would have significant impacts on the outcome of an environmental risk assessment, based upon the red-backed vole as a sentinel species.

3. *Evaluate the "fractionation" characteristics of the dioxin/furan congener emission mixtures in both the environment and within the vole receptor, on a (i) mass ratio and (ii) TEQ ratio. More specifically, the relative congener and isomeric "fingerprint" breakdown of dioxin and furan concentrations present in both environmental (e.g., water, soil, and sediment) and biological (e.g., Labrador tea plants and voles) sinks are highly dependent upon a variety factors. For example, each specific congener group has differing physico-chemical properties, leading to differing physiological disposition, metabolism and ultimately toxicological impacts on biological receptors, such as the red-backed vole. These "fractionation" characteristics provide much of the basis for the TEQ methodology for evaluating the toxicity of individual dioxin-like congeners as an overall functional group.*

When evaluating the PCDD/F congener-specific fractionation characteristics in both the environment (using Labrador tea as a surrogate for ambient environmental concentrations) and the vole sentinel receptors, at each of the three primary monitoring sites (*i.e.*, sites 11, 107, and 114), an interesting pattern emerges (see Table 5.4 and Figures 5.7 and 5.8). Environmental sampling conducted on Labrador tea indicates that 2,3,7,8-TCDF dominates the congener fingerprint pattern on a mass basis, typically representing between 50 and 60% of the total PCDD/F mass, with 2,3,4,7,8-PeCDF representing a further 10 to 20% of the total PCDD/F mass. As expected, this particular congener-specific pattern closely mirrors the PCDD/F emission pattern of the SHTC facility, arising from the PCB incineration process (Ferguson, 1998). However, when these congener-specific concentrations are adjusted to TCDD TEQ-equivalent concentrations, 2,3,4,7,8-PeCDF typically dominates representing between 45 and 60% of the total TEQ-adjusted PCDD/F concentration, with 2,3,7,8-TCDF a close second (typically 30 to 40% of the total TCDD TEQ-eqivalent concentration).

When one examines the congener-specific pattern observed in the vole samples, 2,3,4,7,8-PeCDF is by far the most important congener, typically representing 65 to 80% of the total PCDD/F mass, with the HxCDF isomeric group providing approximately 10% of the total PCDD/F mass, and TCDF less than 5% of the total congener mass. On a TEQ-equivalent basis, the 2,3,4,7,8-PeCDF congener represents more than 90% of the total. While the TCDF congener was a heavy contributor to the pattern viewed in ambient concentrations, the lack of hepatic sequestration and

its rapid excretion rate resulted in no significant disposition in the voles over time. The 2,3,4,7,8-PeCDF congener, on the other hand, was heavily stored in the liver due to CYP1A2 sequestration, which resulted in significant bioaccumulation and dominance of the overall mass- and TEQ-based congener-specific fractionation within the vole. As such, this particular pattern is as expected based upon the research presented in this project.

Interestingly enough, the congener-specific fingerprint patterns do not appear to differ significantly in relative contribution percentages, for both mass- and TEQ-based concentrations, between pre-incident (summer 1996) and post-incident (winter 1996), for either biota sampling set. The only noticeable differences in the pattern are the significant elevation in ambient PCDD/F, particularly the PCDF congeners, in post-incident biota sampling when compared to those observed immediately prior to the October 1996 release incident, and the slightly elevated environmental concentrations of 2,3,7,8-TCDF. Both of these observations are consistent with stack monitoring data during and immediately following the October 1996 incident event.

During the incident, dioxin concentrations were ten times higher than normal, while HxCDDs, which normally accounts for 33% of dioxin emissions, were not present during the process gas release. Overall, the concentrations of total dioxin were also much higher during the release (2.5 $\mu g/m^3$ *versus* 4.9 ng/m^3) when compared to normal operational conditions (CanTox, 1998). Furthermore, the typical incinerator stack gas composition demonstrates that PeCDFs and HxCDFs are important emission constituents, accounting for a majority of total furans on a mass basis. However, during the incident, the TCDF congener was a more important emission constituent, accounting for approximately 47% of the total furans in the stack gas (as opposed to 16% under normal conditions). As with the dioxins, the concentrations of total furans were much higher during the incident release than under normal operational specifications (520 $\mu g/m^3$ *versus* 56 ng/m^3 in normal stack gas) (CanTox, 1998). As such, the similar but elevated PCDD/F congener-specific concentration pattern and the observable spike in TCDF concentrations noted in the winter 1996 ambient sampling data can be directly linked to the congener-specific emission pattern arising from the October 1996 incident event. A more detailed discussion of the incident emissions and the corresponding environmental congener-specific fingerprint can be found in this researcher's Masters thesis report (Ferguson, 1998).

6.3 Application Issues

1. *Discuss the implications of research results on mammalian (both vole and human) risk assessments, and the applicability of laboratory developed TEF values under environmental conditions.*

In the past, hazard and risk assessment of PCDD/Fs have focused on the quantitation of TCDD concentrations in various environmental media. However, with development of high-resolution analytical techniques coupled with studies on structure-toxicity relationships, it has become apparent that the bulk of the toxicity induced by most PCDD/F mixtures is not due to TCDD alone, but has significant contribution from other less-studied congeners. Furthermore, as confirmed in sampling done as part of the SHTC monitoring program, TCDD has been demonstrated to represent only a very small portion of the overall PCDD/F mass present in the environment (typically < 1%).

As a result, the complex nature of environmental mixtures of persistent organic pollutants, such as PCDD/Fs and PCBs, greatly complicates the task of risk evaluation for humans, fish, and wildlife. For this purpose, the concept of toxic equivalency factors (TEFs) was developed and introduced to facilitate risk assessment and regulatory control of exposure to these mixtures. While widely accepted, it is also generally understood that the TEF concept is based on assumption that the individual compounds all act through the same biologic or toxic pathway (*i.e.*, Ah receptor mediated effects), and that the combined effects of the different congeners are dose or concentration additive.

While many studies support this assumption (summarized in Van den Berg *et al.*, 1998), research has indicated that the TEF for each 2,3,7,8-substituted congener compared to TCDD is variable among cell types, laboratory animal species, target organs, and responses. For example, recent studies done by Safe (1998c) with immunotoxicity-derived TEFs for several HAHs in mouse models has indicated that the TEFs for inhibition of the plaque-forming cell response to trinitrophenyl-lipopolysaccharide by 2,3,4,7,8-pentachlorodibenzofuran in C57BL/6, DBA/2, and B6C3F 1 mice varied by approximately 7-fold, and in some assays this congener was more potent than TCDD. Over a broader spectrum of responses, TEFs for individual PCDD/PCDF

congeners have been shown to vary by over 100-fold (Safe, 1998c). As such, the broad range of potencies for a specific congener compromises the use of a single TEF for this congener and may over- or underestimate the calculated TEQ for a mixture. While this overall variability in calculated TEF values is due to many factors, it is primarily a result of the differential pharmacokinetics and metabolism of HAHs in different exposed species.

Given this variability in potency values and the potential implications this variability has on the predictive power of human and ecological risk assessments, validation of its applicability under mixture conditions typically observed in the environment, becomes a vital concern. Validation of the TEF value can be investigated by determining the *in vitro* or *in vivo* toxicities of reconstituted mixtures of PCDDs and PCDFs and comparing their observed *versus* calculated potencies. In a limited number of validation studies using mixtures, a good correlation was found between the observed *in vivo* or *in vitro* response and TEQ values calculated from the relative concentrations of individual congeners in the mixture using multiple end points (Van den Berg *et al.*, 1998; Schrenk *et al.*, 1990; Eadon *et al.*, 1986). However, for more complex mixtures containing compounds that act through multiple pathways to give both similar and different toxic responses, recent thought is that the TEF/TEQ approach may not be appropriate (Safe, 1998c). For example, even for PCDDs/PCDFs, there is some evidence that TEFs do not always predict relative congener potency in different rat strains (Pohjanvirta *et al.*, 1995).

Several studies have also demonstrated that the coplanar PCBs (*i.e.*, 3,3′,4,4′-tetra-, 3,3′,4,4′,5-penta, and 3,3′,4,4′,5,5′-hexachlorobiphenyl) bind to the AhR and induce a broad spectrum of AhR-mediated biochemical and toxic responses (summarized in Safe, 1994). Provisional TEFs have been proposed for coplanar and mono- ortho coplanar PCBs and these values are used routinely for determining total TEQs in risk assessments (Van den Berg *et al.*, 1998). While the relative TEQ contributions of different classes of HAHs are variable, there are numerous examples that demonstrate that PCB TEQs contribute >50% of total TEQs (Safe, 1998c).

While many of these PCBs integrate well into the TEF approach, one of the major problems associated with the TEF approach for HAHs is the potential nonadditive antagonistic interactions

between AhR agonists (*i.e.*, PCDDs/PCDFs and certain PCBs) and PCB congeners that exhibit response and cell/species-specific antagonistic activity. Table 6.3, below, provides a few examples of the antagonistic impacts of various HAHs have on the AhR-mediated HAHs, such as TCDD.

Table 6.3 Examples of Antagonistic Interactions of Halogenated Aromatic Hydrocarbons through Inhibition of TCDD or 3,3',4,4',5-PentaCB-induced Responses (Safe, 1998c).

Antagonists	Antagonistic Response (Animal Cell)
1,3,6,8-TetraCDF 2,3,6,8-TetraCDF Aroclor 1254	AHH/EROD activities (H4IIE cells)
2,2',4,4',5',6-HexaCB	EROD activity (chick embryo hepatocytes)
2,2',5,5'-TetraCB	Luciferase activity (mouse and rat cell lines)
Aroclors 1232, 1242, 1248, 1254, and 1260 Reconstituted PCB mixtures 1,3,6,8-TetraCDF 2,3,3',4,5'-PentaCB 2,3,3',4,4',5-HexaCB 2,3,3',4,5,5'-HexaCB 2,3,4,4',5,6-HexaCB 2,2',4,4',5,6'-HexaCB 2,2',4,4',6,6'-HexaCB 2,2',4,4',5,5'-HexaCB	Splenic plaque-forming cell response to sheep red blood cells or trinitrophenyl-lipopolysaccharide (mouse strains)
2,2',4,4',5,5'-HexaCB	Serum IgM units (mice)
Aroclor 1254 2,2',5,5'-TetraCB 2,2',4,4',5,5'-HexaCB	Fetal cleft palate and hydronephrosis (mice)
2,2',4,4',5,5'-HexaCB	Chick embryotoxicity, malformations ,edema, liver lesions

For example, 2,2′,4,4′,5,5′-hexachlorobiphenyl (PCB 153), a major persistent congener in environmental samples, inhibits the following TCDD or 3,3′,4,4′,5-pentachlorobiphenyl-induced responses: i) induction of ethoxyresorufin O -deethylase activity in chick embryo hepatocytes; ii) inhibition of the plaque-forming cell response to sheep red blood cells in mice; iii) inhibition of the plaque-forming cell response to trinitrophenyl lipopolysaccharide in mice; iv) inhibition of serum IgM units in mice; v) induction of fetal cleft palate in mice; vi) induction of chick embryo malformations; vii) induction of chick embryo edema; viii) induction of chick embryo liver lesions, and; ix) induction of fetal hydronephrosis in mice (Safe, 1998c).

While not discussed directly in the current research project, the implications of such antagonistic HAHs on the ligand binding kinetics and overall tissue-specific disposition of PCDD/Fs are quite far-reaching. Humans and wildlife are constantly environmentally exposed (primarily through diet) to complex mixtures of these persistent HAHs. Hazard and risk assessment of these mixtures is a difficult process and the TEF approach has been utilized to attempt to address these issues. However, these nonadditive interactions, coupled with the unusually broad range of TEF values observed for some PCB congeners (*e.g.*, 3,3′,4,4′-tetraCB), compromises the utility of the TEF approach for hazard and risk assessment of HAHs that contain PCBs (Safe, 1998c).

These and other uncertainties that impact upon the applicability and utility of the TEF concept (*e.g.*, differences in shape of the dose-response curve, species responsiveness, *etc.*) were discussed in detail at an expert meeting organized by the World Health Organization (WHO) and held in Stockholm on June 15-18, 1997. In spite of these uncertainties, it was concluded that the TEF concept is still the most plausible and feasible approach for risk assessment of HAHs with dioxin-like properties. In view of the available scientific evidence from studies with mixtures, it was concluded that it is unlikely for the use of this additive model to result in a great deal of error in predicting the concentrations of TCDD-TEQs or responses at environmentally relevant levels due to non-additive interactions (Van den Berg *et al.*, 1998).

Despite these assurances, these uncertainties may have significant implications on the predictions of toxicological impacts in environmental risk assessments. For example, based upon the tissue sampling conducted on voles living in the area surrounding the SHTC following the October 1996 release incident, the PCDD/F and PCB whole body concentrations (on a TEQ-basis) were sufficiently elevated as to result in the prediction of an observable population-wide negative impact on reproductive success. However, vole populations levels have actually increased in the years following the incident, with no obvious short- or long-term deleterious impacts appearing as a result of the significant short-term increase in environmental HAH levels (Chem-Security Ltd, 1999).

Obviously there is still a significant amount of uncertainty present in the current TEF methodology, likely arising from some of the inter-species pharmacokinetic and

pharmacodynamic issues identified in the current research project. Therefore, while the prediction of TEQs according to the TEF model is considered to be plausible and to be the most feasible approach for risk assessment of HAHs with dioxin-like properties, given these uncertainties, the application of TEFs to evaluate overall toxicity in environmental risk assessments of facilities such as the SHTC must be made with caution. As aptly concluded by Safe (1998c), TEFs/TEQs for HAHs must be used very selectively, and more research on the utility, applications, and limitations of this method should be conducted.

2. *Using uncertainty analyses, evaluate the potential impacts of leverage variables on the PBPK model, and accordingly the results of a health assessment involving these variables.*

Results of the uncertainty analyses conducted on the steady-state PBPK model for the Sprague-Dawley rat provided some very interesting indications of the key leverage variables, and the relative dose-dependencies involved. At low doses, general physiological parameters (*i.e.*, body weight, biliary excretion rate) and compartment-specific equilibrium ratios play the most significant role in TCDD disposition. However, as the exposure dose increases (*i.e.*, above the 0.1 μg/kg bodyweight level), ligand-receptor pharmacodynamics appear to become the dominant factor, with binding kinetic parameters providing the largest leverage on the model outcome. At the lower doses (*i.e.*, around the 0.316 μg/kg bodyweight dose level), the CYP1A2 binding kinetic parameters appear to play the largest role in model outcome. While at the more elevated doses (*i.e.*, around the 1 μg/kg bodyweight dose level), the contribution of Ah receptor binding parameters to overall variance in TCDD disposition has a dominant impact on model outcome. Finally, as the administered dose increases beyond the 3.16 μg/kg bodyweight dose level, the contribution to variance from ligand-receptor parameters returns to the levels observed at the very low doses (*i.e.*, ≤0.1 μg/kg bodyweight), while the parameters related to compartmental permeability, as well as TCDD absorption and elimination, become the key leverage variables in the pattern of TCDD whole-body disposition.

This dose-dependent pattern of leverage parameter impacts on TCDD disposition is as expected based upon the research presented in this paper. At low doses, there are not sufficient levels of TCDD within the body to result in significant occupancy of the Ah receptors or CYP1A2 proteins. Furthermore, the levels of TCDD-Ah receptor complexes are too low to result in a significant induction of CYP1A2 protein levels. As such, TCDD disposition is controlled by tissue-specific equilibrium and permeability parameters related the lipophilicity of the compound, as well as relative rates of elimination *via* urinary and fecal/biliary excretion.

However, as the concentration of TCDD within the organism increases, the Ah receptor occupancy level increases leading to further induction of CYP1A2 protein within the liver. The binding to the Ah receptor and CYP1A2 protein results in sequestration of the TCDD within the

liver, dramatically impacting upon the whole-body disposition and elimination pattern. This hepatic sequestration results in CYP1A2 binding kinetic parameters (primarily the concentration resulting in half maximum induction folds) initially playing the largest role in TCDD disposition. It is important to remember that the Ah receptor is a constitutive high affinity, low-capacity receptor, while CYP1A2 are inducible, low-affinity, and high-capacity receptor proteins. As such, as the concentration of ligand increases, the Ah receptors become more saturated and result in significant induction of CYP1A2 protein in response. Thus, at concentrations approaching levels which result in saturation of available Ah receptor, ligand-Ah receptor binding kinetics become a dominant factor over those related to CYP1A2 sequestration.

Similar results were observed in sensitivity analyses conducted by Evans and Andersen (2000) on Sprague-Dawley rats. Their research indicated that, at elevated doses nearing 0.1 μg/kg bodyweight, the inflection point indicative of the major shift in liver-to-fat ratio was more related to characteristics of DNA binding/induction steps of the Ah receptor-DNA complex than by the CYP1A2 affinity of TCDD or concentrations of CYP1A2.

Finally, once the concentration of TCDD within the body reaches a sufficient level as to result in complete saturation of both the available Ah receptors and CYP1A2 protein pool, remaining free TCDD can no longer be sequestered within the liver and pharmacokinetic processes (primarily compartmental permeability and TCDD absorption and excretion rates) begin to dominate its disposition throughout the body (*i.e.*, disposition in the adipose tissue increases as the liver-to-fat ratio begins to fall).

Given the obvious importance of ligand-receptor pharmacodynamics on the dose-dependent nature of PCDD/F absorption, disposition, metabolism, and excretion, it is vital that any inherent uncertainty within these pharmacodynamic parameters be minimized. Results of the uncertainty/sensitivity analyses indicate that the pharmacodynamic parameters which have the greatest impact on PCDD/F disposition are: concentration to cause half of the maximum CYP1A2 induction folds; maximum CYP1A2 induction folds over the basal rate; Ah receptor binding capacity in each of the key compartments; CYP1A2 physiological delay time, and; the Hill coefficient (see Tables 5.13 and 5.14). Unfortunately, these parameters are also the most

difficult to characterize, not only on a chemical-specific basis, but particularly on a species-specific basis. While QSAR research provides significant promise in bridging these data gaps, a considerable amount of research is still required to better characterize the uncertainty inherent within these key leverage variables.

3. Discuss the value of the results of the research as well as future empirical research needs.

Based upon a limited set of validation exercises, it appears that the current research has successfully developed an integrated PBPK model system for evaluating the absorption, disposition, metabolism, and excretion of key PCDD/F congeners (*i.e.*, TCDD, TCDF, 1-PeCDF, and 4-PeCDF) in three separate test organisms (*i.e.*, the Sprague-Dawley rat, the C57BL/6J mouse, and the Gapper's red-backed vole). As a result of the research, significant differences in tissue-specific disposition of key congeners (*i.e.*, TCDD and 4-PeCDF) has been noted between the laboratory rat and the vole. These differences have significant implications for the application of congener-specific TEF values, and the overall predicted toxicity (on a TCDD-TEQ equivalency basis) to the vole population evaluated as part of an ongoing environmental risk assessment process.

As noted previously, there are a number of uncertainties and conservative assumptions inherent within the development of the current PBPK modelling system, especially as it pertains to the red-backed vole. In addition to the relative strengths and weaknesses of the selected PBPK model discussed previously, other areas of uncertainty include:

- Due to the limited data set on which the model was developed, the appropriateness and accuracy of the model predictions at very low and very high doses has not been validated.
- Due to a lack of species-specific data, many of the pharmacokinetic and pharmacodynamic parameters used for the red-backed vole were based upon those used for the C57BL/6J mouse (based upon similar size and body composition). Given the lack of time-series congener-specific data for vole, it is difficult to determine whether these parameter selections are appropriate or not.
- Differences in pharmacokinetic disposition due to the chemical-specific lipophilicity were incorporated into the model by using a lipophilicity adjustment factor calculated for each congener based upon the ratio of its octanol-water partition coefficient (K_{ow}) to that of TCDD. While likely an acceptable measure of variability in tissue-to-blood equilibrium ratios, more accurate data can be easily gathered through simple tissue-based assays.

- Based on the similarities in lipophilicity of the assessed congeners, the fraction of the total dose absorbed (K_{abs}) *via* the GI tract was assumed to be equal to that used for TCDD. While likely reasonable for these congeners, such an assumption would be highly inappropriate for the higher chlorinated congeners should they be assessed with the current model methodology (*i.e.*, research has demonstrated that very little of the OCDD and OCDF congeners is absorbed through the gut wall and is quickly excreted following an oral administration dose).
- Ah and CYP1A2 ligand-receptor binding affinities (K_D values) were estimated and modelled based upon their relative differences to the TCDD base ligand. Due to the lack of suitable chemical- and species-specific pharmacodynamic data, this is likely the largest source of uncertainty in the current model methodology.
- Congener-specific metabolism (specifically CYP1A1 modulated) was included as part of the overall urinary and biliary/fecal excretion rates, and excretion half-lives were used to calculate chemical-specific excretion rate adjustment factors. Depending on the administered dose and treatment scenario, excretion half-lives can vary dramatically from study to study and species to species.

Results of the model-based uncertainty/sensitivity analyses indicates that one would get the most "bang for your buck" by investing resources into gathering more detailed pharmacodynamic information related to Ah and CYP1A2 ligand-receptor interactions (*i.e.*, concentration to cause half of the maximum CYP1A2 induction folds; maximum CYP1A2 induction folds over the basal induction rate; Ah receptor binding capacity in each of the key compartments; CYP1A2 physiological delay time, and the Hill coefficient). As indicated previously, these parameters are also the most difficult to characterize, not only on a chemical-specific basis, but particularly on a species-specific basis. While QSAR research provides significant promise in bridging these data gaps, a considerable amount of research is still required to better characterize the uncertainty inherent within these key leverage variables.

On important issue for resolution in future research is the conversion of the model basis to allow for a better approximation of whole body concentrations under chronic dosing conditions. The current model is designed based upon an initial acute oral bolus exposure to a particular

congener, and appears to be able to effectively predict short-term whole body concentrations when faced with sudden elevated ambient PCDD/F levels (*i.e.*, immediately following a release incident). However, the model is less successful in predicting body loads when the vole is chronically exposed to low levels of PCDD/Fs, particularly when assessing the more bioaccumulative congeners (*i.e.*, TCDD, 4-PeCDF, and some HxCDFs). This discrepancy is obvious when one compares modelled vole-to-plant BAF values to those estimated based upon environmental sampling (see Tables 5.28 and 5.29). Given their much longer metabolic/excretion half-lives, elevated concentrations of the bioaccumulative congeners would concentrate in the liver and adipose tissue over time. While short-term levels may not be sufficiently elevated as to result in a threshold-based toxic outcome, bioaccumulation of these congeners may result in significant toxicological impacts in the longer term. Unfortunately, the version of the PBPK model used in the current research is unable to assist in the assessment of these risks.

7.0 CONCLUSIONS

Exposure concentrations of contaminants found in air, water, soil, dust, food, or other environmental media to which populations are in contact are typically the dose scales most commonly used when evaluating potential health effects for environmental or occupational pollutants. However, research has indicated that external exposure is often only a rough approximation for the overall internal exposure delivered at the critical target sites in the body. This discrepancy can have significant implications on the overall toxicity manifested based upon a given environmental concentration and exposure scenario.

Pharmacokinetic models have been shown to provide the much needed functional relationship between external measures of chemical exposure and internal, target tissue measures of exposure to the actual toxic moiety. Accordingly, physiologically based pharmacokinetic modelling has become a scientifically attractive method of conducting this aspect of toxicological risk assessment. A number of recent toxicological evaluations (*e.g.*, arsenic, trichloroethylene, benzene, *etc.*), conducted by the U.S. EPA, have incorporated PBPK modelling in its decision making process. This methodology has been shown to be particularly appropriate for the evaluation of the potential impacts that pharmacokinetics and pharmacodynamics may have on the ultimate toxicity of persistent organic pollutants, such as dioxins and furans.

Around midday on July 10th, 1976, an explosion occurred in a 2,4,5-trichlorophenol reactor of the ICMESA chemical plant on the outskirts of Meda, a small town about 20 kilometres north of Milan, Italy. A toxic cloud containing TCDD and other related compounds was accidentally released into the atmosphere. The "dioxin" cloud contaminated a densely populated area about six kilometres long and one kilometre wide, lying downwind from the site. This event became internationally known as the Seveso disaster, after the name of a neighbouring municipality that was most severely affected. The Seveso accident, in addition to the outcry arising from the U.S. military's use of dioxin-contaminated Agent Orange during the Vietnam war, triggered a rarely precedented global surge of interest in one single class of chemical substances, the polyhalogenated dibenzo-p-dioxins and dibenzofurans. One member of this group of several

hundred individual compounds, TCDD, suddenly became the focus of media attention and in the ensuing years dominated the public debate all over the world.

This public interest and scrutiny has resulted in a considerable amount of research into the dispersion, deposition, and bioaccumulation of these compounds in the environment. Unfortunately, the history of PBPK modelling use by regulatory agencies, such as the U.S. EPA, is a rather checkered one. In April 1991, EPA announced that it would undertake a reassessment of the risks of exposure to dioxin. When released in draft form in 1994 (U.S. EPA, 1994), most of the chapters in the reassessment had been appropriately reviewed at peer review workshops. Strangely, Chapter 9 - "Risk Characterization of 2,3,7,8-Tetrachlorodibenzo-*p*-dioxin (TCDD) and Related Compounds" was not subjected to early peer review and did not appear to have the significant involvement of anyone in the scientific community outside the EPA. In particular, a group of well-known dioxin researchers stated that "[t]he conclusions in the EPA's current risk characterization are thus heavily dependent upon many unproven assumptions and untested hypotheses that deserve careful scrutiny by the scientific community" (Conolly, 1994). In response to the criticisms put forward by the EPA's own Science Advisory Board (SAB), public comments, and newly available scientific information EPA has been working to revise and update the 1994 draft, and recently issued a revised draft document (U.S. EPA, 2000) which provides a more complete review of the current state of scientific knowledge surrounding the pharmacokinetics and pharmacodynamics of dioxin.

In an effort to provide an on-going assessment of the potential environmental impacts related to the inadvertent release of these anthropogenic compounds, regulatory agencies (in response to public concern) have also mandated that extensive long-term monitoring programs be typically undertaken, as part of the facility approval and operation licence. These programs endeavour to monitor and assess emission releases, as well as measure ambient environmental concentrations in a variety of key sentinel biota species (*e.g.*, red-backed voles, Labrador tea, moss, *etc.*), to provide a better indication of the current and future human and ecological health risks related to facility emissions.

While emission release and dispersion kinetics play a significant role in the ultimate congener-specific fingerprint observed in environmental biota, as discussed previously, pharmacokinetics can have considerable impact on congener-specific disposition, metabolism and excretion rates. Alteration of the disposition and elimination behaviour of a particular congener can have particularly significant implications on tissue-specific sequestration. Given the importance of these congener-specific differences on the overall toxicity observed in a variety of species, it is vital that a reasonably accurate model of the congener-specific pharmacokinetic and pharmacodynamic processes be developed to better characterize the toxicodynamic properties of the compound. This would also allow for a truer evaluation of the appropriateness of the congener-specific TEF values used as part of the toxicological risk assessment process, on a species-specific basis.

Results of the current application of the PBPK model developed using laboratory rodents for use with the vole sentinel species has indicated that this model methodology appears to provide a reasonable estimation of chemical-specific disposition and elimination patterns within the vole sentinel species, at least under short-term acute exposure scenarios. Accordingly, it appears that the vole is a useful and relevant sentinel species to evaluate the pharmacokinetic and pharmacodynamic issues surrounding the environmental impacts of PCDD/Fs released as a result of anthropogenic activities. PBPK model systems, such as the one developed based upon the Wang *et al.* (1997) methodology, may provide valuable tools for evaluating data from long-term environmental monitoring programs, such as that in place at the Swan Hills Treatment Centre.

However, the current PBPK modelling systems still have a considerable amount of inherent uncertainty associated with the parameter and methodological assumptions. Research is continuing to attempt to provide a better comprehension of the intricate ligand-receptor mechanisms at play within hepatic and extrahepatic tissues, particularly at the P450 isozyme molecular level. While great strides forward have been taken in the past decade, it is only through further detailed research into the pharmacokinetic and pharmacodynamic properties of these compounds, will a more accurate and precise understanding of the disposition and ultimate toxicity of these intriguing persistent organic pollutants be achieved.

8.0 REFERENCES

Aarons, L., Clewell, H.J., Conolly, R.B., Delic, J.L., Houston, J.B., Jarabek, A.M., Loizou, G., Mason, H.J., Nestorov, I., Rowland, M., Tran, C-L., and G.T. Tucker. 1999. Physiologically-based pharmacokinetic modelling: A potential tool for use in risk assessment. Government/Research Councils Initiative on Risk Assessment and Toxicology. University of Leicester: Institute for Environmental and Health. ISBN 1899110259.

Acharya, P., Decicco, S.G., and R.G. Novak. 1991. Factors that can influence and control the emissions of dioxins and furans from hazardous waste incinerators. J. Air. Waste Manage. Assoc. 41:1605-1615.

AGRA. 1997. Draft Soil and Vegetation Monitoring Study. Swan Hills Treatment Centre 1997. Submitted to Bovar Waste Managment Ltd. AGRA Earth & Environmental Limited. Calgary, Alberta.

Alexander, D.L., Zhang, L., Foroozesh, M., Alworth, W.L., and C.R. Jefcoate. 1999. Metabolism-Based Polycyclic Aromatic Acetylene Inhibition of CYP1B1 in 10T1/2 Cells Potentiates Aryl Hydrocarbon Receptor Activity. Toxicol. Appl. Pharmacol. 161:123-139.

Allen, J.R., Van Miller, J.P. and D.H. Norback. 1975. Tissue distribution, excretion and biological effects of [^{14}C]tetrachlorodibenzo-*p*-dioxin in rats. Food. Cosmet. Toxicol. 13:501-505. Cited in: Wang *et al.*, 1997a.

Andersen, M.E., Birnbaum, L.S., Barton, H.A. and C.R Eklund. 1997a. Regional Hepatic CYP1A1 and CYP1A2 Induction with 2,3,7,8-Tetrachlorodibenzo-*p*-dioxin Evaluated with a Multicompartment Geometric Model of Hepatic Zonation. Toxicol. Appl. Pharmacol. 144:145-155.

Andersen, M.E., Mills, J.J., Gargas, M.L., Kedderis, L., Birnbaum, L.S., Neubert, D., and W.F. Greenlee. 1993. Modeling Receptor-Mediated Processes with Dioxin: Implications for Pharmacokinetics and Risk Assessment. Risk Analysis 13(1):25-36.

Andersen, M.E. 1995. Physiologically based pharmacokinetic (PB-PK) models in the study of the disposition and biological effects of xenobiotics and drugs. Toxicology Letters 82/83:341-348.

Andersen, M.E. 1994. Physiologically-Based Pharmacokinetic Modeling. Drug Information Journal 28:247-254.

Angove, K., and B. Bancroft. 1983. A Guide to Some Common Plants of the Southern Interior of British Columbia. B.C. Ministry of Forests. H28-82057.

Bailer, A.J. and D.A. Dankovic. 1997. An introduction to the use of physiologically based pharmacokinetic models in risk assessment. Stat Methods Med Res 6(4):341-58.

Ballenger, L. 1996. Species account narrative of *Clethrionomys gapperi*. Animal Diversity Web, University of Michigan. http://animaldiversity.ummz.umich.edu/.

Bernillon, P. and F.Y. Bois. 2000. Statistical Issues in Toxicokinetic Modeling: A Bayesian Perspective. Environ Health Perspect 108(Suppl. 5):883-893.

Birnbaum, L.S. 1999. TEFs: A Practical Approach to a Real-World Problem. Human and Ecological Risk Assessment: 5(1):13-24.

Birnbaum, L.S. 1994. The mechanism of dioxin toxicity: Relationship to risk assessment. Environ. Health Perspect. 102(Suppl. 9):157-167.

Birnbaum, L.S. 1986. Distribution and excretion of 2,3,7,8-tetrachlorodibenzo-*p*-dioxin in congenic strains of mice which differ at the Ah locus. Drug Metab. Disp. 14:34-40.

Birnbaum, L.S., Decad, G.M., and H.B. Matthews. 1980. Disposition and excretion of 2,3,7,8-tetrachlorodibenzofuran in the rat. Toxicol. Appl. Pharmacol 55:342-351. Cited in: Wang *et al.*, 1997a.

Birnbaum, L.S. and M.J. DeVito. 1995. Use of toxic equivalency factors for risk assessment for dioxin and related compounds. Toxicology 105:391-401.

Boddington, M. 1988. Final plenary session - Risk management considerations. Dioxin '87, Las Vegas, U.S. In *Guiding Principles for the Development of Multi Media Standards for Dioxins*. Draft document produced by Health and Welfare Canada and the Ontario Ministry of the Environment.

Borlakoglu, J.T. and K.D. Haeglele. 1991. Comparative aspects of bioaccumulation, metabolism, and toxicity with PCBs. Comp. Biochem. Physiol. 100(3):327-338.

Brewster, D.W. and L.S. Birnbaum. 1987. Disposition and Excretion of 2,3,4,7,8-Pentachlorodibenzofuran in the Rat. Toxicol Appl Pharmacol 90:243-252.

Brown, R.P., Delp, M.D., Lindstedt, S.L., Rhomberg, L.R., and R.P. Beliles. 1997. Physiological Parameter Values for Physiologically Based Pharmacokinetic Models. Toxicol Indust Health 13(4):407-484.

Brown, M.M., McCready, T.L., and N.J. Bunce. 1992. Factors affecting the toxicity of dioxin-like toxicants: a molecular approach to risk assessment of dioxins. Toxicology Letters 61:141-147.

Buckley, L.A. 1995. Biologically-based Models of Dioxin Pharmacokinetics. Toxicology 102:125-131.

Bunce, N.J. 1997. Is there a regulatory role for mechanism-based bioassays? Chemosphere 34(5-7):1481-1486.

Burt, W.H. and R.P. Grossenheider. 1976. The Peterson Field Guide Series: A Field Guide to the Mammals. Peterson, R.A. (Ed.) Boston: Houghton Mifflin Company.

CanTox Inc. 1998. Accidental Release of PCBs, Dioxins and Furans from the Swan Hills Treatment Centre: Ecological Impacts and Human Health Risks. Preliminary Draft. March 20, 1998. Prepared for BOVAR Waste Management Ltd.

Carrier, G., Brunet, R.C., and J. Brodeur. 1995. Modeling of the toxicokinetics of polychlorinated dibenzo-*p*-dioxins and dibenzofurans in mammalians, including humans: I. Nonlinear distribution of PCDD/PCDF body burden between liver and adipose tissues. Toxicol Appl Pharmacol 131:253-266.

CEPA. 1990. Priority Substance List Assessment Report No. 1: Polychlorinated Dibenzodioxins and Polychlorinated Dibenzofurans. Canadian Environmental Protection Act (CEPA). Ministry of Supply and Services Canada. Beauregard Printers Ltd. ISBN 0-662-17644-8. DSS Cat. En40-215/1E.

Chem-Security (Alberta) Ltd. 1999. Annual Assessment Report of the ongoing SHTC Environmental Monitoring Study. April 29, 1999.

Chem-Security (Alberta) Ltd. 1991. Environmental Impact Assessment for Proposed Expansion of the Alberta Special Waste Treatment Centre. Volume II: Main Report. June 1991.

Clewell III, H.J., Lee, T-S., and R.L. Carpenter. 1994. Sensitivity of Physiologically Based Pharmacokinetic Models to Variation in Model Parameters: Methylene Chloride. Risk Analysis 14(4):521-531.

Clewell III, H.J. 1995. The application of physiologically based pharmacokinetic modeling in human health risk assessment of hazardous substances. Toxicology Letters 79:207-217.

Conolly, R.B. 1994. U.S. EPA Reassessment of the Health Risks of 2,3,7,8-Tetrachlorodibenzo-*p*-dioxin (TCDD). CIIT Activities 14(12):1-9. Chemical Industry Institute of Toxicology (CIIT). December 1994.

Czuczwa, J.M. and R.A. Hites. 1985. Dioxins and dibenzofurans in air, soil and water. In: Kamrin, M.A. and P.W. Rodgers (Eds). *Dioxins in the Environment*. Washington, D.C.: Hemisphere Publications.

Dark, J. and I. Zucker. 1986. Photoperiodic Regulation of Body Mass and Fat Reserves in the Meadow Vole. Physiology & Behavior 38:851-854.

Dayneka, N.L., Garg, V., and W.J. Jusko. 1993. Comparison of four basic models of indirect pharmacodynamic response. J. Dyn. Sys. Meas. Control Sept:255-258. Cited in: Wang *et al.*, 1997a.

Delzell, E., Doull, J., Giesy, J., Mackay, D., Munro, I., and G. Williams. 1994. Interpretive Review of the Potential Adverse Effects of Chlorinated Organic Chemicals on Human Health and the Environment.

DeVito, M.J., Ménache, M.G., Diliberto, J.J., Ross, D.G., and L.S. Birnbaum. 2000. Dose-Response Relationships for Induction of CYP1A2 and CYP1A2 Enzyme Activity in Liver, Lung, and Skin in Female Mice Following Subchronic Exposure to Polychlorinated Biphenyls. Toxicol Appl Pharmacol 167:157-172.

DeVito, M.J., Ross, D.G., Dupuy Jr., A.E., Ferrario, J., McDaniel, D. and L.S. Birnbaum. 1998. Dose-Response Relationships for Disposition and Hepatic Sequestration of Polyhalogenated Dibenzo-*p*-dioxins, Dibenzofurans, and Biphenyls Following Subchronic Treatment in Mice. Toxicological Sciences 46:223-234.

DeVito, M.J., Diliberto, J.J., Ross, D.G., Menache, M.G., and L.S. Birnbaum. 1997. Dose-Response Relationships for Polyhalogenated Dioxins and Dibenzofurans Following Subchronic Treatment in Mice. Toxicol Appl Pharmacol 147:267-280.

DeVito, M.J., Beebe, L.E., Menache, M., and L.S. Birnbaum. 1996. Relationship between CYP1A enzyme activities and protein levels in rats treated with 2,3,7,8-tetrachlorodibenzo-*p*-dioxin. J Toxicol Environ Health 47:379-394.

DeVito, M.J. and L.S. Birnbaum. 1995. The Importance of Pharmacokinetics in Determining the Relative Potency of 2,3,7,8-Tetrachlorodibenzo-*p*-dioxin and 2,3,7,8-Tetrachlorodibenzofuran. Fundam Appl Toxicol 24:145-148.

Diliberto, J.J., Burgin, D.E., and L.S. Birnbaum. 1999. Effects of CYP1A2 on disposition of 2,3,7,8-tetrachlorodibenzo-*p*-dioxin, 2,3,4,7,8-pentachlorodibenzofuran, and 2,2',4,4',5,5'-hexachlorobiphenyl in CYP1A2 knock-out and parental (C57BL/6N and 129/Sv) strains of mice. Toxicol Appl Pharmacol 159:52-64.

Diliberto, J.J., Burgin, D., and L.S. Birnbaum. 1997. Role of CYP1A2 in hepatic sequestration of dioxin: Studies using CYP1A2 knockout mice. Biochem Biophys Res Comm 236:431-433.

Diliberto, J.J., Jackson, J.A. and L.S. Birnbaum. 1996. Comparison of 2,3,7,8-tetrachlorodibenzo-*p*-dioxin (TCDD) disposition following pulmonary, oral, dermal, and parenteral exposures to rats. Toxicol. Appl. Pharmacol. 138:1-11.

Douglas, G.W., Straley, G.B., and D. Meidinger. (Eds.) 1990. The Vascular Plants of British Columbia. Part 2 - Dicotyledons. B.C. Ministry of Forests. April 1990.

Eadon, G., Kaminsky, L., Silkworth, J., Aldous, K., Hilker, D., O'Keefe, P., Smith, R., Gierthy, J., Hawley, J., Kim, N. and A. DeCaprio. 1986. Calculation of 2,3,7,8-TCDD equivalent concentrations of complex environmental contaminant mixtures. Environ Health Perspect 70:221-227. Cited In: Van den Berg *et al.*, 1998.

eNature. 2001. eNature Field Guide: Southern Red-backed Vole (*Clethrionomys gapperi*). www.eNature.com.

Environment Canada. 1997a. Toxic Substances Management Policy: Polychlorinated Biphenyls.

Environment Canada. 1997b. Toxic Substances Management Policy: Polychlorinated Dibenzo-p-Dioxins and Polychlorinated Dibenzofurans.

Erwin, R.J. 2000. Photo of the Southern Red-backed Vole (*Clethrionomys gapperi*). http://www.enature.com/fotog/fotog_gallery.asp?fotogID=905.

Evans, M.V. and M.E. Andersen. 2000. Sensitivity Analysis of a Physiological Model for 2,3,7,8-Tetrachlorodibenzo-*p*-dioxin (TCDD): Assessing the Impact of Specific Model Parameters on Sequestration in Liver and Fat in the Rat. Toxicological Sciences 54:71-80.

Ferguson, G.M. 1999. Field Study of the Potential Impact of a Hazardous Waste Incinerator on Nearby Populations of Red-Backed Voles. University of Waterloo. Research Practicum (HLTH 741). March 25, 1999.

Ferguson, G.M. 1998. Use of Congener-Specific Chemical Fingerprints in the Environmental Health Risk Assessment of Releases from a PCB Incineration Facility. Masters thesis. University of Waterloo. Waterloo, Ontario.

Frederick, C.B. 1995. Summary of panel discussion on the 'advantages/limitations/uncertainties in the use of physiologically based pharmacokinetic and pharmacodynamic models in hazard identification and risk assessment of toxic substances'. Toxicology Letters 79:201-206.

Gasiewicz, T.A., Kende, A.S., Rucci, G., Whitney, B. and J.J. Willey. 1996. Analysis of Structural Requirements for Ah Receptor Antagonist Activity: Ellipticines, Flavones, and Related Compounds. Biochemical Pharmacology 52:1787-1803.

Gasiewicz, T.A. and G. Rucci. 1984. Cytosolic receptor for 2,3,7,8-tetrachlorodibenzo-*p*-dioxin evidence for a homologous nature among various mammalian species. Mol. Pharmacol. 26:90-98.

Gonzalez, F.J. 1988. The molecular biology of cytochrome P450s. Pharmacol Rev 40:232-288.

Haddad, S. and K. Krishnan. 1998. Physiological Modeling of Toxicokinetic Interactions: Implications for Mixture Risk Assessment. Environmental Health Perspectives 106(Supplement 6):1377-1384.

Hahn, M.E. 1998. The aryl hydrocarbon receptor: a comparative perspective. Comp Biochem Physiol C Pharmacol Toxicol Endocrinol 121(1-3):23-53.

Hahn, M.E., Poland, A., Glover, E., and J.J. Stegeman. 1994. Photoaffinity labeling of the Ah receptor: Phylogenetic survey of diverse vertebrate and invertebrate species. Arch Biochem Biophys 310:218-228.

Hall, E.R. 1981. The Mammals of North America. New York: John Wiley & Sons. p. 782.

Hankinson, O., Bacsi, S.G, Fukunaga, B.N., Kozak, K.R., McNulty, S.E., Minehart, E., Probst, M.R., Reisz-Porszasz, S., Sun, W. and J. Zhang. 1996. Role of the aryl hydrocarbon receptor in carcinogenesis. In: Hengstler, J.G and F. Oesch (Eds.) *Control Mechanisms of Carcinogenesis*. Druckerei Thieme, Mainz. Cited In: Hengstler *et al.*, 1999.

Henck, J.W., New, M.A., Kociba, R.J. and K.S. Rao. 1981. 2,3,7,8-Tetrachlorodibenzo-*p*-dioxin: Acute oral toxicity in hamsters. Toxicol Appl Pharmacol 59:405-407. Cited In: Delzell *et al.*, 1994.

Hengstler, J.G., Van Der Burg, B., Steinberg, P. and F. Oesch. 1999. Interspecies Differences in Cancer Susceptibility and Toxicity. Drug Metabolism Reviews 31(4):917-940.

Hestermann, E.V., Stegeman, J.J., and M.E. Hahn. 2000. Relative Contributions of Affinity and Intrinsic Efficacy to Aryl Hydrocarbon Receptor Ligand Potency. Toxicol Appl Pharmacol 168:160-172.

Hoffmeister, D.F. 1986. Mammals of Arizona. Tucson: University of Arizona Press. p. 432-3.

Hu, K. and N.J. Bunce. 1999. Metabolism of Polychlorinated Dibenzo-*p*-dioxins and Related Dioxin-Like Compounds. J. Toxicol. Environ. Health B 2:183-210.

Huff, J., Lucier, G., and A. Tritscher. 1994. Carcinogenicity of TCDD: experimental, mechanistic and epidemiologic evidence. Annu Rev Pharmacol Toxicol 34:343-72.

Hushka, L.J., Williams, J.S., and W.F. Greenlee. 1998. Characterization of 2,3,7,8-Tetrachlorodibenzofuran-Dependent Suppression and AH Receptor Pathway Gene Expression in the Developing Mouse Mammary Gland. Toxicol Appl Pharmacol 152:200-210.

ILSI. 1994. Physiological Parameter Values for PBPK Models. International Life Sciences Institute. U.S. EPA. Cited in: Wang *et al.*, 1997a.

Jackson, J.A., Birnbaum, L.S., and J.J. Diliberto. 1998. Effects of Age, Sex, and Pharmacologic Agents on the Biliary Elimination of 2,3,7,8-Tetrachlorodibenzo-*p*-dioxin (TCDD) in F344 Rats. Drug Metab Dispos 26(7): 714-719.

Kazlauskas, A., Poellinger, L., and I. Pongratz. 1999. Evidence that the co-chaperone p23 regulates ligand responsiveness of the dioxin (aryl hydrocarbon) receptor. J Biol Chem 274:13519-13524.

Kedderis, L.B., Diliberto, J.J. and L.S. Birnbaum. 1991. Disposition and excretion of intravenous 2,3,7,8-tetrabromodibenzo-*p*-dioxin in rats. Toxicol. Appl. Pharmacol 108:397-406.

King, F.G., Dedrick, R.L., Collins, J.M., Matthews, H.B. and L.S. Birnbaum. 1983. Physiological Model for the Pharmacokinetics of 2,3,7,8-Tetrachlorodibenzofuran in Several Species. Toxicol Appl Pharmacol 67:390-400.

Klaassen, C.D. and D.L. Eaton. 1991. Principles of Toxicology. In: Klaassen, C.D., Amdur, M.O., and J. Doull (Eds.). Casarett and Doull's Toxicology, the Basic Science of Poisons. Fourth Edition. New York: Pergamon Press.

Klaassen, C.D. and K. Rozman. 1991. Absorption, Distribution, and Excretion of Toxicants. In: Klaassen, C.D., Amdur, M.O., and J. Doull (Eds.). Casarett and Doull's Toxicology, the Basic Science of Poisons. Fourth Edition. New York: Pergamon Press.

Klinge, C.M., Kaur, K. and H.I. Swanson. 2000. The Aryl Hydrocarbon Receptor Interacts with Estrogen Receptor Alpha and Orphan Receptors COUP-TFI and ERRα1. Archives of Biochemistry and Biophysics 373(1):163-174.

Kohn, M.C., Lucier, G.W., Clark, G.C., Sewall, C., Tritscher, A.M., and C.J. Portier. 1993. A Mechanistic Model of Effects of Dioxin on Gene Expression in the Rat Liver. Toxicol Appl Pharmacol 120:138-154.

Krewski, D., Wang, Y., Bartlett, S. and K. Krishnan. 1995. Uncertainty, Variability, and Sensitivity Analysis in Physiological Pharmacokinetic Models. Journal of Biopharmaceutical Statistics 5(3):245-271.

Krishnan, K. and M.E. Andersen. 1994. Physiologically-based pharmacokinetic modeling in toxicology. In: Hayes, W.A. (Ed.). *Principles and Methods of Toxicology, 3rd edition.* New York: Raven Press. pp. 149-188.

Kurta, A. 1995. Mammals of the Great Lakes Region. Michigan: The University of Michigan Press.

Lakshmanan, M.R., Campbell, B.S., Chirtel, S.J., Ekarohita, N., and M. Ezekiel. 1986. Studies on the mechanism of absorption and distribution of 2,3,7,8-tetrachlorodibenzo-*p*-dioxin in the rat. J Pharmacol Exp Ther 239:673-677.

Larsen, J.C. 1995. Levels of pollutants and their metabolites: exposures to organic substances. Toxicology 101:11-27.

Lauffenburg, D.A. and J.J. Lindermann. 1993. Receptors-Models for Binding, Trafficking and Signalling. Oxford Univ. Press, New York, NY. Cited in: Wang *et al.*, 1997a.

Lee, C.C., and G.L. Huffman. 1990. Minimization of Combustion By-Products: Characteristics of Hazardous Waste. (U.S.) EPA, Cincinnati, OH. PB91-162396.

Lee, D. C., Barlow, K. D., and K.W. Gaido. 1996. The actions of 2,3,7,8-tetrachlorodibenzo-p-dioxin on transforming growth factor-beta2 promoter activity are localized to the TATA box binding region and controlled through a tyrosine kinase-dependent pathway. Toxicol Appl Pharmacol 137:90-9.

Leung, H-W. and D.J. Paustenbach. 1995. Physiologically based pharmacokinetic and pharmacodynamic modeling in health risk assessment and characterization of hazardous substances. Toxicology Letters 79:55-65.

Leung, H-W. 1993. Physiologically-Based Pharmacokinetic Modelling. In: Ballantyne, B., Marrs, T., and P. Turner (Eds.) *General & Applied Toxicology: Volume I.* New York: Stockton Press.

Leung, H.W., Paustenbach, D.J., Murray, F.J. and M.E. Andersen. 1990a. A physiological pharmacokinetic description of the tissue distribution and enzyme-inducing properties of 2,3,7,8-tetrachlorodibenzo-*p*-dioxin in the rat. Toxicol. Appl. Pharmacol. 102:399-410.

Leung, H.W., Poland, A., Paustenbach, D.J., Murray, F.J., and Andersen, M.E. 1990b. Pharmacokinetics of [^{125}I]-2-iodo,3,7,8-trichlorodibenzo-*p*-dioxin mice: Analysis with a physiological modeling approach. Fundam. Appl. Toxicol. 27:70-76.

Leung, H.W., Ku, R.H., Paustenbach, D.J., and M.E. Andersen. 1988. A physiological-based pharmacokinetic model for 2,3,7,8-tetrachlorodibenzo-*p*-dioxin in C57BL/6J and DBA/2J mice. Toxicol. Lett. 42:15-28.

Li, X., Weber, L.W. and K.K. Rozman. 1995. Toxicokinetics of 2,3,7,8-tetrachlorodibenzo-p-dioxin in female Sprague- Dawley rats including placental and lactational transfer to fetuses and neonates. Fundam Appl Toxicol 27:70-6.

Lin, J.H. 1998. Applications and Limitations of Interspecies Scaling and *In vitro* Extrapolation in Pharmacokinetics. Drug Metabolism and Disposition 26(12):1202-1212.

Lioy, P.J. 1995. Measurement methods for human exposure analysis. Environmental Health Perspectives 103(Suppl 3):35-44.

Lucier, G.W., Portier, C.J., and M.A. Gallo. 1993. Receptor Mechanisms and Dose-Response Models for the Effects of Dioxins. Environ Health Perspect 101(1):36-44.

Mahanty, H.K. 1990. Polychlorinated biphenyls: Accumulation and effect on plants. In: Waid, J.S. (ed.). PCBs and the Environment, Volume II. CRC Press. Boston. Cited In: AGRA, 1997.

Mallory, F.F. 2001. Database of Red-backed vole sampling data. Department of Biology, Laurentian University. *Confidential.* Contact: fmallory@nickel.laurentian.ca.

Martin, M.H., and P.J. Coughtrey. 1982. Biological monitoring of heavy metal pollution. Applied Science Publishers. London and New York. Cited In: AGRA, 1997.

Mason, H. and K. Wilson. 1999. Biological Monitoring: The Role of Toxicokinetics and Physiologically Based Pharmacokinetic Modeling. AIHA Journal 60:237-242.

McConnell, E.E., Moore, J.A., Jaseman, J.K. and M.W. Harris. 1978. The comparative toxicity of chlorinated dibenzo-*p*-dioxins in mice and guinea pigs. Toxicol Appl Pharmacol 44:335-356. Cited In: Delzell *et al.*, 1994.

McManus, J.J. 1974. Bioenergetics and Water Requirements of the Redback Vole, *Clethrionomys gapperi*. J Mammal 55(1):30-44.

Micka, J., Milatovich, A., Menon, A., Grabowski, G.A., Puga, A., and D.W. Nebert. 1997. Human Ah receptor (AHR) gene: Localization to 7p15 and suggestive correlation of polymorphism with CYP1A1 inducibility. Pharmacogenetics 7:95-101.

Morgan, M.G. and M. Henrion. 1990. Uncertainty: A guide to dealing with uncertainty in quantitative risk and policy analysis. New York: Cambridge University Press.

Nerurkar, P.V., Park, S.S., Thomas, P.E., Nims, R.W. and R.A. Lubet. 1993. Methoxyresorufin and benzyloxyresorufin: Substrates preferentially metabolized by cytochromes P4501A2 and 2B, respectively, in the rat and mouse. Biochemical Pharmacology 46(5):933-943.

Nims, R.W. and R.A. Lubet. 1995. Induction of cytochrome P-450 in the norway rat, *Rattus norvegicus*, following exposure to potential environmental contaminants. J Toxicol Environ Health 46:271-292.

Nowak, R.M. and J.L. Paradiso. 1983. Walker's Mammals of the Word. Fourth Edition. Baltimore, Maryland: John Hopkin University Press.

NRC. 1989. Biologic Markers in Reproductive Toxicology. National Research Council (NRC). Washington, DC: National Academy Press.

Okey, A.B., Giannone, J.V., Smart, W., Wong, J.M., Manchester, D.K. *et al.* 1997. Binding of 2,3,7,8-tetrachlorodibenzo-p-dioxin to AH receptor in placentas from normal versus abnormal pregnancy outcomes. Chemosphere 34:1535-47.

Olson, J.R., McGarrigle, B.P., Gigliotti, P.J., Kumor, S. and J.H. McReynolds. 1994. Hepatic Uptake and Metabolism of 2,3,7,8-Tetrachlorodibenzo-*p*-dioxin and 2,3,7,8-Tetrachlorodibenzofuran. Fund. Appl. Toxicol. 22:631-640.

Olson, J.R., Holscher, M.A. and R.A. Neal. 1980. Toxicity of 2,3,7,8-tetrachlorodibenzo-*p*-dioxin in the golden syrian hamster. Toxicol Appl Pharmacol 55:67-78. Cited In: Delzell *et al.*, 1994.

Pegram, R.A., Diliberto, J.J., Moore, T.C., Gao, P. and L.S. Birnbaum. 1995. 2,3,7,8-Tetrachlorodibenzo-*p*-dioxin (TCDD) distribution and cytochrome P4501A induction in young adult and senescent male mice. Toxicology Letters 76:119-126.

Penner, D.F. 1994. Alberta Special Waste Treatment Centre, Environmental Monitoring Program Annual Report: 1993 monitoring, Section 4: Wildlife. Prepared by Penner and Associates Ltd. for Chem-Security (Alberta) Ltd.

Poellinger, L. 2000. Mechanistic aspects - the dioxin (aryl hydrocarbon) receptor. Food Additives and Contaminants 17:261-266.

Pohjanvirta, R. and J. Tuomisto. 1994. Short-term toxicity of 2,3,7,8-tetrachlorodibenzo-*p*-dioxin in laboratory animals: Effects, mechanisms, and animal models. Pharmacol Rev 46:483-549.

Pohjanvirta, R., Unkila, M., Lindén, J., Tuomisto, J.T., and J. Tuomisto. 1995. Toxic equivalency factors do not predict the acute toxicities of dioxins in rats. Eur J Pharmacol 293:341-353.

Poland, A. and E. Glover. 1990. Characterization and strain distribution pattern of murine Ah receptor specified by the Ah^d and Ah^{b-3} alleles. Mol Pharmacol 38:306-12.

Poland, A., Glover, E., and B.A. Taylor. 1987. The murine Ah locus: a new allele and mapping to chromosome 12. Mol Pharmacol 32:471-78.

Poland, A., Palen, D., and E. Glover. 1994. Analysis of the four alleles of the murine aryl hydrocarbon receptor. Mol Pharmacol 46:915-921.

Portier, C., Tritscher, A., Kohn, M., Sewall, C., Clark, G., Edler, L., Hoel, D. and G. Lucier. 1993. Ligand/Receptor Binding for 2,3,7,8-TCDD: Implications for Risk Assessment. Fund. Appl. Toxicol 20:48-56.

Rappe, C., Anderson, R., Bergqvist, P.A., Brohede, C., Hansson, M., Kjeller, L.O., Lindstron, G., Marklund, S., Nygren, M., Swanson, S.E., Tysklind, M., and K. Wiberg. 1987. Overview of environmental fate of chlorinated dioxins and dibenzofurans. Sources, levels and isomeric patterns in various matrices. Chemosphere 16:1603.

Rhodes, C., Thomas, M. and J. Athis. 1993. Principles of Testing for Acute Toxic Effects. In: Ballantyne, B., Marrs, T., and P. Turner (Eds.). *General & Applied Toxicology: Volume 1*. New York: The Macmillan Press Limited.

Rose, J.Q., Ramsey, J.C., Wentzler, T.H., Hummel, R.A. *et al.* 1976. The fate of 2,3,7,8-tetrachlorodibenzo-p-dioxin following single and repeated oral doses to the rat. Toxicol Appl Pharmacol 36:209-226.

Rosengren, R., Safe, S., and N.J. Bunce. 1992. Kinetics of the Association of Several Tritiated Polychlorinated Dibenzo-*p*-dioxin and Dibenzofuran Congeners with Hepatic Cytosolic Ah Receptor from the Wistar Rat. Chem Res Toxicol 5:376-382.

Roth, W.L., Weber, L.W.D., and K.K. Rozman. 1995. Incorporation of First-Order Uptake Rate Constants from Simple Mammillary Models into Blood-Flow Limited Physiological Pharmacokinetic Models via Extraction Efficiencies. Pharmaceutical Research 12(2):263-269.

Roth, W.L., Ernst, S., Weber, L.W.D., Kerecsen, L., and K.K. Rozman. 1994. A pharmacodynamically responsive model of 2,3,7,8-tetrachlorodibenzo-*p*-dioxin. Mol. Pharmacol. 49:391-398.

Roth, W.L., Freeman, R.A. and A.G.E. Wilson. 1993. A physiologically based model for gastrointestinal absorption and excretion of chemical carried by lipids. Risk Anal. 13:531-543.

Safe, S.H. 1998a. Development Validation and Problems with the Toxic Equivalency Factor Approach for Risk Assessment of Dioxins and Related Compounds. J Anim Sci 76:134-141.

Safe, S.H. 1998b. Limitations of the Toxic Equivalency Factor Approach for Risk Assessment of TCDD and Related Compounds. Teratogenesis, Carcinogenesis, and Mutagenesis 17:285-304.

Safe, S.H. 1998c. Hazard and Risk Assessment of Chemical Mixtures Using the Toxic Equivalency Factor Approach. Environ Health Persp 106(Suppl. 4):1051-1058.

Safe, S. 1994. Polychlorinated biphenyls (PCBs): Rnvironmental impact, biochemical and toxic responses, and implications for risk assessment. CRC Crit Rev Toxicol 24:87-149.

Safe, S. 1990. Polychlorinated biphenyls (PCBs), dibenzo-*p*-dioxins (PCDDs), dibenzofurans (PCDFs), and related compounds: Environmental and mechanistic considerations which support the development of toxic equivalency factors (TEFs). CRC Crit Rev Toxicol 21:51-88.

Safe, S.H. 1988. The aryl hydrocarbon (Ah) receptor. ISI Atlas Sci. 2:78-83.

Safe, S. 1986. Comparative toxicology and mechanism of action of polychlorinated dibenzo-*p*-dioxins and dibenzofurans. Annu. Rev. Pharamcol. Toxicol. 26:371-399.

Safe, S., Wang, F., Porter, W., Duan, R. and A. McDougal. 1998. Ah receptor agonists as endocrine disruptors: antiestrogenic activity and mechanisms. Toxicology Letters 103:343-347.

Santostefano, M., Liu, H., Wang, X., Chaloupka, K., and S. Safe. 1994. Effect of Ligand Structure on Formation and DNA Binding Properties of the Transformed Rat Cytosolic Aryl Hydrocarbon Receptor. Chem Res Toxicol 74:544-550.

Santostefano, M.J., Wang, X., Richardson, V.M., Ross, D.G., DeVito, M.J. and L.S. Birnbaum. 1998. A Pharmacodynamic Analysis of TCDD-Induced Cytochrome P450 Gene Expression in Multiple Tissues: Dose- and Time-Dependent Effects. Tox. Appl. Pharmacol. 151:294-310.

Santostefano, M., Piskorska-Pliszczynska, J., Morrison, V. and S. Safe. 1992. Effects of ligand structure on the in vitro transformation of the rat cytosolic aryl hydrocarbon receptor. Arch Biochem Biophys 297:73-9.

Schmidt, J.V. and C.A. Bradfield. 1996. Ah Receptor Signaling Pathways. Annu Rev Cell Dev Biol 12:55-89.

Schrenk, D., Lipp, H.P., Wiesmüller, T., Hagenmaier, H., and K.W. Bock. 1990. Assessment of biological activities of mixtures of polychlorinated dibenzo-p-dioxins: Comparison between defined mixtures and their constituents. Arch Toxicol 65:114-118. Cited In: Van den Berg *et al.*, 1998.

Schwetz, B.A., Norris, J.M., Sparschu, G.L., Rowe, V.K., Gehring, P.J., Emerson, J.L. and C.G. Gerbig. 1973. Toxicology of chlorinated dibenzo-*p*-dioxins. Environ Health Perspect 5:87-99. Cited In: Delzell *et al.*, 1994.

Sewall, C.H. and G.W. Lucier. 1995. Receptor-mediated events and the evaluation of the Environmental Protection Agency (EPA) of dioxin risks. Mutation Research 333:111-122.

Sloop, T.C. and G.W. Lucier. 1987. Dose-dependent elevation of Ah receptor binding by TCDD in rat liver. Toxicol Appl Pharmacol 88:329-337.

Smith, A.G., Clothier, B., Robinson, S., Scullion, M.J., Carthew, P., Edwards, R., Luo, J., Lim, C.K., and M. Toledano. 1998. Interaction between Iron Metabolism and 2,3,7,8-Tetrachlorodibenzo-*p*-dioxin in Mice with Variants of the Ahr Gene: A Hepatic Oxidative Mechanism. Molecular Pharmacology 53:52-61.

So, S-S. and M. Karplus. 1997. Three-Dimensional Quantitative Structure-Activity Relationships from Molecular Similarity Matrices and Genetic Neural Networks. 2. Applications. J Med Chem 40:4360-4371.

Swanson, H.I. and C.A. Bradfield. 1993. The AH-receptor: genetics, structure and function (Review). Pharmacogenetics 3:213-30.

Travis, C.C. and S.C. Cook. 1989. Hazardous Waste Incineration and Human Health. CRC Press. Boca Raton, Florida.

Tritscher, A.M., Goldstein, J.A., Portier, C.J., McCoy, Z., Clark, G.C. and G.W. Lucier. 1992. Dose-response relationships for chronic exposure to 2,3,7,8-tetrachlorodibenzo-*p*-dioxin in a rat tumor promotion model: Quantification and immunolocalization of CYP1A1 and CYP1A2 in the liver. Cancer Res. 52:3436-3442.

Tukey, R.H., Hannah, R.R., Negishe, M., Nebert, D.W. and H.J. Eisen. 1982. The Ah locus: Correlation of intranuclear appearance of inducer-receptor complex with induction of cytochrome P1-450 mRNA. Cell 31:275-284.

Tuppurainen, K. and J. Ruuskanen. 2000. Electronic eigenvalue (EEVA): a new QSAR./QSPR descriptor for electronic substituent effects based on molecular orbital energies. A QSAR approach to the Ah receptor binding affinity of polychlorinated biphenyls (PCBs), dibenzo-*p*-dioxins (PCDDs) and dibenzofurans (PCDFs). Chemosphere 412:843-848.

U.S. EPA. 2000. Exposure and Human Health Reassessment of 2,3,7,8-Tetrachlorodibenzo-*p*-Dioxin (TCDD) and Related Compounds. Office of Research and Development. U.S. Environmental Protection Agency. EPA/600/P-00/001Bb. September 2000.

U.S. EPA. 1997. Guiding Principles for Monte Carlo Analysis. Risk Assessment Forum. U.S. Environmental Protection Agency. EPA/630/R-97/001. March 1997.

U.S. EPA. 1994. Estimating Exposure to Dioxin-Like Compounds. Volume II: Properties, Sources, Occurrence and Background Exposures. U.S. Environmental Protection Agency. EPA/600/6-88/005Cb.

Van den Berg, M., Birnbaum, L., Bosveld, A.T.C., Brunström, B., Cook, P., Feeley, M., Giesy, J.P., Hanberg, A., Hasegawa, R., Kennedy, S.W., Kubiak, T., Larsen, J.C., van Leeuwen, F.X.R., Liem, A.K.D., Nolt, C., Peterson, R.E., Poellinger, L., Safe, S., Schrenk, D., Tillitt, D., Tysklind, M., Younes, M., Wærn, F., and T. Zacharewski. 1998. Toxic Equivalency Factors (TEFs) for PCBs, PCDDs, PCDFs for Humans and Wildlife. Environmental Health Perspectives 106(12):775-792.

Van den Berg, M., De Jongh, J., Poiger, H., and J.R. Olson. 1994. The toxicokinetics and metabolism of polychlorinated dibenzo-*p*-dioxins (PCDDs) and dibenzofurans (PCDFs) and their relevance for toxicity. CRC Critical Reviews in Toxicology 24:1-74.

Van de Berg, M., De Jongh, J., Eckhart, P., and F.W.M. Van der Wielen. 1989. Disposition and Elimination of Three Polychlorinated Dibenzofurans in the Liver of the Rat. Fund Appl Toxicol 12:738-747.

Waller, C.L. and J.D. McKinney. 1995. Three-Dimensional Quantitative Structure-Activity Relationships of Dioxins and Dioxin-like Compounds: Model Validation and Ah Receptor Characterization. Chem Res Toxicol 8:847-858.

Wang, X., Santostefano, M.J., DeVito, M.J., and L.S. Birnbaum. 2000. Extrapolation of a PBPK Model for Dioxins across Dosage Regimen, Gender, Strain, and Species. Toxicological Sciences 56:49-60.

Wang, X., Santostefano, M.J., Evans, M.V., Richardson, V.M., Diliberto, J.J., and L.S. Birnbaum. 1997a. Determination of Parameters Responsible for Pharmacokinetic Behavior of TCDD in Female Sprague-Dawley Rats. Toxicol. Appl. Pharmacol 147:151-168.

Wang, X., Santostefano, M.J., DeVito, M.J., and L.S. Birnbaum. 1997b. Extrapolation of a previous PBPK model for TCDD across routes of exposure, gender, and from rats to mice.

Weber, L.W.D., Ernst, S.W., Stahl, B.U. and K. Rozman. 1993. Tissue distribution and toxicokinetics of 2,3,7,8-tetrachlorodibenzo-*p*-dioxin in rats after intravenous injection. Fundam. Appl. Toxicol. 21:523-534.

Wen, Y.H., Kalff, J. and R.H. Peters. 1999. Pharamacokinetic modeling in toxicology: A critical perspective. Environ Rev 7:1-18.

Westworth Associates Environmental Ltd. Natural Resource Consultants. 1998. 1997 Mammal Monitoring Program. Prepared by Douglas L. Skinner. Edmonton, January 1998.

Westworth, Brusnyk & Associates Ltd. 1997. Alberta Special Waste Management Centre: Protocols for Wildlife Monitoring. Prepared for Chem-Security (Alberta) Ltd. May 1997.

WHO. 1993. Polychlorinated Biphenyls and Terphenyls (Second Edition): Environmental Health Criteria 140. World Health Organization. Geneva.

Woodruff, T.J., Bois, F.Y., Auslander, D. and R.C. Spear. 1992. Structure and parameterization of pharmacokinetic models: Their impact on model predictions. Risk Anal. 12(2):189-201.

Wormke, M., Stoner, M., Saville, B., and S. Safe. 2000. Crosstalk between estrogen receptor α and the aryl hydrocarbon receptor in breast cancer cells involves unidirectional activation of proteasomes. FEBS Letters 478:109-112.

Xu, L., Li, A.P., Kaminski, D.L., and M.F. Ruh. 2000. 2,3,7,8 Tetrachlorodibenzo-*p*-dioxin induction of cytochrome P4501A in cultured rat and human hepatocytes. Chemico-Biological Interactions 124:173-189.

Ziegler, D.M. 1991. Unique properties of the enzymes of detoxication. Drug Metab Dispos 19:847-852.

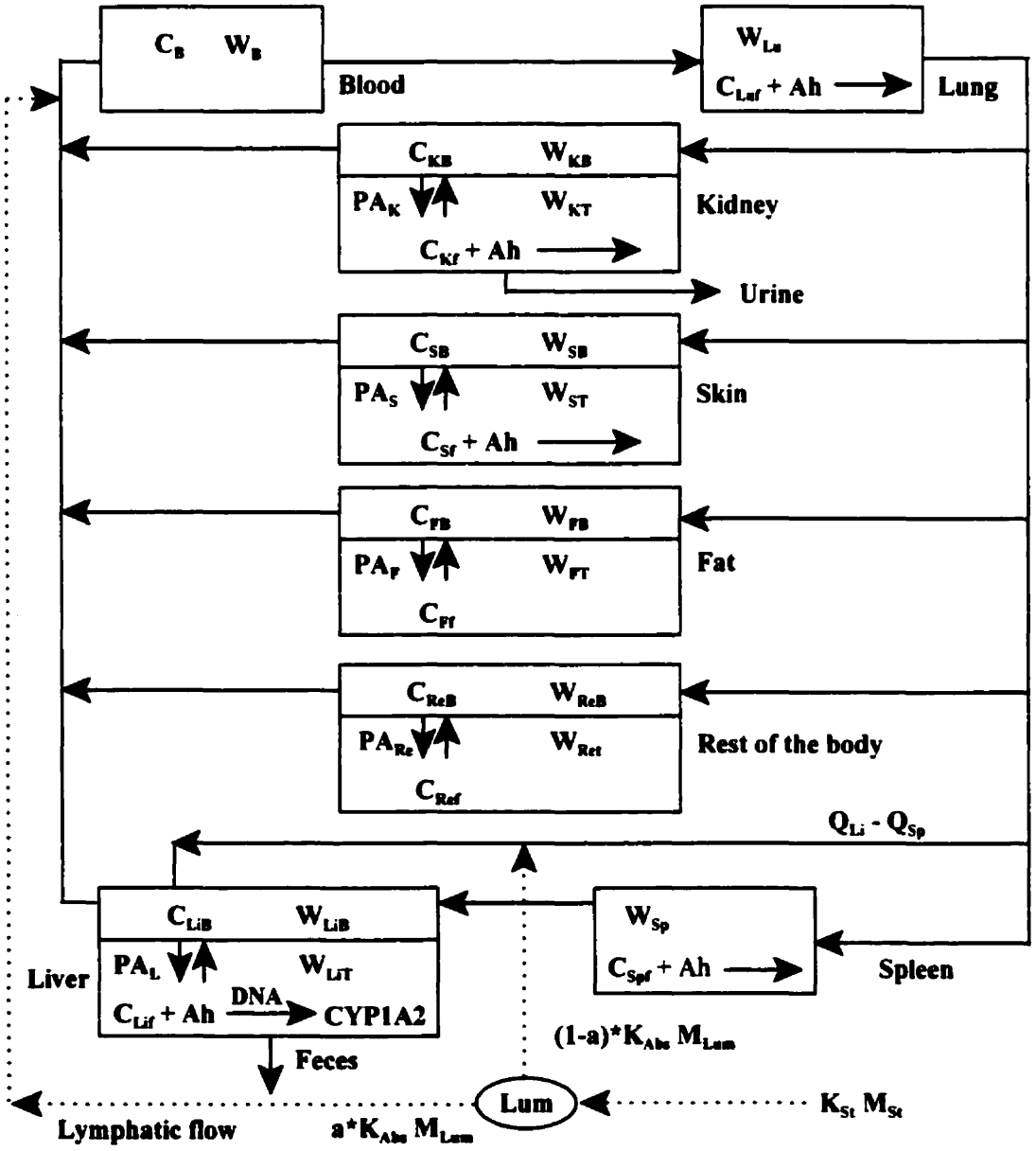
APPENDIX A

Detailed Overview of Mathematical Equations used in Prototype PBPK Models

A-1.0 Prototype Steady-State PBPK Model (Wang *et al.*, 1997)

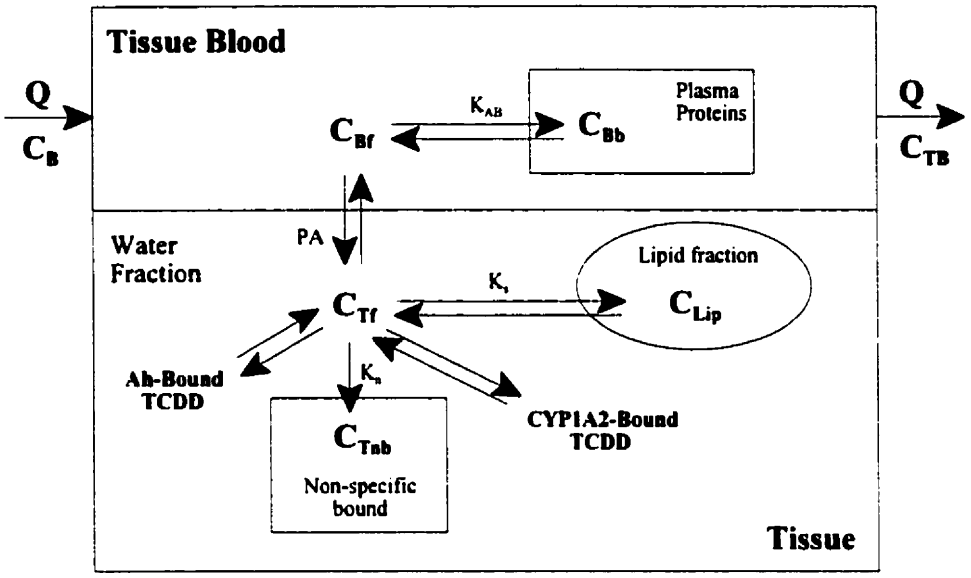
The following section provides the detailed mathematical equations used in the development of the prototype steady-steate PBPK model for the current research on PCDD/F pharmacokinetics. The model methodology is based upon the Wang *et al.* (1997) published model, with a considerable amount of information added (based upon other published source material) to fill in gaps in the methodology provided by the Wang *et al.* (1997) source paper.

Figure A-1 A schematic representation of the equilibrium TCDD PB-PK model (Wang *et al.*, 1997)



TCDD Distribution in a Generic Tissue Compartment

Figure A-2 TCDD Distribution in a Generic Tissue Compartment (Wang *et al.*, 1997)



The total concentration of TCDD in a typical intracellular domain can be simulated as:

$$C_T = f_w C_{Tf} + f_{Lip} C_{Lip} + f_{nb} C_{nb} + C_{sb1} + C_{sb2}$$

Where:

C_T	=	Total concentration of TCDD in the intracellular tissue (nmoles/g tissue)
C_{Tf}	=	Concentration of TCDD in the water fraction of the tissue (nmoles/g tissue)
C_{Lib}	=	Concentration of TCDD in the lipid fraction of the tissue (nmoles/g tissue)
C_{nb}	=	Concentration of TCDD non-specifically bound in the tissue (nmoles/g tissue)
C_{sb1}	=	Concentration of TCDD bound to resident Ah receptors (nmoles/g tissue)
C_{sb2}	=	Concentration of TCDD bound to resident CYP1A2 (nmoles/g tissue)
f_w	=	Water-filled volume fraction in the tissue compartment (unitless)
f_{Lip}	=	Lipid-filled volume fraction in the tissue compartment (unitless)
f_{nb}	=	Volume fraction of linear binding constituents in the tissue compartment (unitless)

The concentration of TCDD bound to proteins and other cellular constituents (C_{nb}) can be calculated as:

$$C_{nb} = K_n C_{Tf}$$

Where:

K_n = the linear binding constant for that tissue compartment (unitless)

Therefore, the concentration of TCDD non-specifically bound to proteins and other linear binding constituents of the tissue (*i.e.*, not bound to Ah receptors or CYP1A2 metabolic sites) can be represented as:

$$C_{t\,(specific\ bound)} = fw\ Ctf + fLip\ Ks\ CTf + fnb\ Kn\ CTf$$

Linear Binding of TCDD to Plasma Proteins

The total TCDD concentration in the blood entering this compartment can be expressed as:

$$C_B = f_{wb}\ C_{Bf} + (1 - f_{wb})\ C_{Bb}$$

Where:

C_B = Total TCDD concentration in the compartment blood supply (nmoles/g)
C_{Bf} = Free TCDD concentration in the compartment blood supply (nmoles/g)
C_{Bb} = Plasma-bound TCDD concentration in the compartment blood supply (nmoles/g)
f_{wb} = Water fraction of the compartment blood supply (unitless)

and,

$$C_{Bb} = K_{AB}\ C_{Bf}$$

Where:

K_{AB} = the linear binding constant of TCDD to plasma proteins.(unitless)

TOTAL BODY WEIGHT CHANGE

$$W_t = W_{t0}\left(1 + \frac{(a_0 \times t)}{(b_0 + t)}\right)$$

Where:

W_t	=	Body weight at time t (g)
W_{t0}	=	Body weight at time of exposure (g)
a_0	=	Body weight fitting parameter A (0.41)
b_0	=	Body weight fitting parameter B (1402.5)
t	=	Elapsed time following exposure (hours)

CALCULATION OF COMPARTMENT VOLUMES

Tissue Volume

$$V = V_c \; W_t$$

Where:

V	=	Tissue volume within the compartment (g tissue)
V_c	=	Allometric constant used to calculate arterial compartment volume (g tissue/g bodyweight)
W_t	=	Body weight at time t (g)

Tissue Blood Volume

$$V_b = V_{bc} \; V$$

Where:

V_b	=	Tissue blood volume within the compartment (g tissue)
V_{bc}	=	Tissue blood volume as a fraction of tissue volume (unitless)

CALCULATION OF CARDIAC OUTPUT

$$Q_{TOT} = Q_{car} \times 60 \times \left(\frac{W_t}{1000}\right)^{0.75}$$

Where:

Q_{TOT}	=	Total cardiac output for the test species (ml/hour)
Q_{car}	=	Allometric coefficient to calculate cardiac output from bodyweight (ml/kg/min)
W_t	=	Body weight at time t (g)

CALCULATION OF ABSORBED DOSE

a) Flow rate of delivery of administered oral dose of TCDD to the stomach (nmoles/hour)

$$R_{St} = \frac{dM_{St}}{dt} = K_{St}\, M_{St}\, BA_{TCDD}$$

b) Flow rate of absorption of TCDD from stomach through the gut wall into the lumen (nmoles/hour)

$$R_{Abs} = \frac{dM_{Lum}}{dt} = K_{St}\, M_{St}\, BA_{TCDD} - K_{Abs}\, M_{Lum}$$

$\mathbf{M_{Lum}}$ is calculated through an integration of $\mathbf{R_{Abs}}$ over time, using A_0 as the initial amount of TCDD present in the lumen.

c) Flow rate of TCDD transfer from lumen to venous blood supply *via* lymphatic flow (nmoles/hour)

$$R_{Lymph} = a \times K_{Abs}\, M_{Lum}$$

d) Flow rate of TCDD transfer from lumen to liver *via* portal vein (nmoles/hour)

$$R_{Arterial} = (1 - a) \times K_{Abs}\, M_{Lum}$$

Where:

a	=	Proportion of absorbed oral dose entering venous blood *via* lymphatic flow from the GI tract (unitless)
A_0	=	Initial amount of TCDD in the lumen (nmoles)
BA_{TCDD}	=	Fraction of the total dose absorbed/bioavailable (unitless)
K_{abs}	=	TCDD absorption rate from the lumen to the systemic circulation (1/hour)
K_{St}	=	the stomach emptying rate (1/hour)
M_{Lum}	=	the amount of TCDD absorbed into the lumen (nmoles)
M_{St}	=	the amount of TCDD in the stomach (nmoles)
R_{Abs}	=	Flow rate of absorption of TCDD from stomach through the gut wall into the lumen (nmoles/hour)
$R_{Arterial}$	=	Flow rate of TCDD transfer from lumen to liver *via* portal vein (nmoles/hour)
R_{Lymph}	=	Flow rate of TCDD transfer from lumen to venous blood supply *via* lymphatic flow (nmoles/hour)
R_{St}	=	Flow rate of delivery of administered oral dose of TCDD to the stomach (nmoles/hour)

VENOUS BLOOD SUPPLY

$$\frac{dW_B C_B}{dt} = Q_K(C_{KB} - C_B) + Q_S(C_{SB} - C_B) + Q_F(C_{FB} - C_B) + Q_{Re}(C_{ReB} - C_B) + Q_{Li}(C_{LiB} - C_B) + R_{Lymph}$$

Where:

W_B	=	Weight of the blood (g)
C_B	=	Concentration of TCDD in the arterial blood (nmoles/g tissue)
C_{KB}	=	Concentration of TCDD in the kidney venous blood (nmoles/g tissue)
C_{LuB}	=	Concentration of TCDD in the lung venous blood (nmoles/g tissue)
C_{SB}	=	Concentration of TCDD in the skin venous blood (nmoles/g tissue)
C_{FB}	=	Concentration of TCDD in the venous blood of the adipose tissue (nmoles/g tissue)
C_{ReB}	=	Concentration of TCDD in the venous blood of the rest of the body (nmoles/g tissue)
C_{LiB}	=	Concentration of TCDD in the liver venous blood (nmoles/g tissue)
Q_K	=	Blood flow in the kidneys (ml/hour)
Q_S	=	Blood flow in the skin (ml/hour)
Q_F	=	Blood flow in the adipose tissue (ml/hour)
Q_{Re}	=	Blood flow in the rest of the body (ml/hour)
Q_{Li}	=	Blood flow in the liver (ml/hour)
R_{Lymph}	=	Flow rate of TCDD transfer from lumen to venous blood supply *via* lymphatic flow (nmoles/hour)

LUNGS ***Flow-Limited Compartment***
(only blood flow rate controls tissue uptake)

a) Concentration of unbound (free) TCDD in lung compartment (nmol/g tissue)

$$C_{Luf} = C - \left[C_{Luf} \times P_{Lu} + \frac{C_{Luf} \times B_{max}}{K_d + C_{Luf}} \right]$$

b) Concentration of TCDD in lung tissue blood (nmol/g tissue)
(this is the concentration leaving the lungs into the arterial blood supply)

$$C_{LuB} = C_{Luf}$$

Note: As membrane permeability has no impact on tissue concentrations in flow-limited compartments, such as the lungs, the outgoing TCDD blood concentration would be equal to the concentration of unbound TCDD found within the lung compartment (*i.e.*, flow-through except for those bound to compartmental tissue constituents).

c) Overall tissue concentration of TCDD in lung compartment (nmol/g tissue)

$$C = \frac{A_{Lu}}{V_{Lu} + \frac{V_{LuB}}{P_{Lu}}}$$

d) Rate of change of TCDD in compartment (nmol/hour)

$$R_{Lu} = \frac{d\left(W_{Lu} + \frac{W_{LuB}}{P_{Lu}} \right) C_{Lu}}{dt} = Q_{Lu} \left(C_B - \frac{C_{Lu}}{P_{Lu}} \right)$$

e) Overall TCDD concentration (tissue and blood) in the lungs (nmol/g tissue)

$$C_{LuLu} = \frac{(C \times V_{Lu} + C_{Lub} \times V_{Lub})}{(V_{Lu} + V_{Lub})}$$

Where:

A_{Lu} = Amount of TCDD concentration in the lungs (nmol)
(Based on integration of R_{Lu} at a specific time slice)
B_{max} = Ah receptor nonlinear binding capacity (nmol/g)
C = Concentration of TCDD in the lung tissue at a specific time (nmol/g)
C_B = Concentration of TCDD in the blood entering the lungs (nmol/g)
C_{Lu} = Concentration of bound TCDD in the lungs (nmol/g)
C_{Luf} = Concentration of unbound TCDD in the lungs (nmol/g)
C_{LuB} = Concentration of TCDD in the lung tissue blood (nmol/g)
C_{LuLu} = Overall TCDD concentration (tissue and blood) in the lungs (nmol/g tissue)
K_d = Equilibrium dissociation constant for Ah receptor binding (nmol/g)
P_{Lu} = Equilibrium ratio of the lung tissue concentration to blood concentration (unitless)
Q_{Lu} = Blood flow in the lungs (ml/hour)
R_{Lu} = Rate of change of TCDD concentration in the lungs (nmol/hour)
V_{Lu} = Tissue volume of the lungs (g)
V_{LuB} = Tissue blood volume within the lungs (g)
W_{Lu} = Tissue weight of the lungs (g)
W_{LuB} = Weight of blood in the lungs (g)

KIDNEYS ***Membrane-Limited Compartment***
(only membrane transfer controls tissue uptake)

a) Concentration of unbound (free) TCDD in kidney compartment (nmol/g tissue)

$$C_{Kf} = C - \left[C_{Kf} \times P_K + \frac{C_{Kf} \times B_{max}}{K_d + C_{Kf}} \right]$$

b) Overall tissue concentration of TCDD in kidney compartment (nmol/g tissue)

$$C = \frac{A_K}{V_K}$$

c) Rate of change of TCDD in compartment (nmol/hour)

$$R_K = \frac{dW_K C_K}{dt} = PA_K(C_{KB} - C_{Kf}) - R_{Urinary}$$

d) Flow rate of TCDD lost due to renal urinary excretion (nmol/hour)

$$R_{Urinary} = K_K C_{Kf} V_K$$

e) Concentration of TCDD in kidney tissue blood (nmol/g tissue)
(this is the concentration leaving the kidneys in the venous blood supply)

$$C_{KB} = \frac{\left(C_B + \frac{PA_k}{Q_K} \times C_{Kf} \right)}{\left(1 + \frac{PA_k}{Q_K} \right)}$$

f) Overall TCDD concentration (tissue and blood) in the kidney (nmol/g tissue)

$$C_{KK} = \frac{(A_K + C_{Kb} \times V_{Kb})}{(V_K + V_{Kb})}$$

Where:

A_K = Amount of TCDD concentration in kidneys (nmol) (based on integration of R_K at a specific time slice)
B_{max} = Ah receptor nonlinear binding capacity (nmol/g)
C = Concentration of TCDD in the kidney tissue at a specific time (nmol/g)
C_B = Concentration of TCDD in the blood entering kidneys (nmol/g)
C_K = Concentration of bound TCDD in the kidney (nmol/g)
C_{KB} = Concentration of TCDD in the kidney tissue blood (nmol/g)
C_{Kf} = Concentration of unbound TCDD in the kidney (nmol/g)
C_{KK} = Overall TCDD concentration (tissue and blood) in the kidney (nmol/g tissue)
K_d = Equilibrium dissociation constant for Ah receptor binding (nmol/g)
K_K = Urinary linear elimination constant (1/hour)
P_K = Equilibrium ratio of the kidney tissue concentration to blood concentration (unitless)
PA_K = Permeability of the kidney (ml/hour)
Q_K = Blood flow in the kidney (ml/hour)
R_K = Rate of change of TCDD concentration in the kidneys (nmol/hour)
$R_{Urinary}$ = Flow rate of TCDD lost due to renal urinary excretion (nmol/hour)
V_K = Tissue volume of the kidneys (g)
V_{KB} = Tissue blood volume within the kidneys (g)
W_K = Tissue weight of the kidneys (g)

REST OF BODY ***Membrane-Limited Compartment***
(only membrane transfer controls tissue uptake)

a) Overall tissue concentration of TCDD in the rest of the body (nmol/g tissue)

$$C = \frac{A_{Re}}{V_{Re}}$$

b) Rate of change of TCDD in compartment (nmol/hour)

$$R_{Re} = \frac{dW_{Re}C_{Re}}{dt} = PA_{Re}(C_B - \frac{C}{P_{Re}})$$

c) Concentration of TCDD in tissue blood within the compartment (nmol/g tissue)
(this is the concentration leaving the rest of the body in the venous blood supply)

$$C_{ReB} = \frac{\left(C_B + \frac{PA_{Re}}{Q_{Re}} \times \frac{C}{P_{Re}}\right)}{\left(1 + \frac{PA_{Re}}{Q_{Re}}\right)}$$

d) Overall TCDD concentration (tissue and blood) in the rest of the body (nmol/g tissue)

$$C_{ReRe} = \frac{(A_{Re} + C_{Reb} \times V_{Reb})}{(V_{Re} + V_{Reb})}$$

Where:

A_{Re}	=	Amount of TCDD concentration in the rest of the body (nmol) (based on integration of R_{Re} at a specific time slice)
C	=	Concentration of TCDD in the rest of the body tissue at a specific time (nmol/g)
C_B	=	Concentration of TCDD in the blood entering the rest of the body (nmol/g)
C_{ReB}	=	Concentration of TCDD in the tissue blood within the rest of the body (nmol/g)
C_{ReRe}	=	Overall TCDD concentration (tissue and blood) in the rest of the body (nmol/g tissue)
P_{Re}	=	Equilibrium ratio of the tissue concentration to blood concentration in the rest of the body (unitless)
PA_{Re}	=	Permeability of the rest of the body (ml/hour)
Q_{Re}	=	Blood flow in the rest of the body (ml/hour)
R_{Re}	=	Rate of change of TCDD concentration in the rest of the body (nmol/hour)
V_{Re}	=	Tissue volume of the rest of the body (g)
V_{ReB}	=	Tissue blood volume within the rest of the body (g)
W_{Re}	=	Tissue weight of the rest of the body (g)

SKIN ***Membrane-Influenced Compartment***

(Both blood flow rate and membrane transfer control tissue uptake)

a) Concentration of unbound (free) TCDD in the skin (nmol/g tissue)

$$C_{Sf} = C - \left[C_{Sf} \times P_S + \frac{C_{Sf} \times B_{max}}{K_d + C_{Sf}} \right]$$

b) Overall tissue concentration of TCDD in the skin (nmol/g tissue)

$$C = \frac{A_S}{V_S}$$

c) Concentration of TCDD in tissue blood within the skin (nmol/g tissue)
(this is the concentration leaving the skin in the venous blood supply)

$$C_{SB} = \frac{A_{SB}}{V_{SB}}$$

d) Rate of change of TCDD in compartment (nmol/hour)

Blood

$$R_{Sb} = \frac{dW_{SB}\,C_{SB}}{dt} = Q_S(C_B - C_{SB}) - PA_S(C_{SB} - C_{Sf})$$

Tissue

$$R_S = \frac{dW_S\,C_S}{dt} = PA_S(C_{SB} - C_{Sf})$$

e) Overall TCDD concentration (tissue and blood) in the skin (nmol/g tissue)

$$C_{SS} = \frac{(A_S + A_{SB})}{(V_S + V_{SB})}$$

Where:

A_S = Amount of TCDD concentration in the skin (nmol) (based on integration of R_S at a specific time slice)
A_{SB} = Amount of TCDD concentration in the skin blood (nmol) (based on integration of R_{SB} at a specific time slice)
B_{max} = Ah receptor nonlinear binding capacity (nmol/g)
C = Concentration of TCDD in the skin tissue at a specific time (nmol/g)
C_B = Concentration of TCDD in the blood entering the skin (nmol/g)
C_S = Concentration of bound TCDD in the skin (nmol/g)
C_{SB} = Concentration of TCDD in the skin tissue blood (nmol/g)
C_{Sf} = Concentration of unbound TCDD in the skin (nmol/g)
C_{SS} = Overall TCDD concentration (tissue and blood) in the skin (nmol/g tissue)
K_d = Equilibrium dissociation constant for Ah receptor binding (nmol/g)
P_S = Equilibrium ratio of the skin tissue concentration to blood concentration (unitless)
PA_S = Permeability of the skin (ml/hour)
Q_S = Blood flow in the skin (ml/hour)
R_S = Rate of change of TCDD concentration in the skin (nmol/hour)
R_{SB} = Rate of change of TCDD concentration in the skin blood (nmol/hour)
V_S = Tissue volume of the skin (g)
V_{SB} = Tissue blood volume within the skin (g)
W_S = Tissue weight of the skin (g)
W_{SB} = Weight of blood in the skin (g)

ADIPOSE TISSUE/FAT *Membrane-Limited Compartment*

(only membrane transfer controls tissue uptake)

a) Overall tissue concentration of TCDD in the adipose tissue (nmol/g tissue)

$$C = \frac{A_F}{V_F}$$

b) Rate of change of TCDD in compartment (nmol/hour)

$$R_F = \frac{dW_F C_F}{dt} = PA_F(C_F - \frac{C}{P_F})$$

c) Concentration of TCDD in tissue blood within the compartment (nmol/g tissue)
(this is the concentration leaving the adipose tissue in the venous blood supply)

$$C_{FB} = \frac{\left(C_B + \frac{PA_F}{Q_F} \times \frac{C}{P_F}\right)}{\left(1 + \frac{PA_F}{Q_F}\right)}$$

d) Overall TCDD concentration (tissue and blood) in the adipose tissue (nmol/g tissue)

$$C_{FF} = \frac{(A_F + C_{Fb} \times V_{Fb})}{(V_F + V_{Fb})}$$

Where:

- A_F = Amount of TCDD concentration in the adipose tissue (nmol) (based on integration of R_F at a specific time slice)
- C = Concentration of TCDD in the adipose tissue at a specific time (nmol/g)
- C_B = Concentration of TCDD in the blood entering the adipose tissue (nmol/g)
- C_{FB} = Concentration of TCDD in the tissue blood within the adipose tissue (nmol/g)
- C_{FF} = Overall TCDD concentration (tissue and blood) in the adipose tissue (nmol/g tissue)
- P_F = Equilibrium ratio of the tissue concentration to blood concentration in the adipose tissue (unitless)
- PA_F = Permeability of the adipose tissue (ml/hour)
- Q_F = Blood flow in the adipose tissue (ml/hour)
- R_F = Rate of change of TCDD concentration in the adipose tissue (nmol/hour)
- V_F = Tissue volume of the adipose tissue (g)
- V_{FB} = Tissue blood volume within the adipose tissue (g)
- W_F = Tissue weight of the adipose tissue (g)

SPLEEN ***Flow-Limited Compartment***
(only blood flow rate controls tissue uptake)

a) Concentration of unbound (free) TCDD in spleen (nmol/g tissue)

$$C_{Spf} = C - \left[C_{Spf} \times P_{Sp} + \frac{C_{Spf} \times B_{max}}{K_d + C_{Spf}} \right]$$

b) Concentration of TCDD in spleen tissue blood (nmol/g tissue)
(this is the concentration leaving the spleen into the portal vein)

$$C_{SpB} = C_{Spf}$$

Note: As membrane permeability has no impact on tissue concentrations in flow-limited compartments, the outgoing TCDD blood concentration would be equal to the concentration of unbound TCDD found within the spleen (*i.e.*, flow-through except for those bound to compartmental tissue constituents).

c) Overall tissue concentration of TCDD in spleen (nmol/g tissue)

$$C = \frac{A_{Sp}}{V_{Sp} + \frac{V_{SpB}}{P_{Sp}}}$$

d) Rate of change of TCDD in compartment (nmol/hour)

$$R_{Sp} = \frac{d\left(W_{Sp} + \frac{W_{SpB}}{P_{Sp}} \right) C_{Sp}}{dt} = Q_{Sp} \left(C_B - \frac{C_{Sp}}{P_{Sp}} \right)$$

e) Overall TCDD concentration (tissue and blood) in the spleen (nmol/g tissue)

$$C_{SpSp} = \frac{(C \times V_{Sp} + C_{Spb} \times V_{Spb})}{(V_{Sp} + V_{Spb})}$$

Where:

A_{Sp} = Amount of TCDD concentration in the spleen (nmol) (based on integration of R_{Sp} at a specific time slice)
B_{max} = Ah receptor nonlinear binding capacity (nmol/g)
C = Concentration of TCDD in the spleen tissue at a specific time (nmol/g)
C_B = Concentration of TCDD in the blood entering the spleen (nmol/g)
C_{Sp} = Concentration of bound TCDD in the spleen (nmol/g)
C_{Spf} = Concentration of unbound TCDD in the spleen (nmol/g)
C_{SpB} = Concentration of TCDD in the spleen tissue blood (nmol/g)
C_{Spsp} = Overall TCDD concentration (tissue and blood) in the spleen (nmol/g tissue)
K_d = Equilibrium dissociation constant for Ah receptor binding (nmol/g)
P_{Sp} = Equilibrium ratio of the spleen tissue concentration to blood concentration (unitless)
Q_{Sp} = Blood flow in the spleen (ml/hour)
R_{Sp} = Rate of change of TCDD concentration in the spleen (nmol/hour)
V_{Sp} = Tissue volume of the spleen (g)
V_{SpB} = Tissue blood volume within the spleen (g)
W_{Sp} = Tissue weight of the spleen (g)
W_{SpB} = Weight of blood in the spleen (g)

PORTAL VEIN ***Miscellaneous Compartment***

(Handles mass flow into liver *via* portal vein)

a) Flow rate of TCDD leaving portal vein into liver (nmoles/hour)

$$R_{Portal} = (Q_{Li} - Q_{Sp}) \times C_B + Q_{Sp} \times C_{SpB} + R_{Arterial}$$

Where:

C_B	=	Concentration of TCDD in the blood entering the portal vein (nmol/g)
C_{SpB}	=	Concentration of TCDD in the blood entering from the spleen (nmol/g)
Q_{Li}	=	Blood flow in the liver (ml/hour)
Q_{Sp}	=	Blood flow in the spleen (ml/hour)
$R_{Arterial}$	=	Flow rate of TCDD transfer from lumen to liver *via* portal vein (nmol/hour)
R_{Portal}	=	Flow rate of TCDD in the blood leaving portal vein into the liver (nmol/hour)

LIVER ***Membrane-Influenced Compartment***
(Both blood flow rate and membrane transfer control tissue uptake)

a) Concentration of unbound (free) TCDD in the liver (nmol/g tissue)

$$C_{Lif} = C - \left(C_{Lif} \times P_{Li} + \frac{C_{Lif} \times B_{max}}{K_d + C_{Lif}} + \frac{C_{Lif} \times C_{CYP}}{K_{dCYP} + C_{Lif}} \right)$$

b) Overall tissue concentration of TCDD in the liver (nmol/g tissue)

$$C = \frac{A_{Li}}{V_{Li}}$$

c) Concentration of TCDD in tissue blood within the liver (nmol/g tissue)
(this is the concentration leaving the liver in the venous blood supply)

$$C_{LiB} = \frac{A_{LiB}}{V_{LiB}}$$

d) Rate of change of TCDD in compartment (nmol/hour)

Blood

$$R_{LiB} = \frac{dW_{LiB} C_{LiB}}{dt} = R_{Portal} - Q_{Li} \times C_{LiB} - PA_{Li}(C_{LiB} - C_{Lif})$$

Tissue

$$R_{Li} = \frac{dW_{Li} C_{Li}}{dt} = PA_{Li}(C_{LiB} - C_{Lif}) - R_{bile}$$

d) Flow rate of TCDD lost due to biliary excretion (nmol/hour)

$$R_{bile} = K_{Li} C_{Lif} V_{Li}$$

e) Concentration of Ah receptor occupied by TCDD ligand and available for binding to CYP1A2 (nmol/g)

$$C_{bAh} = \frac{B_{max} \times C_{Lif}}{K_d + C_{Lif}}$$

f) Overall TCDD concentration (tissue and blood) in the liver (nmol/g tissue)

$$C_{LiLi} = \frac{(A_{Li} + A_{LiB})}{(V_{Li} + V_{LiB})}$$

Where:

A_{Li} = Amount of TCDD concentration in the liver (nmol) (based on integration of R_{Li} at a specific time slice)
A_{LiB} = Amount of TCDD concentration in the liver blood (nmol) (based on integration of R_{LiB} at a specific time slice)
B_{max} = Ah receptor nonlinear binding capacity (nmol/g)
C = Concentration of TCDD in the liver tissue at a specific time (nmol/g)
C_{bAh} = Concentration of Ah receptor occupied by TCDD ligand, available for binding to CYP1A2 in the liver (nmol/g)
C_{CYP} = Concentration of unbound CYP1A2 available in the liver (nmol/g)
C_{Li} = Concentration of bound TCDD in the liver (nmol/g)
C_{LiB} = Concentration of TCDD in the liver tissue blood (nmol/g)
C_{Lif} = Concentration of unbound TCDD in the liver (nmol/g)
C_{LiLi} = Overall TCDD concentration (tissue and blood) in the liver (nmol/g tissue)
K_d = Equilibrium dissociation constant for Ah receptor binding (nmol/g)
K_{dCYP} = Equilibrium dissociation constant for binding to CYP1A2 (nmol/g)
K_{Li} = Biliary linear elimination constant (1/hour)
PA_{Li} = Permeability of the liver (ml/hour)
P_{Li} = Equilibrium ratio of the liver tissue concentration to blood concentration (unitless)
Q_{Li} = Blood flow in the liver (ml/hour)
R_{bile} = Flow rate of TCDD lost due to biliary excretion (nmol/hour)
R_{Li} = Rate of change of TCDD concentration in the liver (nmol/hour)
R_{LiB} = Rate of change of TCDD concentration in the liver blood (nmol/hour)
R_{Portal} = Flow rate of TCDD in the blood leaving portal vein into the liver (nmol/hour)
V_{Li} = Tissue volume of the liver (g)
V_{LiB} = Tissue blood volume within the liver (g)
W_{Li} = Tissue weight of the liver (g)
W_{LiB} = Weight of blood in the liver (g)

CYP1A2 Binding

In the current model, the degradation of free CYP1A2 and bound CYP1A2 are assumed to be the same. The change of CYP1A2 with time was obtained from a simulation model proposed by Dayneka *et al.* (1993). As such, the concentration of unbound CYP1A2 available for TCDD-Ah binding was simplified using the following set of equilibrium binding equations:

a) Calculate zero-order basal induction rate for CYP1A2 synthesis (nmoles/g/hour)

$$K_0 = C_{CYP0} \times K_2$$

b) Rate of change of initially available CYP1A2 within the liver (nmol/hour)

$$R_{CYP_i} = \frac{dW_{Li}\, C_{CYP_i}}{dt} = (S_t\, K_0 - K_2\, C_{CYP_i})\, W_{Li}$$

c) The CYP1A2 stimulation function is represented as follows (unitless)

$$S_t = 1 + IN_{A2} \frac{(C_{bAh})^h}{(IC_{A2})^h + (C_{bAh})^h}$$

As the binding of TCDD to available CYP1A2, via Ah-receptor complexing, is not an instanteous process, a set of two interconnected holding periods were used to represent physiological induction delays in the processing of free CYP1A2. The concentration of free CYP1A2, after completion of the two physiological holding periods, is what ultimately is used by the liver compartment to determine the amount of free CYP1A2 available for binding to existing concentrations of the TCDD ligand.

d) Calculation of the concentration of available CYP1A2 in the liver after the first physiological holding period (nmoles/g)

$$R_{CYP_2} = \frac{dC_{CYP_2}}{dt} = \frac{C_{CYP_i} - C_{CYP_2}}{\tau}$$

C_{CYP2} is then calculated based upon its integration with the basal concentration of CYP1A2 within the liver (C_{CYP0}).

e) Calculation of concentration of available CYP1A2 in the liver after the second physiological holding period (nmoles/g)

$$R_{CYP_2} = \frac{dC_{CYP_2}}{dt} = \frac{C_{CYP_2} - C_{CYP}}{\tau}$$

C_{CYP} is then calculated based upon its integration with the basal concentration of CYP1A2 within the liver (C_{CYP0}). This concentration is used by the liver compartment as the amount of free CYP1A2 available for TCDD binding.

Where:

C_{bAh} = Concentration of Ah receptor bound to TCDD ligand and available for binding to CYP1A2 in the liver (nmol/g)

C_{CYP} = Concentration of unbound CYP1A2 available in the liver **after** the two physiological induction holding periods (nmol/g). This concentration is used by the liver compartment as the amount of free CYP1A2 available for TCDD binding.

C_{CYP0} = Basal concentration of unbound CYP1A2 available in the liver (nmol/g)

C_{CYP1} = Concentration of unbound CYP1A2 available in the liver **before** first physiological holding period (nmol/g)

C_{CYP2} = Concentration of unbound CYP1A2 available in the liver **following** first physiological holding period (nmol/g)

C_{Lif} = Concentration of TCDD in the liver tissue (μg/g tissue)

h = the Hill coefficient (unitless)

IC_{A2} = Michaelis-Menten constant of CYP1A2 induction (nmol/g)

IN_{A2} = the maximum induction of CYP1A2 synthesis rate over the basal rate (unitless)

K_0 = the zero-order basal induction rate for CYP1A2 synthesis (nmol/g/hour)

K_2 = the first-order rate constant for CYP1A2 degradation (1/hour)

R_{CYP1} = the rate of change of unbound CYP1A2 available within the liver (nmol/hour)

R_{CYP2} = the rate of change of unbound CYP1A2 available within the liver after the first physiological holding period (nmol/hour)

R_{CYP1} = the rate of change of unbound CYP1A2 available within the liver after the first physiological holding period (nmol/hour)

τ = CYP1A2 induction delay holding time (hours)

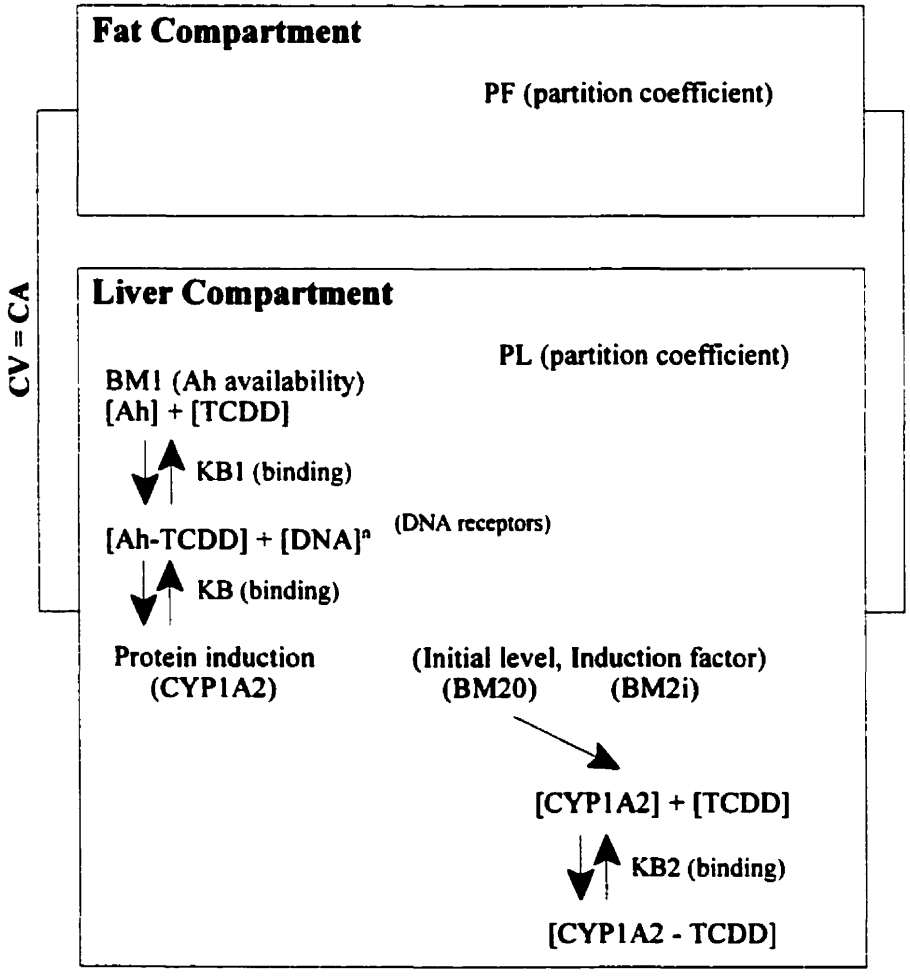
S_t = the stimulation function (unitless)

W_{Li} = the tissue weight of the liver (g)

A-2.0 Prototype Equilibrium-based PBPK Model (Evans and Andersen, 2000)

The following section provides the detailed mathematical equations used in the development of the prototype steady-state PBPK model for the current research on PCDD/F pharmacokinetics. It is based upon the Evans and Andersen (2000) published model, with modifications to correct minor inaccuracies and gaps in the methodology provided by the Evans and Andersen (2000) source paper.

Figure A-3 A schematic representation of the steady-state TCDD PBPK model (Evans and Andersen, 2000)



CALCULATION OF AVAILABLE BINDING RECEPTORS

Ah Receptor Binding

a) Calculation of total amount of Ah-TCDD complex in liver (nmoles)

$$Ah{:}TCDD = C_b \times \frac{BM_1}{KB_1 + C_b}$$

b) Concentration of TCDD bound to Ah receptors in the liver (nM)

$$C_{Ah} = \frac{Ah{:}TCDD}{W_L}$$

CYP1A2 Binding

c) Amount of induced CYP1A2 in the liver (nmoles)

$$BM_{2T} = BM_{2o} + BM_{2o} \times BM_{2i} \times \frac{Ah{:}TCDD^n}{Kd^n + Ah{:}TCDD^n}$$

d) Calculation of total CYP1A2:TCDD complex in liver (nmoles)

$$\text{CYP1A2:TCDD} = C_b \times \frac{BM_{2T}}{KB_2 + C_b}$$

e) Calculation of overall CYP1A2 occupancy by TCDD (unitless)

$$F_{CYP1A2} = \frac{\text{CYP1A2:TCDD}}{BM_{2T}}$$

f) Calculation of overall CYP1A2 fold increase (unitless)

$$IF_{CYP1A2} = \frac{BM_{2T}}{BM_{2o}}$$

f) Concentration of TCDD bound to CYP1A2 in the liver (nM)

$$C_{CYP1A2} = \frac{\text{CYP1A2:TCDD}}{W_L}$$

Where:

Ah:TCDD	=	Amount of TCDD bound to Ah receptors in the liver (nmoles)
CYP1A2:TCDD	=	Amount of TCDD bound to CYP1A2 in the liver (nmoles)
BM_{2o}	=	Basal level of CYP1A2 in the liver (nmoles)
BM_{2i}	=	CYP1A2 fold increase due to induction (unitless)
BM_{2T}	=	Amount of induced CYP1A2 in the liver (nmoles)
C_b	=	Concentration of TCDD in the pooled blood (nM)
C_{Ah}	=	Concentration of TCDD bound to Ah receptors in the liver (nM)
C_{CYP1A2}	=	Concentration of TCDD bound to CYP1A2 in the liver (nM)
C_{CYP1A2}	=	Concentration of TCDD bound to CYP1A2 in the liver (nM)
F_{CYP1A2}	=	Fraction of total CYP1A2 occupied by TCDD (unitless)
IF_{CYP1A2}	=	CYP1A2 induction fold increase over basal level (unitless)
KB_1	=	Ah receptor binding constant (nM)
KB_2	=	Binding affinity for CYP1A2 (nM)
Kd	=	Ah receptor complex/DNA receptor dissociation constant (nM)
n	=	Hill coefficient (unitless)
W_L	=	Liver weight (kg)

CALCULATION OF TCDD BLOOD CONCENTRATION

The following equation is used to calculate the amount of TCDD that is present in the blood pool at steady-state. As the C_b variable is present on both sides, the equation is termed an *implicit equation*, and must be solved with an application capable of resolving the equation to a point of stable convergence. The authors (Evans and Andersen, 2000) recommend the use of Simusolv's IMPL algorithm with the number of points set to 200, supplied with an initial value for blood of zero, a convergence criterion of 0.000001, and the number of allowable iterations set at 10. Other options include using the IMPLC algorithm in ACSL Tox, using the Solver system built into Microsoft Excel, or simply adjust the temporary blood concentration manually in a spreadsheet version of the model until a satisfactory convergence occurs. As multiple solutions are possible, only the maximum value should be used.

For the current research, the methodology was created in an Excel spreadsheet, and solved using both the built-in Solver as well as manual convergence.

a) Concentration of TCDD in blood pool (nM)

$$C_b = \frac{C_D}{V_b + P_L \times V_L + P_F \times V_F + \frac{BM_1}{KB_1 + C_b} + \frac{BM_{2T}}{KB_2 + C_b}}$$

Where:

BM_1	=	Ah receptor maximum availability (nmoles)
BM_{2T}	=	Amount of induced CYP1A2 in the liver (nmoles)
C_b	=	Concentration of TCDD in the pooled blood (nM)
C_D	=	Administered dose of TCDD (nM)
KB_1	=	Ah receptor binding constant (nM)
KB_2	=	Binding affinity for CYP1A2 (nM)
P_F	=	Fat partitioning coefficient (unitless)
P_L	=	Liver partitioning coefficient (unitless)
V_B	=	Blood volume as a percentage of bodyweight (unitless)
V_F	=	Fat volume as a percentage of bodyweight (unitless)
V_L	=	Liver volume as a percentage of bodyweight (unitless)

CALCULATION OF TCDD TISSUE FRACTIONS

Blood Fraction

a) Fraction of TCDD in blood (unitless)

$$FB = \frac{C_b \times V_b}{C_D}$$

Liver Tissue Fraction

b) Concentration of TCDD bound to liver tissue (nM)

$$C_{lt} = C_b \times P_l \times V_l$$

c) Concentration of TCDD bound to Ah receptors in the liver (nM)

$$C_{Ah} = C_b \times \frac{BM_1}{KB_1 + C_b}$$

d) Concentration of TCDD bound to CYP1A2 in the liver (nM)

$$C_{CYP1A2} = C_b \times \frac{BM_{2T}}{KB_2 + C_b}$$

e) Overall concentration of TCDD found in liver tissue (nM)

$$C_L = C_{lt} + C_{Ah} + C_{CYP1A2}$$

f) Calculation of overall fraction of administered TCDD found in the liver (unitless)

$$FH = \frac{C_L}{C_D}$$

Fat Tissue Fraction

g) Fraction of TCDD stored in adipose tissue (unitless)

$$FF = (1 - FH - FB)$$

h) Overall concentration of TCDD found in liver tissue (nM)

$$C_F = C_D * \frac{FF}{V_F}$$

Liver to Fat Mass Ratio

h) Calculation of liver to fat mass ratio (unitless)

$$LTOF = \frac{C_L}{C_F}$$

Where:

FB	=	Fraction of TCDD stored in blood (unitless)
FF	=	Fraction of TCDD stored in adipose tissue (unitless)
FL	=	Fraction of TCDD stored in liver (unitless)
LTOF	=	Liver to fat mass ratio (unitless)
BM_1	=	Ah receptor maximum availability (nmoles)
BM_{2T}	=	Amount of induced CYP1A2 in the liver (nmoles)
C_D	=	Administered dose of TCDD (nM)
C_b	=	Concentration of TCDD in the pooled blood (nM)
C_{Ah}	=	Concentration of TCDD bound to Ah receptors in the liver (nM)
C_{CYP1A2}	=	Concentration of TCDD bound to CYP1A2 in the liver (nM)
C_F	=	Concentration of TCDD in adipose tissue compartment (nM)
C_L	=	Concentration of TCDD in liver compartment (nM)
C_{lt}	=	Concentration of TCDD bound to liver tissue (nM)
KB_1	=	Ah receptor binding constant (nM)
KB_2	=	Binding affinity for CYP1A2 (nM)
P_L	=	Liver partitioning coefficient (unitless)
V_B	=	Blood volume as a percentage of bodyweight (unitless)
V_F	=	Fat volume as a percentage of bodyweight (unitless)
V_L	=	Liver volume as a percentage of bodyweight (unitless)

A-3.0 Evans and Andersen (2000) Simulsolv Source Code

The following source code was provided by the primary author (M. Evans, personal communication, 2001; reproduced with permission), and is designed for the Simulsolv (Dow Chemical Company, Midland, MI, Version 3.0, 1993) computer simulation package.

```
'PROGRAM DIOXIN STEADY STATE MODEL - WITH DATA GAETAN.CSL'
'MEL E. ANDERSEN'
'STEADY STATE MODEL 16 NOV 1993'
INITIAL
CONSTANT   PL=10.  $'BLOOD LIVER PARTITION COEFFICIENT'
CONSTANT   PF=350. $'FAT/BLOOD PARTITION COEFFICIENT'
CONSTANT   PS=10.  $'SLOWLY PERFUSED TISSUE/BLOOD PARTITION'
CONSTANT   PR=10.  $'RICHLY PERFUSED PARITION COEFFICIENT'
CONSTANT   VLC =0.04 $'LIVER VOLUME PROPORTION BW'
CONSTANT   VFC = 0.06 $'FAT VOLUME PROPORTION BW'
CONSTANT   BW=0.215  $'BODY WEIGHT IN KG'
CONSTANT   MW=322   $'MOLECULAR WEIGHT OF DIOXIN'

'*********DIOXIN SECTION FOR LIVER BINDING*************'
CONSTANT   BM1=0.054 $'DIOXIN BINDING CAPACITY TO AHH LOCUS'
CONSTANT   KB1 =0.04 $'DIOXIN BINDING CONSTANT AHH LOCUS'
CONSTANT   BM20 = 10. $'DIOXING BINDING CAPACITY TO P448'
CONSTANT   BM2I = 85. $'INCREASE DUE TO MICROSOMAL INDUCTION'
CONSTANT   KB2 = 7.  $'DIOXIN BINDINB CONSTANT TO P=448'
CONSTANT   N=1.     $'HILL COEFFICIENT'
CONSTANT   KD=1.    $'LIGANDED RECEPTOR-DNA BINDING'
'******************************************************'

'TIMING SECTION'
CONSTANT   PDOSEM = 10.  $'MAXIMUM DOSE FOR CALCULATION'
       LMDOSE = ALOG(PDOSEM)/2.303 $'LOG(10) MAX BURDEN'
CONSTANT   POINTS=100   $'NUMBER OF POINTS IN LOG PLOT'
       CINT = ALOG(PDOSEM)/POINTS  $'INTERVAL FOR OUTPUT'

'INITIAL PARAMETER CALCULATIONS'
VARIABLE  LPDOSE=-6 $'INDEPENDENT VARIABLE-LOG BODY BURDEN'
CLBT=0.0          $'SETS INITIAL VALUE FOR VARIABLE IN IMPL'
VL=VLC*BW          $'LIVER VOLUME'
VF=VFC*BW          $'FAT VOLUME'
FH=0.0           $'INITIAL VALUE OF FRACTION OF DOSE IN LIVER'
fhc=fh
BM2T=BM20          $'INITIAL VALUE OF P450-1A2 IN LIVER'
END   $'END INITIAL'

DYNAMIC
```

```
DERIVATIVE
 PDOSE = 10**LPDOSE
  DOSE = PDOSE*BW/MW*1000
  CLB = AMAX1(IMPL(CLBT,.000001,10,EF,...
  DOSE/(PL*VL+PF*VF+BM1/(KB1+CLB)+BM2T/(KB2+CLB)),...
.0001),0.)
'CLB FREE CONCENTRATION IN BODY'
'SET DUMMY INTEGRATOR SO THAT DERIVATIVE FUNCTION WORKS'
   DUMMY=INTEG(0.,0.)
PROCEDURAL
   DB1 = BM1*CLB/(KB1+CLB)/VL
   BOUND=DB1**N/(DB1**N+KD**N)
   BM2T = BM20+BM2I*BOUND
   FH=(CLB)*(PL*VL+BM1/(KB1+CLB)+BM2T/(KB2+CLB))/(DOSE)
   DERFH=DERIVT(0.0,FH)
   CH=DOSE*FH/VL
   CF=DOSE*(1-FH)/VF
   LTOF = CH/CF
   DERLF = DERIVT(0.0,LTOF)
   CCH=DOSE/BW*MW
END     $'END OF PROCEDURE'
'DB1 CONCENTRATION OF BOUND AH RECEPTOR NM'
'BOUND PROPORTION OCCUPANCY OF DNA BINDING SITES'
'BM2T AMOUNT OF P4501A2 NMOLES'
'FH FRACTION OF BODY BURDEN IN LIVER'
'CH CONCENTRATION IN LIVER NM'
'CF CONCENTRATION IN FAT NM'
'LTOF LIVER FAT RATIO'
'CCH AVERAGE BODY CONCENTRATION NM/KG'


TERMT(LPDOSE.GE.LMDOSE)
END   $'END OF DERIVATIVE'
END   $'END OF DYNAMIC'
END   $'END OF PROGRAM'
```

A-4.0 REFERENCES

Evans, M.V. and M.E. Andersen. 2000. Sensitivity Analysis of a Physiological Model for 2,3,7,8-Tetrachlorodibenzo-*p*-dioxin (TCDD): Assessing the Impact of Specific Model Parameters on Sequestration in Liver and Fat in the Rat. Toxicological Sciences 54:71-80.

Wang, X., Santostefano, M.J., Evans, M.V., Richardson, V.M., Diliberto, J.J., and L.S. Birnbaum. 1997. Determination of Parameters Responsible for Pharmacokinetic Behavior of TCDD in Female Sprague-Dawley Rats. Toxicol. Appl. Pharmacol 147:151-168.

APPENDIX B

Detailed Results of Sensitivity Analyses of PBPK Model System

Table B-1.0 Sensitivity Analysis Results for Contribution to Variance between TCDD PB-PK Model Variables and Sequestration Outcome.

Parameters	8 Hours					24 Hours					72 Hours				
	0.1	0.316	1	3.16	10	0.1	0.316	1	3.16	10	0.1	0.316	3.16	1	10
General Physiological Parameters															
Bodyweight	15.9%	0.0%	0.1%	1.5%	2.2%	11.6%	0.3%	1.3%	1.7%	1.7%	5.4%	1.3%	2.2%	0.3%	1.3%
Qcar	3.8%	2.7%	2.0%	0.1%	2.1%	6.1%	1.3%	4.4%	0.1%	1.7%	3.8%	2.4%	0.1%	5.8%	1.0%
Equilibrium Distribution Ratio															
Pf	0.1%	5.1%	4.7%	2.3%	1.2%	0.0%	5.5%	7.0%	1.4%	2.1%	0.1%	4.7%	0.8%	6.7%	0.6%
Pk	5.2%	1.7%	1.0%	3.4%	0.0%	5.4%	0.5%	0.3%	3.0%	0.0%	8.4%	0.0%	1.9%	0.9%	0.1%
Pli	1.5%	0.2%	2.6%	13.2%	4.5%	1.9%	1.0%	1.6%	13.0%	4.3%	0.5%	0.9%	13.9%	5.1%	4.3%
Plu	0.1%	0.2%	0.6%	2.0%	0.0%	0.0%	0.0%	0.7%	1.8%	0.0%	0.1%	2.0%	1.5%	0.2%	0.2%
Pre	4.9%	0.9%	0.3%	1.7%	5.8%	3.3%	0.1%	0.1%	1.6%	5.7%	2.9%	0.0%	1.0%	0.5%	7.9%
Ps	10.5%	0.2%	3.1%	2.0%	1.7%	7.8%	0.4%	1.2%	1.1%	1.2%	3.8%	0.8%	0.9%	0.9%	0.2%
Psp	4.0%	0.9%	0.0%	0.4%	0.0%	3.6%	0.6%	0.1%	0.5%	0.0%	0.9%	2.8%	0.5%	0.1%	0.0%
Permeability															
PAc - Fat	0.0%	0.5%	1.4%	1.0%	10.8%	0.9%	0.0%	4.0%	1.1%	11.6%	1.8%	0.0%	1.8%	1.5%	12.6%
PAc - Kidney	1.9%	0.9%	0.7%	4.7%	3.0%	0.8%	1.6%	0.8%	5.6%	4.0%	0.0%	1.4%	6.4%	0.2%	3.2%
PAc - Liver	0.2%	0.5%	7.1%	0.3%	10.4%	0.3%	0.0%	11.2%	0.4%	9.7%	0.9%	0.0%	0.1%	7.5%	9.0%
PAc - Rest	1.8%	5.1%	0.8%	0.4%	0.0%	1.4%	4.4%	0.2%	0.3%	0.0%	0.8%	4.3%	0.2%	0.8%	0.0%
PAc - Skin	3.0%	3.6%	0.8%	7.5%	1.1%	3.9%	6.2%	0.0%	7.1%	1.8%	3.7%	14.0%	6.4%	0.4%	1.3%
Compartment Volumes															
Vc	2.4%	4.8%	1.1%	0.8%	1.4%	2.2%	3.0%	0.3%	1.1%	1.8%	2.8%	2.9%	1.4%	1.6%	2.8%
Vfc	0.3%	1.8%	0.0%	1.7%	0.3%	1.6%	2.2%	0.0%	2.4%	0.2%	1.7%	5.2%	3.0%	0.0%	1.0%
Vkc	0.3%	2.0%	4.8%	5.8%	2.2%	0.8%	4.1%	3.7%	6.4%	2.7%	0.9%	1.3%	4.5%	3.2%	1.0%
Vlc	0.1%	0.2%	2.1%	0.0%	0.2%	0.1%	0.2%	0.8%	0.0%	0.5%	1.2%	0.1%	0.0%	1.0%	0.2%
Vluc	3.8%	0.0%	4.2%	3.6%	2.0%	4.8%	0.4%	3.8%	2.9%	2.7%	9.2%	0.0%	2.6%	5.1%	2.2%
Vrec	3.0%	0.3%	0.1%	11.7%	0.0%	0.7%	1.9%	1.7%	12.5%	0.0%	1.2%	2.0%	12.1%	0.4%	0.3%
Vsc	3.1%	3.9%	2.6%	0.1%	4.2%	2.0%	5.1%	3.6%	0.2%	3.9%	2.0%	3.5%	1.0%	3.2%	4.9%
Vspc	0.1%	0.1%	0.1%	3.3%	0.9%	0.1%	0.1%	0.1%	3.8%	1.0%	0.0%	0.0%	5.3%	0.0%	2.2%

Table B-1.0 Sensitivity Analysis Results for Contribution to Variance between TCDD PB-PK Model Variables and Sequestration Outcome.

Parameters	8 Hours					24 Hours					72 Hours				
	0.1	0.316	1	3.16	10	0.1	0.316	1	3.16	10	0.1	0.316	3.16	1	10
Absorption and Elimination															
BAtcdd	0.2%	10.0%	3.1%	1.1%	1.5%	0.0%	12.3%	2.9%	1.2%	1.5%	0.3%	7.9%	1.0%	3.7%	1.6%
Kabs	5.7%	0.1%	1.1%	0.1%	10.1%	5.5%	0.0%	0.7%	0.0%	8.1%	5.1%	1.3%	0.0%	3.0%	9.1%
Kk	3.8%	1.4%	6.3%	2.0%	2.5%	3.8%	2.2%	6.2%	2.3%	1.5%	5.7%	0.9%	3.2%	5.4%	1.5%
Kli	7.5%	0.1%	4.0%	2.1%	4.6%	8.6%	1.1%	1.7%	1.8%	4.1%	8.8%	1.5%	1.8%	2.4%	2.6%
Ah Receptor Pharmacodynamics															
Bmax - Kidney	0.0%	0.0%	0.8%	0.1%	1.4%	0.1%	0.3%	0.0%	0.1%	1.3%	0.3%	0.6%	0.1%	0.1%	3.1%
Bmax - Liver	0.5%	6.4%	0.8%	2.7%	0.2%	0.3%	2.8%	0.9%	4.3%	0.5%	1.1%	1.1%	5.5%	0.5%	0.9%
Bmax - Lungs	1.2%	1.1%	5.0%	0.3%	0.0%	2.5%	1.0%	7.1%	0.1%	0.1%	0.4%	1.7%	0.0%	1.4%	0.0%
Bmax - Skin	0.0%	6.1%	17.9%	5.4%	0.5%	0.0%	2.3%	19.4%	4.6%	0.5%	0.1%	3.2%	4.1%	20.6%	0.1%
Bmax - Spleen	0.1%	4.0%	5.3%	1.0%	0.2%	0.2%	2.7%	2.3%	1.3%	0.1%	2.4%	4.4%	1.8%	3.3%	0.1%
Kd	2.3%	1.2%	5.9%	0.1%	3.3%	2.2%	0.6%	2.6%	0.2%	3.8%	0.3%	0.0%	0.5%	1.7%	4.7%
CYP1A2 Receptor Pharmacodynamics															
Ccyp0	3.1%	0.0%	4.0%	4.8%	1.1%	4.4%	0.0%	2.6%	5.2%	0.7%	4.2%	0.2%	5.6%	3.3%	0.0%
h	3.2%	3.7%	2.4%	0.5%	0.2%	2.9%	4.6%	2.6%	0.1%	0.8%	8.0%	4.7%	0.0%	1.8%	0.9%
ICa2	1.0%	21.1%	0.0%	2.3%	5.2%	1.9%	15.7%	0.0%	1.5%	4.5%	0.6%	16.1%	0.9%	0.0%	3.9%
INa2	0.0%	4.6%	0.7%	7.5%	7.3%	0.0%	7.1%	0.7%	7.5%	7.4%	0.7%	5.0%	7.0%	0.6%	8.4%
K2	1.2%	1.1%	0.0%	0.2%	7.3%	1.7%	2.5%	0.0%	0.1%	8.3%	2.2%	0.1%	0.0%	0.0%	5.3%
Kdcyp	2.2%	0.9%	2.1%	1.2%	0.0%	3.7%	0.4%	2.1%	0.6%	0.1%	3.7%	0.0%	0.1%	4.4%	0.3%
tau	1.7%	2.7%	0.2%	1.2%	0.6%	2.8%	5.3%	1.2%	1.1%	0.2%	4.0%	1.7%	0.8%	2.2%	0.9%

Table B-2.0 Detailed Descriptions for each Parameter Evaluated in the Sensitivity Analysis.

Abbreviation	Parameter Description
General Physiological Parameters	
Bodyweight	Body weight of receptor
Qcar	Allometric coefficient for cardiac output from bodyweight
Equilibrium Distribution Ratio	
Pf	Equilibrium ratio of adipose tissue to blood concentrations
Pk	Equilibrium ratio of kidney tissue to blood concentrations
Pli	Equilibrium ratio of liver tissue to blood concentrations
Plu	Equilibrium ratio of lung tissue to blood concentrations
Pre	Equilibrium ratio of Rest of the Body tissue to blood concentrations
Ps	Equilibrium ratio of skin tissue to blood concentrations
Psp	Equilibrium ratio of spleen tissue to blood concentrations
Permeability	
PAc - Fat	Membrane permeability of fat compartment
PAc - Kidney	Membrane permeability of kidney compartment
PAc - Liver	Membrane permeability of liver compartment
PAc - Rest	Membrane permeability of rest of the body compartment
PAc - Skin	Membrane permeability of skin compartment
Compartment Volumes	
Vc	Venous blood volume as percentage of body weight
Vfc	Adipose tissue blood volume as percentage of bodyweight
Vkc	Kidney tissue blood volume as percentage of bodyweight
Vlc	Liver tissue blood volume as percentage of bodyweight
Vluc	Lung tissue blood volume as percentage of bodyweight
Vrec	Rest of the body tissue blood volume as percentage of bodyweight
Vsc	Skin tissue blood volume as percentage of bodyweight
Vspc	Spleen tissue blood volume as percentage of bodyweight
Absorption and Elimination	
BAtcdd	Oral bioavailability of compound
Kabs	Chemical absorption rate constant from GI tract to blood
Kk	Urinary excretion rate
Kli	Biliary excretion rate
Ah Receptor Pharmacodynamics	
Bmax - Kidney	Ah receptor binding capacity in the kidney
Bmax - Liver	Ah receptor binding capacity in the liver
Bmax - Lungs	Ah receptor binding capacity in the lungs
Bmax - Skin	Ah receptor binding capacity in the skin
Bmax - Spleen	Ah receptor binding capacity in the spleen
Kd	Dissociation constant of Ah receptor binding

Table B-2.0 Detailed Descriptions for each Parameter Evaluated in the Sensitivity Analysis.

Abbreviation	Parameter Description
CYP1A2 Receptor Pharmacodynamics	
Ccyp0	Basal level of CYP1A2 within the liver
h	Hill coefficient
ICa2	Concentration resulting in half maximum induction folds
INa2	Maximum induction folds over the basal induction rate
K2	CYP1A2 first-order degradation rate constant of binding
Kdcyp	Dissociation constant of binding to CYP1A2
tau	CYP1A2 physiological delay time